16th International Online Mini-Symposium of The Protein Society of Thailand

17-18 November 2021

09:00– 16:30
via **Zoom Meeting**

ABSTRACTS AND PROCEEDINGS

pstsymposium2021@gmail.com
https://science.mahidol.ac.th/pst2021
Mahidol Science
The Protein Society of Thailand

ABSTRACTS AND PROCEEDINGS

16th International Online Mini-Symposium of the Protein Society of Thailand

November 17-18, 2021

Hosted by

Faculty of Science, Mahidol University

Via

Zoom Meeting

ISBN: 978-616-92908-5-8

Published by Protein Society of Thailand
Printed by Ink On Paper Co., Ltd., Bangkok, Thailand

TABLE OF CONTENT

RATIONALE AND REMARK

Since its foundation in 2006, Protein Society of Thailand (PST) has arranged annual symposia for protein researchers and students to exchange their knowledge, experience, and expertise. This year, due to the current COVID-19 pandemic situation, Faculty of Science, Mahidol University collaborates with the Protein Society of Thailand to organize the 16th annual symposium as a free virtual conference titled "16th International Online Mini-Symposium of the Protein Society of Thailand." This symposium demonstrates that advanced research can still be carried on albeit difficulties the pandemic has brought about to all researchers. Most of the invited speakers are rising young scientists conducting frontier research on protein and/or related fields. Participants also have opportunities to present and exchange their research through poster and/or oral presentation. Option to publish a proceeding is also available. The manuscripts of which are as critically reviewed with the same quality standard as any of the preceding PST conferences in previous years.

On behalf of the Organizing Committee, I would also like to thank companies that provide support for this symposium. As always, this kind interaction between academia and industry has been an important hallmark of the PST symposium.

Lastly, I hope that all participants can enjoy and benefit from scientific program and interactions through this virtual conference.

Associate Professor Kittisak Yokthongwattana, Ph.D.
Chair of the Organizing Committee
16th International Online Mini-Symposium of the Protein Society of Thailand

ORGANIZING COMMITTEE

Advisory Committee
Prof. Dr. MR. Jisnuson Svasti
Assoc. Prof. Dr. Palangpon Kongsaeree
Dr. Chantragan Phiphobmongkol

Chairperson
Assoc. Prof. Dr. Kittisak Yokthongwattana

Scientific Committee
Mahidol University
Asst. Prof. Dr. Adisak Romsang
Asst. Prof. Dr. Danaya Pakotiprapha
Assoc. Prof. Dr. Jirundon Yuvaniyama
Asst. Prof. Dr. Pramvadee Y. Wongsaengchantra
Asst. Prof. Dr. Puey Ounjai
Asst. Prof. Dr. Ruchanok Tinikul
Dr. Sakonwan Kuhaudomlarp
Dr. Sittinan Chanarat
Assoc. Prof. Dr. Varodom Charoensawan

Protein Society of Thailand
Asst. Prof. Dr. Anuchit Phanumartwiwath
Asst. Prof. Dr. Atit Silsirivanit
Dr. Churat Weeraphan
Assoc. Prof. Dr. Dumnoensun Pruksakorn
Asst. Prof. Dr. Dumrongkiet Arthan
Dr. Hansuk Buncherd
Prof. Dr. James Ketudat-Cairns
Dr. Nilubol Paricharttanakul
Dr. Sittiruk Roytrakul
Dr. Somchai Chutipongtanate
Asst. Prof. Dr. Sutin Kingtong
Dr. Voraratt Champattanachai

Event and MC Committee
Assoc. Prof. Dr. Nuttawee Niamsiri
Asst. Prof. Dr. Patompong Johns Saengwilai

IT Backoffice and Registration Committee
Varasaya Soonthornsarathool
Pichit Leerungnavarat
Arisara Rakdamrongtham
Nootsara Boonkrong
Orn-Aree Thanitpipat
Supawadee Phetnoi
Jirapat Eiamjareanlab
Direk Ounkaew

SCIENTIFIC PROGRAM

16th International Online Mini-Symposium of the Protein Society of Thailand

Wednesday November 17, 2021

09:00 – 09:15	Opening Session
09:15 – 09:45	**Invited Lecture 1 – Dr. Erik Procko** Engineered decoy receptors as potent neutralizers of SARS-CoV-2 variants and therapeutic candidates for the treatment of COVID
09:45 – 10:15	**Invited Lecture 2 – Dr. Kittikhun Wangkanont** Inhibitor discovery and a novel inhibitor binding assay for SARS-CoV-2 main protease
10:15 – 10:45	**Invited Lecture 3 – Dr. Bunyarit Meksiriporn** An engineered survival selection strategy for synthetic binding proteins against difficult-to-drug targets
10:45 – 11:00	Break
11:00 – 11:30	**Invited Lecture 4 – Dr. Sakonwan Kuhaudomlarp** Development of inhibitors targeting pathogenic sugar binding proteins
11:30 – 12:00	**Bruker Academic Talk – Dr. Sri Ramarathinam** Immunopeptidomic analysis of SARS-CoV2 infected lung epithelial cells reveals new targets for antiviral immunity
12:00 – 13:00	Lunch Break
13:00 – 14:00	**PST Annual Meeting / Poster Session**
14:00 – 15:00	**Poster Session** (continued)
15:00 – 15:30	**Invited Lecture 5 – Dr. Patompon Wongtrakoongate** Science and translation toward prevention and treatment of COVID-19
15:30 – 16:00	**Invited Lecture 6 – Dr. Somchai Chutipongtanate** Breast Milk, BigMAC and Crab Cracker: My research on therapeutic peptides

Thursday November 18, 2021

09:00 – 09:30	**Invited Lecture 7 – Dr. Waranyoo Phoolcharoen** Towards clinical trial phase I of plant-based COVID-19 vaccine in Thailand
09:30 – 10:00	**Invited Lecture 8 – Dr. Vimvara Vacharathit** Antibody and cytokine responses in COVID-19 patients and vaccines
10:00 – 10:30	**Invited Lecture 9 – Dr. Waradon Sungnak** Cellular immune response to COVID-19 deciphered by single-cell multi-omics
10:30 – 10:50	Break
10:50 – 11:10	**Oral Presentation 1 – Ms. Wichuda Phothichaisri** Host-derived cell-wall-binding domain of phage endolysin CD16/50L anchors to the surface polysaccharide of *Clostridioides difficile* to preserve neighboring host cells and ensure progeny expansion
11:10 – 11:30	**Oral Presentation 2 – Ms. Kankamol Kerdkumthong** Proteomic analysis of 5-Fluorouracil resistant cholangiocarcinoma cell line
13:30 – 13:00	Lunch Break
13:00 – 13:30	**Waters Academic Talk – Dr. Dhaval Patel** How LC-MS can support our fight against Covid-19
13:30 – 15:00	**Poster Session** (continued)
15:00 – 15:15	Break
15:15	**Closing Session**

Invited Lectures

Company Academic Talks

Oral Presentations

IL-01

Engineered decoy receptors as potent neutralizers of SARS-CoV-2 variants and therapeutic candidates for the treatment of COVID

Erik Procko

School of Molecular and Cell Biology, University of Illinois at Urbana-Champaign, 387 Morrill Hall, MC-119 505 South Goodwin Avenue, Urbana, IL 61801 USA

E-mail: procko@illinois.edu

ABSTRACT

Soluble receptors can act as decoys to neutralize virus infections with reduced risk for the emergence of resistance. However, in the case of SARS-CoV-2, the ACE2 receptor lacks tight affinity and potency. Using deep mutagenesis, decoys are engineered for SARS-CoV-2 that resolve these challenges and are demonstrated to be safe and effective in animal infection models. The decoys broadly bind virus variants with tight affinity and limited potential for escape.

IL-02

Inhibitor discovery and a novel inhibitor binding assay for SARS-CoV-2 main protease

Peerapon Deetanya[1,2], Kowit Hengphasatporn[3], Patcharin Wilasluck[1,2], Yasuteru Shigeta[3], Thanyada Rungrotmongkol[4,5], **Kittikhun Wangkanont[1,2,*]**

[1] Center of Excellence for Molecular Biology and Genomics of Shrimp, Department of Biochemistry, Faculty of Science, Chulalongkorn University, Bangkok 10330 Thailand
[2] Molecular Crop Research Unit, Department of Biochemistry, Faculty of Science, Chulalongkorn University, Bangkok 10330 Thailand
[3] Center for Computational Sciences, University of Tsukuba, 1-1-1 Tennodai, Tsukuba, Ibaraki 305-8577, Japan
[4] Program in Bioinformatics and Computational Biology, Faculty of Science, Chulalongkorn University, Bangkok, 10330, Thailand
[5] Structural and Computational Biology Research Unit, Department of Biochemistry, Faculty of Science, Chulalongkorn University, Bangkok 10330 Thailand

*** E-mail:** kittikhun.w@chula.ac.th

ABSTRACT

The main protease of SARS-CoV-2 is responsible for viral polyprotein cleavage. This process is crucial for viral multiplication. Thus, the main protease is a promising target for antiviral drug development. Traditional enzyme activity assays for inhibitor identification rely on peptide-based substrates. However, the COVID-19 pandemic has limit or delay access to peptide synthesis services, especially for researchers in developing countries. We explored the application of 8-anilinonaphthalene-1-sulfonate (ANS) as a fluorescent probe for inhibitor identification. Fluorescence enhancement upon binding of ANS to the main protease was observed. This interaction was competitive with a peptide substrate, indicating that ANS bound within the active site. The utility of ANS-based competitive binding assay to identify main protease inhibitors was demonstrated with the flavonoid natural products baicalein and rutin. The molecular details of ANS and rutin interaction with the main protease was investigated with molecular modeling. Our results suggested that ANS could be utilized in a competitive binding assay to facilitate the identification of novel SARS-CoV-2 antiviral agents.

IL-03

An engineered survival-selection strategy for synthetic binding proteins against difficult-to-drug targets

Bunyarit Meksiriporn

Department of Biology, King Mongkut's Institute of Technology Ladkrabang, Bangkok, 10520, Thailand

Email: bunyarit.me@kmitl.ac.th

ABSTRACT

Protein phosphorylation plays an important role in the regulation of protein function and many cellular processes. Aberrant phosphorylation has been shown to be a cause of cell death as well as maligination. As such, there is an urgent need for affinity reagents that target phospho-modified sites on individual proteins. Currently, generation of phospho-specific antibodies relies primarily on hybridoma technology which requires phospho-epitope mapping through mass spectrometry, selection of the phospho-epitope to be targeted, and synthesis of a short phosphopeptide to be injected. As an alternative to immunization, protein display technologies (*e.g.*, phage, yeast, and ribosome display) have been employed as a viable approach to specifically select for binders against phospho-modified sites on individual targets. Though up-front phospho-amino acid identification is eliminated in protein display technologies, purification of kinases is still required. Another challenge is that the resulting antibody fragments require intradomain disulfide bonds for conformational stability, thus precluding their use as "intrabodies" in the reducing intracellular environment where most phosphoproteins of interest naturally reside. This bottleneck can be overcome by using alternative non-antibody binding scaffolds for molecular recognition such as designed ankyrin repeat proteins (DARPins), which contain no disulfide bonds and can be expressed in soluble form with high yields in the cytoplasm of living cells. Here, we describe a genetic selection strategy for routine laboratory isolation of phospho-specific designed ankyrin repeat proteins (DARPins) by linking in vivo affinity capture of a phosphorylated target protein with antibiotic resistance of *Escherichia coli* cells. The assay is validated using an existing panel of DARPins that selectively bind the nonphosphorylated (inactive) form of extracellular signal-regulated kinase 2 (ERK2) or its doubly phosphorylated (active) form (pERK2). We then use the selection to affinity-mature a phospho-specific DARPin without compromising its selectivity for pERK2 over ERK2 and to reprogram the substrate specificity of the same DARPin towards non-cognate ERK2. Collectively, these results establish our genetic selection as a useful and potentially generalizable protein engineering tool for studying phospho-specific binding proteins and customizing their affinity and selectivity.

IL-04

New glycomimetics inhibitors targeting sugar-binding proteins from pathogenic bacteria

Sakonwan Kuhaudomlarp[1±$], Eike Siebs[2,3,4$] , Elena Shanina[5,6] , Jérémie Topin[1,7] , Ines Joachim[2,3,4], Priscila da Silva Figueiredo Celestino Gomes[8] , Annabelle Varrot[1] , Didier Rognan[8] , Christoph Rademacher[5,6] , Anne Imberty[1*] , and Alexander Titz[2,3,4*]

[1] Université Grenoble Alpes, CNRS, CERMAV, 38000 Grenoble, France
[2] Chemical Biology of Carbohydrates (CBCH), Helmholtz-Institute for Pharmaceutical Research Saarland (HIPS), Helmholtz Centre for Infection Research, 66123 Saarbrücken, Germany
[3] Department of Chemistry, Saarland University, 66123 Saarbrücken, Germany
[4] Deutsches Zentrum für Infektionsforschung (DZIF), Standort Hannover-Braunschweig, Germany
[5] Department of Biomolecular Systems, Max Planck Institute of Colloids and Interfaces, 14424 Potsdam, Germany
[6] Institute of Chemistry and Biochemistry, Department of Biology, Chemistry and Pharmacy, Freie Universität Berlin, 14195 Berlin, Germany
[7] Institute of Chemistry-Nice, UMR 7272 CNRS, Université Côte d'Azur, 06108 Nice, France
[8] Laboratoire d'Innovation Thérapeutique, UMR 7200 CNRS-Université de Strasbourg, 67400 Illkirch, France
[±] Present address: Department of Biochemistry, Faculty of Science, Mahidol University, Bangkok, 10400, Thailand
[$] These authors contributed equally
[*] Corresponding emails: anne.imberty@cermav.cnrs.fr and alexander.titz@helmholtz-hzi.de

Email: sakonwan.kuh@mahidol.edu

ABSTRACT

Pathogenic bacteria utilise glycan epitopes on host tissue for specific recognition and host infection, the processes which are mediated by the interaction between host glycan epitopes and the pathogenic sugar-binding protein called lectins. Opportunistic pathogens such as *Pseudomonas aeruginosa* produces multivalent sugar-binding proteins, LecA and LecB, which plays crucial roles in host infection and biofilm formation. Through rational design and drug screening approaches, our research works aimed at developing new glycomimetics inhibitors targeting these proteins to interfere with host glycan binding process. In drug screening approach, we performed virtual drug screen against chemical libraries to identify hit molecules that were subsequently validated by several orthogonal biophysical assays (surface plasmon resonance, thermal shift assays, fluorescent polarisation, and nuclear magnetic resonance). X-ray crystallographic study was used to determine the binding mode of the hit molecules to LecA, providing the first evidence of non-carbohydrate glycomimicry for lectins from pathogens. The identified non-carbohydrate inhibitors can be used as a starting point for the development of a new class of LecA inhbitors.

Bruker Academic Talk

Immunopeptidomic analysis of SARS-CoV2 infected lung epithelial cells reveals new targets for antiviral immunity

Sri Ramarathinam

Department of Biochemistry and Molecular Biology and Infection and Immunity Program, Monash Biomedicine Discovery Institute, Monash University, Clayton, Victoria, Australia

Email: Sri.Ramarathinam@monash.edu

ABSTRACT

Peptides presented by Human Leukocyte antigen (HLA) class I and II molecules form an important target of the adaptive immune response against viruses, bacteria and tumours. Identifying HLA-bound peptides is therefore crucial to understand the specificity of T cell responses in cancer and infectious disease. This mode of antigen presentation facilitates broad immunosurveillance by T-lymphocytes (T-cells) which can recognize foreign or abnormal peptides associated with these HLA molecules and elicit an appropriate immune response to eradicate the infected or malignant cells. It is therefore vital to identify these peptides to enable better design of vaccines and immunotherapies.

Mass spectrometry is emerging as a gold-standard to identify the peptide cargo of HLA molecules and the study of these peptides is termed immunopeptidomics. We applied this approach to understand the antigenic landscape of SARS-CoV2 infected Calu3 lung epithelial cells. Virus infected and uninfected cells were lysed and the HLA complexes immunoprecipitated using antibodies specific for HLA class I and II molecules. The peptide cargo was then separated and analysed using a Bruker timsTOF PRO coupled with a NanoElute nano-UHPLC. Leveraging the high sensitivity and trapped ion mobility features of this instrument aided the identification of over 9000 Class I and 10000 class II ligands, that included over 100 SARS-CoV2 derived peptides. We show that peptides spanning the entire viral proteome contribute to the SARS-CoV2 immunopeptidome, revealing new opportunities for rational vaccine design that extend beyond the currently targeted viral Spike protein.

IL-05

Science and translation toward prevention and treatment of COVID-19

Patompon Wongtrakoongate

Department of Biochemistry, Faculty of Science, Mahidol University, 272 Rama 6 Rd., Bangkok 10400 Thailand

Email: patompon.won@mahidol.ac.th

ABSTRACT

In this talk, I will discuss three technologies in prevention and treatment of COVID-19 which have been developed under our COVID-19 research group. First, we have identified two small molecule derivatives of a plant-derived compound which possess a strong anti-SARS-CoV-2 activity. Preliminary data suggest that the two compounds exert their effect via both viral entry and egress pathways. Second, we have recently shown a neutralizing activity of sera collected from mice receiving a prime-boost regimen of HexaPro spike subunit vaccine; this conformation of the SARS-CoV-2 spike glycoprotein is employed by NDV-HXP-S vaccine developed by Mahidol-GPO. Third, we isolated spleenocytes from the mice and used them to create hybridomas. Monoclonal antibody derived from one of these clones possesses a strong neutralizing activity against live viruses. cDNA isolated from this hybridoma clone will be utilized to create a humanized therapeutic monoclonal antibody. Lastly, I will discuss our ongoing work on a novel class of mRNA vaccine. We have demonstrated that this novel class of mRNA vaccine is more potent than a conventional linear mRNA counterpart. Moreover, the mRNA technology will be applied not only for other infectious diseases, but also for genetic diseases, regenerative medicine, and cancers.

IL6

Breast milk, BigMAC and Crab Cracker: My Research on Therapeutic Peptides

Somchai Chutipongtanate[1,2,3,*]

[1] Pediatric Translational Research Unit, Faculty of Medicine Ramathibodi Hospital, Mahidol University, Bangkok 10400 Thailand
[2] Department of Clinical Epidemiology and Biostatistics, Faculty of Medicine Ramathibodi Hospital, Mahidol University, Bangkok 10400 Thailand
[3] Chakri Naruebodindra Medical Institute, Faculty of Medicine Ramathibodi Hospital, Mahidol University, Samut Prakan 10540 Thailand

***Email**: schuti.rama@gmail.com, somchai.chu@mahidol.edu

ABSTRACT

Peptides have gained much attention during the last few years as new therapeutic agents, particularly for cancers. While the exact mechanisms and cancer selectivity have yet to be elucidated, anti-cancer peptides may have oncolytic activities depending on their intrinsic characteristics. Some of these anti-cancer properties are predictable from amino acid sequences. Here, our group has explored the advent of Big data and Machine learning to facilitate the discovery of new Anti-Cancer peptides (Big-MAC). We applied this approach to breast milk peptidomics and recently reported HMP-S7 as a novel anti-leukemic peptide against leukemic cells *in vitro* and patient-derived cells *ex vivo*. Further investigations using a more extensive peptide library and a new algorithm for anti-cancer peptide mutagenesis may be enable the right way to crack the crab by therapeutic peptides in the future.

This research was supported by the New Discovery and Frontier Research Grant of Mahidol University, Thailand (NDFR19/2563).

IL-07

Towards Clinical Trial Phase I of Plant-based COVID-19 Vaccine in Thailand

Waranyoo Phoolcharoen

Baiya Phytopharm Co. Ltd., Bangkok, Thailand

Email: phwaranyoo@gmail.com

ABSTRACT

SARS-CoV-2 causes the COVID-19 outbreak since January 2020 and the virus spreads rapidly worldwide. Within one year of its outbreak, COVID-19 vaccines were developed and approved under emergency application. Several countries have begun mass administration of COVID vaccines from early 2021. However, the accessibility of the vaccines in most countries have been questioned as the vaccines are reserved by wealthy nations. Hence the people in low-income and middle-income countries are still waiting to get a vaccine shot due to the unequal distribution of COVID-19 vaccines around the globe. In view of the vaccine security, plant-based COVID-19 vaccine production has been initiated in Thailand as plants offer many advantages, including high scalability, rapid production time, and low infrastructural cost. Plant-produced COVID-19 vaccine was developed by producing SARS-CoV-2 RBD-Fc fusion protein in *Nicotiana benthamiana* (Baiya SARS-CoV-2 Vax 1). SARS-CoV-2 RBD-Fc showed specific binding to ACE2 protein. The immunogenic potential of Baiya SARS-CoV-2 Vax 1 was demonstrated in mice. The results showed that a single dose of Baiya SARS-CoV-2 Vax 1adjuvanted with alum could induce immune response in mice, however the titer of RBD-specific antibody and neutralizing antibody was increased after the second dose. Also of note, the *in vitro* neutralization of live SARS-CoV-2 virus with the sera collected from Baiya SARS-CoV-2 Vax 1 immunized mice and monkeys was evaluated. Further, the results from SARS-CoV-2 challenge study suggest that Baiya SARS-CoV-2 Vax1 reduces the symptoms and mortality associated with SARS-CoV-2 infection in K18hACE2 mice. The toxicity study also showed that Baiya SARS-CoV-2 Vax1 was well tolerated in Wistar rats with no unanticipated findings or toxicity observed up to 100 μg dose. Collectively, the results from mice, rats and monkeys have shown that Baiya SARS-CoV-2 Vax1 induced potent neutralizing antibody response against SARS-CoV-2, including the variants of concern.

IL-08

Antibody and cytokine responses in COVID-19 patients and vaccines

Vimvara Vacharathit

Department of Microbiology, Faculty of Science, Mahidol University, 272 Rama 6 Rd., Bangkok 10400 Thailand

Email: vimvara.vac@mahidol.ac.th

ABSTRACT

The ongoing COVID-19 pandemic necessitates continued monitoring of both naturally acquired and vaccine-induced immunity against SARS-CoV-2 and its variants of concern (VOCs). A longitudinal study of neutralizing antibody (NAb) titers in patients hospitalized in early 2020 with mild symptoms, pneumonia, or severe pneumonia revealed that peak NAb titers correlated with disease severity and that NAb titers declined over the course of 1 year regardless of severity. Serum-derived inflammatory cytokine profiling in all severity groups unveiled key cytokines linked to severe pneumonia, and cytokine networks were found to be distinct between severity groups. Furthermore, assessment of NAb titers in a separate cohort of healthcare workers who had received 2 doses of CoronaVac revealed that the regimen conferred relatively low levels of NAb-mediated protection against SARS-CoV-2 VOCs compared to WT, and that vaccine-induced NAb potency was lower than that derived from natural infection. Our results highlight the need for constant vigilance and appropriate vaccine monitoring, especially against the highly transmissible delta strain, which was found to be most refractory to neutralization.

IL-09

Cellular immune response to COVID-19 deciphered by single-cell multi-omics

Waradon Sungnak

Department of Microbiology, Faculty of Science, Mahidol University, 272 Rama 6 Rd., Bangkok 10400 Thailand

Email: waradon.sun@mahidol.ac.th

ABSTRACT

Single-cell gene and multi-omic profilings have provided insights into the biology of COVID-19. We surveyed expression of viral entry-associated genes in single-cell RNA-sequencing data from multiple tissues from healthy human donors and co-detected these transcripts in specific respiratory, corneal, and intestinal epithelial cells, potentially explaining the high efficiency of SARS-CoV-2 transmission. Subsequently, we performed single-cell transcriptome, surface proteome, and T and B lymphocyte antigen receptor analyses of over 780,000 peripheral blood mononuclear cells from a cross-sectional cohort of 130 patients with varying severities of COVID-19. We identified the expansion of nonclassical monocytes expressing complement transcripts (*CD16*$^{+}$*C1QA/B/C*$^{+}$) that sequester platelets and were predicted to replenish the alveolar macrophage pool in COVID-19. Early, uncommitted CD34^{+} hematopoietic stem/progenitor cells were primed toward megakaryopoiesis, accompanied by expanded megakaryocyte-committed progenitors and increased platelet activation. Clonally expanded CD8^{+} T cells and an increased ratio of CD8^{+} effector T cells to effector memory T cells characterized severe disease while circulating follicular helper T cells accompanied mild disease. We observed a relative loss of IgA2 in symptomatic disease despite an overall expansion of plasmablasts and plasma cells. Our study highlights the coordinated immune response that contributes to COVID-19 pathogenesis and reveals discrete cellular components that can be targeted for therapy.

Waters Academic Talk

How LC-MS can support our fight against Covid-19

Dhaval Patel

Waters Pacific Pte Ltd, Singapore

ABSTRACT

Research organizations have risen to the challenge of fighting the covid-19 pandemic across the globe. Key areas of research related to covid-19 include improving fundamental understanding of COVID-19 infection; characterizing the virus and how it causes infection; development of rapid and accurate assays for the diagnosis; identifying and evaluating potential treatments for COVID-19 infection and development of safe and effective vaccines.

The presentation will provide high-level context to explain the role of LC-MS based approaches for covid-19 research related applications.

OR-01

Host-derived cell-wall-binding domain of phage endolysin CD16/50L anchors to the surface polysaccharide of *Clostridioides difficile* to preserve neighboring host cells and ensure progeny expansion

Wichuda Phothichaisri,[1] Jirayu Nuadthaisong,[1] Tanaporn Phetreun,[1] Tavan Janvilisri,[1] Robert Fagan,[2] Surang Chankhamhaengdecha,[3] Sittinan Chanarat [1,4,*]

[1] Department of Biochemistry, Faculty of Science, Mahidol University, Bangkok, Thailand
[2] Department of Molecular Biology and Biotechnology, Florey Institute, University of Sheffield, Sheffield, S10 2TN, UK
[3] Department of Biology, Faculty of Science, Mahidol University, Bangkok, Thailand
[4] Laboratory of Molecular Cell Biology, Center for Excellence in Protein and Enzyme Technology, Faculty of Science, Mahidol University, Bangkok, Thailand

*Email: sittinan.cha@mahidol.edu

Abstract

Endolysin is a phage-encoded cell-wall hydrolase which degrades the peptidoglycan layer of the bacterial cell wall. The enzyme is often expressed at the late stage of the phage lytic cycle and is required for progeny escape. Endolysin of bacteriophage that infects Gram-positive bacteria often comprises two domains: a peptidoglycan hydrolase and a cell-wall binding domain (CBD). Although the catalytic domain of endolysin is relatively well-studied, the precise role of CBD is largely unknown and remains controversial. For example, while certain endolysins absolutely require CBD for their lytic activity, others do not need it at all, raising the question of its necessity. Here, we focus on the function of CBD of endolysin encoded in the genome of recently isolated *Clostridioides difficile* phages. We found that CBD of this endolysin is not required for the lytic activity, which is strongly prevented by the surface layer of *C. difficile*. Intriguingly, hidden Markov model (HMM) analysis suggested that the endolysin CBD is likely derived from the cell-wall-binding-2 domain of host's cell-wall proteins but possesses a higher binding affinity to polysaccharide components of bacterial cell wall. Moreover, the CBD is able to form a homodimer, formation of which is necessary for interaction with the peptidoglycan layer. Importantly, endolysin diffusion and sequential cytolytic assays showed that CBD of endolysin is required for anchoring to cell-wall remnants, suggesting its physiological roles in controlling diffusion of the enzyme, preserving neighboring host cells, and thereby enabling phage progeny to initiate new rounds of infection. Taken together, this study provides an insight into regulation of endolysin through CBD and can potentially be applied for endolysin treatment against *C. difficile* infection.

Acknowledgement

This research was supported by Science Achievement Scholarship of Thailand (SAST).

OR-02

Proteomic analysis of 5-Fluorouracil resistant cholangiocarcinoma cell line

Kankamol Kerdkumthong[1], Kawinnath Songsurin[1], Sittiruk Roytrakul[2], Sumalee Obchoei[1,*]

[1] Division of Health and Applied Sciences, Department of Biochemistry, Faculty of Science, Prince of Songkla University, Songkhla 90110, Thailand
[2] National Center for Genetic Engineering and Biotechnology, National Science and Technology Development Agency, Pathumtani 12120, Thailand

***Email**: sumalee.o@psu.ac.th

ABSTRACT

Resistance to commonly used chemotherapeutic drugs is a major problem of cholangiocarcinoma (CCA) treatment, therefore more effective treatment strategy is urgently needed. Drug resistant cell lines have been used for elucidating drug resistance mechanism in various cancers leading to the discovery of novel treatments. Here in, we have established 5-Fluorouracil resistant (FR) CCA cell line by culturing the parental CCA cell line (KKU-213A) in the stepwise increased concentration of 5-Fluorouracil (5-FU). The established cell line was designated as KKU-213A-FR, confirmed for drug resistance, and use for further analyses. The results showed that, under low serum condition, KKU-213A-FR had slower growth rate than its parental cell line. Conversely, cell migration and invasion ability were increased significantly. Moreover, the proteomic analysis using LC/MS/MS identified the total of 5,680 proteins. In which, 431 were identified only in parental cells, 1,105 were found only in FR cells, whereas 4,144 were expressed in both cell lines. Heatmap analysis showed the 25 most up- and down-regulated proteins in KKU-213A-FR. The up-regulated proteins were further analyzed. Gene ontology revealed that most of these proteins were classified in cellular process group. The protein-protein interaction analysis showed 3 clustering groups that involve in N-linked glycosylation, ubiquitin-dependent protein catabolic process, and organic substance catabolic process. In conclusion, the KKU-213A-FR exhibits aggressive phenotypes and a unique proteomic profile as compared to KKU-213A. More in-depth study on the differentially expressed proteins may lead to better understanding of drug resistance mechanism and more effective treatment for CCA.

Poster Abstracts

PP001

In silico prediction and experimental validation of a novel anti-cancer peptide

Tassanee Lertsuthirat[1#], Pasinee On-yam[2#] Sermsiri Chitphuk[1], Wasana Stitchantrakul[1], Suradej Hongeng[3], Wararat Chiangjong[3*], Somchai Chutipongtanate[3]*

[1] Research Center, Faculty of Medicine Ramathibodi Hospital, Mahidol University, Bangkok 10400 Thailand
[2] Faculty of Medicine Ramathibodi Hospital, Mahidol University, Bangkok 10400 Thailand
[3] Department of Pediatrics, Faculty of Medicine Ramathibodi Hospital, Mahidol University, Bangkok 10400 Thailand
[#] Shared equal contribution *Co-correspondence

***Email**: wararat.chi@mahidol.ac.th, somchai.chu@mahidol.edu

ABSTRACT

INTRODUCTION: Cancer is the leading cause of death worldwide. To improve patient outcomes, a more effective treatment agent is required. Our previous work on discovering human milk peptides that selectively kill leukemia cells has shown the approach of using mass spectrometry to identify the candidate anticancer peptides. It is limited by the small peptide library. Thus, we propose to expand the peptide library by using *in silico* generation of peptides from the protein of interest.

MATERIALS AND METHODS: We *in silico* produced peptides from a protein with anticancer potential, alpha-lactalbumin. On-line tools were used to predict anticancer properties of the filtered peptides. Lastly, we chose four candidates for *in vitro* testing on cancer cells.

RESULTS AND DISCUSSION: We *in silico* obtained four candidates (A1-A4) peptides with the highest anticancer scores for further *in vitro* testing on five cancer cell lines, SH-SY5Y, MDA-MB-231, A549, HT29, and K562. A2 was able to solubilize in media, whereas three peptides (A1, A3, and A4) precipitated. Preliminary screening revealed A2 demonstrated the most anticancer activity. To avoid the interference of peptide precipitants on cell viability, we therefore solubilized peptide in DMSO. A1, A3, and A4 exhibited dose-dependent cytotoxicity toward A549, but none of the three exhibited significant cytotoxicity toward the remaining cancer cells.

CONCLUSION: This approach enables us to rapidly identify potential anticancer candidates prior to conducting *in vitro* experiments, while also expanding the pool of bioactive peptides that may be missed by mass spectrometry analysis.

REFERENCE: Chiangjong, W., et al., HMP-S7 Is a Novel Anti-Leukemic Peptide Discovered from Human Milk. Biomedicines, 2021. 9(8): p. 981.

PP002

Identification of protein A, B, C, D and E as biomarkers to distinguish between hepatocellular carcinoma and cholangiocarcinoma in 3D culture using Label-free quantitative proteomics

Penchatr Diskul-Na-Ayudthaya[1], Meghna Phanichkrivalkosil[1], Daranee Chokchaichamnankit[1], Churat Weeraphan[1], Jisnuson Svasti[1,2] and Chantragan Srisomsap[1]*

[1] Laboratory of Biochemistry, Chulabhorn Research Institute, Bangkok 10210, Thailand
[2] Applied Biological Sciences Program, Chulabhorn Graduate Institute, Bangkok 10210, Thailand

***Email**: chantragan@cri.or.th

ABSTRACT

Precise monitoring and diagnosis of cancer patients are the key to cancer therapeutic. Therein, to find the new specific biomarker is the challenge for cancer prevention and treatment. Discovery of new protein markers employ high throughput of sample characterization by mass spectrometry. Here, 3D cell culture was used as a model to mimic tumor environment. Cells were digested and identified by label-free mass spectrometry to differentiate candidate cancer biomarkers between hepatocellular carcinoma and cholangiocarcinoma, which located at nearby area and difficult to diagnose. Mass spectrometry results were then analyzed by Progenesis QI software. More 500 proteins were changed between two types of cancer. All changed proteins involved in protein binding, catalytic activity, structural molecule activity, transport regulator activity and transporter activity. Among these proteins, we found that 4 proteins named protein A, B, C and D were highly expressed in cholangiocarcinoma cells compared to hepatocellular carcinoma. Furthermore, we also found protein E was highly express in hepatocarcinoma compared to cholangiocarcinoma. All candidate proteins were validated by immunoblotting. All of these proteins were analyzed by String and Cytoscape software. However, tissue samples from patients are needed for further study. Taken together, our results provide 5 candidate biomarkers to distinguish the difference between hepatocellular carcinoma and cholangiocarcinoma.

This research was supported by the Chulabhorn Research Institute

PP004

Design of enzyme immobilization system for chitin bioconversion

Ailada Charoenpol[1], Daniel Crespy[2], Albert Schulte[1], Wipa Suginta[1]*

[1] School of Biomolecular Science and Engineering (BSE), Vidyasirimedhi Institute of Science and Technology (VISTEC), Payupnai, Wangchan Valley, Rayong 21210, Thailand
[2] School of Molecular Science and Engineering (MSE), Vidyasirimedhi Institute of Science and Technology (VISTEC), Payupnai, Wangchan Valley, Rayong 21210, Thailand

***Email**: wipa.s@vistec.ac.th

ABSTRACT

Chitooligosaccharides (COS) produced by the enzymatic hydrolysis of chitin are of significant interest; their high value indicates that they have interesting bioactivities such as anticancer, antifungal, and anti-inflammatory properties, making them a viable pharmaceutical product. Utilizing of immobilized enzyme for COS production is interesting, as long as the enzyme is stable enough for industrial application. In this study, chitinase A from the marine bacterium *Vibrio harveyi* (*Vh*ChiA) was fermented and purified by a Ni-NTA column. Chitosan coated magnetic nanoparticles (CS@MNPs) were synthesized by in situ co-precipitation method and were then functionalized with hemin through amidation reaction. *Vh*ChiA was immobilized on to three different types of magnetic nanoparticles including uncoated MNPs, CS@MNPs, and Hemin@CS@MNPs. Transmission electron microscopy (TEM), Scanning electron microscopy (SEM), Fourier-transform infrared spectroscopy (FTIR), and thermal gravimetric analysis (TGA) were used to illustrate the MNPs and immobilized *Vh*ChiA. Among of three types of magnetic nanoparticles, CS@MNPs provided the highest immobilization yield around 95%, followed by Hemin@CS@MNPs, and uncoated MNPs which gave 87% and 29%, respectively.

PP005

Virtual screening of novel *M. tuberculosis* PknA/PknB dual inhibitors as anti-tuberculosis agents

Pharit Kamsri[1,*], Auradee Punkvang[1], Paptawan Thongdee[2], Khomson Suttisintong[3], Prasat Kittakoop[4,5,6], James Spencer[7], Adrian J. Mulholland,[8] Galina V. Mukamolova[9], Pornpan Pungpo[2]

[1] Division of Chemistry, Faculty of Science, Nakhon Phanom University, 48000 NakhonPhanom, Thailand
[2] Department of Chemistry, Faculty of Science Ubon Ratchathani University, 34190 Ubon Ratchathani, Thailand
[3] National Nanotechnology Center, National Science and Technology Development Agency, Thailand Science Park, 12120 Pathumthani, Thailand
[4] Chulabhorn Research Institute, 10210 Bangkok, Thailand
[5] Chulabhorn Graduate Institute, Chemical Biology Program, Chulabhorn Royal Academy, 10210 Bangkok, Thailand
[6] Center of Excellence on Environmental Health and Toxicology (EHT), CHE, Ministry of Education, 10300 Bangkok, Thailand
[7] School of Cellular and Molecular Medicine, University of Bristol, Biomedical Sciences Building, University Walk, BS8 1TD Bristol, United Kingdom
[8] Centre for Computational Chemistry, School of Chemistry, University of Bristol, BS8 1TS Bristol, United Kingdom
[9] Department Respiratory Sciences, University of Leicester, Leicester LE1 7RH, United Kingdom

***Email**: pharit.kamsri@npu.ac.th

ABSTRACT

In this research, we applied virtual screening and pharmacokinetic predictions to identify novel PknA/PknB dual inhibitors for tuberculosis agents from kinase inhibitor database. The obtained results demonstrated that four compounds were identified as new *M. tuberculosis* PknA/PknB dual inhibitors which showed strong biding affinity with ATP binding site. These compounds shared hydrogen bond interaction at the hinge residue of Val98 and Val95 backbone of PknA and PknB, respectively. In addition, sigma-pi andhydrophobic interactions of hit compounds with amino acid residues enhanced the binding affinity in the ATP binding site. Based on the pharmacokinetic prediction, the Caseum FU was ranging from 0.20 to 18.97 % which indicated that compounds will inhibit mycobacterialwith low MIC value. The low maximum tolerated dose and oral rat acute toxicity suggested that hits compounds should be low toxicity. Therefore, this work aided to identify novel PknA/PknB dual inhibitors as potent anti-tuberculosis agents.

This research was supported by Royal Society-Newton Mobility Grant and Office of Permanent Secretary, Ministry of Higher Education Science Research and Innovation (NMG\R1\201061). The EPSRC for funding via BristolBridge (EP/M027546/1) and CCP-BioSim (EP/M022609/1). We would like to thank Faculty of Science, Ubon Ratchathani University, Nakhon Phanom University, Kasetsart University, NECTEC, NANOTEC and the University of Bristol for their support and facilities.

PP006

Elucidating the binding interaction of pyrimido[4,5-b]indol-8-amine derivatives as potential GyrB inhibitors against *M. tuberculosis* using molecular docking calculations

Paptawan Thongdee[1], Bongkochawan Pakamwong[1], Bandit Khamsri[1], Naruedon Phusi[1], Somjintana Taveepanich[1], Jidapa sangswan[2], Pharit Kamsri[3], Auradee Punkvang[3], Patchreenart Saparpakorn[4], Supa Hannongbua[4], Khomson Suttisintong[5], Prasat Kittakoop[6,7,8], Noriyuki Kurita[9], James Spencer[10], Adrian J. Mulholland[11], and Pornpan Pungpo[1,*]

[1] Department of Chemistry, Faculty of Science, Ubon Ratchathani University, Ubon Ratchathani 34190, Thailand
[2] Department of Biological Science, Faculty of Science, Ubon Ratchathani University, Ubon Ratchathani 34190, Thailand
[3] Division of Chemistry, Faculty of Science, Nakhon Phanom University, Nakhon Phanom 48000, Thailand
[4] Department of Chemistry, Faculty of Science, Kasetsart University, Bangkok 10900, Thailand
[5] National Nanotechnology Center, NSTDA, 111 Thailand Science Park, Klong Luang, Pathum Thani 12120, Thailand
[6] Chulabhorn Research Institute, Kamphaeng Phet 6 Road, Laksi, Bangkok 10210, Thailand
[7] Chulabhorn Graduate Institute, Chulabhorn Royal Academy, Bangkok 10210, Thailand
[8] Center of Excellence on Environmental Health and Toxicology (EHT)
[9] Department of Computer Science and Engineering, Toyohashi University of Technology, Tempaku-cho, Toyohashi, Aichi, 441-8580, Japan
[10] School of Cellular and Molecular Medicine, Biomedical Sciences Building, University of Bristol, Bristol, BS8 1TD, United Kingdom
[11] Centre for Computational Chemistry, School of Chemistry, University of Bristol, Bristol, BS8 1TS, United Kingdom

***Email**: pornpan_ubu@yahoo.com

ABSTRACT

Tuberculosis (TB) caused by *M. tuberculosis* remains as a major world health problem due to drug resistance of *M. tuberculosis*. DNA gyrase subunit B (GyrB) has been studied. GyrB is a significant target for *M. tuberculosis* because it is required for DNA replication and transcription. The pyrimido[4,5-b]indol-8-amine derivatives have been reported as GyrB ATPase inhibitors against tuberculosis. In this work, to understand the binging mode, binding interaction and binding energy of compounds, molecular docking calculations were carried out against GyrB. The crucial interactions showed H-bond interactions between pyrimido[4,5-b]indol-8-amine derivatives with Asn52 and Arg141 residues. The hydrophobic interactions between compounds with Val49, Ile84, Val99, Val123, Val125, Ile171 residues were obtained. In addition, the binding affinity increase with pi-cation between pyrimido[4,5-b]indol-8-amine derivatives and Arg82 residue of GyrB pocket. Based on the results, molecular docking calculations of the pyrimido[4,5-b]indol-8-amine derivatives showed crucial interactions between ligands and binding pocket. It may be said that the antitubercular property of the molecule could be via the inhibition of ATPase domain of GyrB enzyme. Therefore, the docking studies of pyrimido[4,5-b]indol-8-amine derivatives are important results for further rational design of novel GyrB inhibitor to combat drug resistant tuberculosis.

This research was supported by the Health Systems Research Institute (HSRI.60.083), Ubon Ratchathani University (DR2564SC01200) and the Excellence for Innovation in Chemistry (PERCH-CIC). Thailand Graduate Institute of Science and Technology (TGIST) Ph.D. Program (SCA-CO-2561-6946TH) to P. Thongdee is appreciated. Faculty of Science, Ubon Ratchathani University, Faculty of Science, Kasetsart University, Faculty of Science, Nakhon Phanom University, School of Chemistry, University of Bristol, and Thailand: National Electronics and Computer Technology (NECTEC) are gratefully acknowledged for supporting this research. We thank EPSRC for funding via BristolBridge (grant number EP/M027546/1) and CCP-BioSim (grant number EP/M022609/1).

PP007

Discovery of novel and potential InhA inhibitors based on virtual screening approaches

Naruedon Phusi[1], Thimpika Pornprom[1], Chayanin Hanwarinroj[1], Chan Inntam[1], Somjintana Taveepanich[1], Jidapa sangswan[2], Sasithorn Lorroengsil[2], Pharit Kamsri[3], Auradee Punkvang[3], Patchreenart Saparpakorn[4], Supa Hannongbua[4], Khomson Suttisintong[5], Prasat Kittakoop[6,7,8], Noriyuki Kurita[9], James Spencer[10], Adrian J. Mulholland[11], and Pornpan Pungpo[1,*]

[1] Department of Chemistry, Faculty of Science, Ubon Ratchathani University, Ubon Ratchathani 34190, Thailand
[2] Department of Biological Science, Faculty of Science, Ubon Ratchathani University, Ubon Ratchathani 34190, Thailand
[3] Division of Chemistry, Faculty of Science, Nakhon Phanom University, Nakhon Phanom 48000, Thailand
[4] Department of Chemistry, Faculty of Science, Kasetsart University, Bangkok 10900, Thailand
[5] National Nanotechnology Center, NSTDA, 111 Thailand Science Park, Klong Luang, Pathum Thani 12120, Thailand
[6] Chulabhorn Research Institute, Kamphaeng Phet 6 Road, Laksi, Bangkok 10210, Thailand
[7] Chulabhorn Graduate Institute, Chulabhorn Royal Academy, Bangkok 10210, Thailand
[8] Center of Excellence on Environmental Health and Toxicology (EHT)
[9] Department of Computer Science and Engineering, Toyohashi University of Technology, Tempaku-cho, Toyohashi, Aichi, 441-8580, Japan
[10] School of Cellular and Molecular Medicine, University of Bristol, Bristol, BS8 1TD, United Kingdom
[11] Centre for Computational Chemistry, School of Chemistry, University of Bristol, Bristol, BS8 1TS, United Kingdom

***Email**: pornpan_ubu@yahoo.com

ABSTRACT

The virtual screening from Specs database was carried out to identify novel 2-*trans* enoyl-acyl carrier protein reductase (InhA) inhibitors as anti-tuberculosis agents. 6 compounds were started from similarity search of cannabigerol (CBG) as potential InhA inhibitor with IC_{50} value of 5.2 μM. 5 compounds passed filtering cutoff with Lipinski's rule of five employed to investigate the binding energy, binding mode, and binding interactions via molecular docking calculations. 3 hit compounds were obtained from the predicted biological activity by way2drug program and anti-bacterial prediction focused on the inhibition of *M. tuberculosis* H37Rv and H37Ra strains. Therefore, the virtual screening provides useful information for rational design new and more potent InhA inhibitors as anti-tuberculosis agents.

This work was supported Thailand Graduate Institute of Science and Technology (TGIST) (SCA-CO-2563-12135-TH) to N. Phusi and the Excellence for Innovation in Chemistry (PERCH-CIC) are appreciated. Faculty of Science, Ubon Ratchathani University, Kasetsart University, Nakhon Phanom University, School of Chemistry, University of Bristol, and Thailand: National Electronics and Computer Technology (NECTEC) are gratefully acknowledged for supporting this research.

PP008

CRISPR-based Detection for Identifying Snake Species from Snakebite Envenoming

Rodjarin Kongkaew*, Kanokpol Aphicho, Surased Suraritdechachai, Maturada Patchsung, and Chayasith Uttamapinant

School of Biomolecular Science and Engineering (BSE), Vidyasirimedhi Institute of Science and Technology (VISTEC), Rayong 21210 Thailand

***Email**: rodjarin.k_s19@vistec.ac.th

ABSTRACT

Snakebite envenoming is a neglected tropical disease which causes broad symptoms ranging from mild to high severity, affecting healthcare management and economy of tropical developing countries including Thailand. Multiple venomous snake species are distributed throughout different regions in Thailand, and it is not trivial to identify snake species upon getting bitten or threated based on old-fashioned means, rendering timely administration of the antivenom difficult or impossible. Here, we propose the development of a point-of-care genotyping tool based on CRISPR for rapid and accurate identification of snake species from bite wounds. DNA regions within the mitochondrial *cytochrome b* (*cytb*) gene of eight venomous snake species endemic to Thailand—*O. hannah*, *N. kaouthia*, *C. rhodostromata*, *D. russelii*, *D. siamensis*, *T. albolabris*, *B. fasciatus*, and *B. candidus*—were chosen as targets for CRISPR-Cas13a-mediated detection, which utilizes recombinase-polymerase amplicification (RPA) and *Leptotrichia wadei* (Lwa) Cas13a for maximal detection sensitivity and specificity. We successfully prepared all biomolecular components necessary for the RPA/LwaCas13-based detection of the *cytb* gene from different snake species, optimized their detection conditions, validated their specificity, and assessed their analytical sensitivity upon detection of surrogate DNA substrates. Detection modules with sufficiently high sensitivity will be used to detect the *cytb* gene from biological fluids obtained from snakes in the near future.

PP010

Global analysis of protein expression of A549 cells after prolonged nicotine exposure by using label-free quantification

Sasikarn Komkleow[1], Churat Weeraphan[2], Daranee Chokchaichamnankit[2], Papada Chaisuriya[2], Chris Verathamjamras[2], Theetat Ruangjaroon[2], Jisnuson Svasti[2,3], Polkit Sangvanich[4], and Chantragan Srisomsap[2,*]

[1] Program in Biotechnology, Faculty of Science, Chulalongkorn University, Bangkok, Thailand
[2] Laboratory of Biochemistry, Chulabhorn Research Institute, Bangkok, Thailand
[3] Applied Biological Sciences Program, Chulabhorn Royal Academy, Bangkok, Thailand
[4] Department of Chemistry, Faculty of Science, Chulalongkorn University, Bangkok, Thailand

***Email**: chantragan@cri.or.th

ABSTRACT

Lung cancer is the leading cause of cancer death worldwide, and cigarette smoke is considered as the most important risk factor for development of lung cancer. Nicotine, an addictive component in cigarettes, is generally considered as non-carcinogenic. However, growing evidence indicates that prolonged nicotine exposure is a potential factor associated with tumorigenesis. Therefore, there is a need to gain insight into the molecular events during prolonged exposure to nicotine. Here, the effect of prolonged nicotine exposure on A549 lung adenocarcinoma cells was investigated, using label-free quantitative proteomic analysis. Selection of invasive subpopulation from A549 cell line was performed to reveal the differential expression and functional annotation of proteins in relation to prolonged nicotine exposure, using Boyden chamber assays in combination with the proteomics approach. One hundred proteins from the NicoA549-L5 subline were identified showing significant change in expression compared to those from A549-L5 subline and their A549 parental cell line. Western blotting was then employed to validate the candidate proteins. The results indicated that prolonged exposure of nicotine promoted invasion on A549 cells. Interestingly, legumain, heat shock protein HSP 90-alpha, heat shock related 70 kDa protein 2, protein disulfide isomerase A3 and profilin-1 were found to show higher expression in A549 cells after prolonged exposure to nicotine. Our findings suggested that these aberrant proteins might serve as novel cancer biomarkers for cigarette smokers.

This research was supported by The 100th Anniversary Chulalongkorn University Fund for Doctoral Scholarship, The 90th Anniversary of Chulalongkorn University Fund (Ratchadaphiseksomphot Endowment Fund) and The Chulabhorn Research Institute (grant no. 302/2131).

PP011

Investigation of malathion sensitivity in *Saccharomyces cerevisiae* lacking the mitophagy receptor Atg32p

Myat Shwe Yee, Thitipa Thosapornvichaia, and Laran T. Jensen*

Department of Biochemistry, Faculty of Science, Mahidol University, Bangkok Thailand

***Email:** laran.jen@mahidol.ac.th

ABSTRACT

Organophosphate (OP) insecticides are widely used in agriculture for controlling insects that can damage crops. Malathion is among the most commonly used of this class. Misapplication and extensive use of insecticides has contributed to the development of OP resistance in insect populations as well as decreasing efficacy of insecticides resulting in crop loss and the spread of insect-borne diseases. In addition, increased insecticide use can lead to environmental contamination and human exposure. However, the limited genetic tools available for insect systems prevents comprehensive screening for mutations or deletions of genes that promote insecticide sensitivity directly. Simple model systems such as the baker's yeast *Saccharomyces cerevisiae* can be utilized to aid in the identification of pathways that lead to insecticide sensitivity. A collection of yeast deletion strains was screened for malathion sensitivity under conditions requiring respiratory growth. This screen identified *ATG32* as being required for malathion tolerance. However, the role of this protein in autophagic processes under other stress conditions has not been previously examined. Using the dual fluorescence Rosella system increased levels of autophagy were observed WT and yeast lacking Atg32p following malathion exposure. In contrast, increased levels of mitophagy were not apparent due to malathion treatment. It appears that malathion sensitivity in yeast lacking Atg32p is not due to disruption in autophagy. Overall, these findings suggest that loss of Atg32p can promote malathion sensitivity. Further characterization of pathways affected in yeast lacking Atg32p may identify molecular targets with utility in the development of agents to sensitize cells to malathion.

PP012

Elucidating the binding mode and binding interactions of 1,2,4-triazole-5-thione derivatives as InhA inhibitor using molecular docking calculations

Thimpika Pornprom[1], Naruedon Phusi[1], Chayanin Hanwarinroj[1], Chan Inntam[1], Somjintana Taveepanich[1], Pharit Kamsri[2], Auradee Punkvang[2], Patchreenart Saparpakorn[3], Supa Hannongbua[3], Khomson Suttisintong[4], Prasat Kittakoop[5,6,7], James Spencer[8], Adrian J. Mulholland[9], and Pornpan Pungpo[1,*]

[1] Department of Chemistry, Faculty of Science, Ubon Ratchathani University, Ubon Ratchathani 34190, Thailand
[2] Division of Chemistry, Faculty of Science, Nakhon Phanom University, Nakhon Phanom 48000, Thailand
[3] Department of Chemistry, Faculty of Science, Kasetsart University, Bangkok 10900, Thailand
[4] National Nanotechnology Center, NSTDA, 111 Thailand Science Park, Klong Luang, Pathum Thani 12120, Thailand
[5] Chulabhorn Research Institute, Kamphaeng Phet 6 Road, Laksi, Bangkok 10210, Thailand
[6] Chulabhorn Graduate Institute, Chulabhorn Royal Academy, Bangkok 10210, Thailand
[7] Center of Excellence on Environmental Health and Toxicology (EHT)
[8] School of Cellular and Molecular Medicine, University of Bristol, Bristol, BS8 1TD, United Kingdom
[9] Centre for Computational Chemistry, School of Chemistry, University of Bristol, Bristol, BS8 1TS, United Kingdom

***Email**: pornpan_ubu@yahoo.com

ABSTRACT

Tuberculosis (TB) is caused by *Mycobacterium tuberculosis* remains a major worldwide public health problem. The enoyl-acyl carrier protein reductase, InhA has been focused on numerous drug discovery efforts as this is the target of the first line prodrug isoniazid. However, resistance to this drug has been becoming more common. Direct InhA inhibitors are remain effective against InhA variants with mutations associated with isoniazid resistance. 1,2,4-triazole-5-thione derivatives were reported as antimycobacterial agents against *Mycobacterium tuberculosis*. 1,2,4-triazole-5-thione derivative was identified as anti-mycobacterial direct InhA inhibitor. In this study, binding mode and binding interactions of 1,2,4-triazole-5-thione derivatives in InhA binding site were evaluated using molecular docking calculations. The results indicating the crucial interactions of 1,2,4-triazole-5-thione derivatives in InhA binding site were found. 1,2,4-triazole-5-thione derivatives formed pi-pi interaction with Phe149. Hydrogen bond interaction was found with Met199. Moreover, hydrophobic interactions were found with Met161, Pro156, Ala198, Val203, Met193, Ala157 Met155, Leu218. Finally, the obtained results from these studies are fruitful to further design the promising InhA inhibitors to overcome tuberculosis drug resistance.

This research was supported by the Health Systems Research Institute (HSRI.60.083), Ubon Ratchathani University (DR2564SC01200) and the Excellence for Innovation in Chemistry (PERCH-CIC). Royal Golden Jubilee (RGJ) Ph.D. Program to T. Pornprom is appreciated. Faculty of Science, Ubon Ratchathani University, Faculty of Science, Kasetsart University, Faculty of Science, Nakhon Phanom University, School of Chemistry, University of Bristol, and Thailand: National Electronics and Computer Technology (NECTEC) are gratefully acknowledged for supporting this research. We thank EPSRC for funding via BristolBridge (grant number EP/M027546/1) and CCP-BioSim (grant number EP/M022609/1).

PP013

Identification of *Pseudomonas pseudomallei* FabI1 inhibitors of antimicrobial agents against melioidosis using virtual screening approaches

Darunee Sukchit[1], Siripen Modmung[1], Sirintip Sangsawang[1], Chayanin Hanwarinroj[1], Bandit Khamsri[1], Somjintana Taweepanich[1], Chan Inntam[1], Jidapa Sangswan[2], Sasithorn Lorroengsil[2], Pharit Kamsri[3], Auradee Punkvang[3], Jiraporn Leanpolchareanchai[4], Narisara Chantratita[5], Warinthorn Chavasiri[6], Khomson Suttisintong[7], Prasat Kittakoop[8,9,10], Noriyuki Kurita [11], Pornpan Pungpo[1]*

[1] Department of Chemistry, Faculty of Science, Ubon Ratchathani University, Ubon Ratchathani 34190, Thailand
[2] Department of Biological Science, Faculty of Science, Ubon Ratchathani University, Ubon Ratchathani 34190, Thailand
[3] Division of Chemistry, Faculty of Science, Nakhon Phanom University, Nakhon Phanom 48000, Thailand
[4] Faculty of Pharmacy, Mahidol University, 10400 Bangkok, Thailand
[5] Department of Microbiology and Immunology, Faculty of Tropical Medicine, Mahidol University, 10400 Bangkok, Thailand
[6] Department of Chemistry, Faculty of Science, Chulalongkorn University, 10330 Bangkok, Thailand
[7] National Nanotechnology Center, NSTDA, 111 Thailand Science Park, Klong Luang, Pathum Thani, Thailand
[8] Chulabhorn Research Institute, Kamphaeng Phet 6 Road, Laksi, Bangkok 10210, Thailand
[9] Chulabhorn Graduate Institute, Chemical Biology Program, Chulabhorn Royal Academy, Kamphaeng Phet 6 Road, Laksi, Bangkok 10210, Thailand
[10] Center of Excellence on Environmental Health and Toxicology (EHT)
[11] Department of Computer Science and Engineering, Toyohashi University of Technology, Toyohashi 441-8580, Japan

***Email**: pornpan_ubu@yahoo.com

ABSTRACT

Melioidosis is a complex disease because of its rapid progression and tendency to generate latent infections. The etiologic agent of melioidosis is the gram-negative organism *Burkholderia pseudomallei*. To identify new and potential melioidosis inhibitors, Zinc database was applied to screen novel melioidosis inhibitor. Then, drug-likeness properties and antibacterial predictions were elucidated. Molecular docking calculations using Glide program were then performed. Based on the obtained results, top three compounds which showed docking score closed to x-ray ligand including **ZINC93953430, ZINC94081106** and **ZINC94708668** were selected. The crucial interactions are hydrogen bond interactions with Gly93 residue and NAD^+ cofactor and hydrophobic interactions with Phe94, Ile100, Ile153, Pro154, Met159, Pro191, Ile192, Ala196, Ala197, Ile200, Phe203 and Ile206 residues were found as crucial interactions. The integrated results provide fruitful information for discovery of melioidosis inhibitor with highly and more potent.

This work was supported Thailand Graduate Institute of Science and Technology (TGIST) (SCA-CO-2563-12097-TH) to D. Sukchit. Faculty of Science, Ubon Ratchathani University, Nakhon Phanom University, and Thailand: National Electronics and Computer Technology (NECTEC) are gratefully acknowledged for supporting this research.

PP014

Discovery of novel main protease inhibitors of SARS-CoV-2 using virtual screening and pharmacokinetic predictions

Siripen Modmung[1], Sirintip Sangsawang[1], Chayanin Hanwarinroj[1], Bandit Khamsri[1], Somjintana Taweepanich[1], Chan Inntam[1], Jidapa Sangswan[2], Sasithorn Lorroengsil[2], Pharit Kamsri[3], Auradee Punkvang[3], Jiraporn Leanpolchareanchai[4], Narisara Chantratita[5], Warinthorn Chavasiri[6], Khomson Suttisintong[7], Prasat Kittakoop[8,9,10], Noriyuki Kurita [11], Pornpan Pungpo[1]*

[1] Department of Chemistry, Faculty of Science, Ubon Ratchathani University, Ubon Ratchathani 34190, Thailand
[2] Department of Biological Science, Faculty of Science, Ubon Ratchathani University, Ubon Ratchathani 34190, Thailand
[3] Division of Chemistry, Faculty of Science, Nakhon Phanom University, Nakhon Phanom 48000, Thailand
[4] Faculty of Pharmacy, Mahidol University, 10400 Bangkok, Thailand
[5] Department of Microbiology and Immunology, Faculty of Tropical Medicine, Mahidol University, 10400 Bangkok, Thailand
[6] Department of Chemistry, Faculty of Science, Chulalongkorn University, 10330 Bangkok, Thailand
[7] National Nanotechnology Center, NSTDA, 111 Thailand Science Park, Klong Luang, Pathum Thani, Thailand
[8] Chulabhorn Research Institute, Kamphaeng Phet 6 Road, Laksi, Bangkok 10210, Thailand
[9] Chulabhorn Graduate Institute, Chemical Biology Program, Chulabhorn Royal Academy, Kamphaeng Phet 6 Road, Laksi, Bangkok 10210, Thailand
[10] Center of Excellence on Environmental Health and Toxicology (EHT)
[11] Department of Computer Science and Engineering, Toyohashi University of Technology, Toyohashi 441-8580, Japan

***Email**: pornpan_ubu@yahoo.com

ABSTRACT

An infectious disease, COVID-19 disease caused by SARS-CoV-2 virus is the major health concerned. The main protease enzyme has been validated as a drug development target to stop SARS-CoV-2. Herein, we attempted to identified new promising main protease inhibitors from Specs commercial database to prepose as novel main protease inhibitors of SAES-CoV-2 Based on virtual screening and pharmacokinetic prediction, three compounds, **AA-504/07472048**, **AK-968/40046672** and **AH-034/04906059** with good binding affinity and pharmacokinetic properties were obtained. Hydrogen bond interactions with Asn142 residue, pi-sigma interactions with Met165 residue and hydrophobic interactions with Met165, Gly143 and Leu27 residues in the SARS-CoV-2 main protease binding site were found as crucial interactions. Based on pharmacokinetic properties predictions, these compounds were suitable to propose for biological assay evaluation and develop as anti-COVID-19 agents.

This research was supported by Ubon Ratchathani University, Nakhon Phanom University, Kasetsart University and National Nanotechnology Center (NANOTEC) are gratefully acknowledged for supporting this research.

PP015

Investigating crucial interactions of the 2-(benzylideneamino)-*N*'-(7-chloroquinolin-4-*yl*)benzohydrazide derivatives and GyrB as potent GyrB inhibitors through molecular docking calculations

Bundit Kamsri[1], Bongkochawan Pakamwong[1], Paptawan Thongdee[1], Naruedon Phusi[1], Kanchiyaphat Ariyachaokun[2], Pharit Kamsri[3], Auradee Punkvang[3], Patchreenart Saparpakorn[4], Supa Hannongbua[4], Khomson Suttisintong[5], Prasat Kittakoop[6,7,8], James Spencer[9], Adrian J. Mulholland[10], Pornpan Pungpo[1,*]

[1] Department of Chemistry, Faculty of Science, Ubon Ratchathani University, Ubon Ratchathani 34190, Thailand
[2] Department of Biological Science, Faculty of Science, Ubon Ratchathani University, Ubon Ratchathani 34190, Thailand
[3] Division of Chemistry, Faculty of Science, Nakhon Phanom University, Nakhon Phanom 48000, Thailand
[4] Department of Chemistry, Faculty of Science, Kasetsart University, Bangkok 10900, Thailand
[5] National Nanotechnology Center, National Science and Technology Development Agency, Pathum Thani 12120, Thailand
[6] Chulabhorn Research Institute, Bangkok 10210, Thailand
[7] Chulabhorn Graduate Institute, Chemical Biology Program, Chulabhorn Royal Academy, Bangkok 10210, Thailand
[8] Center of Excellence on Environmental Health and Toxicology (EHT)
[9] School of Cellular and Molecular Medicine, University of Bristol, Bristol, BS8 1TD, United Kingdom
[10] Centre for Computational Chemistry, School of Chemistry, University of Bristol, Bristol, BS8 1TS, United Kingdom

***Email**: pornpan_ubu@yahoo.com

ABSTRACT

Multi-drug resistant tuberculosis is considered as major bottleneck in the treatment and cure of tuberculosis. So, developing of new tuberculosis drugs to overcome drug resistant have been carried out to develop effective anti-TB drugs. *Mycobacterium tuberculosis* DNA gyrase is a tetrameric A_2B_2 protein. The A subunit (GyrA) carries the breakage-reunion active site, whereas the B subunit (GyrB) promotes ATP hydrolysis. GyrB of DNA gyrase is an attractive target for developing inhibitors against drug resistant tuberculosis. The 2-(benzylideneamino)-*N*′-(7-chloroquinolin-4-*yl*)benzohydrazide derivatives were reported as antimycobacterial activity against *Mycobacterium tuberculosis.* In the present work, the binding mode, binding interactions and binding energy between the 2-(benzylideneamino)-*N*′-(7-chloroquinolin-4-*yl*)benzohydrazide derivatives and GyrB were performed using molecular docking calculations. The crucial interactions showed hydrogen bond interactions via mediated interactions the carbonyl substituent on benzohydrazide with Asp79 residue and nitrogen atom of *N*-benzylidene with Asn52 residue. The 2-(benzylideneamino)-*N*'-(7-chloroquinolin-4-*yl*)benzohydrazide derivatives formed hydrophobic interactions with Ile84, Prp85, Val99, Val123 and Val125 residues. Therefore, our results obtained from this study aid to better understand the crucial binding characteristic of the 2-(benzylideneamino)-*N*′-(7-chloroquinolin-4-*yl*)benzohydrazide derivatives with GyrB are beneficial for rational design of novel GyrB inhibitors as potential anti-tuberculosis agents.

This research was supported by the Health Systems Research Institute (HSRI.60.083), Ubon Ratchathani University (DR2564SC01200) and the Excellence for Innovation in Chemistry (PERCH-CIC). Royal Golden Jubilee (RGJ) Ph.D. Program (PHD/0132/2559) to B. Kamsri are appreciated. Faculty of Science, Ubon Ratchathani University, Faculty of Science, Kasetsart University, Faculty of Science, Nakhon Phanom University, School of Chemistry, University of Bristol, and Thailand: National Electronics and Computer Technology (NECTEC) are gratefully acknowledged for supporting this research. We thank EPSRC for funding via BristolBridge (grant number EP/M027546/1) and CCP-BioSim (grant number EP/M022609/1).

PP016

Investigation of the binding mode and binding interactions of ML300-derivatives as potential anti-SARS-CoV-2 agents through molecular docking calculations

Juthamat Natongho[1], Siripen Modmung[1], Sirintip Sangsawang[1], Bandit Khamsri[1], Somjintana Taweepanich[1], Chan Inntam[1], Jidapa sangswan[2], Sasithorn Lorroengsil[2], Pharit Kamsri[3], Auradee Punkvang[3], Khomson Suttisintong[4], Patchreenart Saparpakorn[5], Supa Hannongbua[5], Prasat Kittakoop[6,7,8], Jiraporn Leanpolchareanchai[9], Noriyuki Kurita[10], James Spencer[11], Adrian J. Mulholland[12], Pornpan Pungpo[1]*

[1] Department of Chemistry, Faculty of Science, Ubon Ratchathani University, Ubon Ratchathani 34190, Thailand
[2] Department of Biological Science, Faculty of Science, Ubon Ratchathani University, Ubon Ratchathani 34190, Thailand
[3] Division of Chemistry, Faculty of Science, Nakhon Phanom University, Nakhon Phanom 48000, Thailand
[4] National Nanotechnology Center, NSTDA, 111 Thailand Science Park, Klong Luang, Pathum Thani 12120, Thailand
[5] Department of Chemistry, Faculty of Science, Kasetsart University, Bangkok, 10900 Thailand
[6] Chulabhorn Research Institute, Kamphaeng Phet 6 Road, Laksi, Bangkok 10210, Thailand
7 Chulabhorn Graduate Institute, Chemical Biology Program, Chulabhorn Royal Academy, Kamphaeng Phet 6 Road, Laksi, Bangkok 10210, Thailand
[8] Center of Excellence on Environmental Health and Toxicology (EHT)
[9] Faculty of Pharmacy, Mahidol University, Bangkok 10400, Thailand
[10]Department of Computer Science and Engineering, Toyohashi University of Technology, Toyohashi 441-8580, Japan
[11]School of Cellular and Molecular Medicine, Biomedical Sciences Building, University of Bristol, Bristol, BS8 1TD, United Kingdom
[12]Centre for Computational Chemistry, School of Chemistry, University of Bristol, Bristol, BS8 1TS, United Kingdom

***Email**: pornpan_ubu@yahoo.com

ABSTRACT

Coronaviruses 19 (COVID-19) are a group of enveloped positive-strand RNA pathogenic viruses that can cause a variety of acute and chronic illnesses, including central nervous system disorders, the common cold, lower respiratory tract infections, and diarrhea. COVID-19 is a serious health risk caused by the severe acute respiratory syndrome coronavirus 2 (SARS-CoV-2). The main protease (M^{pro}) is an enzyme of SARS-CoV-2. The M^{pro} protein of the virus has also been investigated as a development target for inhibiting SARS-CoV-2 virus. Noncovalent inhibitors, ML300 derivatives have been developed against SARS-CoV-2. Herein, we attempted to elucidate ML300-derivatives as novel M^{pro} inhibitors of SARS-CoV-2 based on molecular docking calculations. Hydrogen bond interactions between OH group of all selected compounds with Asn142 and Glu166 residues, pi-sigma interactions between benzene ring with Gln189 residue, and hydrophobic interactions with Met49, Met165 and Pro168 residues in the SARS-CoV-2 M^{pro} binding site were found as crucial interactions. Therefore, the obtained docking results of selected ML300-derivatives are beneficially informative for further rational design of new and potential inhibitors to combat COVID-19.

This research was supported by Faculty of Science, Ubon Ratchathani University, Nakhon Phanom University, Kasetsart University and National Nanotechnology Center (NANOTEC) are gratefully acknowledged for supporting this research.

PP017

Insight into binding mode and crucial interaction of aminopyrimidine derivatives as potential PknB inhibitors using molecular docking calculations

Pongsatorn Wongsri[1], Sirintip Sangsawang[1], Sarannuch Pholangka[1], Siripen Modmung[1], Paptawan Thongdee[1] Chayanin Hanwarinroj[1], Somjintana Taweepanich[1], Chan Inntam[1], Jidapa Sangswan[2], Sasithorn Lorroengsil[2], Pharit Kamsri[3], Auradee Punkvang[3], Patchreenart Saparpakorn[4], Supa Hannongbua[4], Jiraporn Leanpolchareanchai[5], Narisara Chantratita[6], Warinthorn Chavasiri[7], Khomson Suttisintong[8], Prasat Kittakoop[9,10,11], James Spencer[12], Adrian J. Mulholland[13] Noriyuki Kurita[14] and Pornpan Pungpo[1*]

[1] Department of Chemistry, Faculty of Science, Ubon Ratchathani University, Ubon Ratchathani 34190, Thailand
[2] Department of Biological Science, Faculty of Science, Ubon Ratchathani University, Ubon Ratchathani 34190, Thailand
[3] Division of Chemistry, Faculty of Science, Nakhon Phanom University, Nakhon Phanom 48000, Thailand
[4] Department of Chemistry, Faculty of Science, Kasetsart University, Bangkok 10900, Thailand
[5] Faculty of Pharmacy, Mahidol University, 10400 Bangkok, Thailand
[6] Department of Microbiology and Immunology, Faculty of Tropical Medicine, Mahidol University, 10400 Bangkok, Thailand
[7] Department of Chemistry, Faculty of Science, Chulalongkorn University, 10330 Bangkok, Thailand
[8] National Nanotechnology Center, NSTDA, 111 Thailand Science Park, Klong Luang, Pathum Thani, Thailand
[9] Chulabhorn Research Institute, Kamphaeng Phet 6 Road, Laksi, Bangkok 10210, Thailand
[10] Chulabhorn Graduate Institute, Chemical Biology Program, Chulabhorn Royal Academy, Kamphaeng Phet 6 Road, Laksi, Bangkok 10210, Thailand
[11] Center of Excellence on Environmental Health and Toxicology (EHT)
[12] School of Cellular and Molecular Medicine, University of Bristol, Bristol, BS8 1TD, United Kingdom
[13] Centre for Computational Chemistry, School of Chemistry, University of Bristol, Bristol, BS8 1TS, United Kingdom
[14] Department of Computer Science and Engineering, Toyohashi University of Technology, Toyohashi 441-8580, Japan

***Email**: pornpan_ubu@yahoo.com

ABSTRACT

Tuberculosis caused by *mycobacterium tuberculosis* is major global public health concern. Protein serine/threonine kinase B or PknB is an attractive drug development target because of its central importance in several critical signaling cascades. Here, molecular docking calculations were applied to investigate the binding mode and crucial interactions of aminopyrimidine derivatives as anti-tuberculosis agents. The obtained result indicated that crucial interactions are including, hydrogen bond interaction with Val95 residue, pi-sigma interactions with Met145 and Met155 residues. Hydrophobic interactions with Leu17, Phe19, Ser23, Val25, Ala38, Val72, Met92 and Ala142. Based on the obtained results, it could be fruitful guideline for rational design of novel PknB inhibitor as anti-tuberculosis agents.

This research was supported by Ubon Ratchathani University, Nakhon Phanom University and Kasetsart University. National Electronics and Computer Technology Center (NECTEC) is gratefully acknowledged for supporting this research.

PP018

Insight into binding mode and crucial interaction of tetrahydropyran derivatives as potential InhA inhibitors using molecular docking calculations

Sarannuch Pholangka[1], Naruedon Phusi[1], Chayanin Hanwarinroj[1], Chan Inntam[1], Somjintana Taveepanich[1], Pharit Kamsri[2], Auradee Punkvang[2], Patchreenart Saparpakorn[3], Supa Hannongbua[3], Khomson Suttisintong[4], Jiraporn Leanpolchareanchai[5], Prasat Kittakoop[6,7,8], James Spencer[9], Adrian J. Mulholland[10], Noriyuki Kurita[11] and Pornpan Pungpo[1,*]

[1] Department of Chemistry, Faculty of Science, Ubon Ratchathani University, Ubon Ratchathani 34190, Thailand
[2] Division of Chemistry, Faculty of Science, Nakhon Phanom University, Nakhon Phanom 48000, Thailand
[3] Department of Chemistry, Faculty of Science, Kasetsart University, Bangkok 10900, Thailand
[4] National Nanotechnology Center, NSTDA, 111 Thailand Science Park, Klong Luang, Pathum Thani 12120, Thailand
[5] Faculty of Pharmacy, Mahidol University, 10400 Bangkok, Thailand
[6] Chulabhorn Research Institute, Kamphaeng Phet 6 Road, Laksi, Bangkok 10210, Thailand
[7] Chulabhorn Graduate Institute, Chulabhorn Royal Academy, Bangkok 10210, Thailand
[8] Center of Excellence on Environmental Health and Toxicology (EHT)
[9] School of Cellular and Molecular Medicine, University of Bristol, Bristol, BS8 1TD, United Kingdom
[10] Centre for Computational Chemistry, School of Chemistry, University of Bristol, Bristol, BS8 1TS, United Kingdom
[11] Department of Computer Science and Engineering, Toyohashi University of Technology, Toyohashi 441-8580, Japan

***Email**: pornpan_ubu@yahoo.com

ABSTRACT

Tuberculosis (TB) remains a major global health problem, caused by *Mycobacterium tuberculosis* (*M. tuberculosis*). Enoyl-ACP reductase or InhA is an attractive target responsible for mycolic acid synthesis by preventing the fatty acid biosynthesis pathway. Tetrahydropyran derivatives were selected to study because it is a classical substructure for glycomimetics inhibition of proteins and exhibits good InhA inhibitory potency withmoderate antimycobacterial activity. In this work, molecular docking calculations were applied to investigate binding mode and crucial interactions of tetrahydropyran derivatives using Glide program. The obtained results indicated that hydrogen bond interaction between oxygen atom of tetrahydro-2H-pyran ring with Gln100 residue, pi-sigma interactions with between aromatic ring of ligand with Tyr 158 residue and hydrophobic interactions with Phe97, Met103, Ala201, Leu207 and Ile215 residues were found as crucial interaction in InhA binding pocket. These results provide beneficial guideline to rational design new and effective inhibitor against *M. tuberculosis.*

This research was supported by Ubon Ratchathani University, Nakhon Phanom University and Kasetsart University. School of Chemistry, University of Bristol, and Thailand: National Electronics and Computer Technology (NECTEC) are gratefully acknowledged for supporting this research. We thank EPSRC for funding via BristolBridge (grant number EP/M027546/1) and CCP-BioSim (grant number EP/M022609/1).

PP019

Identification of novel JAK2 inhibitors as erythropoiesis stimulant agents for thalassemia therapy

Sirintip Sangsawang[1], Siripen Modmung[1], Bandit Khamsri[1], Somjintana Taweepanich[1], Chan Inntam[1], Jidapa Sangswan[2], Pharit Kamsri[3], Auradee Punkvang[3], Khomson Suttisintong[4], Kanjana Pangjit[5], Noriyuki Kurita[6] and Pornpan Pungpo[1]*

[1] Department of Chemistry, Faculty of Science, Ubon Ratchathani University, Ubon Ratchathani 34190, Thailand
[2] Department of Biological Science, Faculty of Science, Ubon Ratchathani University, Ubon Ratchathani 34190, Thailand
[3] Division of Chemistry, Faculty of Science, Nakhon Phanom University, Nakhon Phanom 48000, Thailand
[4] National Nanotechnology Center, NSTDA, 111 Thailand Science Park, Klong Luang, Pathum Thani, Thailand
[5] College of Medicine and Public Health, Ubon Ratchathani University, Warin Chamrap, Ubon Ratchathani, 34190, Thailand
[6] Department of Computer Science and Engineering, Toyohashi University of Technology, Toyohashi 441-8580, Japan

***Email**: pornpan_ubu@yahoo.com

ABSTRACT

Janus kinase 2 (JAK2) is an enzyme responsible for regulating erythropoiesis. associated with the ineffective erythropoiesis process. This is currently a key target for developing inhibitors in the new pathway therapeutic option for thalassemia. Herein, we applied the computer aided molecular design to identify novel JAK2 inhibitors for erythropoiesis stimulating agent (ESA) from Specs database. Based on multistage virtual screening process, seventy-six compounds were predicted to be active against both JAK2 and ESA. Based on pharmacokinetic properties prediction, two promising compounds, **AN-979/41713534** and **AN-648/15101115** were obtained. In addition, the binding mode and binding interactions in the ATP binding site of JAK2 were investigated. The obtained results revealed that the hydrogen bond interactions with Leu932 backbone in the ATP binding site of JAK2 are key interaction for binding of new finding compounds. The Caco2 permeability of these two compounds was high. The BBB and CNS permeability values suggested that the selected compounds were poorly distributed to the brain and unable to penetrate the CNS. Therefore, the finding compounds were proposed as novel and potential JAK2 inhibitors as ESA for thalassemia therapy.

This research was supported by National Science, Research and Innovation Fund (NSRF), Ubon Ratchathani University and Nakhon Phanom University. National Electronics and Computer Technology Center (NECTEC) is gratefully acknowledged for supporting this research.

PP020

In-house production of brain-derived neurotrophic factor (BDNF) for differentiation of SH-SY5Y cells into matured neurons

Chonticha Saisawang[1,*], Suphansa Prewkiew[1], Chutikorn Nopparat[1], Piyarat Govitrapong[1,2]

[1] Institute of Molecular Biosciences, Mahidol University, Nakhon Pathom 73170, Thailand
[2] Chulabhorn Graduate Institute, Chulabhorn Royal Academy, 54 Kamphaeng Phet 6 Road Lak Si, Bangkok 10210, Thailand

***Email**: chonticha.sai@mahidol.ac.th

ABSTRACT

The SH-SY5Y neuroblastoma cell line is extensively used in neuroscience research. This cell expresses tyrosine hydroxylase and dopamine-β-hydroxylase, as well as the dopamine transporter. These proteins are important markers in the dopamine synthesis pathway. Although the cells possess the dopaminergic neuron characteristics, they can be differentiated into a more functionally mature neuronal phenotype. The differentiated cells become flat with neurites that produce longer projections connecting to neighboring cells. These neurite outgrowths display a morphological similarity to mature neurons in the human brain. A number of protocols have been used to differentiate SH-SY5Y cells to a terminally mature neuron-like phenotype. Different protocols induce different neuronal phenotypes with different biochemical properties. In our laboratory, the sequential differentiation of cells is routinely performed with retinoic acid (RA) and then brain-derived neurotrophic factor (BDNF).

For our research interest on Parkinson's disease (PD), the differentiated cells are a very good model. Once cells are differentiated, BDNF must be maintained in all media. As the commercially available BDNF can be a continuous expense we have produced a more economical alternative by cloning, expressing and purifying a recombinant BDNF protein in our laboratory and then comparing it to commercially available protein.

This research was supported by National Research Council of Thailand (NRCT) and Mahidol University (NRCT5-TRG63009-06)

PP021

Sensor for direct detection of *Vibrio cholerae* in frozen seafood

Panwadee Wattanasin[1,*], Suticha Chunta[2], Phanthipha Runsaeng[3], Proespichaya Kanatharana[1], and Panote Thavarangkul[1]

[1] Division of Physical Science, Faculty of Science, Prince of Songkla University, Songkla 90110, Thailand
[2] Department of Department of Clinical Chemistry, Faculty of Medical Technology, Prince of Songkla University, Songkla, 90110, Thailand
[3] Division of Health and Applied Sciences, Faculty of Science, Prince of Songkla University, Songkla 90110, Thailand

***Email**: Panwadee.toy@gmail.com

ABSTRACT

This work was developed a new sensor for Vibrio cholerae based on molecularly imprinting technique coupled with quartz crystal microbalance (QCM). A film of molecularly imprinted polymers (MIPs) coated on quartz was carried out for direct detection. Firstly, V. cholerae O1 was used as a template for imprinting on polyacrylamide (PAA) and washed with 10% acetic acid in 0.1% SDS solution. The characterization of MIP's *V. cholerae O1* was studied by using SEM. Under the optimum of developed method, a good linearity was obtained in the concentration of 1.0 x 103 to 1.0 x 108 CFU/mL with the limit detection of 1.5 x 10^2 CFU/mL. The developed method provided good reproducibility (%RSD < 7) and high selectivity, can be applied in seafood. The method accuracy was evaluated using recovery measurements in standard spiked samples and good recoveries of 84.0–114.3% with relative standard deviations of less than 10% have been achieved

PP022

Investigation of the mechanism of anoikis resistance involving protein X in thyroid carcinoma cells

Phichamon Phetchahwang[1,*], Kittirat Saharat[1], Kriengsak Lirdprapamongkol[1], Jisnuson Svasti[1,2], and N. Monique Paricharttanakul[1]

[1] Laboratory of Biochemistry, Chulabhorn Research Institute, Bangkok 10210, Thailand
[2] Applied Biological Sciences Program, Chulabhorn Graduate Institute, Bangkok 10210, Thailand

***Email**: phichamon@cri.or.th

ABSTRACT

Anoikis resistance is an important characteristic of metastatic tumor cells, thus impairing anoikis resistance can be a promising strategy for the therapy of metastatic cancers. Previously, we have identified protein X to be important in anoikis resistance of thyroid cancer cells. Remarkably, protein X does not trigger anoikis resistance via epithelial mesenchymal transition (EMT) or integrin switch. In other words, there should be an alternative mechanism of anoikis resistance in thyroid cancer cells involving protein X, which may be through receptors A and/or B. In this study, we investigated the underlying molecular mechanism involving protein X using follicular-type (FTC133) and the highly metastatic anaplastic-type (ARO) thyroid carcinoma cells. siRNA knockdown of protein X was used to study the mechanism of anoikis resistance. Anoikis resistance of these cell lines was determined using flow cytometry and the expression of receptors A and B was determined using Western blot and flow cytometry. The percentage of dead floating cells or anoikis increased in protein X-knockdown cells of both cell lines when compared to that of si-Control cells. The expression of receptors A and B was significantly increased in knockdown ARO cells but not in knockdown FTC133 cells. In summary, protein X induces anoikis resistance in highly metastatic anaplastic-type thyroid cancer cells via the reduction in the expression of receptors A and B, consequently promoting thyroid cancer metastasis. Further studies to identify protein X inhibitor(s) will help to treat thyroid cancer metastasis, therefore reducing the mortality of thyroid cancer patients.

This research was supported by the Thailand Science Research and Innovation and the Chulabhorn Research Institute (grant no. 313/2230).

PP023

Vanillin induces apoptosis in floating colorectal cancer cells under a metastasis-associated condition

Runtikan Pochairach[1], Kriengsak Lirdprapamongkol[1,2,*], Thiwaree Sornprachum[1], Papada Chaisuriya[1], Siriporn Keeratichamroen[1], and Jisnuson Svasti[1]

[1] Laboratory of Biochemistry, Chulabhorn Research Institute, Bangkok, Thailand
[2] Center of Excellence on Environmental Health and Toxicology (EHT), Ministry of Education, Bangkok, Thailand

[*]**Email**: kriengsak@cri.or.th

ABSTRACT

Drug resistance is considered as a major cause of treatment failure in 90% of cancer patients with metastatic stage. Metastatic cancer can be studied in vitro by means of non-adherent cell culture. Our previous study suggested that under non-adherent culture conditions, SW480 human colorectal cancer cells naturally developed drug resistance as a result of slow growth rate and cell cycle progression delay. Therefore, finding new compounds that are safe and effectively kill cancer cells, especially metastasizing cancer cells, is an important research topic nowadays. Vanillin is indicated as safe and used as flavoring agent in a variety of food products. Moreover, vanillin has been reported for its potent antioxidant, anti-inflammatory, and anticancer activities. In the present study, we examined the anticancer effect of vanillin on SW480 cells. The cells were cultivated as attached cells by standard monolayer culture to mimic primary cancer, or cultivated under non-adherent culture condition to obtain floating cells which represented metastasizing cancer cells when floating in blood or lymphatic circulation. Treatment of SW480 cells with vanillin led to a dose-dependent decrease in survival rate of both attached and floating cells. In addition, apoptosis analysis showed that vanillin also increased apoptotic rate in both attached and floating cells, in a dose-dependent manner. Interestingly, cytotoxicity of vanillin was stronger in floating cancer cells compared with attached cells. In conclusion, SW480 floating cells under non-adherent conditions were more susceptible to cytotoxicity of vanillin. The mechanism of action of vanillin is under investigation. Our results suggest that vanillin might be an effective anticancer agent for metastatic colorectal cancer treatment.

This research was supported by the Thailand Science Research and Innovation, the Chulabhorn Research Institute (grant no. 302/2205), and the Center of Excellence on Environmental Health and Toxicology (EHT).

PP024

Short-term exposure to a chemotherapeutic drug oxaliplatin increases metastatic potential of well-differentiated hepatocellular carcinoma cells

Naphaphon Iawsipo[1], Kriengsak Lirdprapamonhkol[1,2,*], Thiwaree Sornprachum[1], Papada Chaisuriya[1], Lukana Ngiwsara[1], and Jisnuson Svasti[1]

[1] Laboratory of Biochemistry, Chulabhorn Research Institute, Bangkok, Thailand
[2] Center of Excellence on Environmental Health and Toxicology (EHT), Ministry of Education, Bangkok, Thailand

***Email**: kriengsak@cri.ac.th

ABSTRACT

Hepatocellular carcinoma (HCC) ranks on top of the high mortality cancer types. Chemotherapeutic agents are utilized as common way to cure cancer patients. Nevertheless, numerous evidences demonstrate a new adverse effect of chemotherapeutic drugs contributing to treatment failure by acceleration of invasion and metastasis. Here, we investigated the influence of a short-term treatment (24 h) of chemotherapeutic drug oxaliplatin on invasion process, a critical step of metastasis, in a HCC cell line, HepG2. First of all, cytotoxicity of oxaliplatin on HepG2 cells was determined by MTT assay. A selected sub-lethal concentration (1 μM) was used to explore impact of the drug on cancer cell invasion, using Transwell assay. Oxaliplatin treatment significantly increased invasion rate of HepG2 cells, compared with untreated group. Invasion process involves cell migration and extracellular matrix (ECM)-remodeling enzymes. Oxaliplatin treatment also elevated migration rate of HepG2 cells, determined by Transwell assay. Matrix metalloproteinase-2 (MMP-2) is an ECM-remodeling enzyme that plays a role in cancer cell invasion of several cancer types. Gelatin zymography demonstrated the significant increase in level and activity of MMP-2 secreted by HepG2 cells after oxaliplatin treatment, compared with untreated group. In conclusion, the invasion-promoting effect of oxaliplatin could be observed in HepG2 cells after short-term exposure to the drug, and the underlying mechanism of this effect is the enhancement of cell migration capacity and MMP-2 production induced by oxaliplatin. This study might lead to improve the chemotherapeutic strategies and treatment outcome.

This research was supported by the Thailand Science Research and Innovation, the Chulabhorn Research Institute (grant no. 302/2128), and the Center of Excellence on Environmental Health and Toxicology (EHT).

PP0025

Molecular docking study of benzosuberone-thiazole derivatives for rational design of novel GyrB inhibitors as anti-tuberculosis agents

Bongkochawan Pakamwong[1], Bundit Kamsri[1], Paptawan Thongdee[1], Naruedon Phusi[1], Somjintana Taveepanich[1], Jidapa sangswan[2], Pharit Kamsri[3], Auradee Punkvang[3], Patchreenart Saparpakorn[4], Supa Hannongbua[4], Jiraporn Leanpolchareanchai[5], Khomson Suttisintong[6], Prasat Kittakoop[7,8,9], James Spencer[10], Adrian J. Mulholland[11], Pornpan Pungpo[1,*]

[1] Department of Chemistry, Faculty of Science, Ubon Ratchathani University, Ubon Ratchathani 34190, Thailand
[2] Department of Biological Science, Faculty of Science, Ubon Ratchathani University, Ubon Ratchathani 34190, Thailand
[3] Division of Chemistry, Faculty of Science, Nakhon Phanom University, Nakhon Phanom 48000, Thailand
[4] Department of Chemistry, Faculty of Science, Kasetsart University, Bangkok 10900, Thailand
[5] Department of Pharmacy, Faculty of Pharmacy, Mahidol University, Bangkok 10400, Thailand
[6] National Nanotechnology Center, National Science and Technology Development Agency, Pathum Thani 12120, Thailand
[7] Chulabhorn Research Institute, Bangkok 10210, Thailand
[8] Chulabhorn Graduate Institute, Chemical Biology Program, Chulabhorn Royal Academy, Bangkok 10210, Thailand
[9] Center of Excellence on Environmental Health and Toxicology (EHT)
[10] School of Cellular and Molecular Medicine, University of Bristol, Bristol, BS8 1TD, United Kingdom
[11] Centre for Computational Chemistry, School of Chemistry, University of Bristol, Bristol, BS8 1TS, United Kingdom

***Email**: pornpan_ubu@yahoo.com

ABSTRACT

Tuberculosis (TB) is an infectious disease caused by *Mycobacterium tuberculosis* (MTB). DNA Gyrase is attractive target for antibacterial which is an essential enzyme that has roles in the fundamental biological processes of replication, transcription and recombination. Mutations of DNA gyrase affected to fluoroquinolone drug resistance are the main problem of treating tuberculosis. Therefore, discover of new potential DNA gyrase inhibitors are urgent to overcome this drug resistant problem. Benzosuberone-thiazole moieties were reported for their antibacterial activity against *Mycobacterium tuberculosis* and ATPase activity. In this work, we are objective to evaluate binding mode, binding interaction and binding energy using molecular docking calculations. The result revealed the hydrogen bond interactions of compound 22 and 27 with Arg82 residue in the GyrB pocket. Another hydrogen bond interaction was found to bind between the sulfur atom of thiazole moiety of compound 22 with Arg141 residue of the GyrB active site. The hydrophobic interaction between compound with Val49, Ile84, Pro85, Val99, Val123, Val125 and Ile171 residues were found. Glide docking score was -4.583 for compound 22 and -3.374 for compound 27. In addition, compound 22 has two hydrogen bond interactions to correlate with low Glide docking score. Therefore, the results obtained from this work provide better understanding crucial interactions of benzosuberone-thiazole derivatives with GyrB pocket for rational design new and more potent ATPase inhibitors as novel anti-tuberculosis agents.
This research was supported by the Health Systems Research Institute (HSRI.60.083), Ubon Ratchathani University (DR2564SC01200) and the Excellence for Innovation in Chemistry (PERCH-CIC). Royal Golden Jubilee (RGJ) Ph.D. Program (PHD/0155/2560) to B. Pakamwong is gratefully appreciated. Faculty of Science, Ubon Ratchathani University, Faculty of Science, Kasetsart University, Faculty of Science, Nakhon Phanom University, School of Chemistry, University of Bristol, and Thailand: National Electronics and Computer Technology (NECTEC) are gratefully acknowledged for supporting this research. We thank EPSRC for funding via BristolBridge (grant number EP/M027546/1) and CCP-BioSim (grant number EP/M022609/1).

PP026

Polymer-lipid hybrid nanoparticles improve drug-resistant lung cancer treatment

Sasivimon Pramual[1,*], Kriengsak Lirdprapamongkol[1], Thiwaree Sornprachum[1], Papada Chaisuriya[1], Lukana Ngiwsara[1], Nuttawee Niamsiri[2], Jisnuson Svasti[1]

[1] Laboratory of Biochemistry, Chulabhorn Research Institute, Bangkok 10210, Thailand
[2] Department of Biotechnology, Faculty of Science, Mahidol University, Bangkok 10400, Thailand

***Email**: sasivimon@cri.or.th

ABSTRACT

The purpose of this study was to develop polymer-lipid hybrid nanoparticles for delivery of anticancer drug, paclitaxel (PTX) to overcome multidrug resistance (MDR) of human lung cancer cells. The PTX-loaded polymer-lipid hybrid nanoparticles were prepared through modified nanoprecipitation. Nanoparticles are composed of a biodegradable poly(D,L-lactide-co-glycolide) (PLGA) as polymeric core encapsulating PTX, wrapped with a mixture of lecithin and PEGylated phospholipids as lipid shell. The resulting nanoparticles had an average particle size of 103.0 ± 1.6 nm, the zeta potential value of -52.9 mV with monodisperse distributions. Nanoparticles were further evaluated for the *in vitro* cytotoxicity against two MDR models with different resistant mechanisms originated from the same cell line A549. An MDR cell line, A549RT-eto with overexpression of drug transporter P-glycoprotein, was used as a drug-selected MDR cells model. A model of metastasis-associated MDR cells (A549 floating cells) was obtained by culturing A549 cells under a metastasis-mimic condition to induce acquisition of MDR phenotype without experience of drug exposure. Comparisons were made with A549 cells. Nanoparticles presented superior cytotoxicity by increases PTX potency as indicated by the decrease in IC_{50} values compared to non-encapsulated PTX. The IC_{50} values were decreased by 49-fold and 10-fold in A549 and A549RT-eto cells treated with nanoparticles, respectively. The IC_{50} values of A549 attached and A549 floating cells treated with nanoparticles were decreased by 43-fold and 256-fold, respectively. These findings indicated that the PTX-loaded polymer-lipid hybrid nanoparticles provide a promising delivery system for treatment of drug resistant lung cancer.

This research was supported by the Thailand Science Research and Innovation and the Chulabhorn Research Institute (grant no. 302/2128).

PP027

Characterization and quantitative proteomics of mammospheres-forming cells of triple negative breast cancer

Lalita Lumkul[1], **Photsathorn Mutapat[1]**, Chris Verathamjamras[1], Amnart Khongmanee[2], Jisnuson Svasti[1,3], Voraratt Champattanachai[1,3,*]

[1] Laboratory of Biochemistry, Chulabhorn Research Institute, Bangkok 10210 Thailand
[2] Translational Research Unit, Chulabhorn Research Institute, Bangkok 10210 Thailand
[3] Applied Biological Science, Chulabhorn Graduate Institute Chulabhorn Royal Academy, Bangkok 10210 Thailand

***Email**: voraratt@cri.or.th

ABSTRACT

Breast cancer is a leading cause of death in women worldwide. Although several therapeutic approaches are combined to successfully cure this disease, some cancer cells can escape and are recurrent, especially in triple negative breast cancer (TNBC). Several lines of evidence suggest that cancer cells which possess stemness-related characters are contributed to drug resistance thereby leading to cancer relapse. Thus, this study aims to establish breast cancer cell – derived mammospheres to investigate its stemness properties and identify key protein changes using a label-free proteomics approach. In this study, mammospheres formation was assay using a TNBC cell line, MDA-MB231. MDA-mammospheres showed upregulated stemness-related genes. Moreover, these mammospheres demonstrated a significant resistance to paclitaxel, a first-line chemotherapy medication for patients with TNBC, compared to that of their parental cells, MDA-MB231. Therefore, protein identification and quantification were performed using a nano-LC coupled with Orbitrap mass spectrometer (LC-MS/MS) and label-free quantitative analysis (Progenesis QI), respectively. Then, almost 200 proteins were identified and compared. With a cut-off value of > 1.5 fold change, there were 37 and 10 proteins that up-regulated and down-regulated in MDA-mammosphers, respectively. Furthermore, the levels of some selected proteins were confirmed by westernblotting. Lastly, all altered proteins were subjected to protein-protein interaction network analysis by STRING database. Several altered proteins expressed in mammospheres were categorized into many biological processes including regulation of cell death, cell activation involved in immune responses, and cytoskeletal reorganization. Collectively, these proteins and predicted molecular pathways enlighten potential markers and therapeutic targets within stemness-possessed breast cancer mammospheres.

This study was supported by the Chulabhorn Research Institute (Grant no. 302-2098).

PP0028

Host-derived cell-wall-binding domain of phage endolysin CD16/50L anchors to the surface polysaccharide of *Clostridioides difficile* to preserve neighboring host cells and ensure progeny expansion

Wichuda Phothichaisri,[1] Jirayu Nuadthaisong,[1] Tanaporn Phetreun,[1] Tavan Janvilisri,[1] Robert Fagan,[2] Surang Chankhamhaengdecha,[3] Sittinan Chanarat [1,4,*]

[1] Department of Biochemistry, Faculty of Science, Mahidol University, Bangkok, Thailand
[2] Department of Molecular Biology and Biotechnology, Florey Institute, University of Sheffield, Sheffield, S10 2TN, UK
[3] Department of Biology, Faculty of Science, Mahidol University, Bangkok, Thailand
[4] Laboratory of Molecular Cell Biology, Center for Excellence in Protein and Enzyme Technology, Faculty of Science, Mahidol University, Bangkok, Thailand

*Email: sittinan.cha@mahidol.edu

ABSTRACT

Endolysin is a phage-encoded cell-wall hydrolase which degrades the peptidoglycan layer of the bacterial cell wall. The enzyme is often expressed at the late stage of the phage lytic cycle and is required for progeny escape. Endolysin of bacteriophage that infects Gram-positive bacteria often comprises two domains: a peptidoglycan hydrolase and a cell-wall binding domain (CBD). Although the catalytic domain of endolysin is relatively well-studied, the precise role of CBD is largely unknown and remains controversial. For example, while certain endolysins absolutely require CBD for their lytic activity, others do not need it at all, raising the question of its necessity. Here, we focus on the function of CBD of endolysin encoded in the genome of recently isolated *Clostridioides difficile* phages. We found that CBD of this endolysin is not required for the lytic activity, which is strongly prevented by the surface layer of *C. difficile*. Intriguingly, hidden Markov model (HMM) analysis suggested that the endolysin CBD is likely derived from the cell-wall-binding-2 domain of host's cell-wall proteins but possesses a higher binding affinity to polysaccharide components of bacterial cell wall. Moreover, the CBD is able to form a homodimer, formation of which is necessary for interaction with the peptidoglycan layer. Importantly, endolysin diffusion and sequential cytolytic assays showed that CBD of endolysin is required for anchoring to cell-wall remnants, suggesting its physiological roles in controlling diffusion of the enzyme, preserving neighboring host cells, and thereby enabling phage progeny to initiate new rounds of infection. Taken together, this study provides an insight into regulation of endolysin through CBD and can potentially be applied for endolysin treatment against *C. difficile* infection.

Acknowledgement
This research was supported by Science Achievement Scholarship of Thailand (SAST).

PP029

Understanding the binding mode and binding interactions of novel main protease pyridyl ester derivatives with SARS-CoV-2 using molecular docking calculations

Panadda Srikaew[1], Sirintip Sangsawang[1], Bandit Khamsri[1], Somjintana Taweepanich[1], Chan Inntam[1], Pharit Kamsri[2], Auradee Punkvang[2], Khomson Suttisintong[3], Patchreenart Saparpakorn[4], Supa Hannongbua[4], Pornpan Pungpo[1]*

[1] Department of Chemistry, Faculty of Science, Ubon Ratchathani University, Ubon Ratchathani 34190, Thailand
[2] Division of Chemistry, Faculty of Science, Nakhon Phanom University, Nakhon Phanom 48000, Thailand
[3] National Nanotechnology Center, NSTDA, 111 Thailand Science Park, Klong Luang, Pathum Thani, Thailand
[4] Department of Chemistry, Faculty of Science, Kasetsart University, Bangkok, 10900 Thailand

***Email**: pornpan_ubu@yahoo.com

ABSTRACT

Currently, the infectious disease, COVID-19 disease caused by SARS-CoV-2 virus is spreading over a large number. Resulting in major health problems main protease enzymes (M^{pro})have been investigated as a prime drug development target to inhibit SARS-CoV-2 virus. In this study, pyridyl ester derivatives were selected to investigate the binding mode and crucial interactions in M^{pro} binding site due to the inhibitors are equipped with the unique azanitrile warhead exhibited concomitant inhibition of M^{pro} and cathepsin L, a protease relevant for viral cell entry. Glide program was appled to understand the binding mode and binding interactions of pyridyl ester derivatives. The obtained results showed that hydrogen bond interactions were found between carbonyl group of the ligands with Glu166and Cys145 residues. Moreover, hydrophobic interactions with Phe140, Leu141, Met49 and Met165, residues in the SARS-CoV-2 main protease binding site were found as crucial interactions. These results provide fruitful information for further design of pyridyl ester derivatives as SARS-CoV-2 main protease agent.

This research was supported by Faculty of Science, Ubon Ratchathani University, Nakhon Phanom University, Kasetsart University and National Nanotechnology Center (NANOTEC) are gratefully acknowledged for supporting this research.

PP030

The major peanut (*Arachis hypogaea*) allergens potentially contain antibacterial and antiviral peptides: an *in silico* study

Wren Leanro I. Aguila[1], **Roseanne Mae P. Ortilano[1]**, Alfonso Beato T. Revilla[1], and Nedrick T. Distor[1,2,*]

[1] Department of Biochemistry, College of Allied Sciences, De La Salle Medical and Health Sciences Institute, Dasmariñas City 4114, Cavite, Philippines
[2] Current Affiliation: Department of Biology and Biochemistry, College of Natural Sciences and Mathematics, University of Houston, Texas, USA

***Email:** nedrickdistor@gmail.com

ABSTRACT

One of the problems in biomedical science is the emergence of antibiotic resistance among pathogenic microorganisms. This led to the exploration of potential alternative agents to combat this global concern. Bioactive peptides became interesting molecules to study against microorganisms due to its unique microbicidal mechanisms. In this study, the peanut (*Arachis hypogaea*) major allergens (Ara h 1 or A1, Ara h 2 or A2, and Ara h 3 or A3) were enzymatically hydrolyzed *in silico* to generate potential bioactive peptides, which were then screened for their antibacterial and antiviral probabilities using various computational tools. The determined probabilities were correlated with their hydropathicity index (GRAVY) using Spearman's correlation. Sequentially, the residue-level interactions between the peptide and chosen proteins were visualized through molecular docking. Screening showed that the percentages of potential antibacterial and antiviral peptides using iAMPpred were higher than those screened using MLAMP and Meta-iAVP. Analysis revealed that positive monotonic correlations predominated between GRAVY values and bioactive probabilities obtained. Negligible correlations were obtained for antibacterial probabilities of the peptides derived from A1 and A3 using iAMPpred and antiviral probabilities of peptides from A1 and A3 using MetaiAVP and iAMPpred respectively. The antibacterial ^{393}NAHTIVVA^{400} peptide (prob=0.92, GRAVY=1.138) and antiviral ^{64}QCAGVA^{69} peptide (prob=1.00, GRAVY=1.067), both derived from A3, showed docking-based hydrophobic interactions with the *S. aureus* membrane enzyme and dengue virus-1 envelope protein respectively. These hydrophobic interactions were consistent with the correlated hydrophobicity of the bioactive peptides. Further work should focus on determining the *in vitro* antibacterial and antiviral activities of these peptides.

PP0031

Analysis of NaOCl-sensing transcriptional repressor NieR in *Agrobacterium tumefaciens* C58

Benya Nontaleerak[1], Jintana Duang-nkern[1], Tham Udomkanarat[2], Kritsakorn Saninjuk[1], Rojana Sukchawalit[1,3,4,*], and SkornMongkolsuk[1,4]

[1] Laboratory of Biotechnology, Chulabhorn Research Institute, Bangkok 10210, Thailand
[2] Environmental Toxicology Program, Chulabhorn Graduate Institute, Bangkok, 10210, Thailand
[3] Applied Biological Sciences Program, Chulabhorn Graduate Institute, Bangkok 10210, Thailand
[4] Center of Excellence on Environmental Health and Toxicology (EHT), Ministry of Education, Bangkok, Thailand

***Email**: rojana@cri.or.th

ABSTRACT

Hypochlorous acid (HOCl) is naturally produced by neutrophils in the innate immune system and is commonly used as the active ingredient of household bleach (sodium hypochlorite) for disinfection of various microorganisms. *Agrobacterium tumefaciens* C58, a plant pathogen causing crown gall disease, was used as a model to study the hypochlorite stress response in bacteria. In this study, a NaOCl-sensing transcriptional regulator (NieR) and its target genes were identified. *A. tumefaciens* NieR belonging to TetR family shares a high amino acid identity with the *Escherichia coli* NemR. The C106 and K175 of *E. coli* NemR protein were reported as NaOCl responding residues, whereas C104 and R166 of *A. tumefaciens* NieR were particularly responsible for sensing NaOCl. NieR was autoregulated and repressed the NaOCl-inducible efflux operon (*nieAB-sdh)*. The results from DNase I footprinting assays revealed the NieR-binding motifs (imperfect inverted repeats), 5′-TAGATTTAGGATGCAATCTA-3′ (boxA) and 5′-TAGATTTCACTTGACATCTA-3′ (boxR) locating in an intergenic region of the divergent *nieA* and *nieR* genes. Electrophoretic mobility shift assays demonstrated that NieR specifically bound to these boxes and NaOCl prevented the NieR-DNA interaction. This implied that NieR was sensitive to NaOCl oxidation. The promoter-*lacZ* fusions and mutagenesis of either boxA or boxR further confirmed a crucial role of these boxes for NieR repression. In addition, the *nieR* mutant exhibited a small colony phenotype and hypersensitivity to NaOCl and antibiotics, including ciprofloxacin, nalidixic acid, novobiocin, and tetracycline. In summary, we report a novel NaOCl-inducible transcriptional repressor NieR that controls an expression of genes encoding efflux pump components in *A. tumefaciens*. Understanding of NaOCl-sensing mechanisms in bacteria may be useful for developing new treatments to combat infectious diseases.

This research was supported by Chulabhorn Research Institute (Grant No 313/2231)

PP032

Identification and functional characterization of *gaa* gene mutations in Thai patients with infantile-onset pompe disease

Lukana Ngiwsara*[1], Duangrurdee Wattanasirichaigoon[2], Thipwimol Tim-Aroon[2], Kitiwan Rojnueangnit[3], Saisuda Noojaroen[2], Arthaporn Khongkraparn[2], Phannee Sawangareetrakul[1], James R. Ketudat-Cairns[1,4], Voraratt Champattanachai[1], Ratana Charoenwattanasatien[1,5], Chulaluck Kuptanon[6], Suthipong Pangkanon[6], Jisnuson Svasti [1]

[1] Laboratory of Biochemistry, Chulabhorn Research Institute, Bangkok, Thailand
[2] Division of Medical Genetics, Department of Pediatrics, Faculty of Medicine Ramathibodi Hospital, Mahidol University, Bangkok, Thailand
[3] Pediatrics Department, Faculty of Medicine, Thammasat University, Pathumthani, Thailand
[4] School of Chemistry, Institute of Science, Suranaree University of Technology, Nakhon Ratchasima, Thailand
[5] Current address: Synchrotron Light Research Institute, Nakhon Ratchasima, Thailand
[6] Queen Sirikit National Institute of Child Health, Bangkok, Thailand

***Email**: Lukana@cri.or.th

ABSTRACT

Pompe disease is a lysosomal storage disorder caused by the deficiency of acid alpha-glucosidase (EC. 3.2.1.20) due to mutations in human *GAA* gene. Twelve patients with infantile-onset Pompe disease (IOPD) including 10 Thai, one Burmese, and one Vietnamese were enrolled. To examine the molecular characteristics of Pompe patients, *GAA* gene was analyzed by PCR amplification and direct Sanger-sequencing of 20 exons coding region. The novel mutations were transiently transfected in COS-7 cells for functional verification. The severity of the mutation was rated by study of the GAA enzyme activity detected in transfected cells and culture media, as well as the quantity and quality of the proper sized GAA protein demonstrated by western blot analysis. All patients had hypertrophic cardiomyopathy, generalized muscle weakness, and undetectable or <1% of GAA normal activity. Seventeen pathogenic mutations including four novel variants: c.876C>G (p.Tyr292X), c.1226insG (p.Asp409GlyfsX95), c.1538G>A (p.Asp513Gly), c.1895T>G (p.Leu632Arg), and a previously reported rare allele of unknown significance: c.781G>A (p.Ala261Thr) were identified. The rating system ranked p.Tyr292X, p. Asp513Gly and p. Leu632Arg as class "B" and p. Ala261Thr as class "D" or "E". The present study provides useful information on the mutations of *GAA* gene in the underrepresented population of Asia which are more diverse than previously described and showing the hotspots in exons 14 and 5, accounting for 62% of mutant alleles. Almost all mutations identified are in class A/B. These data can benefit rapid molecular diagnosis of IOPD and severity rating of the mutations can serve as a partial substitute for cross reactive immunological material (CRIM) study.

This research was supported by Thailand Science Research and Innovation (TSRI), Chulabhorn Research Institute (Grant No. 446/2602) and Mahidol University.

PP033

Gymnanthemum extensum extracts exerted dose-dependent cytostatic and cytotoxic effects on A549 human lung carcinoma cells

Siriporn Keeratichamroen[1,*], Kriengsak Lirdprapamongkol[1,2], Sanit Thongnest[3], Jutatip Boonsombat[3], Pornsuda Chawengrum[4], Thiwaree Sornprachum[1], Jitnapa Sirirak[5], Chris Verathamjamras[1], Narittira Ornnork[1], Somsak Ruchirawat[2,4,6], Jisnuson Svasti[1,7]

[1] Laboratory of Biochemistry, Chulabhorn Research Institute, Bangkok 10210, Thailand
[2] Center of Excellence on Environmental Health and Toxicology (EHT), Ministry of Education, Bangkok 10400, Thailand
[3] Laboratory of Natural Products, Chulabhorn Research Institute, Bangkok 10210, Thailand [4]Program in Chemical Sciences, Chulabhorn Graduate Institute, Chulabhorn Royal Academy, Bangkok 10210, Thailand
[5] Department of Chemistry, Faculty of Science, Silpakorn University, Nakhon Pathom 73000, Thailand
[6] Laboratory of Medicinal Chemistry, Chulabhorn Research Institute, Bangkok 10210, Thailand
[7] Program in Applied Biological Sciences, Chulabhorn Graduate Institute, Chulabhorn Royal Academy, Bangkok 10210, Thailand

***Email**: siriporn@cri.or.th

ABSTRACT

Lung cancer remains one of the primary cancer-related causes of death in both men and women worldwide due to drug resistance and disease recurrence. The limited efficiency of current conventional chemotherapies necessitates the search for new effective anticancer agents. The present study demonstrated anti-proliferative effect and apoptosis-inducing activity of three sesquiterpene lactones isolated from *Gymnanthemum extensum*, including vernodalin (VDa), vernolepin (VLe) and vernolide (VLi), on A549 human lung cancer cells. Treatment with sub-cytotoxic doses (cell viability remaining > 75%) of VDa, VLe and VLi, arrested progression of A549 cell cycle in the G0/G1 phase, while cytotoxic doses of the three compounds induced G2/M phase arrest and apoptosis. Mechanistic studies revealed that VDa, VLe and VLi may exert their anti-tumor activity through the JAK2/STAT3 pathway. Molecular docking study confirmed that VDa, VLe and VLi formed hydrogen bonding interactions with the FERM domain of JAK2 protein. The overall finding of the present study highlights the potential therapeutic value of VDa, VLe and VLi to be further developed as anticancer agents for treatment of lung cancer.

This research was supported by the Thailand Science Research and Innovation, Chulabhorn Research Institute (grant no. 302/2205).

PP034

Proteomic profiling of skin fibroblasts from patients with Parkinson's disease carrying heterozygous variants of glucocerebrosidase and parkin genes

Phannee Sawangareetrakul[1], James R. Ketudat Cairns[1,2], Lukana Ngiwsara[1], Permphan Dharmasaroja[3], Teeratorn Pulkes[4], Jisnuson Svasti[1], and Voraratt Champattanachai[1,*]

[1] Laboratory of Biochemistry, Chulabhorn Research Institute, Thailand
[2] School of Biochemistry, Institute of Science, Suranaree University of Technology, Thailand
[3] Faculty of Science, Mahidol University, Thailand
[4] Faculty of Medicine, Ramathibodi Hospital, Mahidol University, Thailand

***E-mail**: voraratt@cri.or.th

ABSTRACT:

Parkinson's diseases (PD) is a neurodegenerative disorder affecting movement and balance which mostly found in aged population. While the exact cause of PD is generally unknown, the development and progression of the disease is believed to be associated with environmental and genetic factors. The variants of glucocerebrosidase (*GBA*), a lysosomal enzyme responsible for Gaucher's disease, and parkin (*PARK2*), a "parkin" protein which is a E3 ubiquitin ligase, are important risk factors for developing PD. However, the mechanisms how these mutations cause PD remain largely unknown. In this study, we aim to investigate the protein expression patterns of skin fibroblasts from PD patients carrying heterozygous variants of *GBA* and *PARK2* genes in comparison to those of healthy controls. Proteins extracted from these fibroblasts were analyzed by a liquid chromatography coupled with tandem mass spectrometer (LC-MS/MS). Protein identification and quantification were performed using a label-free quantitative proteomics by Progenesis QI. A number of proteins was identified and compared among all sample groups. Using label-free quantitative proteomic analysis, several proteins with changed in their expressions in *GBA* and *PARK2* groups were compared to those in the healthy controls and some were confirmed by western blot analysis. In addition to those alterations, analysis of protein-protein interactions (PPI) by STRING analysis revealed potential unique molecular features of skin fibroblasts from PD patients carrying heterozygous variants of *GBA* and *PARK2*. This study may provide additional information about protein network regulation and contribution of *GBA* and *PARK2* variants related to PD.

This work was supported by Thailand Science Research and Innovation (TSRI), Chulabhorn Research Institute (Grant No. 446/2602).

PP035

Different mechanisms of drug resistance in A549 human lung cancer cells under drug pressure or metastasis-associated conditions

Sasivimon Pramual[1], **Kriengsak Lirdprapamongkol**[1,2,*], Thiwaree Sornprachum[1], Papada Chaisuriya[1], Lukana Ngiwsara[1], and Jisnuson Svasti[1]

[1] Laboratory of Biochemistry, Chulabhorn Research Institute, Bangkok, Thailand
[2] Center of Excellence on Environmental Health and Toxicology (EHT), Ministry of Education, Bangkok, Thailand

***Email**: kriengsak@cri.or.th

ABSTRACT

Failure of chemotherapy is due to the drug resistance emerging and the spread of cancer in the body (metastasis). Drug resistance can result from selection of drug-resistant cell populations under drug pressure. Alternatively, during metastasis progression, cellular adaptation to microenvironmental changes can lead to drug-resistant phenotype without prior drug exposure. Both resistances can be co-emerged in the same patient. Here, we explored the differences between two drug resistances originated from the same cell line A549 human lung cancer. A drug-selected cell line A549RT-eto was established from A549 by Etoposide selection (drug pressure condition). In metastasis-associated resistance model, A549 cells were cultured under non-adherent conditions without drug (metastasis-associated condition) to obtain A549 floating cells, which mimic adaptation of metastasizing cancer cells in lymphatic vessels. Comparing to A549 parental attached cells, the Etoposide and Paclitaxel resistances in A549RT-eto cells were 17.4-fold and 1.8-fold, respectively, while the resistances in A549 floating cells were 11.6-fold and 57.8-fold, respectively. Immunoblot detection showed an increased expression of a drug transporter ABCB1 (MDR1/P-gp) by 1.9-fold in A549RT-eto cells compared to A549 parental attached cells, while these change was not found in A549 floating cells. qRT-PCR analysis revealed that A549 floating cells up-regulated expression of a Paclitaxel-resistant β-tubulin isotype βIVa by 2.0-fold compared to A549 parental attached cells, while expression level of the gene in A549RT-eto cells was 0.3-fold. In conclusion, drug-selected and metastasis-associated resistances developed from the same cell line exhibited different drug-resistant profiles and its underlying mechanisms, and this might occur with cancer patients.

This research was supported by the Thailand Science Research and Innovation, the Chulabhorn Research Institute (grant no. 302/2128), and the Center of Excellence on Environmental Health and Toxicology (EHT).

PP037

Plasma proteomic profiling identifies novel biomarkers for cholangiocarcinoma

Thanyanan Watcharathanyachat[1], Daranee Chokchaichamnankit[1], Churat Weeraphan[1], Somchai Chutipongtanate[2], Jisnuson Svasti[1,3] and Chantragan Srisomsap[1,*]

[1] Laboratory of Biochemistry, Chulabhorn Research Institute, Bangkok, Thailand;
[2] Department of Pediatrics, Faculty of Medicine Ramathibodi Hospital, Mahidol University, Bangkok, Thailand;
[3] Applied Biological Sciences Program, Chulabhorn Graduate Institute, Bangkok, Thailand

***Email**: chantragan@cri.or.th

ABSTRACT

Cholangiocarcinoma (CCA) is a malignant tumor derived from bile duct epithelium which occurs with relatively high incidence in Thailand. CCA is also highly lethal because most are locally advanced at patient presentation where therapies have limited benefit. Currently available tumor markers, e.g., CA19-9 and CEA, are not specific to CCA, thereby novel CCA biomarker is an unmet need. We explored the feasibility of a translational proteomic approach on CCA biomarkers discovery. The possible candidates were obtained from our previous work, together with the label-free quantitation technique which employed on 27 plasma specimens (9 CCA, 9 disease controls and 9 normal individuals). After immunoblot verification, four interesting proteins (A, B, C and D) were selected and translated into clinically compatible ELISA immunoassay to examine the diagnostic performances in a larger cohort (n=63; 26 CCA vs. 37 non-CCA including 17 disease controls and 20 healthy controls). Receiver Operating Characteristics showed that protein A had higher performance with the area under the curve (AUC) of 0.835 (80.8% sensitivity, 83.8% specificity) as compared to other proteins. Among the combined indexed models, a combination of protein A, protein B and protein D enhanced the diagnostic performance with the AUC of 0.849 (76.9% sensitivity, 89.2% specificity). Our results supported that the combination of three proteins (A, B and D) hold good promise as a potential multiplexing biomarker of CCA, in which the real performance should be further validated in an independent cohort or multicenter study. Translational proteomic approach is feasible for CCA biomarker investigation.

This research was supported by Chulabhorn Research Institute.

PP038

7-Methoxyheptaphylline sensitizes TRAIL-induced colorectal adenocarcinoma cells death through up-regulation of DR5 expression by activation of JNK

Chantana Boonyarat[1], Chavi Yenjai[2], Prasert Reubroycharoen[3], Suchada Chaiwiwatrakul [4] and Pornthip Waiwut [5,*]

[1] Faculty of Pharmaceutical Sciences, Khon Kaen University, Khon Kaen 40002, Thailand
[2] Natural Products Research Unit, Department of Chemistry and Center of Excellence for Innovation in Chemistry, Faculty of Science, Khon Kaen University, Khon Kaen 40002 Thailand
[3] Department of Chemical Technology, Faculty of Science, Chulalongkorn University, Bangkok 10330, Thailand
[4] Department of English, Faculty of Humanities and Social Sciences, Ubon Ratchathani Rajabhat University, Ubon Ratchathani 34000 Thailand
[5] Faculty of Pharmaceutical Sciences, Ubon Ratchathani University, Ubon Ratchathani 34190, Thailand

***Email**: porntip.w@ubu.ac.th

ABSTRACT

TRAIL (TNF-related apoptosis-inducing ligand) is a cytokine that can selectively induce apoptosis in cancer cells without damaging normal cells. Regarding current research findings, a number of cancer cells are resistant to TRAIL-induced apoptosis. This study was designed to investigate the molecular mechanisms of the antitumor activity of heptaphylline and 7-methoxyheptaphylline from *Clausena harmandiana* on TRAIL-treated HT29 colorectal adenocarcinoma cells. The quantification of cell viability was performed using a cell proliferation assay (MTT assay) and cell morphology was investigated by phase contrast microscopy. The molecular mechanisms were studied by Western blotting, RT-PCR and real-time RT-PCR. The results showed that 7-methoxyheptaphylline induced cancer cell death in a concentration dependent manner without cytotoxic effect on normal colon FHC cells, while hepataphylline showed cytotoxicity to normal cells. In combination with TRAIL, heptaphylline had no significant effects on TRAL-induced HT-29 cell death, while the cleavage of caspase-3 and PARP-1 was increased when combining 7-methoxyheptaphylline with TRAIL. The investigation of mechanism found that 7-methoxyheptaphylline increased TRAIL receptor, death receptor 5 (DR5) mRNA and protein through the JNK pathway. The findings suggested that 7-methoxyheptaphylline of *Clausena harmandiana* sensitized TRAIL-induced HT29 cell death by increasing expression of DR5 via the JNK pathway.

This research was supported by Thailand Research Fund and Ubon Ratchathani Unive

PP039

Anticancer effect of protocatechuic aldehyde

Kriengsak Lirdprapamongkol[1,*], **Pantipa Subhasitanont**[1], Hiroaki Sakurai[3], Keiichi Koizumi[3], Somsak Ruchirawat[2], Jisnuson Svasti[1], and Ikuo Saiki[3]

[1] Laboratory of Biochemistry, Chulabhorn Research Institute, Bangkok, Thailand
[2] Laboratory of Medicinal Chemistry, Chulabhorn Research Institute, Bangkok, Thailand
[3] Division of Pathogenic Biochemistry, Institute of Natural Medicine, University of Toyama, Toyama, Japan

***Email**: kriengsak@cri.or.th

ABSTRACT

Protocatechuic aldehyde (3,4-dihydroxybenzaldehyde) is a water-soluble compound found in the root of *Salvia miltiorrhiza* which is a herbal plant used in traditional Chinese medicine to treat cardiovascular and liver diseases. This study have evaluated anticancer effect of protocatechuic aldehyde *in vitro* and elucidated its mechanism of action. WST-1 assay was used to determine growth inhibitory effect of protocatechuic aldehyde and its structural-related compounds including protocatechuic acid, vanillin, and vanillic acid on 4T1 mouse mammary adenocarcinoma cell line. After 48 h treatment, IC_{50} value of protocatechuic aldehyde was significantly lower than IC_{50} of vanillin (~187 fold). Caspase-3 activation and PARP cleavage were observed in 4T1 cells when treated with protocatechuic aldehyde or vanillin, indicating induction of apoptotic cell death. Effect of protocatechuic aldehyde and vanillin on MAPKs (ERK, p38, JNK) and PI3K/Akt signaling pathways were determined by western blot analysis. Both protocatechuic aldehyde and vanillin could decrease basal level of Akt phosphorylation, but had no effects on p38 phosphorylation. Protocatechuic aldehyde inhibited Erk phosphorylation and activated JNK phosphorylation, whereas vanillin did not have such effects. These might be an explanation for the large fold difference between IC_{50} values of the two compounds in 4T1 cells.

This research was supported by Japanese-Thai Collaborative Scientific Research Fellowship (JSPS-NRCT) and the Chulabhorn Research Institute.

PP040

Proteomic analysis of anti-cancer effects by 5'-deoxy-5'-methylthioadenosine treatment in cholangiocarcinoma cell line

Sutthipong Nanarong[1], Sittiruk Roytrakul[2], Thanawat Pitakpornpreecha[1], Sumalee Obchoei[1,*]

[1] Division of Health and Applied Science, Faculty of Science, Prince of Songkla University, Songkhla 90110, Thailand
[2] National Center for Genetic Engineering and Biotechnology, National Science and Technology Development Agency, Pathumtani 12120, Thailand

***Email**: sumalee.o@psu.ac.th

ABSTRACT

The treatment of advanced cholangiocarcinoma (CCA) is mostly ineffective due to the intrinsic and acquired chemotherapeutic drug resistance phenotypes. Clearly, a novel and effective therapies are urgently needed. 5'-deoxy-5'-methylthioadenosine (MTA) is a natural-derived bioactive compound that has been shown to possess anti-cancer activity in various human cancers. In the present study we demonstrated the MTA exhibited a potent cytotoxic effect against a CCA cell line, KKU-213A in a dose dependent manner. In addition, it strongly inhibited cell migration and invasion of CCA cells. Proteomic analysis using LC/MS/MS identified the total of 5,297 proteins. In which, 507 were identified only in untreated cells, 710 were found only in MTA treated cells, whereas 4,080 were expressed in both. The 25 most up-regulated and down-regulated proteins in MTA-treated KKU-213A cell line were displayed using heatmap analysis. The results showed that MTA significantly suppressed numbers of oncoproteins such as RYR1, RCOR2, KLC1, GRAMD1C, and HLA-DQB1. Protein-protein interaction analysis of 25 most down-regulated proteins predicted 3 major clusters namely calcium ion transmembrane transport, antigen processing and presentation of exogenous peptide, and microtubule motor activity. These clusters were reported to involved in tumor progression and they might be the main target of MTA. The detailed study of molecular mechanisms underlying MTA effect on CCA cells both *in vitro* and *in vivo* should be further explored with the anticipation that this promising natural bioactive compound might be an alternative treatment for CCA in the future.

PP041

Expression and characterization of recombinant alkaline protease from *Aspergillus sojae* in yeast *Pichia pastoris*

Pannaporn Tantimetta[1], Aratee Aroonkesorn[1], Phanthipha Runsaeng[1], Sumalee Obchoei[1, *]

[1] Division of Health and Applied Sciences, Department of Biochemistry, Faculty of Science, Prince of Songkla University, Songkhla 90110, Thailand

***Email**: sumalee.o@psu.ac.th

ABSTRACT

Alkaline protease (AP) is a group of enzymes that breaks peptide bonds within polypeptide chain under alkaline condition. It has been extensively used in many industries in particularly food and detergent industries. AP can be obtained from wide variety of alkalophilic microorganisms including bacteria and fungi. Yeast expression system has been utilized for production of recombinant protein in large scales. In this study, we produced a recombinant alkaline protease (rAP) via cloning AP gene from *Aspergillus sojae* (*A. sojae*) into pPIC9K expression vector and introduce into the yeast *Pichia pastoris* KM71. The rAP was successfully expressed and secreted to culture medium. The resultant rAP was composed of 389 amino acids and had molecular weight of approximately 35 kDa. Two positive clones, rAP-3 and rAP-4, were further analyzed and showed positive on skim milk agar plate. Folin-phenol method using casein as a substrate revealed that the enzyme activity of rAP-3 and rAP-4 were 2.966 and 3.923 U respectively. The rAPs had higher enzyme activity as compared with the commercial alkaline proteases from *Bacillus Subtilis* (*B. subtilis*) whose enzyme activity was 2.026 U. SDS-PAGE analysis showed that rAP-3 and rAP-4 completely digested protein casein and protein from cell line lysate. This result suggests that rAP might have broad range of substrate specificity. In summary, we successfully expressed AP gene from *A. sojae* in *P. pastoris* in the form of secreted enzymes in high quantity and satisfactory activity. This established platform could be used in various applications in the future.

PP042

Proteomic analysis of 5-Fluorouracil resistant cholangiocarcinoma cell line

Kankamol Kerdkumthong[1], Kawinnath Songsurin[1], Sittiruk Roytrakul[2], Sumalee Obchoei[1,*]

[1] Division of Health and Applied Sciences, Department of Biochemistry, Faculty of Science, Prince of Songkla University, Songkhla 90110, Thailand
[2] National Center for Genetic Engineering and Biotechnology, National Science and Technology Development Agency, Pathumtani 12120, Thailand

***Email**: sumalee.o@psu.ac.th

ABSTRACT

Resistance to commonly used chemotherapeutic drugs is a major problem of cholangiocarcinoma (CCA) treatment, therefore more effective treatment strategy is urgently needed. Drug resistant cell lines have been used for elucidating drug resistance mechanism in various cancers leading to the discovery of novel treatments. Here in, we have established 5-Fluorouracil resistant (FR) CCA cell line by culturing the parental CCA cell line (KKU-213A) in the stepwise increased concentration of 5-Fluorouracil (5-FU). The established cell line was designated as KKU-213A-FR, confirmed for drug resistance, and use for further analyses. The results showed that, under low serum condition, KKU-213A-FR had slower growth rate than its parental cell line. Conversely, cell migration and invasion ability were increased significantly. Moreover, the proteomic analysis using LC/MS/MS identified the total of 5,680 proteins. In which, 431 were identified only in parental cells, 1,105 were found only in FR cells, whereas 4,144 were expressed in both cell lines. Heatmap analysis showed the 25 most up- and down-regulated proteins in KKU-213A-FR. The up-regulated proteins were further analyzed. Gene ontology revealed that most of these proteins were classified in cellular process group. The protein-protein interaction analysis showed 3 clustering groups that involve in N-linked glycosylation, ubiquitin-dependent protein catabolic process, and organic substance catabolic process. In conclusion, the KKU-213A-FR exhibits aggressive phenotypes and a unique proteomic profile as compared to KKU-213A. More in-depth study on the differentially expressed proteins may lead to better understanding of drug resistance mechanism and more effective treatment for CCA.

PP043

Label-free quantitative proteomic analysis of plasma protein fractionation using multiple immunoaffinity chromatography revealed biomarker candidates of patients with colorectal cancer

Chris Verathamjamras[1,#], Juthamard Chantaraamporn[1,#], Daranee Chokchaichamnankit[1], Thiwaree Sornprachum[1], Chantragan Srisomsap[1], Somchai Chutipongtanate[2,3] , Jisnuson Svasti[1,4], Voraratt Champattanachai [1,4,*]

[1] Laboratory of Biochemistry, Chulabhorn Research Institute, Bangkok 10210, Thailand
[2] Pediatric Translational Research Unit, Department of Pediatrics, Faculty of Medicine Ramathibodi Hospital, Mahidol University, Bangkok 10400, Thailand
[3] Department of Clinical Epidemiology and Biostatistics, Faculty of Medicine Ramathibodi Hospital, Mahidol University, Bangkok 10400, Thailand
[4] Applied Biological Sciences Program, Chulabhorn Graduate Institute, Chulabhorn Royal Academy, Bangkok 10210, Thailand
[#] These authors contributed equally to this work

* **Email**: Voraratt@cri.or.th

ABSTRACT

Colorectal cancer (CRC) is one of the most common cancer worldwide. Globocan reports in 2020 reveal that it is third ranked incidence (10.0%) and second ranked mortality (9.4%) among all cancers. At present, carcinoembryonic antigen (CEA) is still the only blood-based biomarker approved by the U.S. FDA for colorectal cancer screening when used with other diagnostic means. This is because the CEA level can sometimes be normal in CRC patients and can be abnormal for reasons in other cancers. Nevertheless, searching specific biomarkers from liquid biopsy specimens such as plasma and serum is still an ideal non-invasive approach for primary screening of CRC. However, seeking biomarkers in plasma/serum are challenging because numerous proteins were overshadowed by high abundant proteins such as albumin and immunoglobulins. In our present work, a multiple immunoaffinity chromatography was applied to fractionate pooled plasma samples of healthy control, non-metastasis, and metastasis CRC patients into high abundant and low abundant protein fractions. Each fraction was then analysis by a label-free quantitative proteomics approach using LC-MS/MS and Progenesis QI software. Among 167 MS/MS-identified proteins, 10 proteins showed accumulated changes in a stage-dependent manner and 5 prominent candidates were validated by western blotting and will be subjected for further validation in an independent cohort study. It is hoped that our techniques will be useful in order to find more specific biomarker candidates of CRC patients.

This study was supported by the Chulabhorn Research Institute (Grant no. 302-2098).

PP044

Identification of Potential Key (Hub) Genes Associated with Prognosis of Triple-Negative Breast Cancer in Asian versus non-Asian Populations Based on Bioinformatics Analysis

Rassanee Bissanum[1], Raphatphorn Navakanitworakul[1], Suphawat Laohawiriyakamol[2], Piyanan Wangkulangkul[2], Ayako Nakatake[3], Kazuhiro Morishita[3], Rawikant Kamolphiwong[1], and Kanyanatt Kanokwiroon[1,*]

[1] Department of Biomedical Sciences and Biomedical Engineering, Faculty of Medicine, Prince of Songkla University, Hat Yai, Songkhla, Thailand
[2] Department of Surgery, Faculty of Medicine, Prince of Songkla University, Hat Yai, Songkhla, Thailand
[3] Division of Tumor and Cellular Biochemistry, Department of Medical Sciences, University of Miyazaki, Miyazaki, Japan

***Email**: kkanyana@gmail.com

ABSTRACT

Introduction: Triple negative breast cancer (TNBC) is a heterogeneous disease associated with advanced stage and poor prognosis. There are no prognostic biomarkers of TNBC, especially in Asian women. We aimed to identify the potential key genes and their prognosis association in Asian TNBC patients through bioinformatics. **Materials and Methods:** Microarray datasets of TNBC patients were downloaded from gene expression omnibus (GEO) database. Differentially expressed genes (DEGs) between Asian and non-Asian populations were analyzed. The upregulated DEGs were selected as inputs for Gene Ontology and pathway enrichment analyses using Metascape. The significant modules from protein–protein interaction (PPI) network were screened by MCODE. UALCAN and GEPIA databases were analyzed the prognostic values of the hub genes. **Results:** In Asian population, 686 up-regulated genes were identified and mainly enriched in various pathways including vesicle-mediated transport and membrane trafficking, apoptotic signaling and T cell activation pathways. A PPI network was constructed with 588 nodes and 2,351 edges. Eleven hub genes from the significant module were related to the metabolism of RNA and mRNA splicing which highly expressed in breast cancer patients. High expression levels of *SEC61G, MRPL13* and *LSM5* genes were significantly associated with poor overall survival.
Conclusion: These genes might be beneficial for prognostic markers development TNBC patients.

This research was supported by The Royal Golden Jubilee Ph.D. Program, National Research Council of Thailand (grant no. PHD/0184/2561)

PP045

Analysis of the molecular mechanism in metastasis osteosarcoma using gene expression re-analysis

Rawikant Kamolphiwong[1], Kanyanatt Kanokwiroon[1*], Weerinrada Wongrin[2], Parunya Chaiyawat[3,4], Jeerawan Klangjorhor[3,4], Dumnoensun Pruksakorn[3,4*]

[1] Department of Biomedical Sciences and Biomedical Engineering, Faculty of Medicine, Prince of Songkla University, Songkhla, Thailand
[2] Department of Statistics, Faculty of Science, Chiang Mai University, Chiang Mai, Thailand
[3] Musculoskeletal Science and Translational Research Center, Department of Orthopaedics, Chiang Mai University, Chiang Mai, Thailand
[4] Center of Multidisciplinary Technology for Advanced Medicine (CMUTEAM), Faculty of Medicine, Chiang Mai University, Thailand

***Email**: dumnoensun.p@cmu.ac.th, kanyanatt.k@psu.ac.th

ABSTRACT

Background: Survival rate of osteosarcoma has remained plateaued for the past three decades and mechanism of progression remain unclear. Therefore, our aim is to explore the mechanism and identify new therapeutic targets for metastasis osteosarcoma by using gene expression profile.
Materials and Methods: Metastasis osteosarcoma gene expression microarray data were retrieved from available database. Differential gene expression with ratio ≥ 4 and adjusted *p-value* < 0.05 were identified as primary candidate genes (PCG). PCG were further used to find secondary candidate genes (SCG) which involved in pathways. PCG and SCG were matched with genes target from the Drug repurposing hub. Finally, expression of potential genes and pathway were explored by western blotting.
Results: Eighty-one genes were identified as PCG which 4 genes were able to match with 6 drugs. Sixty genes corresponding to top ten pathways were identified as SCG. However, only 3 pathways (negative regulation of anoikis, regulation of anoikis, surfactant metabolism) with 8 genes were matched with 77 Drugs. CAV1 and CAV2 were identified as PCG and found in anoikis resistance pathway which may play an important role in metastasis disease including osteosarcoma. We found that the CAV1 and CAV2 protein were down regulated in 143B osteosarcoma cell seeded on poly-Hema treated wells (as anoikis resistance condition) and reversed back to the normal levels when the anoikis resistance cells were re-attached.
Conclusion: CAV1 and CAV2 might play role in anoikis resistance in osteosarcoma. However, further validation of downstream molecular mechanism and drug inhibition is needed.

This research was financially supported by the Research Fund of the Faculty of Medicine, Prince of Songkla University (grant no. REC 63-351-4-2); partially supported by the Musculoskeletal Science and Translational Research Center (MSTR), Chiang Mai University; and the National Science and Technology Development Agency (NSTDA), code P-18-5199.

PP046

Frequency distribution of triple negative breast cancer subtype according FUSCC classification using immunohistochemistry and correlation with survival outcome

Marisa Leeha[1], Paramee Thongsuksai[2], Rassanee Bissanum[1], Sirion Danklaoun[2], Suphawat Laohawiriyakamol[3], Kanyanatt Kanokwiroon[1, *]

[1] Department of Biomedical Sciences and Biomedical Engineering, Faculty of Medicine, Prince of Songkla University, Hat Yai, Songkhla 90110, Thailand.

[2] Department of Pathology, Faculty of Medicine, Prince of Songkla University, Hat Yai, Songkhla 90110, Thailand.

[3] Department of Surgery, Faculty of Medicine, Prince of Songkla University, Hat Yai, Songkhla 90110, Thailand.

***Email**: Kanyanatt.k@psu.ac.th

ABSTRACT

Introduction: Triple negative breast cancer (TNBC) is a heterogeneous disease and aggressive behavior. Recently, the molecular subtype of TNBC has been studied by transcriptome profiling identified into 4 subtypes by FUSCC classification as follow: luminal androgen receptor (LAR), mesenchymal-like (MES), basal-like immune-activated (BLIA), and immunomodulatory (IM) subtypes. The purpose of this study was to identify the expression of the subtype-specific-protein markers in order to classify the subtype of TNBC patients. **Materials and Methods:** We included patients diagnosed with TNBC at Songklanakarind hospital between 2016 and 2019. The tissue microarray was constructed and performed IHC stained for androgen receptor (AR), doublecortin Like Kinase 1 (DCLK1), cluster of differentiation 8 (CD8), and forkhead Box C1(FOXC1) antibodies to classify the TNBC subtype regarding FUSCC classification. **Results:** We included 50 TNBC patients, with a mean age of 50 years old (33-77 years). The histological subtype was infiltrating duct carcinoma, not otherwise specified (NOS) (62.0%), and ductal carcinoma, NOS (32.0%). Most of the TNBC patients had high grade (3 grade = 72.0%). The distribution of 50 TNBC samples according to FUSCC classification were classified as LAR subtype (AR^+, n = 9; 18.0%), MES subtype (DCLK1 positive, n = 3; 6.0%), IM subtype (CD8 positive, n = 14; 28.0%), BLIS subtype (FOXC1 positive, n = 23, 46.0%) and unclassifiable type (n = 1; 2%). **Conclusion**: This study revealed the distribution of TNBC subtype in southern Thai population. Molecular subtypes obtained may be beneficial for targeted therapeutic guideline in TNBC patients.

This research was supported by grant from the Research Fund of the Faculty of Medicine, Prince of Songkla University, and Health Systems Research Institute, Thailand (grant no, HSRI 63-107).

PP047

Investigation of multidrug resistance protein expression profile in HepG2 cells and microparticles induced by hypoxia

Kanlaya Khounkaew[1], Pornthip Chaichompoo[1], Kriengsak Lirdprapamongkol[2], Saovaros Svasti[3], Chantragan Srisomsap[2], Jisnuson Svasti[2], Titipatima Sakulterdkiat[1,*]

[1] Department of Pathobiology, Faculty of Science, Mahidol University, Bangkok, 10400, Thailand
[2] Laboratory of Biochemistry, Chulabhorn Research Institute, Bangkok, 10210, Thailand
[3] Thalassemia Research Center, Institute of Molecular Biosciences, Mahidol University, Nakhon Pathom, 73170, Thailand

***Email:** titipatima.sak@mahidol.ac.th

ABSTRACT

Tumor microenvironment such as hypoxia impact tumor aggressiveness and treatment outcome. Hepatocellular carcinoma remains one of the most challenging cancers to treat, as indicated by its high mortality and recurrence rate. One of the main obstacles to treatment is decrease efficacy of chemotherapeutic drugs due to increase multidrug resistance (MDR). As the tumor grows, the mass is subjected to temporal and spatial hypoxia – a low O_2 condition. Cells experiencing hypoxia can release cellular vesicle mediators called extracellular vesicles (EV) that imparts cell survival mechanisms to nearby cells. We hypothesize that cell survival mechanism such as MDR may be transferable through release of EV induced under hypoxic condition.

HepG2 cells were cultured under hypoxic (1% O_2) or normoxic (20% O_2) conditions for 24 to 72 hours. Expression of HIF-1α as a hypoxic marker was determined by Western blotting. Increased survival rate of HepG2 cells when treated with Sorafenib, Doxorubicin and Curcumin were observed under hypoxic condition. Interestingly, hypoxic conditioned media was able to increase survival rate of normoxic cells by roughly 20%. We, therefore, believe hypoxic-induced drug resistance of the cells are transferred to conditioned media through EV and set out to elucidate the underlying mechanism(s). Profile of drug transporters including MDR1, MRP1 and MRP3 were analyzed on cells under normoxic and hypoxic conditions and on extracted microparticles, using flow cytometry. We found that both cells and microparticles displayed differential expression of drug transporter profile, suggesting that hypoxia may enhance transfer of MDR transporters from cells to microparticles.

PP048

In silico repurposing and side effect studies of first-and second-generation antipsychotic drugs in methamphetamine addiction treatment

Kasidit Wiboonkiat[1], **Napak Vejsureevakul**[1], **Chotiphat Pornthanamongkol**[1], Chonlakran Auychinda[1], Jiraporn Panmanee[2], Sujira Mukda[2]*

[1] Department of Biology and Health Science, Mahidol Wittayanusorn School, Nakhon Pathom, Thailand 73170
[2] Research Center for Neuroscience, Institute of Molecular Biosciences, Mahidol University, Nakhon Pathom, Thailand 73170

***Email**: sujira.muk@mahidol.edu

ABSTRACT

Methamphetamine (METH) is an illicit psychostimulant that is widely abused and associated with psychological morbidity. METH performs its function directly through the central nervous system, especially on the brain reward circuitry. METH passes through a dopamine transporter and induces excess dopamine discharging. Consistently, antipsychotic drugs can efficiently bind with D2 receptors. Thus, these drugs may be able to prevent the effects of dopamine overstimulation caused by METH. Previous studies in mice indicated that antipsychotic drugs may be used as an intervention for METH-induced sensitization and hyperlocomotion. Therefore, this project is focused on the repurposing of antipsychotic drugs including prochlorperazine, haloperidol, olanzapine, zotepine, and aripiprazole in addiction using computational methods to estimate the binding affinity between drugs and binding sites of the dopaminergic D2 and serotonergic 5-HT2A receptors. Molecular docking scores were calculated using the Scoring Function of the AutoDock Vina. According to the results, five tested antipsychotic drugs displayed a higher binding affinity to the D2 receptor when compared to dopamine. They can inhibit the binding of dopamine towards the D2 receptor and thus suppress neuronal overstimulation. Considering appropriate medications, the most suitable antipsychotic drug is determined by the lower side effects indicated by lower D2 and higher 5-HT2A binding affinity. In this study, the first most appropriate drug is prochlorperazine; a typical antipsychotic. The second is olanzapine; an atypical antipsychotic. In addition, the relationship between molecular interactions and binding affinities was also studied, and found that H-bonds, hydrophobic contacts, and amino sequences are associated with the binding affinity values.

Keywords: Antipsychotic drugs; Dopamine D2 receptor; Methamphetamine; Molecular docking; Serotonin 5-HT2A receptor

PP049

Develop *in vivo* and *in vitro* coupling strategies to produce nicotinamide mononucleotide

Utumporn Ngivprom[1], Praphapan Lasin[1], Panwana Khunnonkwao[2], Suphanida Worakaensai[1], Kaemwich Jantama[2], and Rung-Yi Lai[1,3]*

[1] School of Chemistry, Institute of Science, Suranaree University of Technology, Nakhon Ratchasima, 30000, Thailand
[2] Metabolic Engineering Research Unit, School of Biotechnology, Institute of Agricultural Technology, Suranaree University of Technology, Nakhon Ratchasima 30000,Thailand
[3] Center for Biomolecular Structure, Function and Application, Suranaree University of Technology, Nakhon Ratchasima, 30000, Thailand

***Email**: rylai@sut.ac.th

ABSTRACT

Nicotinamide mononucleotide (NMN), a ribonucleotide, is a key intermediate in the biosynthesis of coenzyme, nicotinamide adenine dinucleotide (NAD^+). Recently, NMN has gained lots of attention for self-medication as a nutraceutical. However, the *in vitro* biosynthesis of NMN requires expensive substrates, which makes this approach is difficult for large scale production. Therefore, we tried to develop a pathway with lower cost. In this project, the biosynthesis of NMN could be divided into two modules. The first module is to produce ribose from xylose by engineered *Escherichia coli*. In the first module, we conducted CRISPR-Cas9 to knock out two transketolase genes (*tktA* and *tktB*) and one gene (*ptsG*) encoding glucose-specific PTS enzyme IIBC component in *E. coli* MG1655. The engineered *E. coli* MG1655 could produce 2.47 g/L of ribose from 5g/L of xylose in LB medium after 48 hours. The second module is to construct *in vitro* biosynthetic pathway to convert ribose to NMN. The pathway involves *E. coli* ribose kinase (*Ec*RbsK), *E. coli* PRPP synthase (*Ec*PRPP), and *Chitinophaga pinensis* nicotinamide phosphoribosyl transferase (*Cp*Nampt) to convert ribose in the supernatant of engineered *E. coli* MG1655 medium to NMN with the incubation of excess ATP and stoichiometric nicotinamide. To reduce ATP cost, polyphosphate kinase was incorporated in the reaction to regenerate ATP from AMP and ATP using *Cytophaga hutchinsonii* polyphosphate kinase (PPK2). Furthermore, to improve the yield of NMN, the *Ec*PRPP inhibitor of pyrophosphate was hydrolyzed by the addition of Ppase. With all effort, the developed system could produce NMN from Nam with about 70% yield using the supernatant of engineered *E. coli* MG1655 medium. Currently, we continue to optimize the production protocol.

This research was supported by Suranaree University of Technology (SUT)

PP050

Computer aided molecular design of FabI1 inhibitors as anti-melioidosis agents from natural product compounds of *Morinda coreia* root

Pornpan Pungpo[1,*], Sirintip Sangsawang[1], Siripen Modmung[1], Somjintana Taweepanich[1], Chan Inntam[1], Pharit Kamsri[2], Auradee Punkvang[2], Jidapa Sangswan[3], Sasithorn Lorroengsil[3], Jiraporn Leanpolchareanchai[4], Narisara Chantratita[5], Warinthorn Chavasiri[6], Khomson Suttisintong[7], Prasat Kittakoop[8,9,10]

[1] Department of Chemistry, Faculty of Science, Ubon Ratchathani University, Ubon Ratchathani 34190, Thailand
[2] Division of Chemistry, Faculty of Science, Nakhon Phanom University, Nakhon Phanom 48000, Thailand
[3] Department of Biological Science, Faculty of Science, Ubon Ratchathani University, Ubon Ratchathani 34190, Thailand
[4] Faculty of Pharmacy, Mahidol University, 10400 Bangkok, Thailand
[5] Department of Microbiology and Immunology, Faculty of Tropical Medicine, Mahidol University, 10400 Bangkok, Thailand
[6] Department of Chemistry, Faculty of Science, Chulalongkorn University, 10330 Bangkok, Thailand
[7] National Nanotechnology Center, National Science and Technology Development Agency, Thailand Science Park, 12120 Pathumthani, Thailand
[8] Chulabhorn Research Institute, 10210 Bangkok, Thailand
[9] Chulabhorn Graduate Institute, Chemical Biology Program, Chulabhorn Royal Academy, 10210 Bangkok, Thailand
[10] Center of Excellence on Environmental Health and Toxicology (EHT), CHE, Ministry of Education, 10300 Bangkok, Thailand

***Email**: pornpan_ubu@yahoo.com

ABSTRACT

Melioidosis caused by *Burkholderia pseudomallei* (*B. pseudomallei*) is top infection diseases of Northeastern part, Thailand. This disease is difficult to manage and often fatal in humans. Herein, we applied computer aided molecular design to evaluate thirteen natural product compounds extracted from *Morinda coreia* root as FabI1 inhibitors of *B. pseudomallei*. The obtained results demonstrated that natural product compounds extracted from *Morinda coreia* root were promising compounds for *B. pseudomallei* FabI1 inhibition. Based on docking calculation, all natural compounds from *Morinda coreia* root were favorable for binding in FabI1 binding site with the docking score ranging from -4.52 to -10.39 kcal/mol. Hydrogen bond and sigma-pi interactions were found as the crucial interaction for binding in FabI1 binding site. The anti-bacterial prediction revealed that all compounds were acted as anti-bacterial agents with the predicted values from 0.0628-0.3181 and 0.0846-0.4625 for *B. pseudomallei* and resistant-*B. pseudomallei*, respectively. Therefore, these finding results aided to identify natural compounds and plant for developing of novel anti-melioidosis agents

This research was supported by the Faculty of Science, Ubon Ratchathani University. National Electronics and Computer Technology Center (NECTEC) is gratefully acknowledged for supporting this research.

PP051

Proposal of JAK2 inhibitors from natural chalcone derivatives as erythropoiesis stimulant agents for thalassemia therapy: biological predictions, molecular docking and pharmacokinetic predictions

Auradee Punkvang[1], Siripen Modmung[2], Sirintip Sangsawang[2], Somjintana Taweepanich[2], Malee Prajuabsuk[2], Pharit Kamsri[1], Pornpan Pungpo[2], Khomson Suttisintong[3], Kanjana Pangjit[4,*]

[1] Division of Chemistry, Faculty of Science, Nakhon Phanom University, Nakhon Phanom 48000, Thailand
[2] Department of Chemistry, Faculty of Science, Ubon Ratchathani University, Ubon Ratchathani 34190, Thailand
[3] National Nanotechnology Center, NSTDA, 111 Thailand Science Park, Klong Luang, Pathum Thani, Thailand
[4] College of Medicine and Public Health, Ubon Ratchathani University, Warin Chamrap, Ubon Ratchathani, 34190, Thailand

***Email**: kanjana.pa@ubu.ac.th

ABSTRACT

The ineffective erythropoiesis inhibition by JAK2 inhibitors has been developed as novel thalassemia therapy. Herein, we applied the biological predictions, molecular docking, and pharmacokinetic predictions to identify natural chalcone as JAK2 inhibitor and erythropoiesis simulating agent for developing as novel thalassemia drug candidate. Seven natural chalcone derivatives were identified as JAK2 inhibitors with erythropoiesis simulating agent property. In addition, these finding compounds were strongly bound with JAK2 binding site which the Glide XP docking score ranging from -8.27 to -7.23 kcal/mol. The main interaction of chalcone derivative is hydrogen bond interactions between an oxygen carbonyl or an oxygen atom of meta-substitution on chalcone analog with NH backbone of Leu932. The pharmacokinetic properties predictions demonstrated that collected compounds were suitable for acting as drug. Therefore, these finding results aid to collect the potential compounds for biological assay evaluations and development as novel drug for thalassemia therapy.

This research was supported by National Science, Research and Innovation Fund (NSRF), the Faculty of Science, Ubon Ratchathani University and Faculty of Science, Nakhon Phanom University. National Electronics and Computer Technology Center (NECTEC) is gratefully acknowledged for supporting this research.

PP052

Screening of JAK2 inhibitors from natural curcumin and its derivatives as erythropoiesis stimulant agents for thalassemia therapy: computer aided molecular design approaches

Somjintana Taweepanich[1,*], Sirintip Sangsawang[1], Siripen Modmung[1], Chan Inntam[1], Pharit Kamsri[2], Auradee Punkvang[2], Khomson Suttisintong[3], Pornpan Pungpo[1], Kanjana Pangjit[4]

[1] Department of Chemistry, Faculty of Science, Ubon Ratchathani University, Ubon Ratchathani 34190, Thailand
[2] Division of Chemistry, Faculty of Science, Nakhon Phanom University, Nakhon Phanom 48000, Thailand
[3] National Nanotechnology Center, NSTDA, 111 Thailand Science Park, Klong Luang, Pathum Thani, Thailand
[4] College of Medicine and Public Health, Ubon Ratchathani University, Warin Chamrap, Ubon Ratchathani, 34190, Thailand

***Email**: somjintana.t@ubu.ac.th

ABSTRACT

JAK2 inhibitors has been validated as novel therapeutic process for thalassemia. This research aimed to developed curcumin and its derivatives as JAK2 inhibitors and erythropoiesis stimulant agents. The biological predictions, molecular docking, and pharmacokinetic predictions were applied on curcumin derivatives and these processes revealed that eleven curcumin derivatives will be act as JAK2 inhibitors with the high binding affinity in JAK2 binding site based on Glide XP docking score ranging from –9.65 to -12.09 kcal/mol. Hydrogen bond interaction with NH backbone of Leu932. In addition, sigma-pi interaction of aromatic ring on curcumin analog with Leu983 sidechain. The ADMET predictions suggested that curcumin derivatives were suitable for acting as drug. Therefore, these finding results aid to collect the potential compounds for biological assay evaluations and development as novel drug for thalassemia therapy based on JAK2 inhibition mechanism.

This research was supported by National Science, Research and Innovation Fund (NSRF), the Faculty of Science, Ubon Ratchathani University and Faculty of Science, Nakhon Phanom University. National Electronics and Computer Technology Center (NECTEC) is gratefully acknowledged for supporting this research.

PP053

Flavans from *Desmos cochinchinensis* as highly potent FabI1 inhibitors of *Burkholderia pseudomallei*: *in silico* based rational design approaches

Jidapa Sangswan[1,*], Sirintip Sangsawang[2], Siripen Modmung[2], Somjintana Taweepanich[2], Malee Prajuabsuk[2], Pharit Kamsri[3], Auradee Punkvang[3], Sasithorn Lorroengsil[1], Jiraporn Leanpolchareanchai[4], Narisara Chantratita[5], Warinthorn Chavasiri[6], Khomson Suttisintong[7], Prasat Kittakoop[8,9,10], Pornpan Pungpo[2]

[1] Department of Biological Science, Faculty of Science, Ubon Ratchathani University, Ubon Ratchathani 34190, Thailand
[2] Department of Chemistry, Faculty of Science, Ubon Ratchathani University, Ubon Ratchathani 34190, Thailand
[3] Division of Chemistry, Faculty of Science, Nakhon Phanom University, Nakhon Phanom 48000, Thailand
[4] Faculty of Pharmacy, Mahidol University, 10400 Bangkok, Thailand
[5] Department of Microbiology and Immunology, Faculty of Tropical Medicine, Mahidol University, 10400 Bangkok, Thailand
[6] Department of Chemistry, Faculty of Science, Chulalongkorn University, 10330 Bangkok, Thailand
[7] National Nanotechnology Center, National Science and Technology Development Agency, Thailand Science Park, 12120 Pathumthani, Thailand
[8] Chulabhorn Research Institute, 10210 Bangkok, Thailand
[9] Chulabhorn Graduate Institute, Chemical Biology Program, Chulabhorn Royal Academy, 10210 Bangkok, Thailand
[10] Center of Excellence on Environmental Health and Toxicology (EHT), CHE, Ministry of Education, 10300 Bangkok, Thailand

***Email**: sanom.n@ubu.ac.th

ABSTRACT

Burkholderia pseudomallei (*B. pseudomallei*) is the etiologic agent of melioidosis. Herein, we applied *in silico* based rational design approaches to evaluate natural flavans extracted from *Desmos cochinchinensis* as FabI1 inhibitors. The obtained results suggested that three natural flavans, (2*S*,4*R*)-2-Phenyl-5,7-dimethoxy-6,8-dimethylchroman-4-ol (**1**), (2*S*)-5-Hydroxy-7-methoxy-6,8-dimethylflavanone (**2**) and (2*S*)-5-hydroxy-7-methoxy-8-methyl-2-phenyl-2,3-dihydrochromen-4-one (**3**) extracted from *Desmos cochinchinensis* were promising compounds with the anti-bacterial prediction against resistant-*B. pseudomallei* ranging from 0.0204-0.0912. The highest binding affinity was found between flavan compound **2** (-10.07 kcal/mol) with *B. pseudomallei* FabI1 and hydrogen bond interaction between hydroxyl (OH) with an oxygen carbonyl backbone of Gly93 and pi-pi interaction of phenyl ring with Phe203 sidechain were suggested as the crucial interaction for binding. Therefore, these results aided to identify natural compounds and medicinal plant for developing of novel anti-melioidosis agents.

This research was supported by the Faculty of Science, Ubon Ratchathani University. National Electronics and Computer Technology Center (NECTEC) is gratefully acknowledged for supporting this research.

PP054

Potential FabI1 inhibitors of *B. pseudomallei* from the heartwoods of *Mansonia gagei* Drumm.: biological prediction and molecular docking calculations

Sasithorn Lorroengsil[1,*], Sirintip Sangsawang[2], Siripen Modmung[2], Somjintana Taweepanich[2], Chan Inntam[2], Saisamorn Lumlong[2], Pharit Kamsri[3], Auradee Punkvang[3], Jidapa Sangswan[1], Jiraporn Leanpolchareanchai[4], Narisara Chantratita[5], Warinthorn Chavasiri[6], Khomson Suttisintong[7], Prasat Kittakoop[8,9,10], Pornpan Pungpo[2]

[1] Department of Biological Science, Faculty of Science, Ubon Ratchathani University, Ubon Ratchathani 34190, Thailand
[2] Department of Chemistry, Faculty of Science, Ubon Ratchathani University, Ubon Ratchathani 34190, Thailand
[3] Division of Chemistry, Faculty of Science, Nakhon Phanom University, Nakhon Phanom 48000, Thailand
[4] Faculty of Pharmacy, Mahidol University, 10400 Bangkok, Thailand
[5] Department of Microbiology and Immunology, Faculty of Tropical Medicine, Mahidol University, 10400 Bangkok, Thailand
[6] Department of Chemistry, Faculty of Science, Chulalongkorn University, 10330 Bangkok, Thailand
[7] National Nanotechnology Center, National Science and Technology Development Agency, Thailand Science Park, 12120 Pathumthani, Thailand
[8] Chulabhorn Research Institute, 10210 Bangkok, Thailand
[9] Chulabhorn Graduate Institute, Chemical Biology Program, Chulabhorn Royal Academy, 10210 Bangkok, Thailand
[10] Center of Excellence on Environmental Health and Toxicology (EHT), CHE, Ministry of Education, 10300 Bangkok, Thailand

***Email**: sasithorn.l@ubu.ac.th

ABSTRACT

In this research, we applied biological prediction and molecular docking calculation to evaluate natural compounds extracted from *Mansonia gagei* Drumm.as FabI1 inhibitors of *B. pseudomallei,* the novel and promising target for melioidosis treatment. Six compounds, Mansorin B, Mansorin C, Mansonone C, Mansonone G, Mansonone E and Mansonone H were identified as potential FabI1 Inhibitors of *B. pseudomallei* based on anti-bacterial prediction and molecular docking calculations. All compounds were active against resistant-*B. pseudomallei* with the prediction value ranging from 0.0329 to 0.2859. Mansorin B was highest binding affinity with -4.93 kcal/mol for binding in FabI1 binding site. The crucial interaction is hydrogen bond interaction of an oxygen carbonyl on Mansorin B with hydroxyl (OH) of Tyr156 sidechain. In addition, hydrophobic interaction was improved the binding affinity in the FabI1 binding site of *B. pseudomallei*. Therefore, these results aided to identify natural compounds for developing of novel anti-melioidosis agents.

This research was supported by the Faculty of Science, Ubon Ratchathani University. National Electronics and Computer Technology Center (NECTEC) is gratefully acknowledged for supporting this research.

PP055

Molecular modeling analysis for purposing depsidones and diaryl ethers from the endophytic fungus *Corynespora cassiicola* L36 against *Burkholderia pseudomalle* FabI1

Suriya Tingthong[1], Sirintip Sangsawang[2], Siripen Modmung[2], Somjintana Taweepanich[2], Saisamorn Lumlong[2], Pharit Kamsri[3], Auradee Punkvang[3], Sasithorn Lorroengsil[1] Jiraporn Leanpolchareanchai[4], Narisara Chantratita[5], Warinthorn Chavasiri[6], Khomson Suttisintong[7], Prasat Kittakoop[8,9,10], Pornpan Pungpo[2], Jidapa Sangswan[1,*]

[1] Department of Biological Science, Faculty of Science, Ubon Ratchathani University, Ubon Ratchathani 34190, Thailand
[2] Department of Chemistry, Faculty of Science, Ubon Ratchathani University, Ubon Ratchathani 34190, Thailand
[3] Division of Chemistry, Faculty of Science, Nakhon Phanom University, Nakhon Phanom 48000, Thailand
[4] Faculty of Pharmacy, Mahidol University, 10400 Bangkok, Thailand
[5] Department of Microbiology and Immunology, Faculty of Tropical Medicine, Mahidol University, 10400 Bangkok, Thailand
[6] Department of Chemistry, Faculty of Science, Chulalongkorn University, 10330 Bangkok, Thailand
[7] National Nanotechnology Center, National Science and Technology Development Agency, Thailand Science Park, 12120 Pathumthani, Thailand
[8] Chulabhorn Research Institute, 10210 Bangkok, Thailand
[9] Chulabhorn Graduate Institute, Chemical Biology Program, Chulabhorn Royal Academy, 10210 Bangkok, Thailand
[10] Center of Excellence on Environmental Health and Toxicology (EHT), CHE, Ministry of Education, 10300 Bangkok, Thailand

***Email**: sanom.n@ubu.ac.th

ABSTRACT

An infectious disease, melioidosis caused by the bacterium *Burkholderia pseudomallei* is public health problem of people from Northeastern part of Thailand. Herein, we applied molecular modeling approaches to evaluate depsidones and diaryl ethers from the endophytic fungus *Corynespora cassiicola* L36 as FabI1 inhibitors. Five compounds based on were identified as potential FabI1 inhibitors which displayed the biological activity prediction against resistant- *Burkholderia pseudomallei* (0.0294 - 0.2629). The binding affinity based on docking score raining from -5.15 to -6.92 kcal/mol. 2,3',4-Trihydroxy-5',6-dimethyldiphenyl ether was highest binding affinity which shown H-bond interaction with NH and an oxygen carbonyl of Gly96 backbone in FabI1 binding site. In addition, H-bond interaction of OH of diphenyl ether with OH of NAD^+ was obtained. Consequently, these results aided to identify natural compounds and understand the binding mechanism for developing of novel anti-melioidosis agents based on FabI1 Inhibitors.

This research was supported by the Faculty of Science, Ubon Ratchathani University. National Electronics and Computer Technology Center (NECTEC) is gratefully acknowledged for supporting this research.

PP056

Discovery of novel JAK2 inhibitors as erythropoiesis stimulant agents for thalassemia therapy through virtual screening approaches

Siripen Modmung[1], Sirintip Sangsawang[1], Bandit Khamsri[1], Somjintana Taweepanich[1], Chan Inntam[1], Pornpan Pungpo[1], Auradee Punkvang[2], Pharit Kamsri[2], Kanjana Pangjit[3], Khomson Suttisintong[4,*]

[1] Department of Chemistry, Faculty of Science, Ubon Ratchathani University, Ubon Ratchathani 34190, Thailand
[2] Division of Chemistry, Faculty of Science, Nakhon Phanom University, Nakhon Phanom 48000, Thailand
[3] College of Medicine and Public Health, Ubon Ratchathani University, Warin Chamrap, Ubon Ratchathani, 34190, Thailand
[4] National Nanotechnology Center, NSTDA, 111 Thailand Science Park, Klong Luang, Pathum Thani, Thailand

***Email**: khomson@nanotec.or.th

ABSTRACT

JAK2 is an enzyme responsible for regulating erythropoiesis associated with the ineffective erythropoiesis process. This is currently a new key target for developing drugs with the new therapeutic option for thalassemia. Herein, we applied the ligand and structure based virtual screening to identify novel JAK2 inhibitors for erythropoiesis stimulating agent (ESA). The obtained results demonstrate that seven compounds were predicted to be active against both JAK2 and ESA and showed strongly bound with JAK2 binding site. In addition, the binding mode, and binding interactions in the ATP binding site of JAK2 were investigated. The obtained results revealed that the hydrogen bond interactions with Leu932 backbone in the ATP binding site of JAK2 are key interaction for binding of new finding compounds. Therefore, the finding compounds were proposed as novel and potential JAK2 inhibitors as ESA for thalassemia therapy.

This research was supported by National Science, Research and Innovation Fund (NSRF), Faculty of Science, Ubon Ratchathani University and Faculty of Science, Nakhon Phanom University. National Electronics and Computer Technology Center (NECTEC) is gratefully acknowledged for supporting this research.

PP057

Understanding binding modes and binding interactions of 4-oxocrotonic acid as highly potential PknB inhibitors through computer aided drug design

Chayanin Hanwarinroj[1], Paptawan Thongdee[1], Chan Inntam[1], Somjintana Taveepanich[1], Jidapa Sangswan[2], Sasithorn Lorroengsil[2], Pharit Kamsri[3], Auradee Punkvang[3], Patchreenart Saparpakorn[4], Supa Hannongbua[4], Khomson Suttisintong[5], Prasat Kittakoop[6,7,8], James Spencer[9], Adrian J. Mulholland[10], and Pornpan Pungpo[1,*]

[1] Department of Chemistry, Faculty of Science, Ubon Ratchathani University, Ubon Ratchathani 34190, Thailand
[2] Department of Biological Science, Faculty of Science, Ubon Ratchathani University, Ubon Ratchathani 34190, Thailand
[3] Division of Chemistry, Faculty of Science, Nakhon Phanom University, Nakhon Phanom 48000, Thailand
[4] Department of Chemistry, Faculty of Science, Kasetsart University, Bangkok 10900, Thailand
[5] National Nanotechnology Center, NSTDA, 111 Thailand Science Park, Klong Luang, Pathum Thani 12120, Thailand
[6] Chulabhorn Research Institute, Kamphaeng Phet 6 Road, Laksi, Bangkok 10210, Thailand
[7] Chulabhorn Graduate Institute, Chulabhorn Royal Academy, Bangkok 10210, Thailand
[8] Center of Excellence on Environmental Health and Toxicology (EHT)
[9] School of Cellular and Molecular Medicine, University of Bristol, Bristol, BS8 1TD, United Kingdom
[10] Centre for Computational Chemistry, School of Chemistry, University of Bristol, Bristol, BS8 1TS, United Kingdom

***Email**: pornpan_ubu@yahoo.com

ABSTRACT

The *Mycobacterium tuberculosis* Ser/Thr protein kinases B or PknB is essential for growth and survival of the pathogen in vitro and in vivo. 4-oxocrotonic acid derivatives which is majority anti-TB activity of minimum inhibitory concentrations (MICs) is falling in micromolar range and significantly higher than other reported PknB inhibitors selected to study. Molecular docking calculations of 4-oxocrotonic acid derivatives were performed via Autodock 4.2 program to get better understanding binding modes and binding interactions in PknB binding site. The result illustrated the hydrogen bond interaction was found between oxygen atom of ligand with carbonyl group of Val95 residue. Another hydrogen bond interaction was formed between carbonyl group of core structure of ligand with carbonyl backbone of Val72 residue. In addition, hydrophobic interaction between ligand and Leu17, Val25, Ala38, Val72, Met92, Tyr94, Met155 and Asp156 residues were found. The obtained result provides beneficially information for further modification of 4-oxocrotonic acid derivatives with highly and more potent against *mycobacterium tuberculosis*.

This research was supported by the Thailand Graduate Institute of Science and Technology (TGIST) (SCA-CO-2560-4375TH) to C. Hanwarinroj and the Excellence for Innovation in Chemistry (PERCH-CIC) are appreciated. Faculty of Science, Ubon Ratchathani University, Kasetsart University, Nakhon Phanom University, School of Chemistry, University of Bristol, and Thailand: National Electronics and Computer Technology (NECTEC) are gratefully acknowledged for supporting this research.

PP058

A protein engineering to create the high thermostable formate dehydrogenase enzyme for biocatalysis applications

Rattima Boonkumkrong[1], Paweenapon Chunthaboon[1], Ruchanok Tinikul[2]

[1] Student of Deparmaent of Biochemistry and Center of Excellence in Protein and Enzyme Technology (CPET), Faculty of Science, Mahidol University, Bangkok 10400, Thailand
[2] Assistant Professor, Department of Biochemistry and Center of Excellence in Protein and Enzyme Technology (CPET), Faculty of Science, Mahidol University, Bangkok 10400, Thailand

***Email:** rattima2014@gmail.com, rattima.boo@student.mahidol.edu

ABSTRACT

Formate dehydrogenase (FDH) catalyzes the generation of NADH from NAD^+ by oxidation of formate to carbondioxide. The enzyme is useful for coenzyme regenerating systems, in which NADH is continuously generated by the FDH enzyme to support the main synthesis enzyme reaction in biotransformations. The novel FDH from *Bacillus simplex* (BsFDH) was recently characterized and revealed the highest catalytic efficiency. However, the major painpoint of BsFDH is low thermostability. Therefore, in this study, we employed a FireProt computational prediction to rational engineer to improve the thermostability of BsFDH. The program suggested 61 variants that may have more thermostability than the wild-type. By complement three criteria, we selected 9 candidate variants to perform site-directed mutagenesis and 7 variants were successfully overexpressed and purified. The enzyme activity and thermostability were investigated in comparison with wild-type enzyme. The results showed that the Q125L, A216I, S50L, and T213C exhibited comparable activity to the wild-type enzyme, while only Q125L had higher thermostability than the wild-type. At 55^{o}C incubation, the Q125L was able to retain more than 50% after 6 h of incubation, while the wild-type activity dropped 35% activity. This result suggests that the Q125L variant of the BsFDH might be suitable for biosynthesis.

Keyword: Thermostability, Formate dehydrogenases, Biocatalysis, Coenzyme regenerating system, FireProt

PP059

Characterization of a cellobiohydrolase from the thermophilic bacterium *Thermothelomyces thermophilus* (TtCel7) produced in recombinant *Escherichia coli*

Chamaipon Beagbandee, Peeranat Jatooratthawichot, and James R. Ketudat Cairns*

School of Chemistry, Institute of Science and Center for Biomolecular Structure, Function and Application, Suranaree University of Technology, Nakhon Ratchasima, 30000, Thailand.

***Email**: cairns@sut.ac.th

ABSTRACT

Cellulose is a major source of biomass monosaccharide, which may be applied as a feedstock for industrial biorefinery. Cellulose is a linear polymer with glucose monomers linked exclusively by β-1,4 glycosidic bonds, tethered to other molecules by a hydrogen bonding network that joins individual cellulose polymers to form crystalline cellulose. Cellobiohydrolases play an important role in hydrolysis of cellulose to smaller molecules, along with endoglucanases and β-glucosidases. In this study, we produced cellobiohydrolase from thermophilic *Thermothelomyces thermophilus* and its recombinant protein TtCel7A, which is a member of glycoside hydrolase family 7. TtCel7A was simply expressed in E. coli system (Origami(DE3)), purified and biochemically characterized. TtCel7 exhibited cellobiohydrolase activity against cellooligosaccharides (C3 to C6), microcrystalline cellulose from commercial and natural sources, respectively, under optimal conditions of 40-50 °C and pH 5.5. It retained over 80% residual activity after incubation at 60◦C for 24 hours. TtCel7A has ability to work in high methanol and ethanol concentrations, and displayed over 80% residual activity after incubated at 20% ethanol or methanol for 30 min. TtCel7A is also active to release glucose and cellooligosaccharides in the presence of various metal ions. TtCel7A hydrolysis of cellotetraose releases glucose, cellobiose, and cellotriose, suggesting that cellotetraose can bind in multiple positions to produce different products. However, the breaking down of cellooligosaccharide and pre-treated agricultural biomass (rice straw, rice husk, and sugarcane leaf) confirmed that cellobiose is the main product of TtCel7 hydrolysis. The properties of TtCel7 make it a potential biocatalyst for the conversion of biomass in contaminated conditions for practical industrial applications and simultaneous saccharification and fermentation conditions to convert agricultural wastes to valuable compounds.

This work is supported by the Thailand Research Fund, the Synchrotron Light Research Institute and Suranaree University of Technology.

PP060

Enzymatic synthesis of glycosylated compounds by rice Os9BGlu31 transglucosidase and its mutants

Eko Suyanto[1,2,3], Sunaree Choknud[1,2], Jaggaiah Naidu Gorantla[1,2], and James R. Ketudat-Cairns[1,2,4*]

[1] School of Chemistry, Institute of Sciences, Suranaree University of Technology, Nakhon Ratchasima, Thailand
[2] Center for Biomolecular Structure, Function and Application, Suranaree University of Technology, Nakhon Ratchasima, Thailand
[3] Biology Department, Faculty of Mathematic and Sciences, Brawijaya University, Malang, Indonesia
[4] Laboratory of Biochemistry, Chulabhorn Research Institute, Bangkok, Thailand

***Email**: cairns@sut.ac.th

ABSTRACT

Rice Os9BGlu31 (EC 3.2.1.21) is one of enzyme in glycoside hydrolase family 1 (GH1), a family that mostly catalyzes hydrolysis reactions. Os9BGlu31, however, mainly has transglycosylation activity that can transfer a glucosyl moiety to another aglycon moiety to form new glycosylated compounds (glycoconjugates) through a retaining mechanism. This reaction may improve the bioactivity, stability, solubility, and physicochemical and physiological properties of the compounds, such as promising functional compounds and pharmaceuticals. In this study, we investigated the ability of rice Os9BGlu31 transglucosidase for glycosylation of phytosterol and phenolic acids to synthesis glycosides or glucosyl esters. Os9BGlu31 and its mutants were expressed in *Escherichia coli* strain Origami B(DE3), then purified by an immobilized metal affinity chromatography (IMAC). The glycosylated products of several glucose acceptor were obtained by transglycosylation reactions, then were detected by thin layer chromatography (TLC), measured by ultra-high performance liquid chromatography (UHPLC) and their structures verified by Nuclear Magnetic Resonance (NMR) spectroscopy. Rice Os9BGlu31 transglucosidase and its mutants transferred a glucosyl moiety from *p*-nitrophenol β-D-glucopyranoside as glucose donor to sterol compounds and phenolic acids. Rice Os9BGlu31 mutants had higher activity than wildtype on phytosterol compounds and phenolic acids to produce glucoside. However, the activity of Os9BGlu31 on phytosterols was lower than on phenolic acids. Meanwhile, Os9BGlu31 wildtype tended to produce a single product of phenolic glucosyl ester. Rice Os9BGlu31 transglucosidase is promising for glycosylation of compounds of interest, which may be improved by engineering the substrate specificity to allow production of a range glycoconjugates.

This research was supported by International Research Network grant IRN62W0004 from the Thailand Research Fund.

PP061

Immobilization of *Thermoanaerobacterium xylanolyticum Tx*GH116 and E441G nuclophile mutant

Salila Pengthaisong[1] and James R. Ketudat Cairns[1,2*]

[1] School of Chemistry, Institute of Science, and the Center for Biomolecular Structure, Function and Application, Suranaree University of Technology, Nakhon Ratchasima, Thailand
[2] Laboratory of Biochemistry, Chulabhorn Research Institute, Bangkok 10210, Thailand

E-mail: cairns@sut.ac.th

ABSTRACT

*Thermoanaerobacterium xylanolyticum Tx*GH116 β-glucosidase belongs to glycoside hydrolase (GH) family 116 and hydrolyzes β-1,3- and β-1,4- linked oligosaccharides. *Tx*GH116 E441G nucleophile mutant catalyzed transfer of glucose from α-glucosyl fluoride (α-GlcF) to cellobiose acceptor without hydrolysis of the products and showed broad specificity for α-glycosyl fluoride donors and *p*-nitrophenyl glycoside acceptors. Moreover, the *Tx*GH116 E441G catalyzed synthesis of α-D-glucosyl azide from sodium azide and *p*NP-β-D-glucoside (*p*NPGlc) or cellobiose for production of α-glucosyltriazoles. Enzyme immobilization promotes high catalytic activity and stability, and convenient handling of reusable enzymes. In order to economize on the enzymes, *Tx*GH116 and E441G were immobilized on Sepharose 4B activated by cyanogen bromide. The optimum pH of *Tx*GH116 was slightly reduced from 5.5 to 5.0 upon immobilization and had lower relative activity than free enzyme from pH 5.5 to 8.0, while the temperature optimum and thermal stability of immobilized *Tx*GH116 was similar to free enzyme. The immobilized *Tx*GH116 remained 94% of its initial activity after 20 cycles. The optimum pH of immobilized E441G was pH 4.5, similar to free enzyme, while immobilized E441G had lower thermal stability than free enzyme. The activity of immobilized E441G remained only 53% after 10 cycles. Small scale immobilization of E441G on immobilized metal affinity chromatography (IMAC) resin gave higher stability than on cyanogen bromide-activated Sepharose 4B, with 100% activity remaining after 10 cycles, but it was unstable in larger scale reactions. Therefore, the immobilization process could not enhance the pH and temperature stability of *Tx*GH116 and E441G, but the immobilized enzymes were reusable.

This research was supported by Suranaree University of Technology, the Synchrotron Light Research Institute, the Thailand Research Fund, and Thailand Science Research and Innovation.

PP062

Development of extracellular vesicle-based liquid biopsy for MYCN-amplified high-risk neuroblastoma

Napat Rojsirikulchai,[1,2#] Jirawan Panachan,[3,#] Nutkridta Pongsakul,[2] Ladawan Khowawisetsut,[4] Wararat Chiangjong,[2] Pongpak Pongphitcha,[3] Usanarat Anurathapan,[3] Kovit Pattanapanyasat,[5] Suradej Hongeng,[3] and Somchai Chutipongtanate[2,6,7]*

[1] Faculty of Medicine Ramathibodi Hospital, Mahidol University, Bangkok 10400 Thailand
[2] Pediatric Translational Research Unit, Department of Pediatrics, Faculty of Medicine Ramathibodi Hospital, Mahidol University, Bangkok 10400 Thailand
[3] Division of Hematology and Oncology, Department of Pediatrics, Faculty of Medicine Ramathibodi Hospital, Mahidol University, Bangkok 10400 Thailand
[4] Department of Parasitology, Faculty of Medicine Siriraj Hospital, Mahidol University 10700 Thailand
[5] Office for Research and Development, Faculty of Medicine Siriraj Hospital, Mahidol University 10700 Thailand
[6] Department of Clinical Epidemiology and Biostatistics, Department of Pediatrics, Faculty of Medicine Ramathibodi Hospital, Mahidol University, Bangkok 10400 Thailand
[7] Chakri Naruebodindra Medical Institute, Faculty of Medicine Ramathibodi Hospital, Mahidol University, Samut Prakan 10540 Thailand
[#] Share equal contributions

***Email**: schuti.rama@gmail.com, somchai.chu@mahidol.edu

ABSTRACT

MYCN amplification is an important marker for detecting high-risk neuroblastoma (NB), an aggressive neuroblast tumor with a poor prognosis. However, detecting MYCN amplification requires invasive procedures, e.g., bone marrow aspiration or tumor biopsies. Extracellular vesicles (EVs) contain molecular signatures (e.g., DNA, RNA, proteins) of originate cells that serve as an invaluable source for a less-invasive liquid biopsy. This study aimed to establish a method for detecting MYCN amplification status in EVs deriving from NB cells. Two EV subtypes, i.e., microvesicles and exosomes, were isolated from NB cell culture supernatants (3 MYCN-amplified and 3 MYCN-non-amplified). After characterizing EV protein and particle evidence, MYCN amplification status in EVs deriving from six different NB cells was detected by qRT-PCR. Interestingly, MYCN amplification status was only detectable in the microvesicles, but not exosomes, of MYCN-amplified NB. The feasibility of this method was successfully demonstrated by using simulated samples prepared by pulsing NB-derived microvesicles into the human serum. This study established a liquid biopsy workflow for detecting MYCN-amplification status in the isolated microvesicles. Further validation using the clinical specimens may enable the use of the microvesicle-based liquid biopsy for the high-risk NB diagnosis in the future.

This research was supported by the Dean Research Novice Award, Faculty of Medicine Ramathibodi Hospital, Mahidol University (257/2563) and the Genomics Thailand Project of Health Systems Research Institute, Thailand (HSRI 64-130).

Proceedings

Proceeding PP004

Design of enzyme immobilization system for chitin bioconversion

Ailada Charoenpol[1], Daniel Crespy[2], Albert Schulte[1], Wipa Suginta[1*]

[1] School of Biomolecular Science and Engineering (BSE), Vidyasirimedhi Institute of Science and Technology (VISTEC), Payupnai, Wangchan Valley, Rayong 21210, Thailand
[2] School of Molecular Science and Engineering (MSE), Vidyasirimedhi Institute of Science and Technology (VISTEC), Payupnai, Wangchan Valley, Rayong 21210, Thailand

***Email**: wipa.s@vistec.ac.th

ABSTRACT

Chitooligosaccharides (COS) produced by the enzymatic hydrolysis of chitin are of significant interest; their high value indicates that they have interesting bioactivities such as anticancer, antifungal, and anti-inflammatory properties, making them a viable pharmaceutical product. Utilizing of immobilized enzyme for COS production is interesting, as long as the enzyme is stable enough for industrial application. In this study, chitinase A from the marine bacterium *Vibrio harveyi* (*Vh*ChiA) was expressed and purified by a Ni-NTA column. Chitosan coated magnetic nanoparticles (CS@MNPs) were synthesized by in situ co-precipitation method and were then functionalized with hemin through amidation reaction. *Vh*ChiA was immobilized on to three different types of magnetic nanoparticles including uncoated MNPs, CS@MNPs, and Hemin@CS@MNPs. Transmission electron microscopy (TEM), Scanning electron microscopy (SEM), Fourier-transform infrared spectroscopy (FTIR), and thermal gravimetric analysis (TGA) were used to illustrate the MNPs and immobilized *Vh*ChiA. Among of three types of magnetic nanoparticles, CS@MNPs provided the highest immobilization yield around 95.96±3.45%, followed by Hemin@CS@MNPs, and uncoated MNPs which gave 87.70±1.95% and 29±4.99%, respectively.

Keywords: Chitinases, chitooligosaccharide production, enzyme immobilization, magnetic nanoparticles.

INTRODUCTION

The development of an efficient enzyme immobilization system for chitin bioconversion have received a lot of attention and challenge. Chitin is the second most abundant natural polysaccharides which derived from the shell of Arthropods such as shrimps, crabs, and insects. The structure of chitin consists of *N*-acetyl-D-glucosamine monomer that link together with β-1,4 glycosidic linkage [1]. Chitinolytic enzymes including chitosanases, chitinases, and *N*–acetyl β glucosaminidases are important enzymes for chitosan and chitin bioconversion. Chitinase is a hydrolytic enzyme that efficiently catalyzes the hydrolysis of chitin by cleaving the glycosidic bonds between *N*-acetyl-D-glucosamine (GlcNAc) units, resulting in the formation of chitooligosaccharides (COS). The chitooligosaccharide (COS) products exhibit antitumor [2], antiviral [3], antimicrobial [4], and anti-inflammatory [5] activities, making them applicable for pharmaceutical applications. However, utilizing chitinase in free form to produce chitooligosaccharides (COS) on a large scale is insufficient and has significant limitations including poor stability of enzyme, complicated process of product purification is needed, and enzyme cannot be reused. To overcome these disadvantages, enzyme immobilization is an alternative technique which can be used to

improve enzyme properties and provides many advantages including increasing productivity efficiency [6], enhancing enzyme thermostability and catalytic activity [7], continuously operating of catalysis process [8], and the enzyme can be easily separated from the reaction solution and reused [9].

The enzyme immobilization system is made up of three main parts including carrier, enzyme, and grafting form of enzyme-carrier. The enzyme can be supported by a variety of carriers such as natural polymer [10], synthetic polymer [11], inorganic and organometallic materials [12], and carbon-based materials [13] in which the carrier should be easily available and inexpensive [14]. In addition, various immobilization methods have been employed to prepare the immobilized enzyme such as physical adsorption [15], covalent bonding [16], entrapment [17], encapsulation [18], and cross-linking [19]. These methods provide a specific interaction between the enzyme and the carrier, and they have both of pros and cons. Many studies have been conducted to immobilize chitinase on various types of carriers with various immobilization methods, however covalent bonding is the most commonly utilized approach [20-23]. These immobilized chitinases can be applied for enhancing the production of chitooligosaccharides (COS) [24] and used as a biosensor for chitin determination from fungal contaminated stored rice grains [23] which are very important in pharmaceutical and food applications.

In this study, an efficient enzyme immobilization system was designed to immobilize the chitinase A enzyme from the marine bacterium *Vibrio harveyi* (*Vh*ChiA) for improving the chitinase A (*Vh*ChiA) activity and enhancing the production of chitooligosaccharides (COS). Magnetic nanoparticles in both uncoated and functionalized versions were utilized as carriers to determine the best chitinase A (*Vh*ChiA) carrier (Scheme 1) and several techniques including scanning electron microscopy (SEM), transmission electron microscopy (TEM), Fourier-transform infrared spectroscopy (FTIR), and thermal gravimetric analysis (TGA) were used to characterize the immobilized *Vh*ChiA.

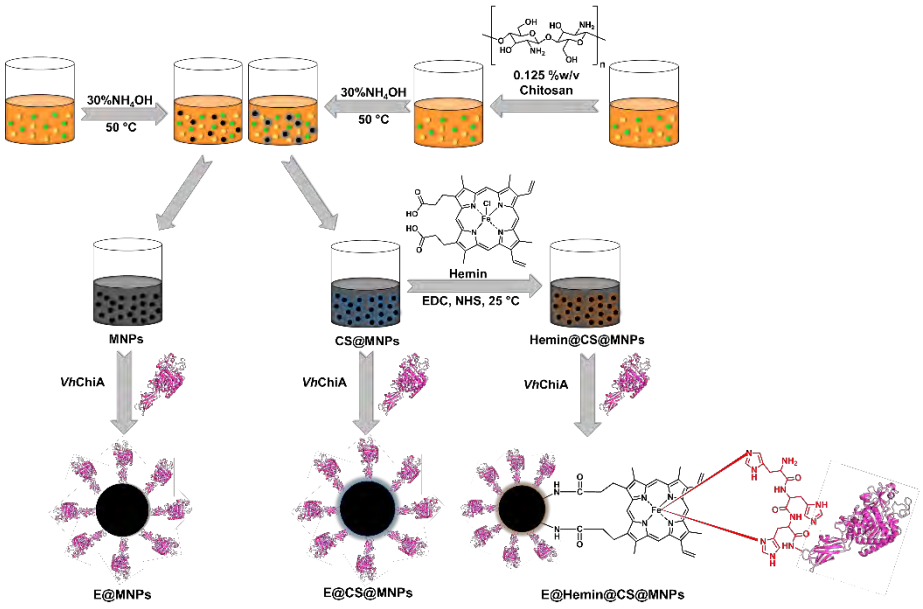

Scheme 1 Schematic representation of *Vh*ChiA immobilization on to MNPs with three different approaches, which are MNPs, CS@MNPs, and Hemin@CS@MNPs.

MATERIALS AND METHODS

VhChiA expression and purification

As previously reported [25], the wild type chitinase A from *Vibrio harveyi* was cloned into the expression vector pQE60 and overexpressed in *E. coli* M15 cells. The transformed cells were cultured at 37 °C in LB medium containing a final concentration of 100 μg/mL ampicillin and 50 μg/mL kanamycin until the OD_{600} of the cell culture reached 0.6-0.8 for recombinant expression. After that, the cell culture was placed on ice to chill before the addition of isopropyl thio-β-D-galactoside (IPTG) to a final concentration of 0.2 mM was used to activate chitinase expression. Cell growth was maintained at 25 °C for 18 hours, after which the cell pellet was recovered by centrifugation at 4,500 rpm, 4 °C for 30 minutes. The pellet was resuspended in freshly made lysis buffer (20 mM Tris-HCl, 150 mM NaCl, pH 8.0, 1 mM PMSF, and 1 mg/mL egg white lysozyme), then lysed on ice with an ultra sonicator (Amp : 30 %, Pulse ON : 20 sec, OFF 40 sec, Timer : 40 minutes). Centrifugation at 12,000 rpm, 4 °C, for 45 minutes was used to eliminate unbroken cells and cell debris. The supernatant was immediately applied to a Ni-charged Resin affinity column (GenScript, Hong Kong), and gravity chromatography was performed at 4 °C. After loading, the column was equilibrated with the buffer containing 20 mM Tris-HCl, 150 mM NaCl, pH 8.0, and 20 mM imidazole. The bound proteins were eluted with 150 mM imidazole in the same buffer and eluted fractions of 5 mL were collected. To validate the purity, 20 μL of each fraction were tested on a 12% SDS-PAGE. For complete removal of imidazole, fractions with chitinase activity were pooled and exposed to repeated rounds of dialysis (Snake SkinTM Dialysis Tubing, 3.5 K MWCO, 35-mm dry I.D, Thermo Scientific) in the same buffer. The purified protein was concentrated using a centrifugal filter unit (Amicon Ultra-15 centrifugal filters Ultra cell-30 K) and stored at -80 °C until used.

Synthesis of magnetic nanoparticles (MNPs) and chitosan coated magnetic nanoparticles (CS@MNPs)

The uncoated MNPs and CS@MNPs were prepared by co-precipitation method described by Osuna et al. [26] with minor modification. For the uncoated MNPs, 50 mL of $FeCl_3 \cdot 6H_2O$ (0.32 M) and 50 mL of $FeSO_4 \cdot 7H_2O$ (0.32 M) were mixed and stirred at 400 rpm. Then, the reaction temperature was raised to 50 °C, and 40 mL of 30% NH_4OH solution was dropped into the mixture solution. After NH_4OH addition was completed, the completion reaction was allowed to proceed for 20 minutes. For the preparation of CS@MNPs, 50 mL of $FeCl_3 \cdot 6H_2O$ (0.32 M) and 50 mL of $FeSO_4 \cdot 7H_2O$ (0.32 M) were mixed and stirred at 400 rpm. Then, 0.125 g of chitosan was added to the reaction mixture and the temperature was raised to 50 °C. After the reaction temperature reached 50 °C, 40 mL of 30% NH_4OH solution was dropped into the mixture solution. After NH_4OH addition was completed, the completion reaction was allowed to proceed for 20 minutes. At the end of the reaction, the particles were recovered by using a permanent magnet, extracted 10 times with deionized (DI) water, and lyophilized to obtain the final product.

Preparation of hemin functionalized chitosan coated magnetic nanoparticles (Hemin@CS@MNPs)

The CS@MNPs was further functionalized by amidation reaction with hemin. To carry out the reaction, 25 mg of hemin was dissolved in 12.5 mL of *N,N*-dimethylformide (DMF), then 2.5 mL of 200 mM 1-Ethyl-3-(3-dimethylaminopropyl)carbodiimide (EDC) and 2.5 mL of 200 mM *N*-hydroxysuccinimide (NHS) were added into the mixture solution, the reaction was shaked at 25 °C, 180 rpm, for 1 hour. Then, 500 mg of CS@MNPs was added into the

mixture solution and the reaction was allowed to proceed for 16 hours. After the reaction completed, the synthesized Hemin@CS@MNPs were extracted 10 times with DI water and lyophilized to obtain the product in the powder form.

Immobilization of VhChiA

To immobilize *Vh*ChiA on to the synthesized MNPs, CS@MNPs, and Hemin@CS@MNPs, 10 mg of nanoparticles were placed into the microplate. Then 31.2 µL of purified *Vh*ChiA (10 mg/mL) and buffer (20 mM Tris-HCl, 150 mM NaCl, pH 8) were added to the final volume 500 µL. Then the immobilized solutions were incubated at 4 °C, 180 rpm, for 18 hours. The immobilized *Vh*ChiA was washed 3 times with buffer (20 mM Tris-HCl buffer, 150 mM NaCl, pH 8) to remove the unbound enzyme. The amount of the enzyme in the solutions before and after the immobilization process were measured by Bradford assay [27] and the immobilization yield were calculated as follows:

$$\%immobilization\ yield = \frac{amount\ of\ enzyme\ immobilized}{starting\ amount\ of\ enzyme} \times 100$$

Note: the amount of enzyme immobilized = starting amount of enzyme (mg/mL) - amount of unbound enzyme (mg/mL).

Characterization of immobilized VhChiA

The morphology and size of nanoparticles, before and after immobilization of *Vh*ChiA, were analyzed using scanning electron microscopy (SEM, JEOL JSM-7610F) and transmission electron microscopy (TEM, JEOL JEM-ARM200F). The infared spectra of all formulations: uncoated MNPs, CS@MNPs, Hemin@CS@MNPs, E@MNPs, E@CS@MNPs, and E@Hemin@CS@MNPs were analyzed with Fourier transform infrared spectroscopy (FTIR, PerkinElmer). Thermogravimetric analysis (TGA) of nanoparticles was performed in a thermogravimetric analyzer (TGA, Linseis STA PT1600).

RESULTS

VhChiA expression and purification

From the **Fig. 1**, the crude *Vh*ChiA extract was purified using a Ni-NTA column and analyzed the purity by SDS-PAGE, which showed more than 95% purity after purification. The molecular mass of the purified *Vh*ChiA was estimated to be 63 kDa on SDS-PAGE. The concentration of concentrated purified *Vh*ChiA fractions was determined to be *approx.* 10 mg/mL, which was appropriate for immobilization.

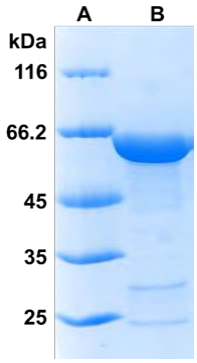

Figure 1 SDS-PAGE analysis of purified *Vh*ChiA. Lane A, protein markers; lane B, purified *Vh*ChiA.

Immobilization yield of immobilized VhChiA

The immobilization yield of immobilized *Vh*ChiA on uncoated MNPs, CS@MNPs, and Hemin@CS@MNPs were determined by Bradford assay, and calculated using equation below;

$$\%immobilization\ yield = \frac{amount\ of\ enzyme\ immobilized}{starting\ amount\ of\ enzyme} \times 100$$

From the Bradford assay result in the **Fig. 2A**, it was clearly observed that the amount of *Vh*ChiA in the supernatant after immobilization was almost dissappeared in CS@MNPs, followed by Hemin@CS@MNPs when compared to the amount of *Vh*ChiA in the supernatant before immobilization (Free *Vh*ChiA). For the uncoated MNPs, the amount of *Vh*ChiA after immobilization was not different from the amount of *Vh*ChiA before immobilization. From the calculation of %immobilization yield, the bar graph represents an average %immobilization yield from 3 replicate experiments, and error bar shows SD. It was found that CS@MNPs gave the highest immobilization yield of around 95.96±3.45%, followed by Hemin@CS@MNPs and uncoated MNPs which gave 87.70±1.95% and 29±4.99%, respectively (**Fig. 2B**).

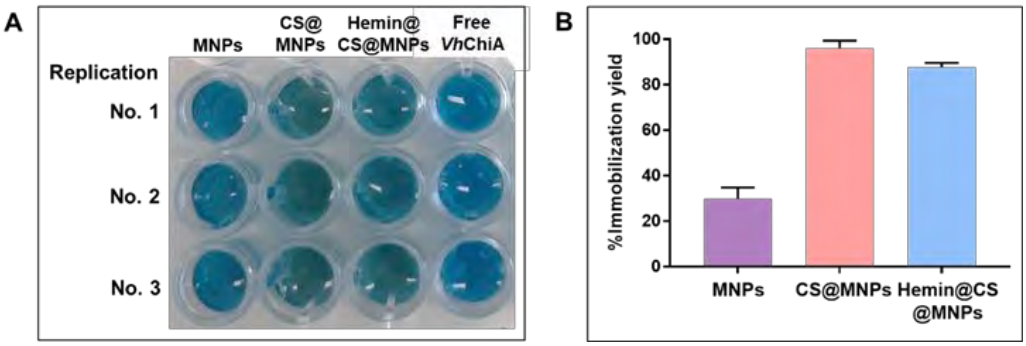

Figure 2 Immobilization yield of immobilized *Vh*ChiA. Bradford assay of free *Vh*ChiA and immobilized *Vh*ChiA on different carrier types (MNPs, CS@MNPs, and Hemin@CS@MNPs) (A). The bar graph represents an average %immobilization yield of immobilized *Vh*ChiA on different carrier types (MNPs, CS@MNPs, and Hemin@CS@MNPs) from 3 replicate experiments, and error bar shows SD (B).

Characterization of immobilized VhChiA using scanning electron microscopy (SEM)

Scanning electron microscopy was used to analyze the morphology surface of all nanoparticles including MNPs, CS@MNPs, and Hemin@CS@MNPs before and after immobilization. From **Fig. 3 (A-C)**, all free nanoparticles have rough spheroidal morphology and strong agglomeration due to the van der Waals forces between the particles. However, after *Vh*ChiA immobilization (**Fig. 3 (D-F)**), the surface of all nanoparticles is smooth. To gain more insight, the SEM-EDS element mapping was employed to examine the elemental components and their distributions. As shown in **Fig. 4 (A-M)**, it could be seen clearly that Fe and O were homogeneously distributed on all nanoparticles. For the CS@MNPs and Hemin@CS@MNPs, the N is distributed uniformly. However, due of the interference of C in the carbon tape used for sample preparation in SEM analysis, the C has a poor distribution. The present of N in CS@MNPs and Hemin@CS@MNPs were assigned as $-NH_2$ group of chitosan and N containing in porphyrin ring of hemin molecule, respectively. The results indicate that chitosan and hemin modification on the MNPs were successfully prepared.

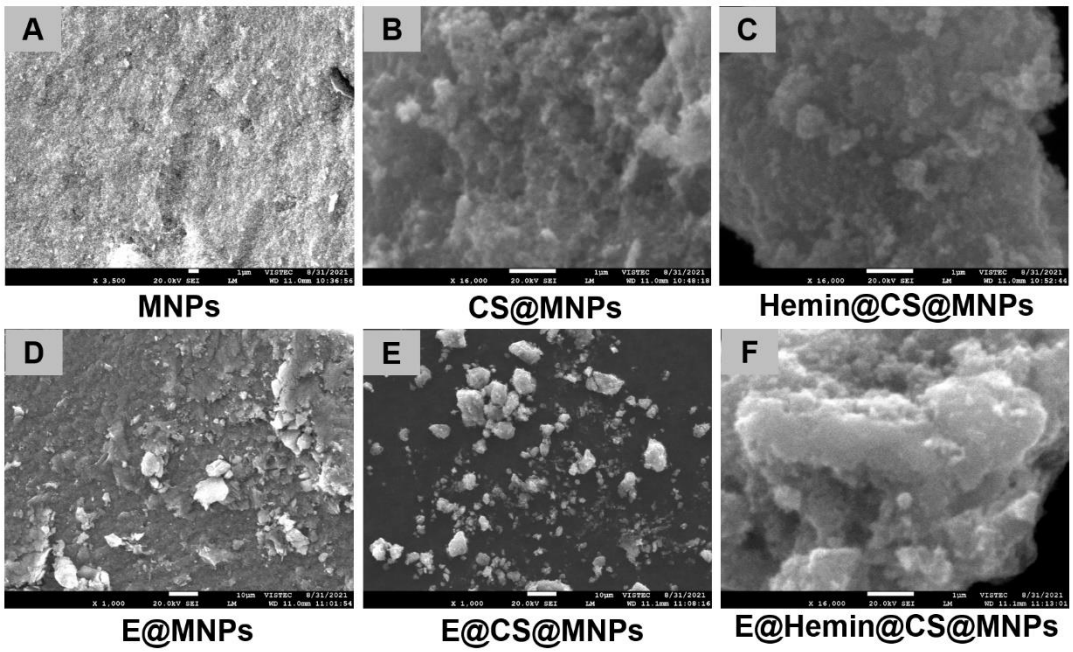

Figure 3 SEM images of all nanoparticles before (A-B) and after immobilization (D-F). MNPs (magnification: 3,500x) (A), CS@MNPs (magnification: 16,000x) (B), Hemin@CS@MNPs (magnification: 16,000x) (C), E@MNPs (magnification: 1,000x) (D), E@CS@MNPs (magnification: 1,000x), and E@Hemin@CS@MNPs (magnification: 16,000x) (F).

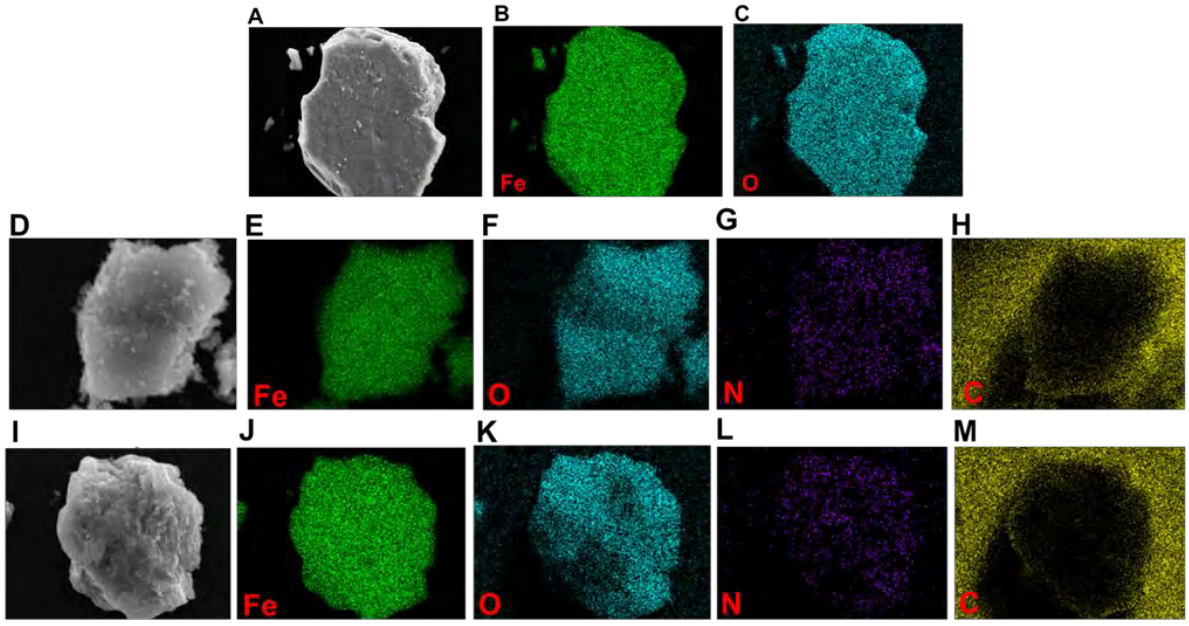

Figure 4 SEM images of all nanoparticles: MNPs (A), CS@MNPs (D), Hemin@CS@MNPs (I). Elemental mapping images of MNPs: Fe element (B), O element (C), CS@MNPs: Fe element (E), O element (F), N element (G), C element (H), Hemin@CS@MNPs: Fe element (J), O element (K), N element (L), C element (M).

Characterization of immobilized VhChiA using transmission electron microscopy (TEM)

Transmission electron microscopy (TEM) was used to observe the size and morphology of CS@MNPs. From the **Fig. 5**, The histogram shows the size of nanoparticles which ranged

from 5 to 15 nm. And in the **Fig. 6**, the nanoparticles have rough spheres shape and form scattered groups due to the forces of attraction between them.

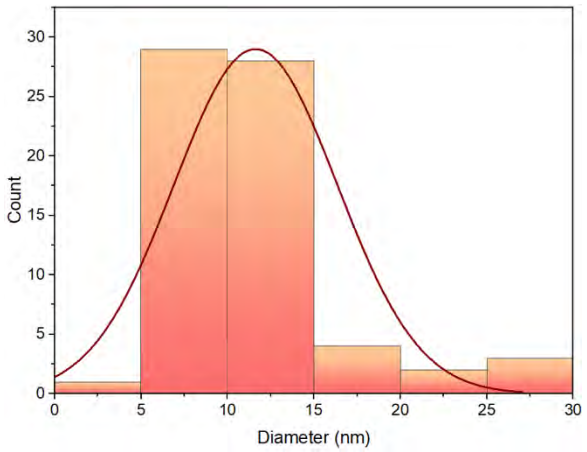

Figure 5 Nanoparticle diameter histogram of CS@MNPs.

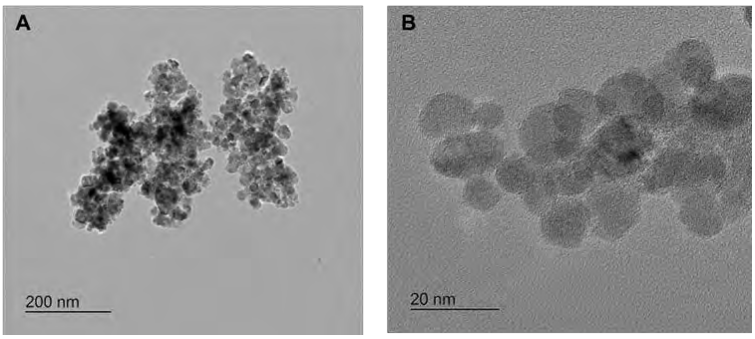

Figure 6 TEM micrographs of nanoparticles prepared by coprecipitation method with 0.125 % (w/v) of chitosan.

Characterization of immobilized VhChiA using Fourier transform infrared spectroscopy (FTIR)

FTIR characterization of all nanoparticles were shown in the **Fig. 7 (A-C)**. For the first formula of **Fig. 7A** (MNPs, blue line), there are two vibrations at 535 cm^{-1} and 1632 cm^{-1} that corresponded to Fe-O, and O-H bending of magnetic nanoparticles, respectively. In the E@MNPs spectrum (**Fig. 7A, dark brown line**), the vibrations of amide bond were observed at 1640 and 1525 cm^{-1} indicating that the *Vh*ChiA was successfully immobilized on the MNPs. For the CS@MNPs formula (**Fig. 7B**, red line), the additional characteristic absorption bands at 3335 cm^{-1} (O-H and N-H stretching vibrations), 1637 cm^{-1} (C=O stretching), and 1067 cm^{-1} (C-O-C stretching) which corresponded to the chitosan spectrum (**Fig. 7B**, purple line) were observed when compared to the MNPs spectrum, indicating that the chitosan was completely incoporated on the MNPs. For the E@CS@MNPs spectrum (**Fig. 7B**, green line), the absorption peak at 1645 cm^{-1} (C=O stretching) and 1531 cm^{-1} (C-N stretching and N-H bending) were assigned to the amide I and II of the peptide bonds [28] which confirming that the *Vh*ChiA was successfully immobilized on the CS@MNPs. For the **Fig. 7C**, there are two peaks were observed at 1539 and 1397 cm^{-1} in hemin@CS@MNPs spectrum (orange line) which corresponded to amide bond (C-N stretching and N-H bending), indicating that hemin functionalization by amidation reaction was completed. In addition, due to the vibration of

amide bond between -COOH group of hemin and -NH_2 of chitosan on MNPs and amide bond of enzyme on Hemin@CS@MNPs are the same, their FTIR spectrum of both formula: Hemin@CS@MNPs spectrum (orange line) and E@Hemin@CS@MNPs (light brown line) were not significantly different.

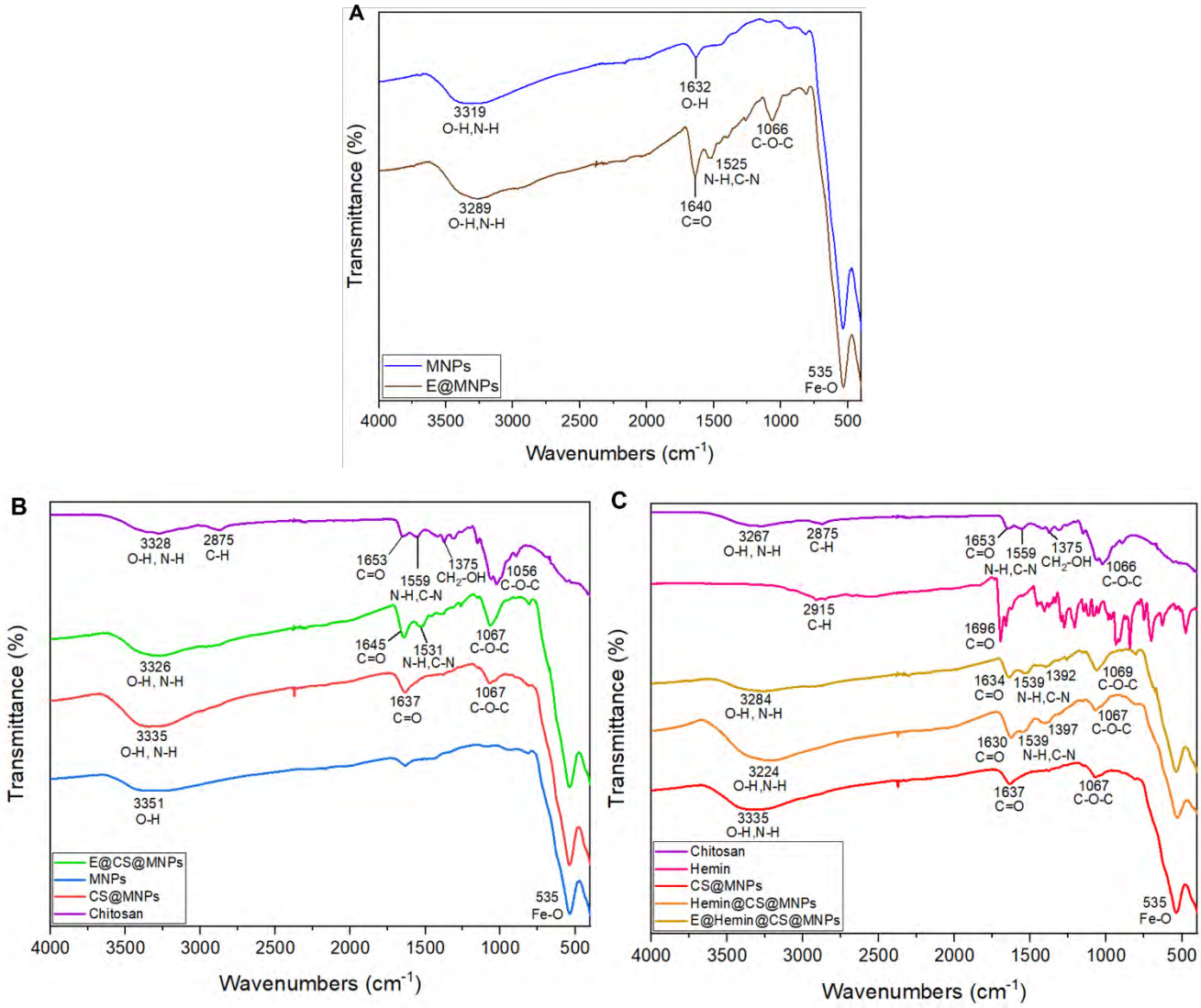

Figure 7 Fourier transform infrared spectroscopy (FTIR) spectra of MNPs (blue line), E@MNPs (dark brown line) (A). MNPs (blue line), CS@MNPs (red line), E@CS@MNPs (green line), and chitosan (purple line) (B). Hemin@CS@MNPs (orange line), E@hemin@CS@MNPs (brown line), hemin (pink line) (C).

Characterization of immobilized VhChiA using thermogravimetric analysis (TGA)

Thermogravimetric analysis was used to analyze thermal decomposition temperature of nanoparticles under nitrogen atmosphere at temperature range between 30 ºC to 900 ºC. As comparison, TGA was performed on CS@MNPs, E@CS@MNPs, and pure chitosan which are shown in the **Fig. 8A**. From these results, the first temperature region from 30 °C to 100 °C indicates the loss of water molecules, and 9.8% weight loss of CS@MNPs (**Fig. 8A, red line**) was observed, which indicated the amount of chitosan content in the MNPs. In addition, E@CS@MNPs (**Fig. 8A, blue line**) showed 18.04% weight loss which belong to the *Vh*ChiA

content in the CS@MNPs, indicating the amount of enzyme that was immobilized on the CS@MNPs. For the Hemin@CS@MNPs (**Fig. 8B, purple line**), the TGA profile showed 8.29 and 7.39% weight loss which were assigned as the hemin and chitosan contents, respectively, while the large region weight loss around 50.122% in E@Hemin@CS@MNPs (**Fig. 8B, blue-green line**) were defined as the hemin and *Vh*ChiA contents on the nanoparticles.

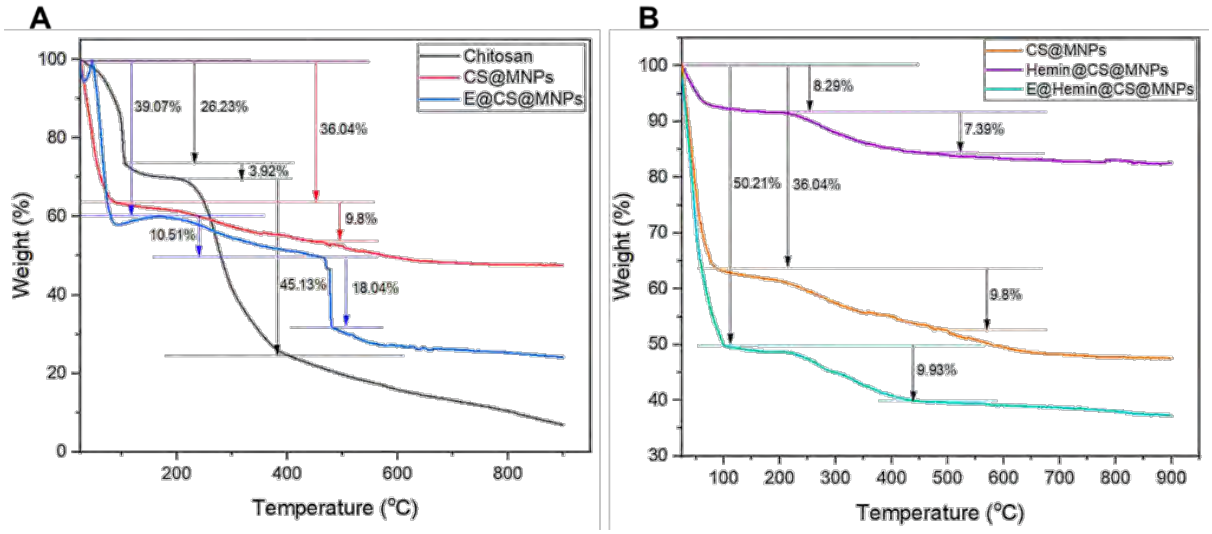

Figure 8 Thermal degradation curves of nanoparticles prepared by co-precipitation method: the down arrows indicate the %weight loss of each component in nanoparticles. TGA analysis of CS@MNPs (red line), E@CS@MNPs (blue line), and pure chitosan (black line) (A). TGA analysis of Hemin@CS@MNPs (purple line), E@Hemin@CS@MNPs (blue-green line), and CS@MNPs (orange line) (B).

DISCUSSION AND CONCLUSION

In this research, *Vh*ChiA was successfully immobilized on all three types of MNPs including uncoated MNPs, CS@MNPs, and Hemin@CS@MNPs. The uncoated MNPs and CS@MNPs grafted the *Vh*ChiA using physical adsorption through electrostatic interaction. According to the biocompatibility of chitosan and large surface area of MNPs making the chitosan coated MNPs is an appropriate carrier for immobilization. In addition, using physical adsorption method through electrostatic interaction between $-NH_3^+$ group of chitosan and $-COO^-$ group of amino acid residue of enzyme provided many advantages such as the conformational of enzyme is not change, the catalytic activity of enzyme is not affected, and high amount of enzyme loading. Moreover, Hemin@CS@MNPs immobilized *VhChiA* through His-tag affinity interaction also not effect to the enzyme structure because the iron center of the hemin molecule coordinates with His-tag of *Vh*ChiA. From the immobilization results, CS@MNPs provided the highest immobilization yield around 95%, followed by Hemin@CS@MNPs and uncoated MNPs that gave 87% and 29%, respectively, which was higher than the recently report in which they immobilized chitinase on the amine functionalized MNPs through covalent bonding using glutaraldehyde as linking agent and provided only 62% immobilization yield [22]. The TEM and SEM characterization showed that the free nanoparticles have rough spherical morphology with diameter in the range of 5-15 nm and form scattered group while after *Vh*ChiA immobilization, the nanoparticles have changed to smooth surface. The SEM-EDS analysis exhibited homogenously elemental distribution of Fe and O in all nanoparticles. In addition, the present of N and C on the CS@MNPs and

Hemin@CS@MNPs indicated the successfully of chitosan and hemin incorporation. The results of the FTIR spectra indicated the enzyme was immobilized on the carrier, the vibration in the range of 1600-1670 and 1500-1570 cm^{-1} was observed in the immobilized *Vh*ChiA which belong to the amide bond of enzyme. Interestingly, the TGA analysis showed 18.04% weight loss in the CS@MNPs which indicated the high content of *Vh*ChiA in the CS@MNPs.The immobilized *Vh*ChiA can expand the use of enzymes in industrial applications in which the enzyme can be easily separated from the reaction and recycled using the external magnetic force.

ACKNOWLEDGEMMENTS

This research was supported by Vidyasirimedhi Institute of Science and Technology (VISTEC) and The Thailand Research Fund (TRF) through The Basic Research Grant (Grant no: BRG610008), and Thailand Science Research and Innovation (TSRI) under the Global Partnership Grant. RT received the full-time PhD Scholarship from VISTEC.

REFERENCES

1. 1. Hamed I, Fatih Oz, Joe MR. Industrial applications of crustacean by-products (chitin, chitosan, and chitooligosaccharides): A review. Trends in food science & technology. 2016;48:40-50.
2. Kim EK, Je JY, Lee SJ, Kim YS, Hwang JW, Sung SH, et al. Chitooligosaccharides induce apoptosis in human myeloid leukemia HL-60 cells. Bioorg Med Chem Lett. 2012;22(19):6136-8.
3. Artan M, Karadeniz F, Karagozlu MZ, Kim MM, Kim SK. Anti-HIV-1 activity of low molecular weight sulfated chitooligosaccharides. Carbohydr Res. 2010;345(5):656-62.
4. Wu SJ, Pan SK, Wang HB, Wu JH. Preparation of chitooligosaccharides from cicada slough and their antibacterial activity. Int J Biol Macromol. 2013;62:348-51.
5. Sánchez Á, Mengíbar M, Fernández M, Alemany S, Heras A, Acosta N. Influence of Preparation Methods of Chitooligosaccharides on Their Physicochemical Properties and Their Anti-Inflammatory Effects in Mice and in RAW264.7 Macrophages. Mar Drugs. 2018;16(11).
6. Garcia-Galan C, Berenguer-Murcia Á, Fernandez-Lafuente R, Rodrigues RC. Potential of Different Enzyme Immobilization Strategies to Improve Enzyme Performance. Advanced Synthesis & Catalysis. 2011;353(16):2885-904.
7. Sheldon RA. Enzyme Immobilization: The Quest for Optimum Performance. Advanced Synthesis & Catalysis. 2007;349(8-9):1289-307.
8. Datta S, Christena LR, Rajaram YR. Enzyme immobilization: an overview on techniques and support materials. 3 Biotech. 2013;3(1):1-9.
9. Sheldon RA, van Pelt S. Enzyme immobilisation in biocatalysis: why, what and how. Chem Soc Rev. 2013;42(15):6223-35.
10. Bezerra C, Lemos CMG, Sousa M, Gonçalves L. Enzyme immobilization onto renewable polymeric matrixes: Past, present, and future trends. Journal of Applied Polymer Science. 2015;132.
11. Cantone S, Ferrario V, Corici L, Ebert C, Fattor D, Spizzo P, et al. Efficient immobilisation of industrial biocatalysts: criteria and constraints for the selection of organic polymeric carriers and immobilisation methods. Chem Soc Rev. 2013;42(15):6262-76.
12. Hartmann M, Kostrov X. Immobilization of enzymes on porous silicas – benefits and challenges. Chemical Society Reviews. 2013;42(15):6277-89.

13. Wang X, Lan PC, Ma S. Metal–Organic Frameworks for Enzyme Immobilization: Beyond Host Matrix Materials. ACS Central Science. 2020;6(9):1497-506.
14. Zdarta J, Meyer AS, Jesionowski T, Pinelo M. A General Overview of Support Materials for Enzyme Immobilization: Characteristics, Properties, Practical Utility. Catalysts. 2018;8(2):92.
15. Jesionowski T, Zdarta J, Krajewska B. Enzyme immobilization by adsorption: a review. Adsorption. 2014;20(5):801-21.
16. Cao L. Covalent Enzyme Immobilization. 2006. p. 169-316.
17. Trevan MD. Enzyme immobilization by entrapment. Methods Mol Biol. 1988;3:491-4.
18. Rother C, Nidetzky B. Enzyme Immobilization by Microencapsulation: Methods, Materials, and Technological Applications. Encyclopedia of Industrial Biotechnology. p. 1-21.
19. Nguyen HH, Kim M. An Overview of Techniques in Enzyme Immobilization. Applied Science and Convergence Technology. 2017;26:157-63.
20. Prasad M, Palanivelu P. Immobilization of a thermostable, fungal recombinant chitinase on biocompatible chitosan beads and the properties of the immobilized enzyme. Biotechnol Appl Biochem. 2015;62(4):523-9.
21. Esawy MA, Awad GEA, Wahab WAA, Elnashar MMM, El-Diwany A, Easa SMH, et al. Immobilization of halophilic Aspergillus awamori EM66 exochitinase on grafted k-carrageenan-alginate beads. 3 Biotech. 2016;6(1):29.
22. Kidibule PE, Costa J, Atrei A, Plou FJ, Fernandez-Lobato M, Pogni R. Production and characterization of chitooligosaccharides by the fungal chitinase Chit42 immobilized on magnetic nanoparticles and chitosan beads: selectivity, specificity and improved operational utility. RSC Advances. 2021;11(10):5529-36.
23. Preety, Hooda V. A novel polyurethane/nano ZnO matrix for immobilization of chitinolytic enzymes and optical sensing of chitin. International Journal of Biological Macromolecules. 2018;106:1173-83.
24. Ismail SA, Hassan ME, Hashem AM. Single step hydrolysis of chitin using thermophilic immobilized exochitinase on carrageenan-guar gum gel beads. Biocatalysis and Agricultural Biotechnology. 2019;21:101281.
25. Suginta W, Vongsuwan A, Songsiriritthigul C, Prinz H, Estibeiro P, Duncan RR, et al. An endochitinase A from Vibrio carchariae: cloning, expression, mass and sequence analyses, and chitin hydrolysis. Arch Biochem Biophys. 2004;424(2):171-80.
26. Osuna Y, Gregorio-Jauregui KM, Gaona-Lozano JG, de la Garza-Rodríguez IM, Ilyna A, Barriga-Castro ED, et al. Chitosan-Coated Magnetic Nanoparticles with Low Chitosan Content Prepared in One-Step. Journal of Nanomaterials. 2012;2012:327562.
27. Bradford MM. A rapid and sensitive method for the quantitation of microgram quantities of protein utilizing the principle of protein-dye binding. Analytical Biochemistry. 1976;72(1):248-54.
28. Tatulian S. Structural Characterization of Membrane Proteins and Peptides by FTIR and ATR-FTIR Spectroscopy. Methods in molecular biology (Clifton, NJ). 2013;974:177-218.

Proceeding PP008

CRISPR-based detection for identifying snake species from snakebite envenoming

Rodjarin Kongkaew*, Kanokpol Aphicho, Surased Suraritdechachai, Maturada Patchsung, and Chayasith Uttamapinant

School of Biomolecular Science and Engineering (BSE), Vidyasirimedhi Institute of Science and Technology (VISTEC), Rayong 21210 Thailand

***Email**: rodjarin.k_s19@vistec.ac.th

ABSTRACT

Snakebite envenoming is a neglected tropical disease which causes broad symptoms ranging from mild to high severity, affecting healthcare management and economy of tropical developing countries including Thailand. Multiple venomous snake species are distributed throughout different regions in Thailand, and it is not trivial to identify snake species upon getting bitten based on old-fashioned means, rendering timely administration of the antivenom difficult or impossible. Here, we propose the development of a point-of-care genotyping tool based on CRISPR for rapid and accurate identification of snake species from bite wounds. DNA regions within the mitochondrial *cytochrome b* (*cytb*) gene of eight venomous snake species endemic to Thailand—*O. hannah*, *N. kaouthia*, *C. rhodostromata*, *D. russelii*, *D. siamensis*, *T. albolabris*, *B. fasciatus*, and *B. candidus*—were chosen as targets for CRISPR-Cas13a-mediated detection, which utilizes recombinase-polymerase amplification (RPA) and *Leptotrichia wadei* (Lwa) Cas13a for maximal detection sensitivity and specificity. We successfully prepared all biomolecular components necessary for the RPA/LwaCas13-based detection of the *cytb* gene from different snake species, optimized their detection conditions, validated their specificity, and assessed their analytical sensitivity upon detection of surrogate DNA substrates. Detection modules with sufficiently high sensitivity will be used to detect the *cytb* gene from biological fluids obtained from snakes in the near future.

Keywords: CRISPR-Cas13; RPA; snakebite; tropical disease

INTRODUCTION

It was estimated in 2005 that more than 5.4 million people were bitten by snakes, with up to 2.7 million envenoming (injection of the venom into the bite) [1,2]. In 2009, approximately 81,000 to 138,000 people die globally from snakebites [2] and in 2017 more than 100,000 snakebite-related deaths occurred [3]. Most cases have occurred in Africa, Asia, and Latin America; in Asia, up to 2 million people were reported to be envenomed in 2017 [3]. Most injuries and disabilities occur in poor, rural communities. Snakebite envenoming thus is an important yet neglected tropical disease in many tropical and subtropical countries, including Thailand [3,4].

Each venomous snake species has different compositions of venom [3,5]. The venom is made of toxins, enzymes, and non-toxic substances, the composition of which is complex and can be highly variable [6]. Venoms are classified into 2 main types: hemotoxins and neurotoxins. Hemotoxic venoms, typically found in Viperidae families, contain proteins that can disrupt the coagulation cascade, the hemostatic system, causing tissue bleeding,

incoagulable blood, and local tissue necrosis, while neurotoxins, found in Elapidae and Hydrophiidae families, primarily affect the peripheral nervous system [6,7]. Bites by venomous snakes can cause severe injuries including: paralysis that may obstruct breathing; bleeding disorders that can lead to fatal hemorrhage; irreversible kidney failure; and tissue damage that may require limb amputation and permanent disability [3]. The only effective treatment for snake envenoming is intravenous administration of a high-quality—and correct—species-specific antivenin/antivenom. Antivenoms are highly specific and can neutralize only the venoms used in their production [7]. Several methods can be used to empirically identify snake species for correct antivenom administration. Examining the captured/killed snake or its photo/image, verbal description by the victim, associated clinical symptoms, and laboratory methods (described in more detail below) are common methods at medical facilities [8]. However, there remain no standardized point-of-care protocols, resulting in a significant risk of snake misidentification and unnecessary or even incorrect antivenom administration. Given the variability in symptom manifestation time, from a few minutes to several days or weeks, misidentification or failure to administer antivenoms at the point of care is often found. Laboratory-based methods that can assist correct antivenom administration include radioimmunoassay, agglutination assay [9], enzyme-linked immunosorbent assay [10], and molecular techniques. In Australia, the widely distributed snake venom detection kit, SVDK, is based on an enzyme immunoassay in which well plates are coated with antibodies specific to various snake venoms [11]. However, such an assay is known to have cross-reactivity problems and misidentification of rare species [11]. Molecular detection of snake types based on PCR amplification of DNA collected from venoms/snake bites have also been developed to identify snake types with high specificity and sensitivity [12]. However, the use of PCR or real-time PCR techniques is cumbersome in resource-limited settings (RLS), requiring laboratory setup and trained staff, and can take a long thermocycling time before obtaining results [13,14,15]. Thus, there is arguably a need for a new snake type identification method that is easy to use, does not require complex setup or instrumentation, is highly specific and sensitive, and can be performed rapidly at point-of-care settings, to facilitate timely administration of correct antivenoms [16].

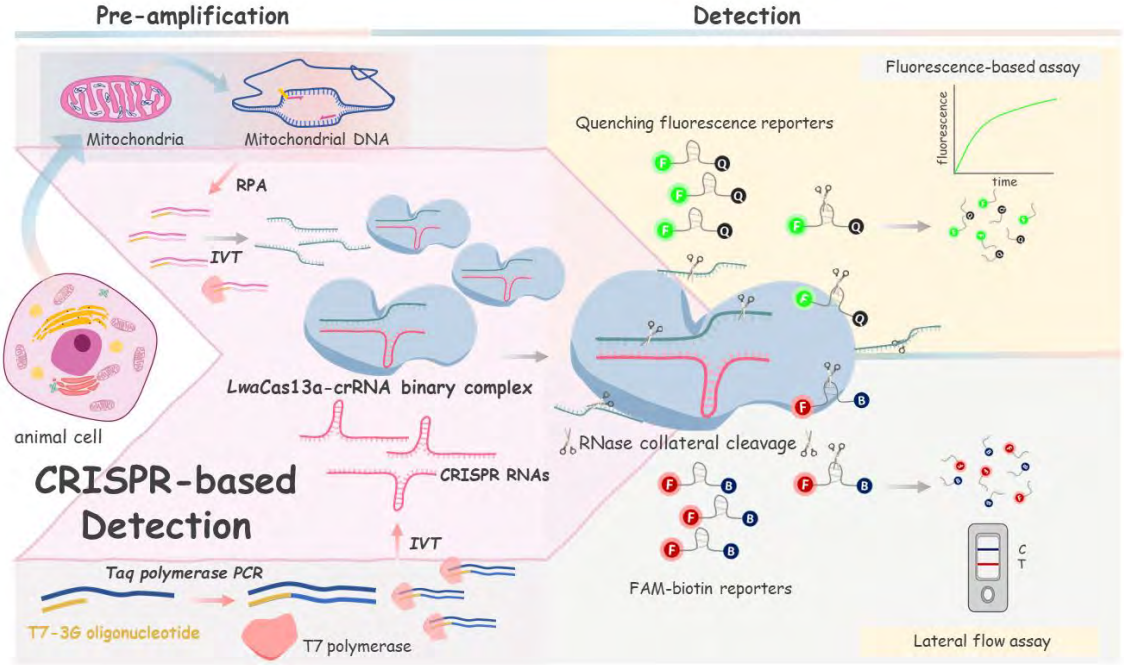

Figure 1 Schematic of the CRISPR-based detection to detect snake mitochondrial DNA

Key to the technology is an RNA-guided/RNA-targeted CRISPR-associated enzyme Cas13a from *Leptotrichia wadei* (LwaCas13a) which exhibits collateral cleavage activity of bystander RNA probes upon activation through recognition of target RNA, via a programmable CRISPR RNA (crRNA). Cas13a does not have a strict PAM requirement, allowing high flexibility in choosing the targeting site, and can be coupled to both DNA- and RNA-based detection via the use of enzymes that can interconvert RNA and DNA i.e., reverse transcriptase and RNA polymerase [17,18,19].

To maximized detection sensitivity and specificity, the LwaCas13a-based CRISPR detection reaction can be coupled to an isothermal amplification technique, such as Recombinase Polymerase Amplification (RPA) [18] or loop-mediated isothermal amplification (LAMP) [26]. This genetic pre-amplification step can also be combined in the same reaction vessel/pot as the CRISPR-Cas reaction, making the assay easier and faster to perform [18,19]. Diverse DNA and RNA species, especially from pathogens, have been demonstrated as a target for detection with SHERLOCK (specific high-sensitivity enzymatic reporter unlocking) and related DETECTR technologies. To date, some demonstrated applications include detection of emerging viruses such as HIV, Zika, and Dengue [19], Ebola and Lassa viruses [20], SAR-CoV-2 [21], and the detection of *Plasmodium* species in a field-ready setup [22].

Here, we propose to apply a CRISPR-Cas13a based assay for snake species-specific detection of the mitochondrial cytochrome b gene (*cytb*) as shown in **Fig. 1**. Previous studies suggested that *cytb* can be used as a genetic marker to differentiate both the genus and species level of snake type according to the intraspecific and interspecific variations [13]. Furthermore, previous studies have shown that both genomic and mitochondrial DNA can be extracted from dried venom and obtained from bitten positions by swabbing [13,14,17]. To detect trace DNA in a sample, we propose to use SHERLOCK, a CRISPR-Based Diagnostic (CRISPR-Dx) platform [17]. SHERLOCK uses a combination of nucleic acid pre-amplification with CRISPR-Cas enzymology for specific recognition of target DNA or RNA. The technology allows multiplexed, portable, and ultra-sensitivity and provide result less than 1 hour, with a setup time of less than 15 min, and is compatible with multiple modes of readout including fluorescence, lateral flow or turbidity-based detection, depending on the reporter molecule of choice [17]. In this study, we examine venomous snake species distributed in Thailand [5,13,23] and design the SHERLOCK fluorescence-based assay for the detection of these snake species. We took into consideration the most prevalent venomous snake species in Thailand, for which there is local production of antivenoms [24]. In total, we selected eight snake species to develop the SHERLOCK-based genotyping technology: *Ophiophagus hannah* (King Cobra), *Naja kaouthia* (Cobra), *Calloselasma rhodostoma* (Malayan Pit Viper), *Daboia russelii* (Russell's Viper), *D. siamensis*, *Trimeresurus albolabris* (Green Pit Viper), *Bungarus fasciatus* (Banded Krait), and *B. candidus* (Malayan Krait) [5,23]. Venoms from all eight species can be neutralized by a selection from nine equine antivenoms: eight for species-specific monovalent antivenoms, and two polyvalent pan-species antivenoms [24].

MATERIALS AND METHODS

Design of specific SHERLOCK: RPA primer pairs, target sites, and their specific crRNAs

We targeted *cytb* of the snake mitochondrial DNA for SHERLOCK detection. DNA sequences of *cytb* were downloaded from the nucleotide database, National Center for Biotechnology Information (NCBI), as Fasta format files. The reference sequence for each species was from isolates collected in Thai or South-East Asia regions. To investigate consensus and non-consensus regions among sequences, the sequences from selected species

were aligned by sequences submission into MAFFT high-speed multiple sequence alignment program [25] by multiple sequence alignment EMBL-EBI tool, and the alignment visualized with Jalview 2.11.1.1 program. Specific sites within *cytb* for SHERLOCK detection were selected for their conservation within species and lack of conservation among different species, and RPA primers were designed for these regions. crRNAs which can detect the RPA amplicons were further designed to allow sequence-specific Cas13a-mediated recognition of the RPA amplicons and subsequent Cas-mediated signal generation for detection. Using two sequence-specific steps in SHERLOCK detection (genetic amplification, then CRISPR-Cas) ensures high specificity of detection and minimal cross-reactivity. RPA primers were designed manually and included a 5'-T7-promoter sequence. The amplicon size was kept short at ~100 bp for efficient amplification. Furthermore, crRNAs were designed according to LwaCas13a preference, with a 28-bp spacer and a 32-bp direct repeat (DR) sequence. To allow the production of crRNAs via T7-based *in vitro* transcription (IVT), we designed crRNAs to contain a T7 promoter. All oligonucleotides were designed using SnapGene 5.2. and purchased from IDT.

Sample preparation

To produce synthetic dsDNA templates for analysis of the limit of detection (LoD) [27], we purchased single-strand sense and antisense oligonucleotides (60-90 bp in length) from IDT. The partially complementary oligonucleotides were annealed then amplified by *Taq* DNA polymerase-mediated PCR. The PCR products were purified using a DNA purification kit (Zymogen). Thereafter, we determined the dsDNA concentration using a spectrophotometer (BioSpectrometer, Eppendorf). A calibration curve of DNA concentrations and absorbance at 260 nm (A_{260}) was generated using 0.001-1 µg/mL λ-phage DNA. Molar concentrations of DNAs were calculated from their weight concentrations using their estimated molecular weights (number of base pairs multiplied by the average molecular weight of a deoxynucleotide unit in DNA, 330 g/mol). We prepared DNA templates for RPA LoD measurements via serial dilutions to generate a concentration range of nanomolar to attomolar (10^{-9}-10^{-18} M). The molar concentrations can be converted to DNA copy numbers per unit volume by multiplying the concentration values with the Avogadro's number (6.022×10^{23} molecules/mole). For the negative control with no DNA template, we used DEPC-treated water.

We have not performed DNA extraction and detection from real snake samples but have conceived of the plan to do so. Saliva samples from snakes with clear species identification by a specialized herpetologist will be obtained through collaboration with Queen Saovabha Memorial Institute (QSMI). DNA can be extracted from the saliva samples using QIAamp DNA Blood Mini Kit and used as the input for RPA. We will also test if we can bypass column-based DNA extraction by employing the HUDSON (heating unextracted diagnostic samples to obliterate nucleases) protocol for rapid cell lysis and DNA release [28]. For HUDSON, cells can be lyzed in 2 steps: heat treatment at 55˚C for 15 minutes followed by heating at 98˚C for 5 minutes with the addition of proteinase K and 100 mM TCEP/1 mM EDTA. The crude lysates can potentially be used directly as the input for RPA.

crRNA production by in vitro transcription and purification

We synthesized CRISPR RNA by *in vitro* transcription (IVT) using an adapted protocol from the RiboMAX Large Scale RNA Production kit. First, we generated a dsDNA template for transcription by amplifying synthetic oligonucleotide (dsDNA) with a primer with a T7 promoter overhang. The PCR products were purified using a DNA purification kit (Zymogen), analyzed for correct size using agarose gel electrophoresis, and concentrations determined via

spectroscopic measurements. The IVT reactions were set up using RiboMAX Large Scale RNA Production System-T7 (Promega), as follows: 4 µL 5x T7 transcription buffer, 6 µL NTP mix 25 mM each, 1 µL of 10 µM crRNA DNA template, 2 µL T7 polymerase, and 7 µL UltraPure water to 20 µL total reaction volume. After incubating at 37°C overnight, the transcribed RNAs were treated with DNase at 37ºC for 15-30 min then purified in two steps: first with VAHTS RNA Clean Beads (Vazyme Biotech), followed by phenol-chloroform precipitation. Precipitated RNAs were resuspended in DEPC-treated water, concentrations spectroscopically determined, and analyzed with 15% 7.5 M urea denaturing PAGE for correct size and purity.

Isothermal amplification via recombinase polymerase amplification (RPA)

RPA reaction mix can be prepared for 5 reactions by resuspending an RPA pellet (TwistAmp Basic kit, TwistDx) with 29.5 µL of rehydration buffer (provided by kit), 5 µL of RPA forward and reverse primers mix, 1 µL DEPC-treated water then mix and aliquot 7.1 µL and transfer to a clean tube following by add 0.7 µL MgOAc and 6.5 µL sample input for each aliquoted reaction. The reactions can be incubated at 42°C for 25 min by using a thermal shaking incubator. The protocol adapted from the protocol [21]. The RPA product was then used as a sample of Cas13 detection reaction according to the two-pot SHERLOCK protocol.

Cas13-SHERLOCK nucleic acid detection via fluorescence-based detection assay

Cas13-SHERLOCK nucleic acid detection signal can be visualized via fluorescence. The CRISPR Cas-13a detection reaction can be prepared using the RPA product as a sample. To set up the reaction, we prepared the detection reaction in a precooled 1.5 mL microcentrifuge tube with the following components: 9.5 µL DEPC-treated water, 0.4 µL HEPES (1 M stock pH 6.8), 1 µL $MgCl_2$ (120 mM stock), 0.8 µL ribonucleotide triphosphate mix (25 mM stock), 2 µL LwaCas13a enzyme in storage buffer (63.3 µg/mL enzyme stock concentration), 1 µL Riboguard RNase inhibitor (40 U/µL; Lucigen), T7 RNA polymerase (0.6 µL, 50 U/µL stock; Lucigen), 1 µL of crRNA (10 ng/µL stock), and 1.25 µL FAM-Iowa Black PolyU reporter (2 µM stock; IDT). The master mix containing sufficient reagents based on individual reactions can be prepared, and 18 µL of the master mix aliquoted to a 384-well plate. The Cas13 reactions were initiated by adding 2 µL of the RPA product. We incubated the reactions at 37°C over 60 min and measured FAM fluorescence kinetics at 1-min intervals in a Varioskan LUX multimode microplate reader.

LoD determination and data analysis

For LoD analysis with synthetic dsDNA input, we varied concentrations from nanomolar to attomolar as described in the sample preparation section. At least 3 replicates of each DNA concentration were performed. For each measurement, background-subtracted fluorescence measurement values were calculated by subtracting fluorescence measurement values from the no-DNA template negative control, at the same measurement time.

RESULTS

The designed sequences for the snake detections

We designed DNA sequences of specific SHERLOCK including crRNA IVT templates, RPA primer pairs, and the synthetic oligonucleotides for analytical LoD and snake species-specific nucleic acid detection shown in **Table 1**.

Table 1 The designed sequences for SHERLOCK snake detection**.**

Name	Sequence	Purpose
synT7crRNA13a_O_hannah 1	AGATGTGCCTTACGGATGAACCATACAAGTTTTAGTCCCCTTCGTTTTTGGGGTAGTCTAAATCCCCTATAGTGAGTCGTATTAATTTC	crRNA IVT template for *O.hannah* target 1
synT7crRNA13a_O_hannah 2	GCGCATCCATATTCTTCATCTGCATTTAGTTTTAGTCCCCTTCGTTTTTGGGGTAGTCTAAATCCCCTATAGTGAGTCGTATTAATTTC	crRNA IVT template for *O. hannah* target 2
N-kaou_crRNA13a	CACGGGACGTGCCTTACGGGTGAATCATGTTTTAGTCCCCTTCGTTTTTGGGGTAGTCTAAATCCCCTATAGTGAGTCGTATTAATTTC	crRNA IVT template for *N. kaoutai*
C-rhod_crRNA13a	ATAACACTGCTAACAACAATAATCACCCGTTTTAGTCCCCTTCGTTTTTGGGGTAGTCTAAATCCCCTATAGTGAGTCGTATTAATTTC	crRNA IVT template for *C. rhodostromata*
D-russ1_crRNA13a	ATCCCTATTCTTTGTTTGTATCTATATAGTTTTAGTCCCCTTCGTTTTTGGGGTAGTCTAAATCCCCTATAGTGAGTCGTATTAATTTC	crRNA IVT template for *D. russelii*
D-siam_crRNA13a	TGACCCAAACATAATAAACGACCCAGAGGTTTTAGTCCCCTTCGTTTTTGGGGTAGTCTAAATCCCCTATAGTGAGTCGTATTAATTTC	crRNA IVT template for *D. siamensis*
T-albo_crRNA13a	CTCAGGCACAACCCTTTTAATCATCTTAGTTTTAGTCCCCTTCGTTTTTGGGGTAGTCTAAATCCCCTATAGTGAGTCGTATTAATTTC	crRNA IVT template for *T. albolabris*
B-fasc_crRNA13a	ATCCATACCATTCCTACAAAGATATATTGTTTTAGTCCCCTTCGTTTTTGGGGTAGTCTAAATCCCCTATAGTGAGTCGTATTAATTTC	crRNA IVT template for *B. fasciatus*
B-cand_crRNA13a	CCGCCCTATTAATCACTCTAATAGCAACGTTTTAGTCCCCTTCGTTTTTGGGGTAGTCTAAATCCCCTATAGTGAGTCGTATTAATTTC	crRNA IVT template for *B. candidus*
O-hannah_cytb_F RPA primer1	GAAATTAATACGACTCACTATAGGGATCTAGCCTTCTCATCCGTAATTCACATCACTCG	RPA primer for pre-amplification of *O. hannah* DNA target 1
O-hannah_cytb_R RPA primer1	ATGAAGAATATGGATGCGCCGATTGCGTGAAGGTT	RPA primer for pre-amplification of *O. hannah* DNA target 1
O-hannah_cytb_F RPA primer2	GAAATTAATACGACTCACTATAGGGTACGGATGAACCATACAAAACCTTCACGCAATCG	RPA primer for pre-amplification of *O. hannah* DNA target 2
O-hannah_cytb_R RPA primer2	AAGATCCATAGTAGATTCCTCGTGCGATGTGGATA	RPA primer for pre-amplification of *O. hannah* DNA target 2
N-kaou_F-RPA-Primer	GAAATTAATACGACTCACTATAGGGTATCAACCTGGCCTTCTCATCAGTAATTCACATCA	RPA primer for pre-amplification of *N. kaouthai*
N-kaou_R-RPA-Primer	AGAATAGGGATGCGCTGATTGTGTGAAGGTTTTGT	RPA primer for pre-amplification of *N. kaouthai*
C-rhod_F-RPA-Primer	GAAATTAATACGACTCACTATAGGGAAATCCCATTTCACCCATATCACTCTTACAAAGAC	RPA primer for pre-amplification of *C. rhodostromata*
C-rhod_R-RPA-Primer	TATATCTGGGCAGAATGATAGGATAATAAATAGAA	RPA primer for pre-amplification of *C. rhodostromata*
D-russ_F-RPA-Primer	GAAATTAATACGACTCACTATAGGGGGCTGAATTATACAAAATTCACACGCCATCGGCGC	RPA primer for pre-amplification of *D. russelii*
D-russ_R-RPA-Primer	AGGTAAGATCCATAATAGAGGCCTCGTGCAATGTG	RPA primer for pre-amplification of *D. russelii*
D-siam_F-RPA-Primer	GAAATTAATACGACTCACTATAGGGATATTAATTACAGCCATACTTATTATCCTATCATT	RPA primer for pre-amplification of *D. siamensis*
D-siam_R-RPA-Primer	TGTGGGGTGACTAGGGGGTTAGCTTTAGAGAAGTT	RPA primer for pre-amplification of *D. siamensis*
T-albo_F-RPA-Primer	GAAATTAATACGACTCACTATAGGGTACTACGGCTCCTATCTTAACAAAGAAGTATGACT	RPA primer for pre-amplification of *T. albolabris*
T-albo__R-RPA-Primer	CATGGTAGTACATAGCCAAAGAAGGCTGTGGCTAT	RPA primer for pre-amplification of *T. albolabris*
B-fasc_F-RPA-Primers	GAAATTAATACGACTCACTATAGGGTGGCACTAACTCAGATATTGATAAAATCCCATTAC	RPA primer for pre-amplification of *B. fasciatus*
B-fasc_R-RPA-Primers	TAATGAATAATATAGTGATTATGATGCTAATTATT	RPA primer for pre-amplification of *B. fasciatus*
B-cand_F-RPA-Primers	GAAATTAATACGACTCACTATAGGGTCTATACCTCAATAAAGAAGTCTGATTATCAGGAA	RPA primer for pre-amplification of *B. candidus*
B-cand_R-RPA-Primers	TTTGTCCTCATGGGAGGACGTAGCCAAAGAAAGCT	RPA primer for pre-amplification of *B. candidus*
O-hann_sense1	ATCTAGCCTTCTCATCCGTAATTCACATCACTCGAGATGTGCCTTACGGATGAACCATACAAAACCTTCACGCAATCGGCGCATCCATAT	primer for synthetic dsDNA template production of *O. hannah* target 1
O-hann_Anti1	GAAGAATATGGATGCGCCGATTGCGTGAAGGTTTTGTATGGTTCATCCGTAAGGCACATCTCGAGTGATGTGAATTACGGATGAGAAGGC	primer for synthetic dsDNA template production of *O. hannah* target 1
O-hann_sense2	TACGGATGAACCATACAAAACCTTCACGCAATCGGCGCATCCATATTCTTCATCTGCATTTATATCCACATCGCACGAGGAATCTACTAT	primer for synthetic dsDNA template production of *O. hannah* target 2
O-hann_Anti2	AAGATCCATAGTAGATTCCTCGTGCGATGTGGATATAAATGCAGATGAAGAATATGGATGCGCCGATTGCGTGAAGGTTTTGTATGGTTC	primer for synthetic dsDNA template production of *O. hannah* target 2
N-kaou_Sense	TATCAACCTGGCCTTCTCATCAGTAATTCACATCACACGGGACGTGCCTTACGGGTGAAT	primer for synthetic dsDNA template production of *N. kaouthai*
N-kaou_Anti	AGAATAGGGATGCGCTGATTGTGTGAAGGTTTTGTATGATTCACCCGTAAGGCACGTCCC	primer for synthetic dsDNA template production of *N. kaouthai*
C-rhod_Sense	AAATCCCATTTCACCCATATCACTCTTACAAAGACATAACACTGCTAACAACAATAATCA	primer for synthetic dsDNA template production of *C. rhodostromata*

C-rhod_Anti	TATATCTGGGCAGAATGATAGGATAATAAATAGAAGGGTGATTATTGTTGTTA GCAGTGT	primer for synthetic dsDNA template production of *C. rhodostromata*
D-russ_Sense	GGCTGAATTATACAAAATTCACACGCCATCGGCGCATCCCTATTCTTTGTTTGT ATCTAT	primer for synthetic dsDNA template production of *D. russelii*
D-russ_Anti	AGGTAAGATCCATAATAGAGGCCTCGTGCAATGTGTATATAGATACAAACAAA GAATAGG	primer for synthetic dsDNA template production of *D. russelii*
D-siam_Sense	ATATTAATTACAGCCATACTTATTATCCTATCATTTGACCCAAACATAATAAAC GACCCA	primer for synthetic dsDNA template production of *D. siamensis*
D-siam_Anti	TGTGGGGTGACTAGGGGGTTAGCTTTAGAGAAGTTCTCTGGGTCGTTTATTATG TTTGGG	primer for synthetic dsDNA template production of *D. siamensis*
T-albo_Sense	TACTACGGCTCCTATCTTAACAAAGAAGTATGACTCTCAGGCACAACCCTTTTA ATCATC	primer for synthetic dsDNA template production of *T. albolabris*
T-albo_Anti	CATGGTAGTACATAGCCAAAGAAGGCTGTGGCTATTAAGATGATTAAAAGGGT TGTGCCT	primer for synthetic dsDNA template production of *T. albolabris*
B-fasc_Sense	TGGCACTAACTCAGATATTGATAAAATCCCATTACATCCATACCATTCCTACAA AGATAT	primer for synthetic dsDNA template production of *B. fasciatus*
B-fasc_Anti	TAATGAATAATATAGTGATTATGATGCTAATTATTAATATATCTTTGTAGGAAT GGTATG	primer for synthetic dsDNA template production of *B. fasciatus*
B-cand_Sense	GGTCTATACCTCAATAAAGAAGTCTGATTATCAGGAACCGCCCTATTAATCACT CTAATA	primer for synthetic dsDNA template production of *B. candidus*
B-cand_Anti	TTTGTCCTCATGGGAGGACGTAGCCAAAGAAAGCTGTTGCTATTAGAGTGATTA ATAGGG	primer for synthetic dsDNA template production of *B. candidus*

Preparation of double-stranded cytb DNA segments

We produced the double-stranded *cytb* DNA segments to be RPA templates as synthetic dsDNA templates to analyze the limit of detection (LoD). The partially complementary oligonucleotides (sense and anti-sense) were annealed then amplified by *Taq* DNA polymerase-mediated PCR. The PCR products (**Fig. 2A**) were purified using a DNA purification kit (Zymogen). The purified dsDNAs are illustrated in **Fig. 2B**. After measured the concentrations and converted to Molar unit, we prepared DNA templates for RPA LoD measurements via serial dilutions to generate a concentration range of nanomolar to attomolar.

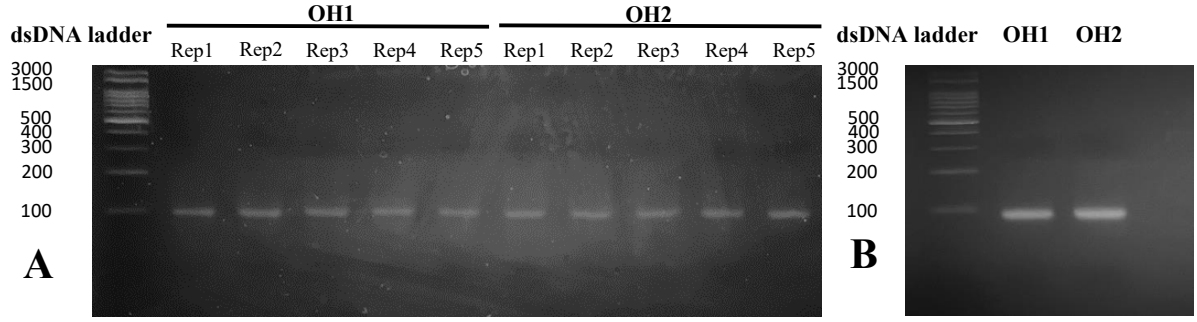

Figure 2 The double-stranded *cytb* DNA segments in agarose gel (3%) after 100 mV running in 0.5X TBE running buffer for 25 min with 100 bp DNA Ladder (biotech rabbit). **(A)** The double-stranded DNAs produced from *Taq* polymerase PCR with expected 95-bp size subsequent by **(B)** purifying with a DNA purification kit (Zymogen). Where OH1-2 refers to the dsDNA of *O. hannah* target 1-2, rep1-5 refers to the experimental replicate 1-5.

CRISPR RNA production using T7 RNA polymerase-based in vitro transcription

CRISPR RNAs (crRNAs) needed for LwaCas13a-based detection of the *cytb* gene of different snake species were prepared using the Ribomax Large Scale RNA Production System-T7 (Promega) and purified in two steps via magnetic bead enrichment and phenol-chloroform precipitation. Purified crRNAs were analyzed for correct size and sufficient purify using denaturing acrylamide gel electrophoresis. Representative gels from crRNAs for *O. hannah cytb* gene detection are shown in **Fig. 3**.

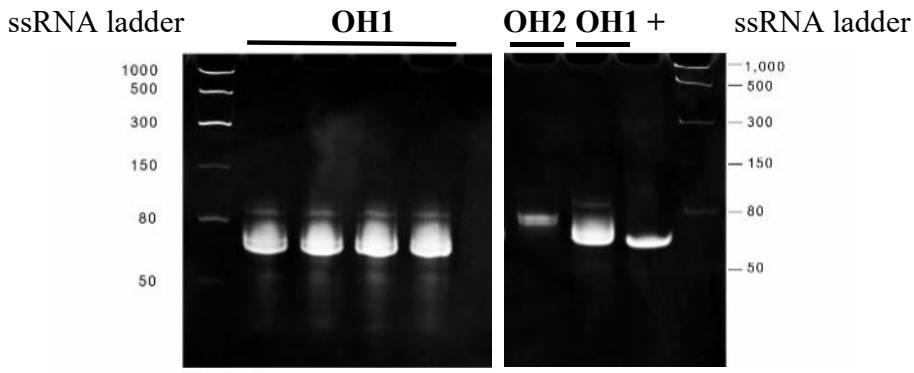

Figure 3 crRNA analysis in 7.5 M urea denaturing polyacrylamide gel (15%) after 150 mV running PAGE for 1 h 30 min. A single-stranded RNA ladder (NEB) was shown, along with a reference LwaCas13a crRNA (for the detection of Orf1ab of SARS-CoV-2, 64-bp) as a positive control (+) and a negative control with RNA input omitted (-). OH1 and OH2 refer to the crRNAs (67-bp) of *O. hannah* target 1 and 2 respectively.

The LoD of synthetic dsDNA template for species-specific detection

We first determined the analytical sensitivity, or the limit of detection (LoD) of SHERLOCK-based detection of *O. hannah cytb* gene segment. We made serial dilutions of the double-stranded *O. hannah cytb* gene segment, to obtain a range of DNA concentrations from nanomolar to attomolar (10^{-9}, 10^{-12}, 10^{-15}, and 10^{-18} M). Each dilution was prepared with at least 3 replicates. For negative controls, we added in DEPC-treated water instead of DNA solutions. A SHERLOCK assay, in which RPA was used to amplify the *cytb* gene segment for 25 min at 42°C, and kinetics of LwaCas13a-mediated detection of the amplified gene segment was monitored in real time, via fluorescence measurements, over 60 min, at 37°C.

We observed that for the desired *cytb* gene segments of *O. hannah*, here referred to as targets OH1 and OH2, SHERLOCK detection was highly sensitive, capable of detecting both targets at attomolar levels (**Fig. 4**).

We expanded the limit of detection measurements of SHERLOCK-based detection to *ctyb* gene segments from seven additional snake species: *N. kaouthia*, *C. rhodostromata*, *D. russelii*, *D. siamensis*, *T. albolabris*, *B. fasciatus*, and *B. candidus*. Double-stranded *cytb* gene segments were prepared, and SHERLOCK detection performed in a similar way as those of *O. hannah*. However, we observed a wider range of limits of detection for these *cytb* gene variants. The detection of *C. rhodostromata, D. siamensis, T. albolabris* and *B. candidus cytb* segments gave the highest sensitivity at attomolar levels (**Fig. 5B, 5D, 5E and 5G**), similar to that of the two *cytb* targets of *O. hannah*, although the signal-to-noise at attomolar target levels for *B. candidus cytb* is much lower compared to those from other species. The detection of *N. kaouthia* and *D. russelii cytb* segments showed markedly lower sensitivity, at femtomolar (10^{-15} M) (**Fig. 5A and 5C**) and for *B. fasciatus cytb* segments given the lowest sensitivity at nanomolar (10^{-9} M) as shown in **Fig. 5F**.

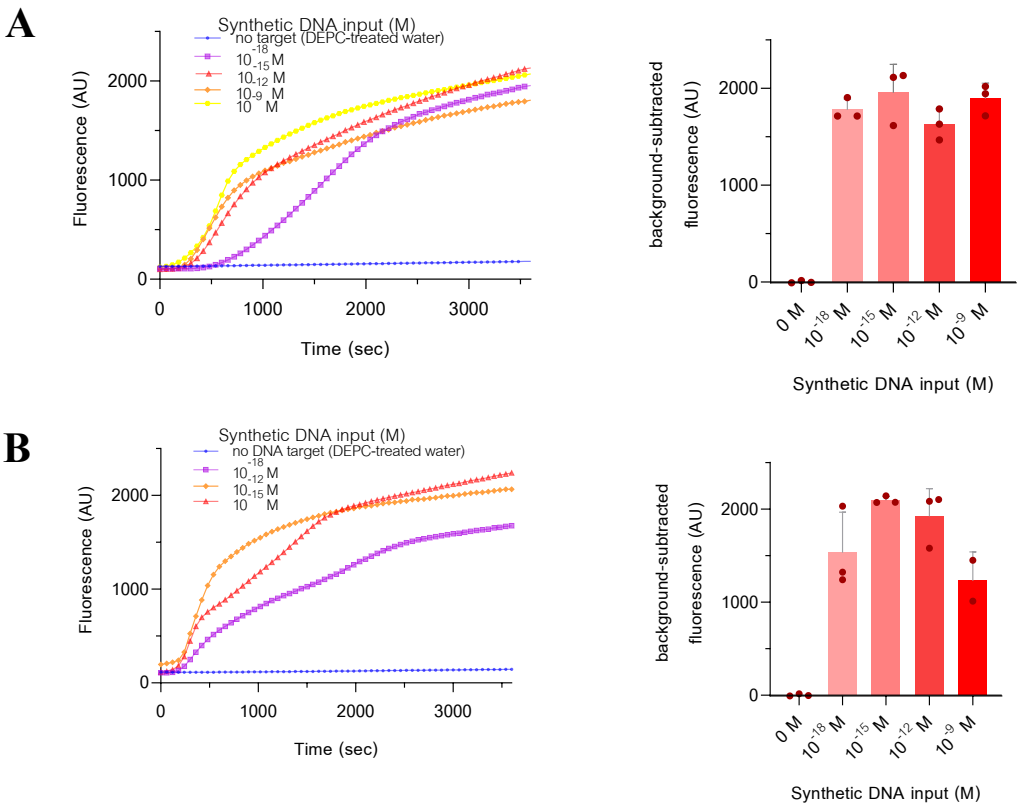

Figure 4 LwaCas13a-mediated detection of synthetic dsDNA inputs corresponding to the *cytb* gene segments from *O. hannah* target 1-2, at different input concentrations. Results from synthetic *cytb* gene segments from **(A)** target 1 and **(B)** target 2. For each sub-figure, LwaCas13a reaction kinetics are shown on the left, and background-subtracted FAM fluorescence generated after 60-min reactions are shown as bar graphs on the right. Circles on the bar graphs represent individual fluorescence values from three replicates, for each reaction condition. Error bars, ± S.D.

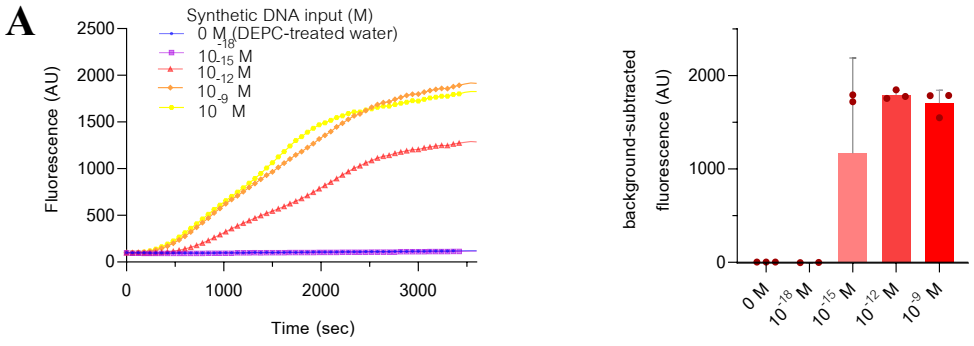

B

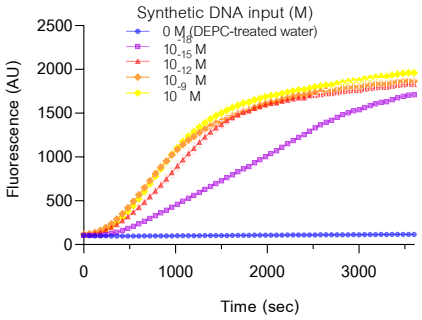
Synthetic DNA input (M)
0 M (DEPC-treated water)
10-18 M
10-15 M
10-12 M
10-9 M
10-6 M
Fluorescence (AU)
Time (sec)

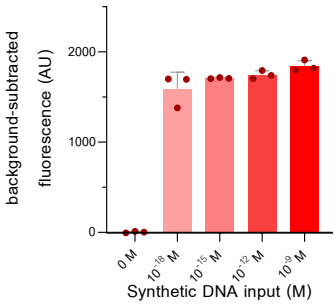
background-subtracted fluorescence (AU)
0 M
10-18 M
10-15 M
10-12 M
10-9 M
Synthetic DNA input (M)

C

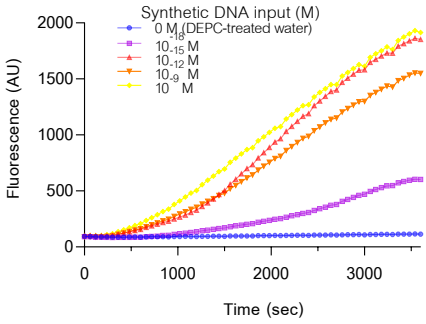
Synthetic DNA input (M)
0 M (DEPC-treated water)
10-18 M
10-15 M
10-12 M
10-9 M
10-6 M
Fluorescence (AU)
Time (sec)

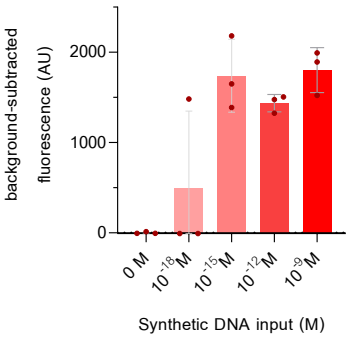
background-subtracted fluorescence (AU)
0 M
10-18 M
10-15 M
10-12 M
10-9 M
Synthetic DNA input (M)

D

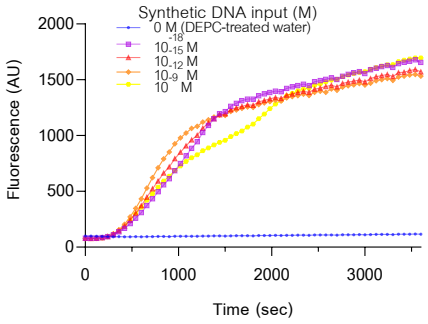
Synthetic DNA input (M)
0 M (DEPC-treated water)
10-18 M
10-15 M
10-12 M
10-9 M
10-6 M
Fluorescence (AU)
Time (sec)

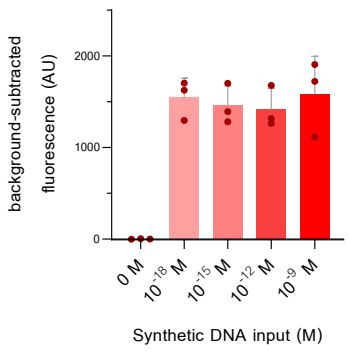
background-subtracted fluorescence (AU)
0 M
10-18 M
10-15 M
10-12 M
10-9 M
Synthetic DNA input (M)

E

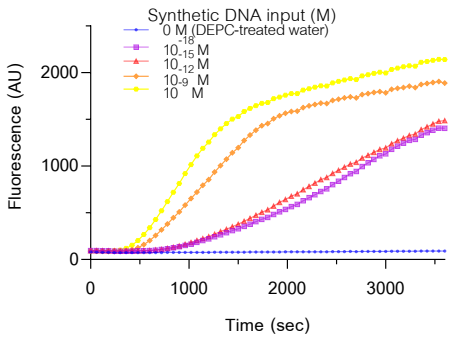
Synthetic DNA input (M)
0 M (DEPC-treated water)
10-18 M
10-15 M
10-12 M
10-9 M
10-6 M
Fluorescence (AU)
Time (sec)

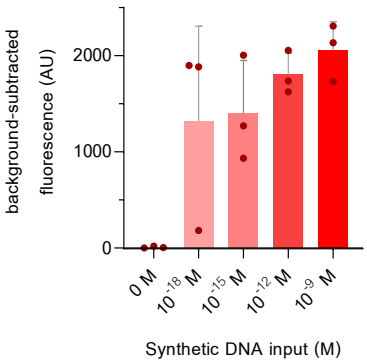
background-subtracted fluorescence (AU)
0 M
10-18 M
10-15 M
10-12 M
10-9 M
Synthetic DNA input (M)

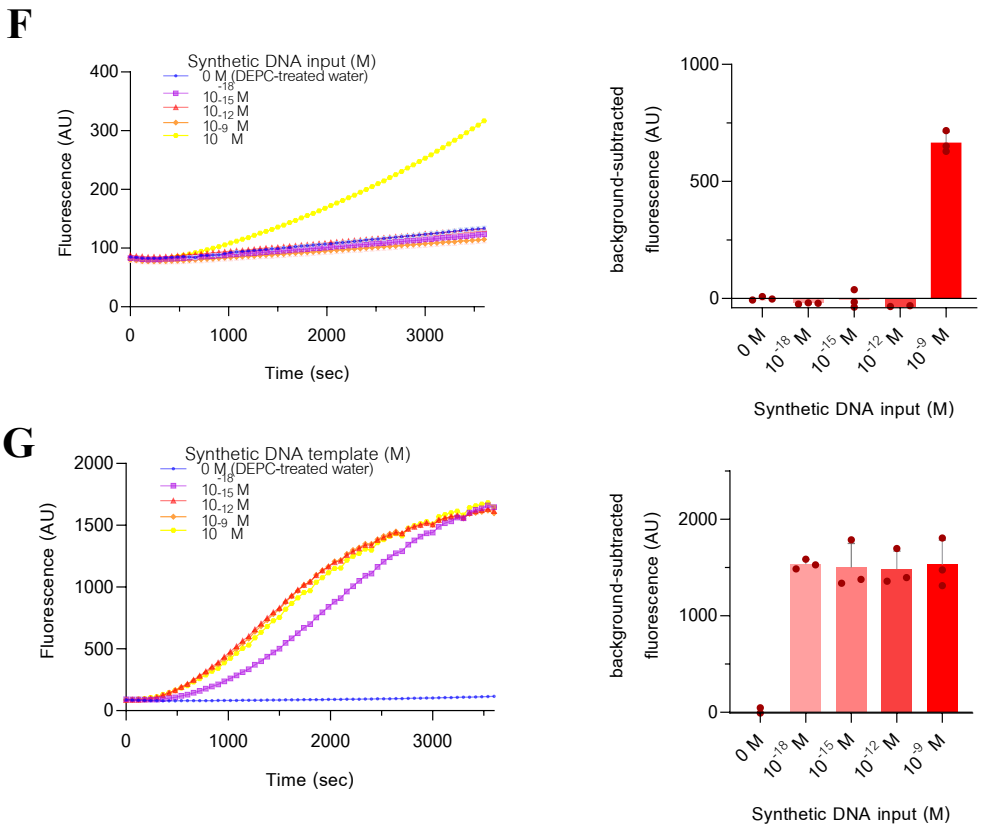

Figure 5 LwaCas13a-mediated detection of synthetic dsDNA inputs corresponding to the *cytb* gene segments from different snake species, at different input concentrations. Results from synthetic *cytb* gene segments from **(A)** *N. kaouthai*, **(B)** *C. rhodostromata*, **(C)** *D. russelii*, **(D)** *D. siamensis*, **(E)** *T. albolabris*, **(F)** *B. fasciatus*, and **(G)** *B. candidus* are shown. For each sub-figure, LwaCas13a reaction kinetics are shown on the left, and background-subtracted FAM fluorescence generated after 60-min reactions are shown as bar graphs on the right. Circles on the bar graphs represent individual fluorescence values from three replicates, for each reaction condition. Error bars, ± S.D.

Optimizations of LwaCas13a and crRNA amount in CRISPR-based detection reactions

We increased final concentration of crRNA targeting *O. hannah* target 1 from 0.5 ng/µL (corresponding to 0.02 µM), the recommended crRNA concentration of use, to 1.0 and 2.5 ng/µL (corresponding to 0.05, and 0.12 µM) with 6.3 µg/mL LwaCas13a (corresponding to 0.05 µM). We found that the reaction kinetics increased with increasing crRNA concentrations (**Fig. 6A**), resulting in higher end-point fluorescence intensity at the high crRNA concentrations after 60 min of CRISPR reactions (**Fig. 6B**), as previous studies showed Cas13-crRNA complexes function best when the molar ratio of Cas13: crRNA is ~1:2 [29].

We also concurrently optimized LwaCas13a concentrations to match the increased crRNA concentrations. We previously used 6.3 µg/mL LwaCas13a, and here, further tested lowering Cas13a concentration to 3.15 µg/mL (corresponding to 0.025 µM). We found the combination of 0.12 µM crRNA and 0.025 µM LwaCas13a to provide the fastest reaction kinetics, followed by 0.06 µM crRNA and 0.025 µM LwaCas13a (**Fig. 6C**). The enhanced reaction kinetics under the optimal reaction condition was also reflected in the end-point fluorescence measurements after 15 min of CRISPR reactions (**Fig. 6D**).

While increasing the crRNA: Cas13 molar ratio is known to increase Cas reaction kinetics and efficiency, our observation that reducing Cas concentrations can lead to better reaction kinetics is surprising, but consistently seen at different relative Cas and crRNA

amounts. Cas13a is not known to form dimers or other forms of oligomerization, and inhibitory states due to the formation of higher-ordered Cas oligomers are unlikely. It may be possible that too high Cas-crRNA complex concentrations can lead to unproductive, non-specific cleavage of unbound crRNAs, which negatively affects the reaction kinetics.

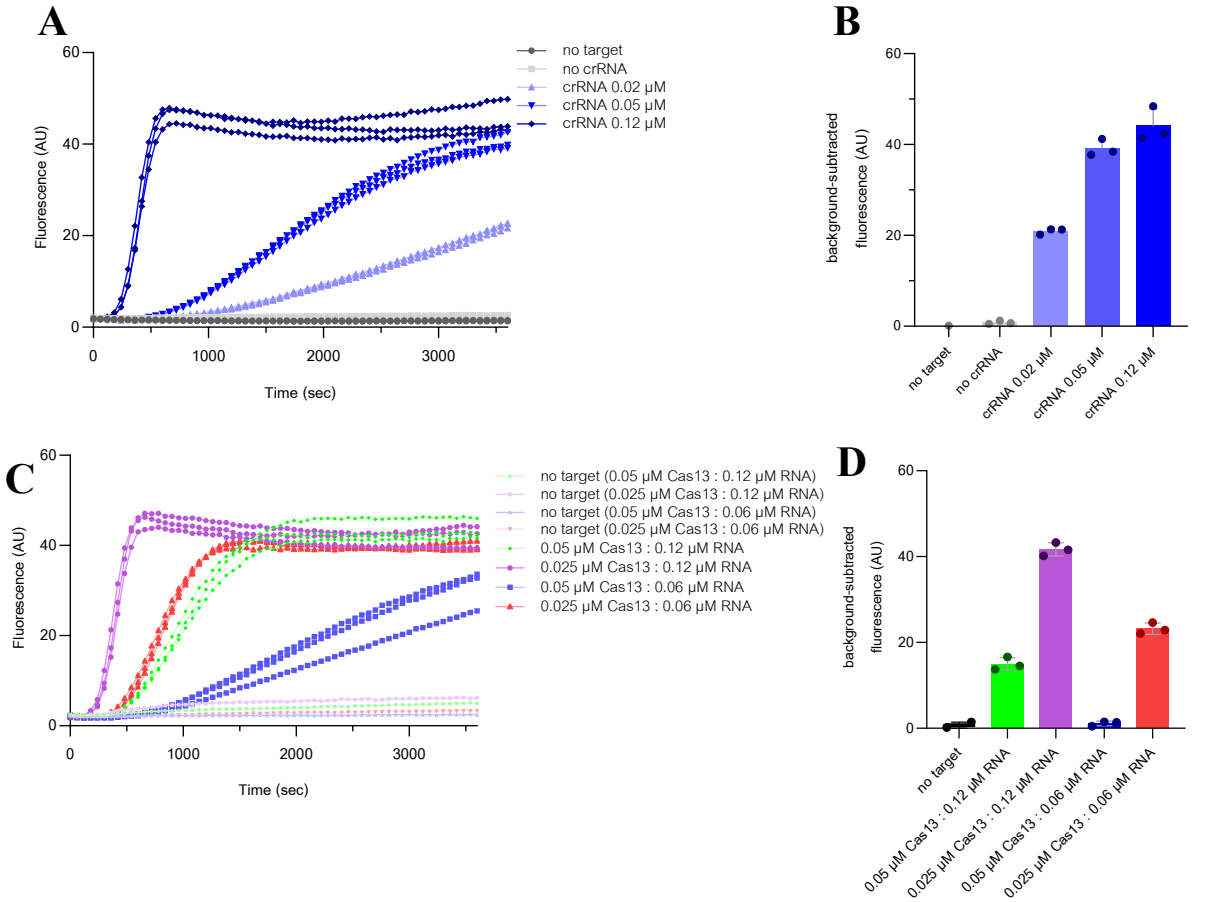

Figure 6 Optimizing Cas13a-based detection via increased crRNA concentration shows **(A)** Cas13a reaction kinetics of the detection targeting *O. hannah* target 1 and **(B)** background-subtracted fluorescence at the 60-min reaction. Increasing crRNA concentration coupled with reducing LwaCas13a concentration shows **(C)** Cas13a reaction kinetics of the detection targeting *O. hannah* target 1 and **(D)** background-subtracted fluorescence at the 15-min reaction.

DISCUSSION AND CONCLUSION

We observed varying limit of detection values upon detecting *cytb* genes from different snake species. We will dissect whether the low sensitivity of *cytb* gene detection, particularly with *N. kaouthia* and *B. fasciatus cytb*, originates from inefficient RPA or CRISPR-Cas13a, and will re-design faulty components (RPA primers, or crRNAs) accordingly.

We currently used purified DNA surrogate substrates to validate the functionality of RPA primers and crRNAs. To extend the detection platform to real samples, we will first test the detection on DNA extracted from snake saliva, which was reported to have at least 0.5 ng of genomic DNA per 20 µL [13]. Such samples will be obtained with ethical approval from Queen Saovabha Memorial Institute (QSMI), in collaboration with Dr. Lawan Chanhome. We will also test the detection on DNA obtained from crudely lysed (through heating and detergent-induced cell lysis) snake saliva. Cross-reactivity of detection upon using different snake species will be fully validated; any non-specific detection modules will be redesigned

and tested. We anticipated that cross-reactivity will be minimal, as the gene regions chosen for detection by RPA primers and crRNAs do not contain a lot of homologies across different snake species (**Fig. 7**).

	RPA forward primer	gRNA Match	RPA Reverse Primer
O. hannah	TACGGATGAACCATACAAAACCTTCACGCAATCG	GCGCATCCATATTCTTCATCTGCATTTA	TATCCACATCGCACGAGGAATCTACTATGGATCTT
N. kaouthai	TACGGGTGAATCATGCAGAACCTTCACACAATCA	GCGCATCCCTATTCTTCATTTGCATCTA	CACCCACATTGCACGAGGGCTCTATTATGGCTTAT
C. rhodostoma	TACGGATGAATCATACAAAACACACACACAATTG	GCGCATCCCTATTTTTTATCTGCATCTA	TATCCACATCGCTCGAGGACTTTACTACGGCTCCT
D. rusellii	TATGGCTGAATTATACAAAATTCACACGCCATCG	GCGCATCCCTATTCTTTGTTTGTATCTA	TATACACATTGCACGAGGCCTCTATTATGGATCTT
T. alobolabris	TACGGCTGAATCATACAAAACACGCATGCTATTG	GCGCATCTATATTCTTTATTTGCATCTA	CATCCACATTGCACGAGGGCTCTACTACGGCTCCT
B. fasciatus	TACGGATGAATCATACAAAACATTCATGCAATCG	GCGCATCCCTATTCTTTATTTGCATCTA	TATCCATATTGCACGAGGACTTTACTACGGCCTTT
B. candidus	TATGGATGAACCATACAAAATATTCATGCAATTA	GCGCATCACTATTCTTTATTTGCATTTA	CATCCATATTGCACGAGGACTATACTATGGTCTAT

Figure 7 Sequence alignment of binding regions of RPA primers and crRNAs on the *cytb* gene from different snake species.

CRISPR-based detection is highly amenable to multiplexed detection; once species-specific detection of DNA extracted from snake saliva is validated for LwaCas13a-based detection, we will extend the detection platform to other orthogonal Cas enzymes to create a one-pot detection reaction for multiple snake species.

ACKNOWLEDGEMENTS

We thank VISTEC for scientific equipment supporting and research financial funding, and studentship funding to R.K. We especially thank all C.U. lab members for their contribution to the research study, and Queen Saovabha Memorial Institute (QSMI) for providing useful information on venomous snakes and for future collaborations.

REFERENCES

1. Kasturiratne A, Wickremasinghe AR, Silva ND, Gunawardena NK, Pathmeswaran A, Premaratna R, et al. The Global Burden of Snakebite: A Literature Analysis and Modelling Based on Regional Estimates of Envenoming and Deaths. PLoS Med. 2008;5(11):e218.
2. Snakebite envenoming [Internet]. Who.int. 2020 [cited 3 November 2020]. Available from: https://www.who.int/news-room/fact-sheets/detail/snakebite-envenoming.
3. Gutiérrez JM, Calvete JJ, Habib AG, Harrison RA, Williams DJ, Warrell DA. Snakebite envenoming. Nat Rev Dis Primers. 2017;3(1):17063.
4. Chippaux JP. Snakebite envenomation turns again into a neglected tropical disease!. J Venom Anim Toxins Incl Trop Dis. 2017;23(1):38.
5. Chanhome L, Cox MJ, Vasaruchapong T, Chaiyabutr N, Sitprija V. Characterization of venomous snakes of Thailand. Asian Biomed (Res Rev News). 2011;5(3):311-328.
6. Costa LG, Giordano G, Aschner M. Snake Venoms. Neurosci Behav Physiol. 2014:227.
7. Antivenom treatments [Internet]. World Health Organization. 2020 [cited 5 November 2020]. Available from: https://www.who.int/snakebites/treatment/Antivenom_treatments/en/.
8. Bolon I, Durso AM, Mesa SB, Ray N, Alcoba G, Chappuis F, et al. Identifying the snake: First scoping review on practices of communities and healthcare providers confronted with snakebite across the world. PLoS One. 2020;15(3):e0229989.
9. Isbister G, Maduwage K, Shahmy S, Mohamed F, Abeysinghe C, Karunathilake H, et al. Diagnostic 20-min whole blood clotting test in Russell's viper envenoming delays antivenom administration. QJM. 2013;106(10):925-932.

10. Maduwage K, O'Leary MA, Isbister GK. Diagnosis of snake envenomation using a simple phospholipase A2 assay. Sci Rep. 2014;4(1):4827.
11. Nimorakiotakis VB, Winkel KD. Prospective assessment of the false positive rate of the Australian snake venom detection kit in healthy human samples. Toxicon. 2016;111:143-146.
12. Hung DZ, Lin JH, Mo JF, Huang CF, Liau MY. Rapid diagnosis of Naja atra snakebites. Clin Toxicol (Phila). 2014;52(3):187-191.
13. Supikamolseni A, Ngaoburanawit N, Sumontha M, Chanhome L, Suntrarachun S, Peyachoknagul S, et al. Molecular barcoding of venomous snakes and species-specific multiplex PCR assay to identify snake groups for which antivenom is available in Thailand. Genet Mol Res. 2015;14(4):13981-13997.
14. Suntrarachun S, Pakmanee N, Tirawatnapong T, Chanhome L, Sitprija V. Development of a polymerase chain reaction to distinguish monocellate cobra (Naja khouthia) bites from other common Thai snake species, using both venom extracts and bite-site swabs. Toxicon. 2001;39(7):1087-1090.
15. Pook CE, McEwing R. Mitochondrial DNA sequences from dried snake venom: a DNA barcoding approach to the identification of venom samples. Toxicon. 2005;46(7):711-715.
16. Williams HF, Layfield HJ, Vallance T, Patel K, Bicknell AB, Trim SA, et al. The Urgent Need to Develop Novel Strategies for the Diagnosis and Treatment of Snakebites. Toxins (Basel). 2019;11(6):363.
17. Kellner MJ, Koob JG, Gootenberg JS, Abudayyeh OO, Zhang F. SHERLOCK: nucleic acid detection with CRISPR nucleases. Nat Protoc. 2019;1(4):2986-3012.
18. Lobato IM, O'Sullivan CK. Recombinase polymerase amplification: Basics, applications and recent advances. Trends Analyt Chem. 2018;98:19-35.
19. Gootenberg JS, Abudayyeh OO, Kellner MJ, Joung J, Collins JJ, Zhang F. Multiplexed and portable nucleic acid detection platform with Cas13, Cas12a, and Csm6. Science. 2018;360(6387):439-444.
20. Barnes KG, Lachenauer AE, Nitido A, Siddiqui S, Gross R, Beitzel B, et al. Deployable CRISPR-Cas13a diagnostic tools to detect and report Ebola and Lassa virus cases in real-time. Nat Commun. 2020;11(1):4131.
21. Patchsung M, Jantarug K, Pattama A, Aphicho K, Suraritdechachai S, Meesawat P, et al. Clinical validation of a Cas13-based assay for the detection of SARS-CoV-2 RNA. Nat Biomed Eng. 2020; 4:1140–1149.
22. Lee RA, Puig HD, Nguyen PQ, Angenent-Mari NM, Donghia NM, McGee JP, et al. Ultrasensitive CRISPR-based diagnostic for field-applicable detection of Plasmodium species in symptomatic and asymptomatic malaria. Proc Natl Acad Sci U S A. 2020;117(41):25722-25731.
23. List of snake species in Thailand [Internet]. Thai National Parks. 2020 [cited 3 November 2020]. Available from: https://www.thainationalparks.com/list-of-snakes-in-thailand.
24. Serum Antivenin Production at QSMI: Queen Saovabha Memorial Institute [Internet]. Saovabha.com. 2020 [cited 3 November 2020]. Available from: https://www.saovabha.com/en/product_serum.asp?nTopic=2.
25. Katoh K, Standley DM. MAFFT Multiple Sequence Alignment Software Version 7: Improvements in Performance and Usability. Mol. Biol. Evol. 2013;30(4):772-780.

26. Schermer B, Fabretti F, Damagnez M, Cristanziano VD, Heger E, Arjune S, et al. Rapid SARS-CoV-2 testing in primary material based on a novel multiplex RT-LAMP assay. PLoS One. 2020;15(11): e0238612.
27. Armbruster DA, Pry T. Limit of blank, limit of detection and limit of quantitation. Clin Biochem Rev. 2008;29 Suppl 1(Suppl 1): S49-S52.
28. Myhrvold C, Freije CA, Gootenberg JS, Abudayyeh OO, Metsky HC, Durbin AF, et al. Field-deployable viral diagnostics using CRISPR-Cas13. Science. 2018;360(6387):444-448.
29. Abudayyeh OO, Gootenberg JS, Essletzbichler P, Han S, Joung J, Belanto JJ, et al. RNA targeting with CRISPR-Cas13a. Nature. 2017;550:280-284.

Proceeding PP011

Investigation of malathion sensitivity in *Saccharomyces cerevisiae* lacking the mitophagy receptor Atg32p

Myat Shwe Yee, Thitipa Thosapornvichai, and Laran T. Jensen*

Department of Biochemistry, Faculty of Science, Mahidol University, Bangkok Thailand

***E-mail:** laran.jen@mahidol.ac.th

ABSTRACT

Organophosphate (OP) insecticides are widely used in agriculture for controlling insects that can damage crops. Malathion is among the most commonly used of this class. Misapplication and extensive use of insecticides has contributed to the development of OP resistance in insect populations resulting in crop loss and the spread of insect-borne diseases. In addition, increased insecticide use can lead to environmental contamination and human exposure. However, the limited genetic tools available for insect systems prevents comprehensive screening for mutations or deletions of genes that promote insecticide sensitivity directly. Simple model systems such as the baker's yeast *Saccharomyces cerevisiae* can be utilized to aid in the identification of pathways that lead to insecticide sensitivity. A collection of yeast deletion strains was screened for malathion sensitivity under conditions requiring respiratory growth. This screen identified *ATG32* as being required for malathion tolerance. However, the role of this protein in autophagic processes under other stress conditions has not been previously examined. Using the dual fluorescence Rosella system increased levels of autophagy were observed WT and yeast lacking Atg32p following malathion exposure. In contrast, increased levels of mitophagy were not apparent due to malathion treatment. It appears that malathion sensitivity in yeast lacking Atg32p is not due to disruption in autophagy. Overall, these findings suggest that loss of Atg32p can promote malathion sensitivity. Further characterization of pathways affected in yeast lacking Atg32p may identify molecular targets with utility in the development of agents to sensitize cells to malathion.

Keywords: Organophosphate, malathion, *Saccharomyces cerevisiae, ATG32*, Rosella, autophagy

INTRODUCTION

More than 40% of the agricultural crops are damaged by insect pests each year globally [1]. Decreased crop yields and poor quality of food production are major global concerns as the world population is growing over time. In addition to agricultural and economic concerns, insect-borne diseases, such as malaria, dengue fever, West Nile fever, yellow fever, tick-borne encephalitis, are responsible for more than 17% of total infectious diseases [2, 3]. To address these issues, insecticides become a critical part of integrated pest management strategies as well as application of everyday needs in household settings. Among the classes of insecticides, organophosphate (OP) insecticides are the most widely used synthetic insecticides in developed and developing countries [4, 5]. Malathion is one of the most widespread used broad-spectrum non-systemic OP insecticides due to its relatively low to moderate toxicity to humans and

mammals [6]. However, it is highly toxic to insects by inhibiting the acetylcholinesterase (AChE) enzymes, resulting in paralysis and death [6].

Because of the beneficial effects of the insecticides for controlling insect pests, people have mainly relied on the use of insecticides since the 1950s [7]. However, misuse or repeated use of insecticides can cause the environmental contamination and insecticide resistance that has become a major growing problem nowadays [8–11]. Insecticide resistance can also lead to increased insecticide application as well as reduction in insecticide efficacy [8]. Among several strategies to overcome insecticide resistance**,** the addition of a second compound known as synergist, that can enhance the efficacy without affecting the economy and environment [8]. Synergists have a role in blocking specific metabolic pathways in which metabolic-based resistance usually occurs [12, 13]. Nevertheless, insect pests may also evolve resistance to the synergist compounds with insecticides [13]. Therefore, targeting independent molecular pathways may increase the effectiveness of insecticides. Some molecular pathways can enhance malathion resistance through mitochondria, endoplasmic reticulum, and others. However, the limitation of genomic data in insect systems hinders the investigation of molecular pathways that promote resistance to insecticides [14].

The budding yeast, *Saccharomyces cerevisiae* is a convenient model system that has been widely utilized in many toxicological investigations due to their similarity with higher organisms and ease of genetic modification [15–17]. Understanding the mechanisms responsible for organophosphate insecticide resistance in yeast cells may reveal pathways that can be targeted for the effectiveness of insecticides.

We screened a collection of *S. cerevisiae* yeast autophagy-related gene deletion arrays that promotes sensitivity to malathion. Our initial screen identified the *atg32*Δ strain as strongly sensitive to malathion. Atg32p is involved in mitophagy in yeast cells following nitrogen starvation and perhaps other stresses. It is localized in the mitochondrial outer membrane with N and C terminal region directed towards the cytosol and the mitochondrial intermembrane space. Autophagy is a conserved catabolic process from yeast to humans. Autophagy can be induced by several stress factors such as starvation or nutrient deprivation, oxidative stress, infections, and other stress conditions [16]. Bulk autophagy or autophagy is a non-selective type of autophagy in which cytosolic components are degraded by sequestering within autophagosomes. Mitophagy is the selective degradation of mitochondria through an autophagic process. Several studies have shown that mitophagy can be induced in *S. cerevisiae* during respiratory growth and under nitrogen starvation [18]. However, little is known about other stress-induced mitophagy in yeast.

The aim of our study was to examine the malathion sensitivity in *S. cerevisiae atg32* mutant yeast strain using the spot test and Rosella system. We used spot test analysis to screen the sensitivity of yeast strains to malathion. To monitor autophagy or mitophagy in cells treated with either malathion or vehicle, we applied Rosella system developed by Rosado et.al. [19]. The Rosella system is a fluorescent protein biosensor with a pH-stable red fluorescent protein (DsRed) fused to a pH-sensitive green fluorescent protein (GFP) [19]. Using plasmids expressing Rosella localized to the cytoplasm (Cyto-Rosella) and mitochondria (Mito-Rosella), the presence of the fluorescent proteins in the vacuoles of cells can be determined. The levels of autophagy and mitophagy in WT and *atg32* mutant cells were observed following malathion exposure. Our results indicate that deletion of the *ATG32* gene enhances malathion sensitivity.

MATERIALS AND METHODS

Yeast strains and medium

Saccharomyces cerevisiae strains used in this study were derived from BY4742 (*Mat α, leu2Δ0, lys2Δ0, ura3Δ0, his3Δ1*). Single deletion strains were obtained from Open Biosystems and include *atg1*Δ:: *kanMX4*, *atg9*Δ:: *kanMX4, atg11*Δ:: *kanMX4, atg27*Δ:: *kanMX4, atg32*Δ:: *kanMX4, atg39*Δ:: *kanMX4*.

Yeast transformations were performed using the lithium acetate procedure [20]. Cells were propagated at 30˚ C either in rich medium (YPD; 1% yeast extract, 2% bacteriological peptone, 2% D-glucose) or synthetic complete media (0.17% yeast nitrogen base, 2% glucose, 0.5% ammonium sulfate and amino acids) with 3% glycerol (SCG) or 2% D-glucose (SC) lacking the appropriate nutrients. For solid media, 2% agar was included.

Plasmids

The Rosella reporter is composed of two fluorescent proteins, a pH-stable RFP (DsRed.T3) and a pH-sensitive GFP variant (super ecliptic pHluorin, SEP), developed by Rosado et.al. [19]. Visualization of the biosensor depends on the pH differences between the vacuole and cellular compartments. Plasmids pAS1NB c Rosella I and pAS1NB m Rosella I were gifts from Mark Prescott (71245 pAS1NB Cyto-Rosella I and 71247 pAS1NB Mito-Rosella I with *LEU2* marker).

Analysis of Malathion sensitivity

Serial dilution assays were utilized to screen for deletion strains exhibiting sensitivity to malathion. 10% malathion (MA) was prepared by dissolving 57% malathion (stock) in 0.4% Tween-80 and sterile water by vigorously mixing. Various concentrations of MA were added while preparing synthetic complete with 3% glycerol (SCG) media.

Yeast strains were pre-cultured on YPD solid media and grown at 30˚ C for 2 to 3 days. Cells were diluted to an OD_{600nm} of 0.33 and ten-fold serial dilution in sterile distilled water was prepared. Yeast (10^4, 10^3, 10^2) were spotted on SCG agar plates containing a range of malathion concentrations or vehicle. Culture plates were incubated at 30˚ C for 7 days. Sensitivity of yeast strains was observed by comparing the growth of each mutant with that of the WT on the same plate. Mutants that exhibited growth retardation compared with the WT on MA plates were scored as sensitive phenotypes.

Liquid Culture Toxicity Test

Rosella transformed strains were pre-cultured on SC-Leu media for 2 to 3 days. Cells (starting at $OD_{600} = 0.05$) were inoculated into 10 mL of SC-Leu liquid medium containing a range of malathion concentrations and grown for 24 hr at 30˚ C in a rotary shaker. The OD_{600} was measured and IC_{50} was determined.

Fluorescence Imaging

Yeast strains were transformed with the indicated Rosella plasmids. Cells expressing the Rosella plasmids were cultured on SC-Leu media for 2 to 3 days. For microscopy experiments, cells were grown in 10 mL of SC-Leu medium with or without malathion overnight at 30˚ C in a rotary shaker. For nitrogen starvation, cells were washed to remove glucose and transferred into fresh SCG-N medium for a further 6 hours. Agarose pads were prepared using 20 μL of SC-Leu medium containing 0.1% agarose by placing the preheated solution onto a glass slide, covering with a second slide, and then cooled on ice. Cells were placed on the agarose pad, covered with a cover slip and sealed with a thin layer of nail polish to prevent dehydration.

Cells were observed using a confocal laser scanning microscope (Olympus FV10i-DOC), Olympus Bioimaging Center, Mahidol University. A magnification of 60X was used with a universal plan super apochromat phase-contrast oil-immersion objective. The induction of autophagy/mitophagy was monitored with excitation wavelengths (EGFP:489, Alexa Fluor:568) and emission wavelengths of 510 nm, respectively [19]. To evaluate vacuolar Rosella 100 cells were examined for each condition.

RESULTS AND DISCUSSION

Deletion of ATG32 sensitized yeast to malathion

Initially, a subset of ATG gene deletion strains was examined for sensitivity to malathion using serial dilution assays. Approximately 40 autophagy-related genes have been characterized and their molecular mechanisms have been investigated under various physiological conditions [21]. Wild-type yeast (BY4742) and yeast strains lacking genes related to pathways: *atg1*Δ, *atg9*Δ, *atg11*Δ, *atg27*Δ, *atg32*Δ, and *atg39*Δ were tested for growth in the presence of malathion. Interestingly, this screen identified *atg32*Δ strain as strongly sensitive to malathion (Fig. 1). In contrast, WT and other mutant strains *atg1*Δ, *atg9*Δ, *atg11*Δ, *atg27*Δ, and *atg39*Δ were resistant to malathion. The functions of the genes analyzed are listed in Table 1.

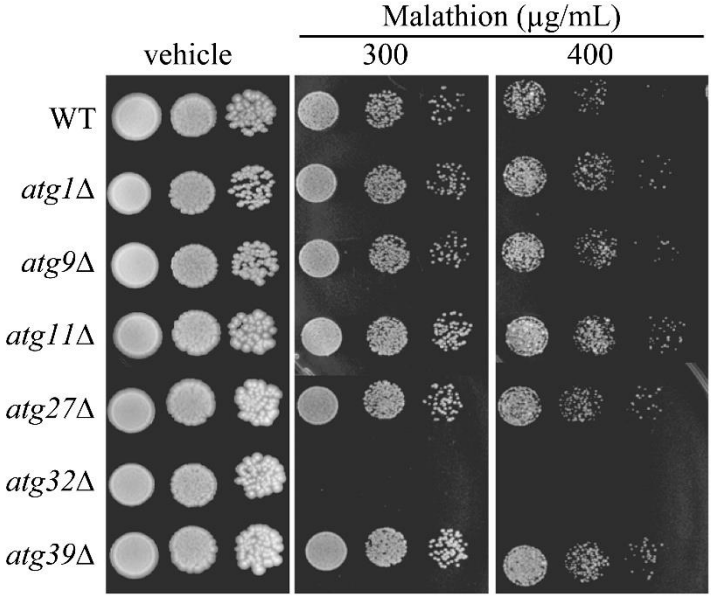

Figure 1 The strains were spotted onto SCG plates supplemented with the indicated concentration of malathion. Plates were incubated at 30˚C for 7 days.

Due to the reported role of Atg32p in mitophagy following nitrogen starvation, we monitored the autophagy/mitophagy in *atg32*Δ yeast exposed to malathion compared to the WT. Both WT and *atg32*Δ strains were transformed with Rosella plasmids to monitor activation of autophagy and mitophagy. Prior to microscopic examination, the half-maximal (50%) inhibitory concentration (IC_{50}) for malathion was determined for the transformed cells. We found that *atg32*Δ Rosella transformants were sensitized to malathion in a concentration dependent manner compared to the wild type, as expected based on the initial observation in the *atg32*Δ strain. IC_{50} concentrations for malathion in yeast expressing either Cyto-Rosella or Mito-Rosella were 100 μg/mL (Fig. 2).

Autophagy is induced following malathion exposure

To investigate whether malathion induces autophagy, we monitored the co-localization of the fluorescent proteins in the vacuoles of cells using plasmids expressing Rosella localized to the cytoplasm (Cyto-Rosella). Overlay of the RFP and GFP signals shows a yellow color in the absence of autophagy. However, if autophagy is induced, the vacuole will appear red [19].

Table 1 Genes involved in autophagy/mitophagy

Gene name	SGD description
ATG1	Protein serine/threonine kinase; required for vesicle formation in autophagy and the cytoplasm-to-vacuole targeting (Cvt) pathway; structurally required for phagophore assembly site formation
ATG9	Transmembrane protein involved in forming Cvt and autophagic vesicles; cycles between the phagophore assembly site (PAS) and other cytosolic punctate structures
ATG11	Adapter protein for pexophagy and the Cvt targeting pathway; directs receptor-bound cargo to the phagophore assembly site (PAS) for packaging into vesicles
ATG27	Type I membrane protein involved in autophagy and the Cvt pathway; may be involved in membrane delivery to the phagophore assembly site
ATG32	Mitochondrial outer membrane protein required to initiate mitophagy; recruits the autophagy adaptor protein Atg11p and the ubiquitin-like protein Atg8p to the mitochondrial surface to initiate mitophagy
ATG39	Autophagy receptor with a role in degradation of the ER and nucleus; involved specifically in autophagy of perinuclear endoplasmic reticulum in response to nitrogen starvation or rapamycin treatment

Gene descriptions were taken from Saccharomyces Genome Database (SGD).

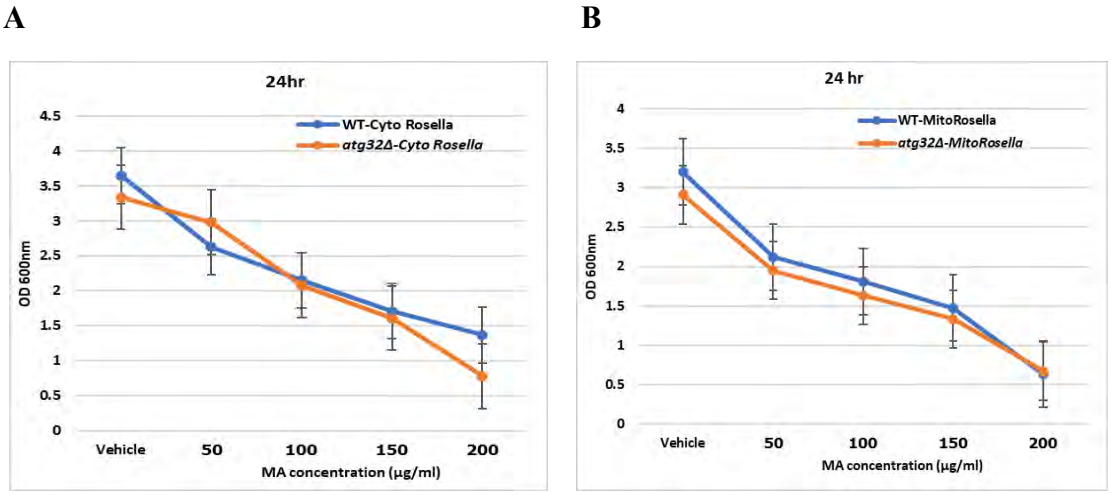

Figure 2 Determination of IC_{50} values for malathion in WT and *atg32*Δ yeast, (A) Growth curve for Cyto-Rosella transformants, and (B) Growth curve for Mito-Rosella transformant

Yeast strains expressing the Cyto-Rosella were treated with either vehicle or malathion (100 µg/mL) and induction of autophagy was examined using confocal microscopy. Cells were harvested during mid-exponential phase of growth in SC-Leu medium. Nitrogen starvation, moving cells to a medium lacking yeast nitrogen base, was utilized as a positive control as this condition has been shown to induce autophagy and mitophagy [19]. Consistent with the previous study, red fluorescence in vacuoles were observed in wild-type cells after nitrogen starvation for 4 hours. Under growth condition containing vehicle, cells showed a slight induction of autophagy. In contrast, increased level of autophagy was observed in the wild-type cells treated with malathion, suggesting that malathion induced autophagy in wild-type yeast (Fig. 3A).

The induction of autophagy was then examined in *atg32*Δ cells using the same growth conditions as described for wild-type cells. Consistent with Atg32p being a mitophagy specific protein, cells lacking this protein did not exhibit defective autophagy [22]. After 4hr nitrogen starvation, the mutant cells show red fluorescence vacuoles. However, in vehicle- treated condition, autophagy was not observed. In contrast, malathion treated cells showed an increase in the level of autophagy compared to the vehicle (Fig. 3B). This result indicates that malathion is capable of inducing the autophagy in cells lacking Atg32p.

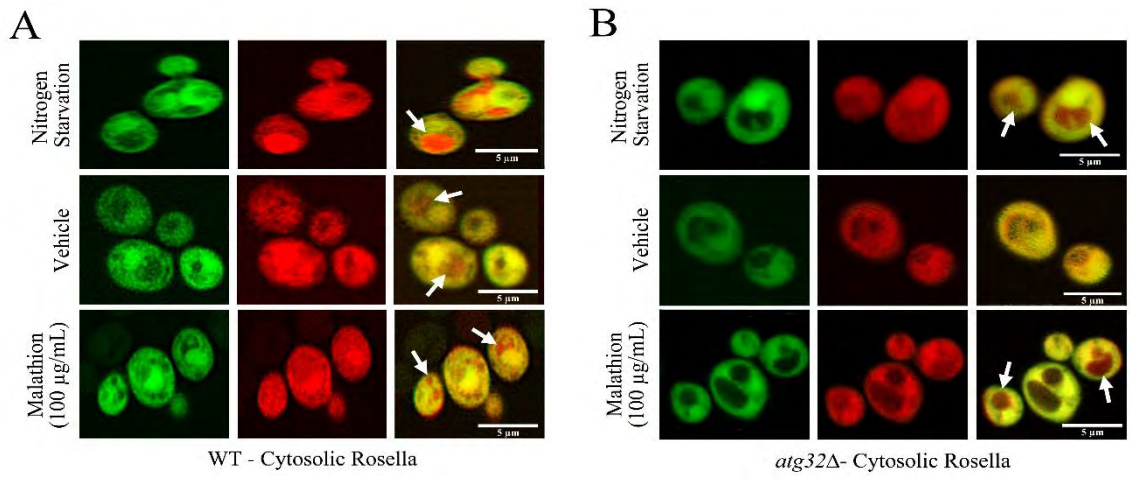

Figure 3 Induction of autophagy following malathion exposure. Wild-type (WT), atg32Δ strains expressing Cyto-Rosella were cultured in SC-Leu medium to mid-log phase, and then starved in SCG-N for 4hr as a positive control. In addition, samples treated with vehicle or 100 µg/mL malathion were also examined for induction of autophagy (A) Wild-type cells and (B) atg32Δ cells. Autophagy can be observed in WT cells and atg32Δ cells by the appearance of red fluorescence regions inside the vacuoles (white arrows). Scale bar, 5µm.

Mitophagy is not elevated by treatment with malathion

Previous studies have shown that loss of the Atg32p receptor results in defective mitophagy [22]. We examined if malathion could stimulate mitophagy activity in WT and atg32Δ cells. Yeast strains expressing the Mito-Rosella were treated with vehicle or malathion (100 µg/mL), or starved for nitrogen starvation.

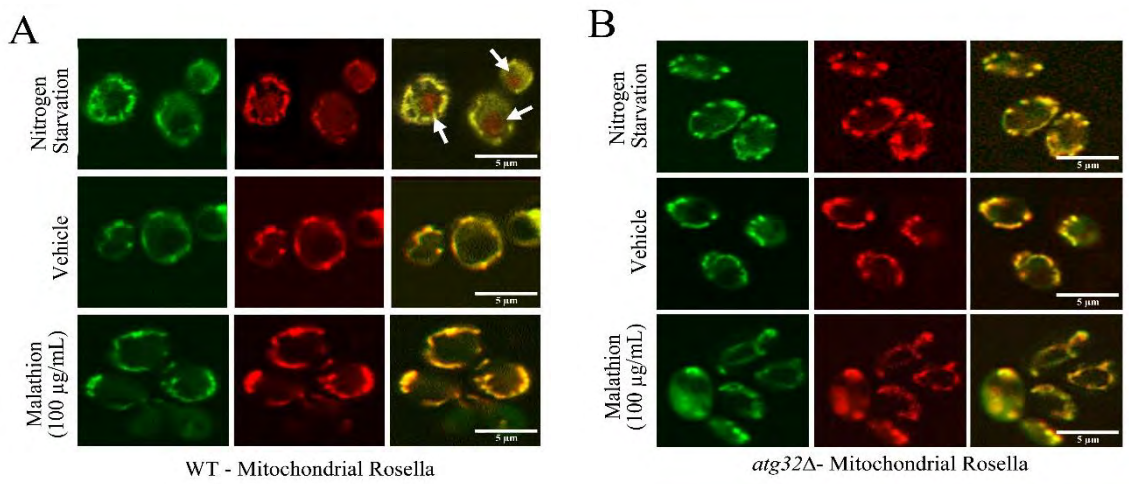

Figure 4 Delivery of Mitochondrial Rosella to the vacuole by mitophagy under nitrogen starvation. Cells grown in SCG-N for 6hr were observed as a positive control. Cells treated with vehicle or 100 µg/mL malathion were also examined for induction of mitophagy (A) WT and (B) *atg32*Δ cells. Mitophagy can be observed in WT cells under nitrogen starvation by the appearance of red fluorescence regions inside the vacuoles (white arrows). Scale bar, 5µm.

Recent studies have reported that mitophagy occurs when cells are pre-cultured in fermentable medium and then shifted to nitrogen starvation medium although few mitochondria are degraded [23]. The growth conditions were the same as utilized for monitoring the Cyto-Rosella. However, the cells were incubated in nitrogen starvation medium up to 6hr.

We found that nitrogen starvation induces mitophagy of WT cells whereas no induction occurs with vehicle or malathion (Fig. 4A). In contrast, atg32Δ cells exhibit lack of mitophagy activity under nitrogen starvation. In addition, vehicle or malathion exposure did not induce mitophagy in atg32Δ cells (Fig. 4B). This is consistent with reports that mitophagy is severely blocked in the atg32Δ cells. Collectively, a role for impaired mitophagy in malathion sensitivity of yeast lacking Atg32p is less clear as malathion exposure did not induce mitophagy in WT yeast.

CONCLUSION

In this study, we showed that malathion stress response pathway is related to autophagy in *S. cerevisiae* yeast. Our Rosella analysis demonstrated that autophagy levels were increased after malathion exposure. Bulk autophagy was elevated in atg32Δ cells following malathion exposure. *In contrast*, atg32Δ cells showed impaired mitophagy compared to the wild type cells under mitophagy-inducing conditions. The transport of damaged mitochondria to the vacuole through the selective autophagy or mitophagy pathways is important for maintaining mitochondrial function and integrity of cells under stress conditions. It is likely that malathion induction of the mitophagy signaling pathway may be regulated by Atg32p. Therefore, Atg32p function in mitophagy may be important for malathion tolerance. In addition, other proteins that interact with Atg32p may be involved in this mechanism. Better understanding of the molecular mechanism and regulatory pathways of Atg32p should assist in finding novel strategies to sensitize cells to malathion.

ACKNOWLEDGEMENTS

This work was supported by the Thailand Research Fund RSA6180082 (LTJ) and a grant from Mahidol University. We thank Dr. Mark Prescott for the Rosellas plasmids and Dr. Amornrat N. Jensen and Dr. Sittinan Chanarat for their helpful discussions.

REFERENCES

1. Field LM, Emyr Davies TG, O'Reilly AO, Williamson MS, Wallace BA. Voltage-gated sodium channels as targets for pyrethroid insecticides. Eur Biophys J. 2017 Oct 1;46(7):675–9.
2. Vector-borne diseases [Internet]. Available from: https://www.who.int/news-room/fact-sheets/detail/vector-borne-diseases
3. Tolle MA. Mosquito-borne diseases. Curr Probl Pediatr Adolesc Health Care. 2009 Apr;39(4):97–140.
4. Salama M, Lotfy A, Fathy K, Makar M, El-emam M, El-gamal A, et al. Developmental neurotoxic effects of Malathion on 3D neurosphere system. Appl Transl Genomics. 2015 Dec;7:13.
5. Wongta A, Sawarng N, Tongchai P, Sutan K, Kerdnoi T, Prapamontol T, et al. The Pesticide Exposure of People Living in Agricultural Community, Northern Thailand. J Toxicol. 2018 Nov 29;2018:e4168034.
6. Badr AM. Organophosphate toxicity: updates of malathion potential toxic effects in mammals and potential treatments. Environ Sci Pollut Res. 2020 Jul 1;27(21):26036–57.
7. Insecticides - Benefits of Insecticide Use [Internet]. Available from: https://science. jrank.org/pages/3599/Insecticides-Benefits-insecticide-use.html
8. Correy GJ, Zaidman D, Harmelin A, Carvalho S, Mabbitt PD, Calaora V, et al. Overcoming insecticide resistance through computational inhibitor design. Proc Natl Acad Sci. 2019 Oct 15;116(42):21012–21.
9. Himeidan YE, Temu EA, Kweka EJ. Insecticides for Vector-Borne Diseases: Current Use, Benefits, Hazard and Resistance [Internet]. Insecticides - Advances in Integrated Pest Management. IntechOpen; 2012
10. Coleman M, Hemingway J, Gleave KA, Wiebe A, Gething PW, Moyes CL. Developing global maps of insecticide resistance risk to improve vector control. Malar J. 2017 Feb 21;16(1):86.
11. Karaağa&#231 SU. Insecticide Resistance [Internet]. Insecticides - Advances in Integrated Pest Management. IntechOpen; 2012.
12. Snoeck S, Greenhalgh R, Tirry L, Clark RM, Van Leeuwen T, Dermauw W. The effect of insecticide synergist treatment on genome-wide gene expression in a polyphagous pest. Sci Rep. 2017 Oct 18;7(1):13440.
13. Lorini I, Galley DJ. Effect of the synergists piperonyl butoxide and DEF in deltamethrin resistance on strains of Rhyzopertha dominica (F.) (Coleoptera: Bostrychidae). An Soc Entomológica Bras. 2000 Dec;29:749–55.
14. Iyison NB, Shahraki A, Kahveci K, Düzgün MB, Gün G. Are insect GPCRs ideal next-generation pesticides: opportunities and challenges. FEBS J. 2021;288(8):2727–45.
15. Estève K, Poupot C, Dabert P, Mietton-Peuchot M, Milisic V. A Saccharomyces cerevisiae-based bioassay for assessing pesticide toxicity. J Ind Microbiol Biotechnol. 2009 Oct 1;36:1529–34.
16. Mamaev DV, Zvyagilskaya RA. Mitophagy in Yeast. Biochem Mosc. 2019 Jan 1;84(1):225–32.
17. Gaytán BD, Loguinov AV, Peñate X, Lerot J-M, Chávez S, Denslow ND, et al. A Genome-Wide Screen Identifies Yeast Genes Required for Tolerance to Technical Toxaphene, an Organochlorinated Pesticide Mixture. PLOS ONE. 2013 Nov 18;8(11):e81253.
18. Abeliovich H, Dengjel J. Mitophagy as a stress response in mammalian cells and in respiring S. cerevisiae. Biochem Soc Trans. 2016 Apr 15;44(2):541–5.

19. Rosado C, Mijaljica D, Hatzinisiriou I, Prescott M, Devenish RJ. Rosella: A fluorescent pH-biosensor for reporting vacuolar turnover of cytosol and organelles in yeast. Autophagy. 2008 Feb 16;4(2):205–13.
20. Gietz RD, Woods RA. 4 Transformation of Yeast by the Lithium Acetate/Single-Stranded Carrier DNA/PEG Method. In: Brown AJP, Tuite M, editors. Methods in Microbiology. Academic Press; 1998; p. 53–66. (Yeast Gene Analysis; vol. 26).
21. Xie Z, Klionsky DJ. Autophagosome formation: core machinery and adaptations. Nat Cell Biol. 2007 Oct;9(10):1102–9.
22. Kanki T, Wang K, Cao Y, Baba M, Klionsky DJ. Atg32 is a mitochondrial protein that confers selectivity during mitophagy. Dev Cell. 2009 Jul;17(1):98–109.
23. Kanki T, Furukawa K, Yamashita S. Mitophagy in yeast: Molecular mechanisms and physiological role. Biochim Biophys Acta. 2015 Oct;1853(10 Pt B):2756–65.

Proceeding PP040

Proteomic analysis of anti-cancer effects by 5′-deoxy-5′-methylthioadenosine treatment in cholangiocarcinoma cell line

Sutthipong Nanarong[1], Sittiruk Roytrakul[2], Thanawat Pitakpornpreecha[1], Sumalee Obchoei[1, *]

[1] Division of Health and Applied Science, Faculty of Science, Prince of Songkla University, Songkhla 90110, Thailand
[2] National Center for Genetic Engineering and Biotechnology, National Science and Technology Development Agency, Pathumtani 12120, Thailand

***Email**: sumalee.o@psu.ac.th

ABSTRACT

The treatment of advanced cholangiocarcinoma (CCA) is mostly ineffective due to the intrinsic and acquired chemotherapeutic drug resistance. Clearly, a novel and effective therapies are urgently needed. 5′-deoxy-5′-methylthioadenosine (MTA) is a natural-derived bioactive compound that has been shown to possess anti-cancer activity in various human cancers. In the present study we demonstrated that MTA exhibited a potent cytotoxic effect against a CCA cell line, KKU-213A in a dose dependent manner. In addition, it strongly inhibited cell migration and invasion of CCA cells. Proteomic analysis, using LC-MS/MS, identified the total of 4,117 proteins. In which, 10 were identified only in untreated cells, 30 were found only in MTA treated cells, whereas 4,077 were expressed in both. The 25 most up-regulated and down-regulated proteins in MTA-treated KKU-213A cell line were displayed using heatmap analysis. The results showed that MTA significantly suppressed numbers of oncoproteins such as RYR1, RCOR2, KLC1, GRAMD1C, and HLA-DQB1. Protein-protein interaction analysis of 25 most down-regulated proteins predicted 3 major clusters namely calcium ion transmembrane transport, antigen processing and presentation of exogenous peptide, and microtubule motor activity. These clusters were reported to involved in tumor progression and they might be the main target of MTA. The detailed study of molecular mechanisms underlying MTA effect on CCA cells both *in vitro* and *in vivo* should be further explored with the anticipation that this promising natural bioactive compound might be an alternative treatment for CCA in the future.

Keywords: 5′-deoxy-5′-methylthioadenosine, cholangiocarcinoma, KKU-213A, proteomics, LC-MS/MS

INTRODUCTION

Cholangiocarcinoma (CCA) is a cancer of the bile duct, which is a rare cancer worldwide but found with high incidence in Thailand in particular the in Northeastern part [1]. CCA patients have a poor prognosis due to the diagnosis at late stages and by nature this cancer is highly invasive and highly resistant to various anticancer drugs [2, 3]. Therefore, it is urgent to search for new anti-cancer agents that are effective with minimal side effects.

5′-deoxy-5′-methylthioadenosine (MTA), a by-product of polyamine biosynthesis, is naturally occurring sulfur-containing nucleoside found in prokaryotes, yeast, plants, and higher eukaryotes [4, 5]. Number of reports demonstrated that MTA possesses pharmacological and anti-cancer activities such as inhibitory effects on cell proliferation and invasion of many

cancers. For instance, it has been reported that MTA inhibits cell proliferation of cervical cancer, lymphoma, erythroleukemia, and promyelocytic cells [6, 7]. In addition, MTA was shown to suppress migration and invasion of colorectal cancer, liver cancer, and HT1080 fibrosarcoma cells [8, 9].

Despite several studies on MTA targets and mechanism of action in various cancers, its effect on CCA has not been explored. In this study, we investigated the effects of MTA on the cell proliferation, migration and invasion of KKU-213A CCA cell line. Finally, using proteomic analysis we identified differential expressed proteins in MTA-treated CCA cell line.

MATERIALS AND METHODS

Reagents and cell cultures

5′-deoxy-5′-methylthioadenosine (MTA) and 3-(4,5-dimethylthiazol-2-yl)-2,5-diphenyltetrazolium bromide (MTT) reagents were purchased from Sigma (Sigma - Aldrich, St. Louis, MO, USA). Matrigel was purchased from BD Bioscience (BD Bioscience, Bedford, MA, USA). A human CCA cell line (KKU-213A) was established from the tissues of Thai CCA patients as previously described [10] and was obtained from the Japanese Collection of Research Bioresources (JCRB) Cell Bank (Osaka, Japan). The cells were cultured in Dulbecco's modified Eagle's medium (DMEM) supplemented with 10% fetal bovine serum (FBS) (Gibco, NY, USA) and 1% antibiotics/antimycotics (Capricorn Scientific), in a humidified atmosphere of 5% CO_2 at 37 ˚C.

Cell viability assay

Cells (3×10^3 cells/100 µL/well) were seeded in a 96-well plate and incubated overnight. On the next day, the attached cells were treated with 0, 3.125, 6.25, 12.5, 25, 50, and 100 µg/mL of MTA. After 72 h of incubation, cell viability was determined using MTT assay. Percentage of cell viability was calculated, using untreated cell as control with 100% cell viability. The same set of data was used for the calculation of the half-maximal inhibitory concentration (IC_{50}).

Cell growth assay

The effect of MTA on cell growth was measured using MTT. Briefly, KKU-213A cells at the density of 1.5×10^3 cells/100 µL/well were seeded onto 96-well plate, treated with 25 µg/mL and subjected to MTT assay at day 0, 2, 4, 6, and 8. Cell proliferation rate was calculated as fold change comparing to day 0.

Wound healing assay

The CCA cells (2×10^5 cells/well) were seeded into a 12-well plate and cultured in complete medium overnight. After achieving approximately 90-100% confluence, cell monolayers were scratched by using sterile pipette tip and then the old medium and cell debris were removed. Cells were incubated with 25 µg/mL of MTA for 48 h, images of the wounds were captured at 12, 24, 36, and 48 h time points. The percentage of wound closure was calculated using ImageJ software (version 1.53e, National Institute of Health, Bethesda, MD, USA).

Cell migration and invasion assay

Cell migration and invasion were performed by modified Boyden chamber method using Transwell® with 8.0 µm pore size (Corning, NY, USA) and 24-well plate as a lower chamber. KKU-213A (2×10^4 cells) in serum-free medium with or without 25 µg/mL MTA

were seeded into the upper part of Transwell®. For invasion assay, the Transwell® was pre-coated with 0.5 mg/mL Matrigel™, prior to use. The lower chamber was filled with 600 µL complete medium. After 12 h of incubation, the non-migrated/non-invaded cells on the upper chamber were removed. The migrated/invaded cells were fixed with 4% paraformaldehyde, stained with 0.4% Sulforhodamine B (SRB), and then pictures were recorded under microscope. The number of migrated/invaded cells was counted from 6 random low-power fields.

Protein preparation for shotgun proteomics

To identify the target of MTA, proteomic analysis using LC-MS/MS was performed. Summary of the workflow is shown in **Fig. 3A**. MTA-treated KKU-213A and control cells were harvested by trypsinization. The cell pellets were lyzed with 0.5% SDS and centrifuged at 10,000xg for 15 min. The supernatant was transferred to a new tube, mixed with 2 volumes of cold acetone, and incubated overnight at -20 ºC. The mixture was thawed and centrifuged at 10,000xg for 15 min. After the supernatant was discarded, the pellet was dried and stored at -80 ºC until use. Protein samples were prepared, digested with sequencing grade porcine trypsin (1:20 ratio) for 16 h at 37 °C and were subjected for injection into an Ultimate3000 Nano/Capillary LC System (Thermo Scientific, UK) coupled to a HCTUltra LC-MS system (Bruker Daltonics Ltd; Hamburg, Germany) equipped with a Nano-captive spray ion source. LC-MS data were operated using DecyderMS [11, 12] and searched against a nonredundant UniProt database (Homo sapiens, 20,386 entries from Swiss-Prot; Homo sapiens, 181,774 entries from TrEMBL). The analysis allowed for a maximum of three missed cleavages from tryptic digest. Carbamidomethylation of Cys as a fixed modification, and oxidation of Met as variable modifications. The level of proteins in each sample were expressed as log2 value.

Proteomic and data analysis

The volcano plot was generated to show the total number of identified proteins and the proteins that differentially expressed in each sample. Log 2 values of the identified proteins were visualized by MultiExperiment Viewer (MeV) [13]. The heatmap was generated from the 25 most upregulated and downregulated proteins in MTA-treated KKU-213A as compared with the untreated control cells. The 25 most down-regulated proteins were furthered analyzed by Protein ANnalysis THrough Evolutionary Relationships (PANTHER) classification system [14], and were analyzed by the STRING version 11 [15] for the prediction of functional interaction networks.

Statistical analysis

The results are presented as a mean ± SEM from three separate experiments. Statistical significance was determined using Student's *t-test*. $P \leq 0.05$ was considered statistically significant.

RESULTS

MTA inhibits CCA cell viability and growth of CCA line in vitro

To determine the cytotoxic effect of MTA on CCA cell line and to obtain the optimal concentration of MTA for use in the subsequent experiments, KKU-213A were treated with various concentrations of MTA and then the cell cytotoxicity assay was performed using MTT test. The results showed that MTA reduced cell viability in a dose-dependent manner (**Fig. 1B**). As shown in **Table 1**, The IC_{50} at 72 h of MTA in KKU-213A was 25.98 ± 3.08 µg/mL. The IC_{50} concentration was used for cell growth assay (**Fig. 1C**). The results showed that MTA at

25 µg/mL inhibited growth of KKU-213A significantly at day 2, 4, 6 and 8 as compared with the untreated control.

Table 1 the half-maximal inhibitory concentrations of MTA on CCA cells at 72 h.

Cell line	**IC_{50} at 72 h of MTA** (µg/mL)
KKU-213A	25.98 ± 3.08

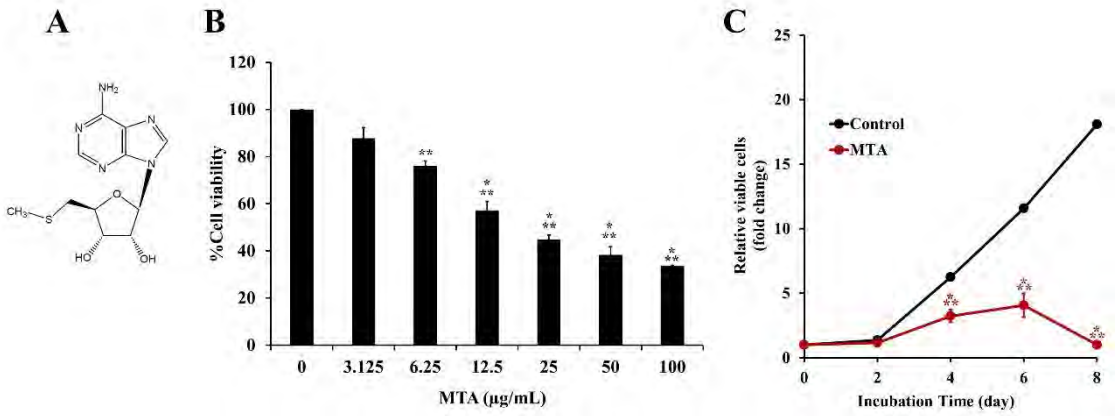

Figure 1 Effect of MTA on cell viability and growth of CCA cell line. (A) chemical structure of MTA. (B) Cell cytotoxicity assay. KKU-213A cells were treated with various concentrations of MTA for 72 h and were determined by MTT. (C) Cell growth assay. Cells were treated with 25 µg/mL MTA and the MTT assay was carried out at day 0, 2, 4, 6, and 8. Data are represented as the mean ± SEM of three independent experiments. *p ≤ 0.05, **p ≤ 0.01, ***p ≤ 0.001.

Effect of MTA on cell migration and invasion.

Wound healing assay was performed to determine the effect of MTA on cell migration. The results showed that the wound closure rate was significantly slower in MTA-treated cells. Percentage of wound closure in MTA-treated vs control cells were 24.9 vs 26.7, 39.5 68.1, and 40.3 vs 77.9 at 24, 36, and 48 h time point respectively (**Fig. 2A**). Similarly, using modified Boyden chamber assay, MTA significantly suppressed cell migration to 57% (**Fig. 2B**) and suppressed cell invasion to 52% (**Fig. 2C**).

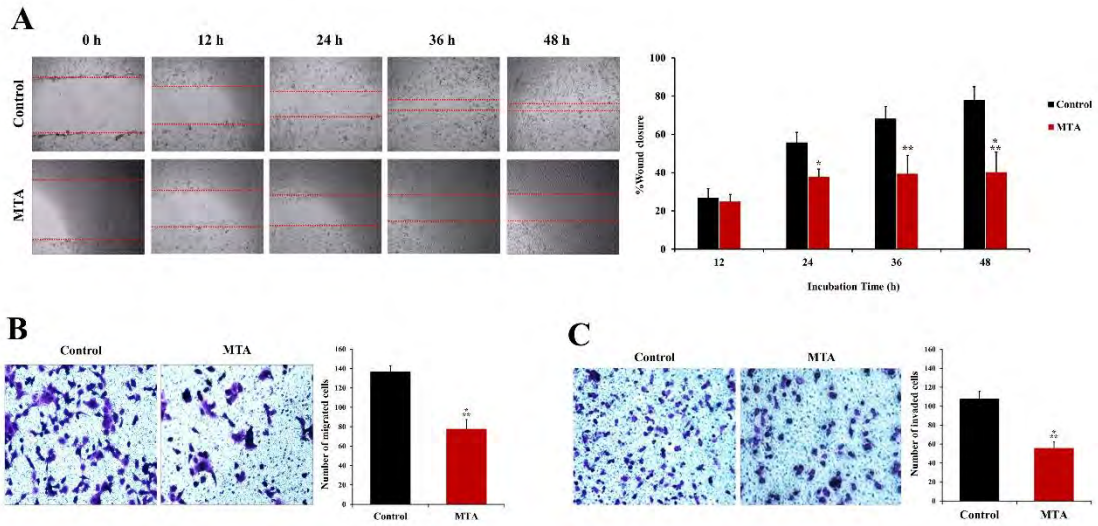

Figure 2 Effects of MTA on cell migration and invasion. (A) Wound healing assay. Confluent monolayer of KKU-213A cells was scratched and treated with MTA, representative images were taken from the same field every 12 h. Percentage of wound closure was calculated by comparing with 0 h. (B) Migration assay. Treated cells were allowed to migrate through Transwell® for 12 h and (C) Matrigel invasion assay. Treated cells were allowed to invade Matrigel-coated Transwell® for 12 h. Cells were fixed, stained and the representative images are shown. The data are represented as the mean ± SEM of three independent experiments. *p ≤ 0.05, **p ≤ 0.01, ***p ≤ 0.001.

Identification of differentially expressed proteins by proteomic analysis

To further investigate the anti-cancer effects and protein targets of MTA, LC-MS/MS was carried out to identify differentially expressed proteins. The summary workflow of the proteomic and data analysis is shown in **Fig. 3A**. The Venn diagram showed that the total of 4,117 unique non-redundant proteins were identified in all 3 biological triplicate samples. In which, 10 proteins were identified only in untreated control cells, 30 proteins were found only in MTA-treated cells, whereas 4,077 were expressed in both treated and untarred samples (**Fig. 3B**). The Venn diagram showed a total of 4,117 unique non-redundant proteins were identified in all 3 biological triplicate samples. In which, 10 proteins were identified only in untreated control cells, 30 proteins were found only in MTA-treated cells, whereas 4,077 were expressed in both treated and untarred samples (**Fig. 3B**). Volcano plot was generated by GraphPad Prism version 8 [16] to show differentially expressed protein (fold change ≥4 and False Discovery Rate (FDR) ≤ 0.05) and unchanged proteins in MTA-treated cells as compared with the control (Fig. 3C). Log 2 values of the identified proteins were visualized by MultiExperiment Viewer (MeV). The heatmap was generated from the 25 most upregulated and downregulated proteins as shown in **Fig 3D**.

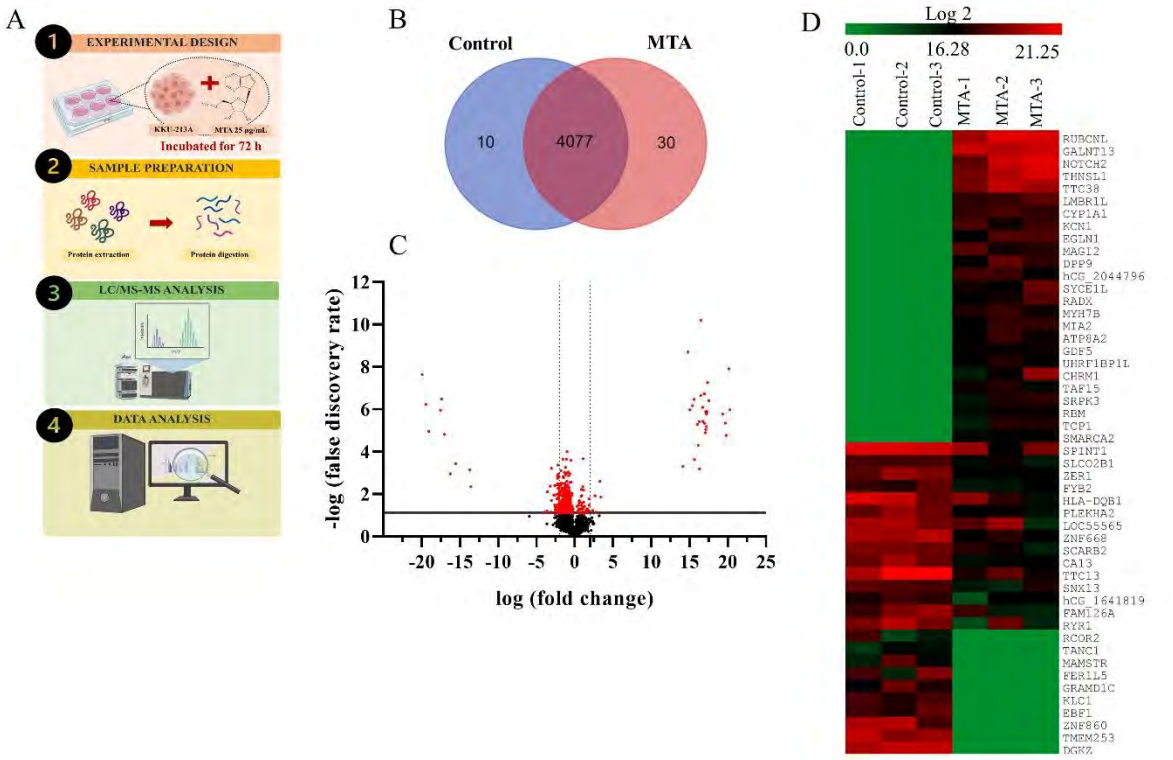

Figure 3 Identification of differentially expressed proteins by proteomics analysis. (A) Illustration of experimental workflow. (B) Total number of identified proteins in all samples were displayed by Venn diagram. (C) Volcano plot of all proteins identified in the proteome database, for untreated and MTA-treated groups ($p \leq 0.05$). (D) Heatmap analysis of 25 most up- and down-regulated proteins.

Gene ontology and protein-protein interaction analyses

The 25 most down-regulated proteins were further classified by molecular function and biological process. The results showed that the down-regulated proteins are involved in molecular function regulator (50.0%), binding (33.30%), and catalytic activity (16.70%) respectively (**Fig. 4A**). Annotation via biological process, revealed that the down-regulated proteins are involved in biological regulation (26.70%), cellular process (26.70%), metabolic process (20.00%), response to stimulus (6.70%), signaling (6.70%), immune system process (6.70%), and localization (6.70%) respectively (**Fig. 4B**). Furthermore, protein-protein interaction was analyzed by STRING software. The results showed interaction between top 25 down-regulated proteins and their predicted protein partners (HLA-DQA1, FKBP1A, KIF5B, CACNA1S, TRDN, KIF5C, FKBP1B, KDM1A, KIF5A, and S100A1). As shown in **Fig. 4C**, the three main protein clusters were, 1) calcium ion transmembrane transport (RYR1, CACNA1S, FKBP1A, FKBP1B, TRDN, S100A1), 2) protein antigen processing and presentation of exogenous peptide (HLA-DQB1, HLA-DQA1), and 3) protein microtubule motor activity (KIF5A, KIF5C, KLC1 KIF5B).

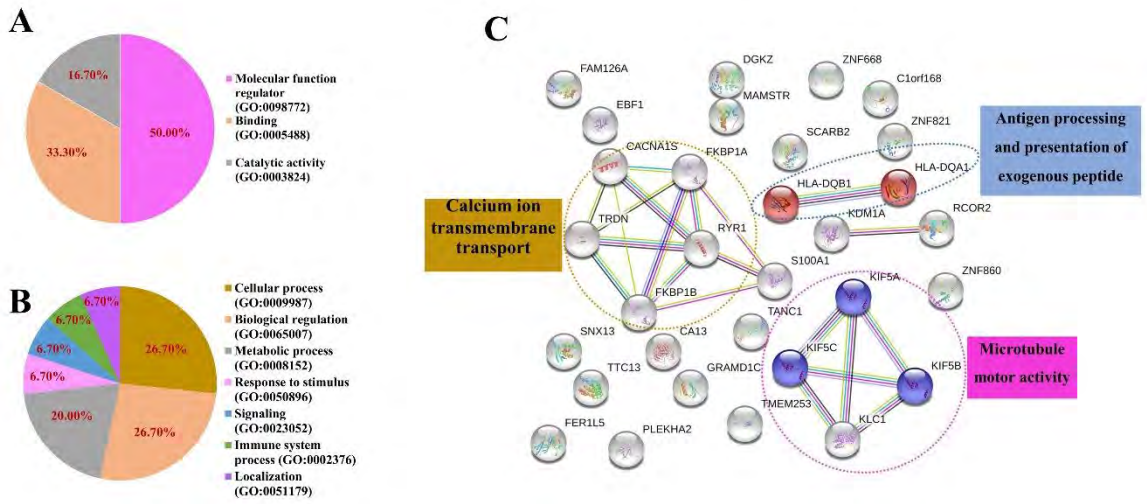

Figure 4 Bioinformatic analyses of the 25 most down-regulated proteins. (A) Gene ontology analysis based on molecular function and (B) Gene ontology analysis based on biological process. (C) Prediction of protein-protein interaction using STRING software.

DISCUSSION AND CONCLUSION

Currently, the only effective treatment for CCA is curative surgery, but more than 80% of the patients are inoperable due to late presentation and delayed diagnosis [17]. Chemotherapy is therefore the most common treatment option for patients with advanced CCA [18]. Apparently, the search for novel and effective treatments is urgently required.

In this study, we showed that MTA exhibited anti-proliferative, anti-migrative and anti-invasive effects on CCA cells. Although this is the first report regarding MTA effect on CCA, but the anti-cancer activity of this compound is well known in many cancers [6, 7].

Cell migration and invasion are aggressive phenotypes that facilitate tumor metastasis that is known to be one of the hallmarks of cancer [19]. Here in, we demonstrated that MTA strongly suppressed CCA cell migration and invasion capability. Concomitant with the previous reports in other cancers such as melanoma [20] and liver cancer [21]. Analysis of down-regulated proteins in MTA-treated KKU-213A and the results of protein-protein interactions showed that RYR1 in association with predicted protein partners forms a protein network that involves in calcium ion transmembrane transport (**Fig. 4C**). Previously, it was reported in colon cancer that abnormal remodeling of the intracellular Ca^{2+} homeostasis enhanced cell proliferation, migration, and survival [22]. In addition, our results showed that the interaction between input proteins and predicted functional partners, for instance the interaction of KLC1 and KIF5, form microtubule motor activity clusters (**Fig. 4C**). Functionally, KLC1 is actively involved in transporting c-MYC which is an oncogenic transcription factor [23], and KIF5 predicted partners protein overexpression in breast cancer, leads to formation of docetaxel resistance [24]. In addition, HLA-DQB1 protein input involved in antigen processing and presentation of exogenous peptide cluster (**Fig. 4C**). The previous study reported that HLA-DQB1 protein highly expressed in tumor cells and led to the tumor recurrence [25].

In summary, this study shows for the first time that MTA exhibits strong anti-cancer effect against CCA cells in *in vitro*. Proteomic analysis demonstrates a unique differentially expressed protein profile in MTA treated cells. More detailed study focusing on these differentially expressed proteins will bring a better knowledge on mechanism of action of MTA. In the future, MTA might serve as a potential anti-cancer agent.

ACKNOWLEDGEMENTS

This study was supported by the budget revenue of Prince of Songkla University to S. Obchoei (SCI6202093S). Sutthipong Nanarong was supported by the Research Grant for Thesis in the Fiscal Year 2020 Scholarships, Graduate School of Prince of Songkla University, Thailand

REFERENCES

1. Khan SA, Thomas HC, Davidson BR, Taylor-Robinson SD. Cholangiocarcinoma. Lancet. 2005;366(9493):1303-14.
2. Braconi C, Patel T. Cholangiocarcinoma: new insights into disease pathogenesis and biology. Infect Dis Clin North Am. 2010;24(4):871-84, vii.
3. Isa T, Kusano T, Shimoji H, Takeshima Y, Muto Y, Furukawa M. Predictive factors for long-term survival in patients with intrahepatic cholangiocarcinoma. Am J Surg. 2001;181(6):507-11.
4. Pegg AE, Jones DB, Secrist JA, 3rd. Effect of inhibitors of S-adenosylmethionine decarboxylase on polyamine content and growth of L1210 cells. Biochemistry. 1988;27(5):1408-15.
5. Williams-Ashman HG, Seidenfeld J, Galletti P. Trends in the biochemical pharmacology of 5'-deoxy-5'-methylthioadenosine. Biochem Pharmacol. 1982;31(3):277-88.
6. Shafman TD, Sherman ML, Kufe DW. Effect of 5'-methylthioadenosine on induction of murine erythroleukemia cell differentiation. Biochem Biophys Res Commun. 1984;124(1):172-7.
7. Vandenbark AA, Ferro AJ, Barney CL. Inhibition of lymphocyte transformation by a naturally occurring metabolite: 5'-methylthioadenosine. Cell Immunol. 1980;49(1):26-33.
8. Tang B, Kadariya Y, Chen Y, Slifker M, Kruger WD. Expression of MTAP inhibits tumor-related phenotypes in HT1080 cells via a mechanism unrelated to its enzymatic function. G3 (Bethesda). 2014;5(1):35-44.
9. Tomasi ML, Cossu C, Spissu Y, Floris A, Ryoo M, Iglesias-Ara A, et al. S-adenosylmethionine and methylthioadenosine inhibit cancer metastasis by targeting microRNA 34a/b-methionine adenosyltransferase 2A/2B axis. Oncotarget. 2017;8(45):78851-69.
10. Sripa B, Leungwattanawanit S, Nitta T, Wongkham C, Bhudhisawasdi V, Puapairoj A, et al. Establishment and characterization of an opisthorchiasis-associated cholangiocarcinoma cell line (KKU-100). World J Gastroenterol. 2005;11(22):3392-7.
11. Johansson C, Samskog J, Sundstrom L, Wadensten H, Bjorkesten L, Flensburg J. Differential expression analysis of Escherichia coli proteins using a novel software for relative quantitation of LC-MS/MS data. Proteomics. 2006;6(16):4475-85.
12. Thorsell A, Portelius E, Blennow K, Westman-Brinkmalm A. Evaluation of sample fractionation using micro-scale liquid-phase isoelectric focusing on mass spectrometric identification and quantitation of proteins in a SILAC experiment. Rapid Commun Mass Spectrom. 2007;21(5):771-8.
13. Howe EA, Sinha R, Schlauch D, Quackenbush J. RNA-Seq analysis in MeV. Bioinformatics. 2011;27(22):3209-10.
14. Mi H, Muruganujan A, Ebert D, Huang X, Thomas PD. PANTHER version 14: more genomes, a new PANTHER GO-slim and improvements in enrichment analysis tools. Nucleic Acids Res. 2019;47(D1):D419-D26.
15. Szklarczyk D, Gable AL, Lyon D, Junge A, Wyder S, Huerta-Cepas J, et al. STRING v11: protein-protein association networks with increased coverage, supporting functional

discovery in genome-wide experimental datasets. Nucleic Acids Res. 2019;47(D1):D607-D13.
16. Niu R, Liu Y, Zhang Y, Zhang Y, Wang H, Wang Y, et al. iTRAQ-Based Proteomics Reveals Novel Biomarkers for Idiopathic Pulmonary Fibrosis. PLoS One. 2017;12(1):e0170741.
17. Sripa B, Pairojkul C. Cholangiocarcinoma: lessons from Thailand. Curr Opin Gastroenterol. 2008;24(3):349-56.
18. Marin JJ, Macias RI. Understanding drug resistance mechanisms in cholangiocarcinoma: assisting the clinical development of investigational drugs. Expert Opin Investig Drugs. 2021;30(7):675-9.
19. Fares J, Fares MY, Khachfe HH, Salhab HA, Fares Y. Molecular principles of metastasis: a hallmark of cancer revisited. Signal Transduct Target Ther. 2020;5(1):28.
20. Stevens AP, Spangler B, Wallner S, Kreutz M, Dettmer K, Oefner PJ, et al. Direct and tumor microenvironment mediated influences of 5'-deoxy-5'-(methylthio)adenosine on tumor progression of malignant melanoma. J Cell Biochem. 2009;106(2):210-9.
21. Kirovski G, Stevens AP, Czech B, Dettmer K, Weiss TS, Wild P, et al. Down-regulation of methylthioadenosine phosphorylase (MTAP) induces progression of hepatocellular carcinoma via accumulation of 5'-deoxy-5'-methylthioadenosine (MTA). Am J Pathol. 2011;178(3):1145-52.
22. Villalobos C, Hernandez-Morales M, Gutierrez LG, Nunez L. TRPC1 and ORAI1 channels in colon cancer. Cell Calcium. 2019;81:59-66.
23. Lee CM. Transport of c-MYC by Kinesin-1 for proteasomal degradation in the cytoplasm. Biochim Biophys Acta. 2014;1843(9):2027-36.
24. De S, Cipriano R, Jackson MW, Stark GR. Overexpression of kinesins mediates docetaxel resistance in breast cancer cells. Cancer Res. 2009;69(20):8035-42.
25. Zhang L, Li M, Deng B, Dai N, Feng Y, Shan J, et al. HLA-DQB1 expression on tumor cells is a novel favorable prognostic factor for relapse in early-stage lung adenocarcinoma. Cancer Manag Res. 2019;11:2605-16.

Proceeding PP041

Expression and characterization of recombinant alkaline protease from *Aspergillus sojae* in yeast *Pichia pastoris*

Pannaporn Tantimetta[1], Aratee Aroonkesorn[1], Phanthipha Runsaeng[1], Sumalee Obchoei[1,*]

[1]Division of Health and Applied Sciences, Department of Biochemistry, Faculty of Science, Prince of Songkla University, Songkhla 90110, Thailand

***Email**: sumalee.o@psu.ac.th

ABSTRACT

Alkaline protease (AP) is a group of enzymes that breaks peptide bonds within polypeptide chain under alkaline condition. It has been extensively used in many industries in particularly food and detergent industries. AP can be obtained from wide variety of alkalophilic microorganisms including bacteria and fungi. Yeast expression system has been utilized for production of recombinant protein in large scales. In this study, we produced a recombinant alkaline protease (rAP) via cloning AP gene from *Aspergillus sojae* into pPIC9K expression vector and introduce into the yeast *Pichia pastoris* KM71. The rAP was successfully expressed and secreted to culture medium. The resultant rAP was composed of 389 amino acids and had molecular weight of approximately 35 kDa. Two positive clones, rAP-3 and rAP-4, were further analyzed and showed positive on skim milk agar plate. Folin-phenol method using casein as a substrate revealed that the enzyme activity of rAP-3 and rAP-4 were 2.966 and 3.923 U respectively. The rAPs had higher enzyme activity as compared with the commercial alkaline proteases from *Bacillus subtilis* whose enzyme activity was 2.026 U. SDS-PAGE analysis showed that rAP-3 and rAP-4 completely digested protein casein and protein from cell line lysate. This result suggests that rAP might have broad range of substrate specificity. In summary, we successfully expressed AP gene from *A. sojae* in *P. pastoris* in the form of secreted enzymes in high quantity and satisfactory activity. This established platform could be used in various applications in the future.

Keywords: alkaline protease, *Aspergillus sojae*, *Pichia pastoris*, recombinant protein, gene cloning.

INTRODUCTION

Alkaline protease accelerates the breakdown of peptide bonds in protein molecules into amino acids and smaller peptides that works under neutral to alkaline conditions. Due to this property, alkaline protease is important and has been used in detergent, leather, food, medical and chemical industries as well as waste management [1]. Alkaline protease can be obtained from most alkalophilic microorganisms including *Bacillus spp.* and *Aspergillus spp.* which can be isolated from the natural sources. The selected organisms are then cultured under appropriate conditions and allowed to produce enzymes. However, this method is time-consuming and often get low enzyme quantity. In addition, the enzyme production and purification process is complicated and difficult to expand the production volume to industrial scale [2].

To serve the needs for use of alkaline protease in high quantity and to obtain high quality enzymes with the desired properties, recombinant DNA technology has been widely applied. The processes involve introducing DNA sequences (genes) of interest, with or without modification, from one organism into another organism (host). The host will then produce recombinant protein in large quantity within a short period of time [3]. The most widely used hosts for protein expression are *Escherichia coli* and yeast. The yeast expression system has several advantages compared to *E. coli*. For instance, yeast cells have the ability to grow in high biomass and also have machinery required for post-translational modification (PTM) processes. Therefore, it can be used for producing fully functional proteins [4]. In addition, in the yeast expression system, recombinant proteins can be selectively secreted from cells into the culture medium using signal peptides known as alpha factors, making the protein purification easier.

P. pastoris is a methylotrophic yeast that can utilize methanol as a carbon and an energy source through the methanol utilization pathway (MUT pathway) because it harbors Alcohol oxidase (AOX) promoters. When methanol is present, the AOX promoter is highly activated, the gene under its control will be highly expressed [5]. Therefore, AOX promotor is included in many expression vectors for recombinant protein production in *P. pastoris*. Methylotrophic yeast can be categorized based on the ability to use methanol into 3 different sub-types namely Mut^-, Mut^+, and Mut^S. The Mut^S, such as *P. pastoris* strain KM71H, who slowly grows on methanol was reported to produce higher recombinant protein than Mut^+ strain that quickly grows on methanol [6]. In this study, we cloned AP gene from *A. sojae* into pPIC9K expression vector, expressed in *P. pastoris* strain KM71H. The rAP was purified, characterized and tested for alkaline protease activity. The overview of this study is shown in **Fig. 1**

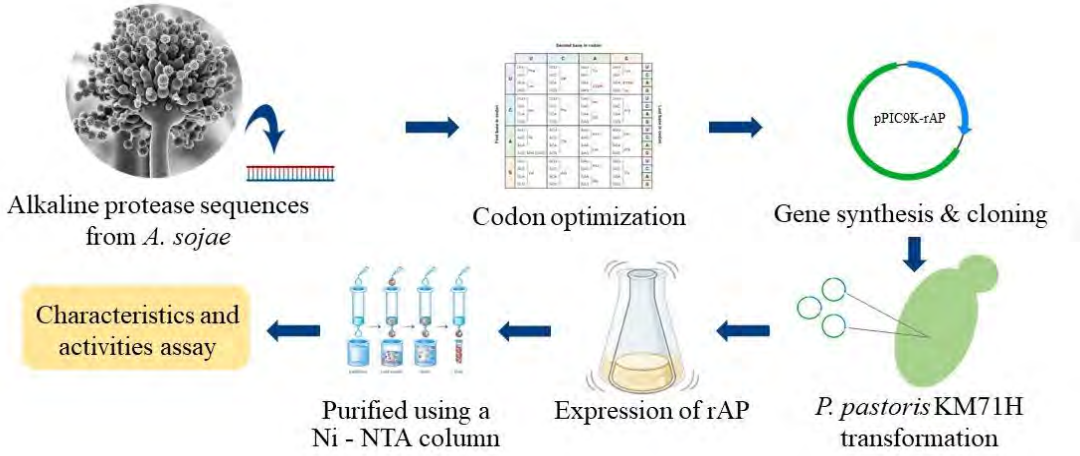

Figure 1 Overview of the study. The AP gene *A. sojae* was retrieved from GenBank and optimized the codon usage for *P. pastoris*. Then the optimized AP gene was cloned into pPIC9K expression vector and transformed into the yeast *Pichia pastoris* KM71. After protein expression was induced, the supernatant was harvested for purification via Ni-NTA column. The rAP was analyzed for protein characteristics and protease activity.

MATERIALS AND METHODS

Yeast and cultured conditions

Pichia pastoris strain KM71H was kindly provided by Dr. Ponsit Sathapondecha, Department of Molecular Biotechnology and Bioinformatics, Faculty of Science, Prince of Songkla University. All the yeast cells were cultured in Yeast Extract Peptone Dextrose (YPD) medium in shaking incubator at 30 °C and shaking 200 rpm. To express the recombinant

proteins, the positive transformant *P. pastoris* was first cultured in a Buffered Glycerol Complex Medium (BMGY) to achieve high biomass, then cultured in Buffered Methanol Complex Medium (BMMY) containing 1% (v/v) methanol. Methanol was added daily into culture flask until harvesting.

Alkaline protease gene from Aspergillus sojae

A reference nucleotide sequence of the alkaline protease (AP) gene from *A. sojae* was selected from GenBank (MG867728.1). The sequence was optimized for expression in *P. pastoris* using the GenSmart Codon Optimization program (Version Beta 1.0). In addition, poly histidine sequence (6xHis tag) was added onto the 3' end of AP gene for detection and purification purposes.

Construction of the pPIC9K-rAP expression plasmid

The codon-optimized AP sequence was sent for gene synthesis and cloning by Gene Universal Inc. The gene was successfully cloned into pPIC9K at *Eco*RI and *Not*I enzyme recognition sites on the multiple cloning site (MCS) of the vector. The resultant pPIC9K-rAP plasmid was transformed into *E. coli* DH5α for propagation. The pPIC9K-rAP was isolated from *E. coli* using miniprep, and analyzed for rAP gene insert by *Eco*RI and *Not*I double enzyme digestion and agarose gel electrophoresis. The whole sequence was then confirmed by DNA sequencing.

Transformation and screening for positive transformant P. pastoris

The pPIC9K-rAP vector was linearized with the restriction enzyme, *Sac*I and transformed into *P. pastoris* KM71 via electroporation and spread on YPD plate containing 0.25-2 mg/mL G418 antibiotic. After 2-3 days of incubation at 30 °C, the G418-resistant clones were selected and analyzed for AP gene integration by PCR (**Fig. 3A**). The primers used for PCR amplification were AOX primers (5′AOX, 5'-GACTGGTTCCAATTGACAAGC-3'; and 3′AOX, 5'-GCAAATGGCATTCTGACATCC-3').

Expression of rAP

The five-positive yeast transformants were grown in YPD medium at 30 °C, 200 rpm for 2 days. Then, the cells were harvested by centrifugation and seeded into BMGY medium and cultured for 1 day before changing the medium to BMMY and incubated at 30 °C to induce the expression of rAP. In this process, methanol was added to obtain a final concentration of 1% (v/v) every day for 7 days to maintain the induction.

Harvesting and purification of rAP

The yeast cells were removed from the fermentation broth via centrifugation at 8,000 g for 10 min at 4 °C. Solid ammonium sulfate was added to the supernatant every 3 h, until the saturation of the solution gradually reached 80% at 4 °C. The mixture was then separated via centrifugation at 12,000 g for 30 min. The precipitate was dissolved in 0.02 M borax-sodium hydroxide buffer (pH 10.0), and dialyzed overnight with the same buffer. The crude rAP was then loaded onto a Nickel-affinity chromatography column. The column was washed with PBS, 20 mM Imidazole, pH 7.0, and then eluted with PBS, 500 mM Imidazole, pH 7.4. The rAp containing fractions were collected and kept at 4 °C.

SDS-PAGE electrophoresis and western blot

Ten micrograms of the purified rAP protein samples were mixed with sample buffer, boiled for 5 min and separated by SDS-PAGE. The gel was stained with Coomassie Brilliant Blue R-250. The excess dye was removed by destain solution until the gel was clear and the protein bands were prominent. For western blot analysis, the separated proteins were transferred from the gel onto polyvinylidene fluoride (PVDF) membrane. The membrane was incubated overnight in blocking solution (0.1% skim milk, 0.1% tween 20 in PBS pH 7.4) at 4 °C to prevent non-specific binding. The blot was then incubated for 1 h at 4 °C with mouse anti-6x-His primary antibody (1:5,000). The membrane was washed and then incubated with secondary antibody (goat anti-mouse IgG-HRP secondary antibody, 1:5,000) for 1 h at room temperature. After washing, the signal was developed by adding the Enhanced Chemiluminescence (ECL) reagent and then visualized by chemiluminescence imager.

Screening of protease activity by skim milk agar plate assay

Skim milk agar plate (1% yeast extract, 2% peptone, 2% dextrose, 2% agar and 2.5% skim milk) was drilled by using blunt end of a sterile 1000 µL pipette tip to generate wells. The 50 µL of filtered cell free supernatant containing rAP or negative control and the purified rAP were added to the wells, and incubated at 37 °C for 24 h. The samples that generate clear zone on the skim milk agar plate were considered positive for protease activity.

Analysis of digested protein by SDS-PAGE

The protein samples, 1% (w/v) casein and whole cell line lysate, were used as substrate for rAP. The samples were incubated with crude rAP solution in 0.02 M borax-sodium hydroxide pH 10.0 in the ratio of 1:1, the mixtures were incubated at 40 °C for 10 min. The digested proteins were then subjected to SDS-PAGE in parallel with non-digested control samples.

Protease activity assay

The activity of rAP was analyzed via the Folin-phenol method. Briefly, 200 µL of diluted rAP was mixed with 200 µL of 1.0% casein solution and the reaction mixture was incubated at 40 °C for 10 min. To terminate the reaction, 400 µL of 0.5 M trichloroacetic acid (TCA) was added and incubated at 40 °C for another 20 min to enhance precipitation of non-digested protein. The mixture was centrifuged at 12,000 g for 10 min, and then 200 µL of supernatant was added to 1 mL of 0.4 M Na_2CO_3 and 200 µL of Folin-phenol reagent. The mixture was re-incubated at 40 °C for 20 min and the absorbance at 660 nm was determined. The amount of released tyrosine was obtained using tyrosine standard curve. A unit of protease activity was defined as the amount of enzyme that produced 1 µg of tyrosine per minute via casein hydrolysis.

RESULTS

Cloning of the AP gene from A. sojae into pPIC9K vector

The optimized sequence of AP gene from *A. sojae* (**Fig. 2A**) was successfully synthesized and cloned into the vector pPIC9K, after α-factor sequence, at *EcoR*I and *Not*I sites and designated as pPIC9K-rAP (**figure 2B and 2C)**. To confirm the present of AP gene, the purified pPIC9K-rAP was digested with *EcoR*I and *Not*I. The agarose gel electrophoresis revealed two bands at approximately 9,000 and 1,100 bp which were close to the actual size of empty plasmid (9,256 bp) and AP gene (1,187 bp) respectively (**Fig. 2D)**. The pPIC9K-rAP was further confirmed by DNA sequencing (data not shown).

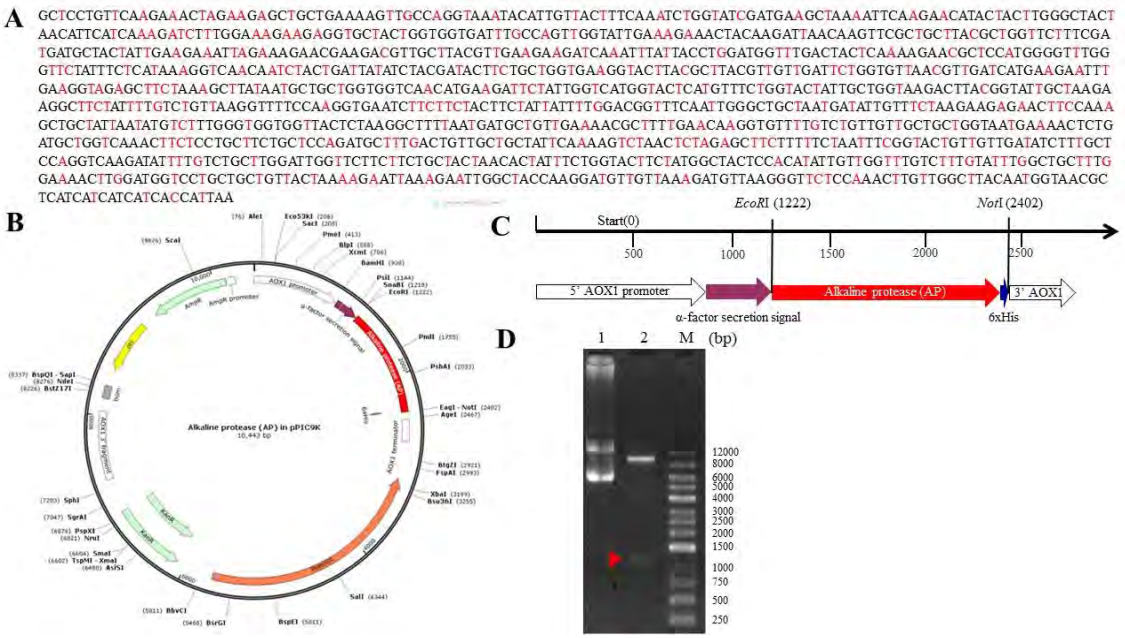

Figure 2 Construction of the expression vector pPIC9K-rAP. A) Optimized AP gene sequence B) pPIC9K-rAP plasmid map C) The AP open reading frame was cloned into pPIC9K vector flanked by α-factor secretion signal and 6xHis tag, at 5′ and 3′ end, respectively. The rAP was downstream of AOX1 promoter. D) *Eco*RI/*Not*I double enzyme digestion of pPIC9K-rAP. Lane M, 1 Kb DNA ladder; lane 1, un-disgusted pPIC9K-rAP; lane 2, digested pPIC9K-rAP.

Yeast transformation and screening for positive transformants

The pPIC9K-rAP was linearized via *Sac*I, and then transformed into *P. pastoris* KM71H. The G418-resistant clones were selected for confirmation of rAP gene integration via PCR (**Fig. 3A**). The results showed that all of the 5 G418-resistant clones were positive as observed by the presence of PCR product at approximately 1,500 bp indicating that the AP gene was successfully integrated into the *P. pastoris* genome (Fig. 3B).

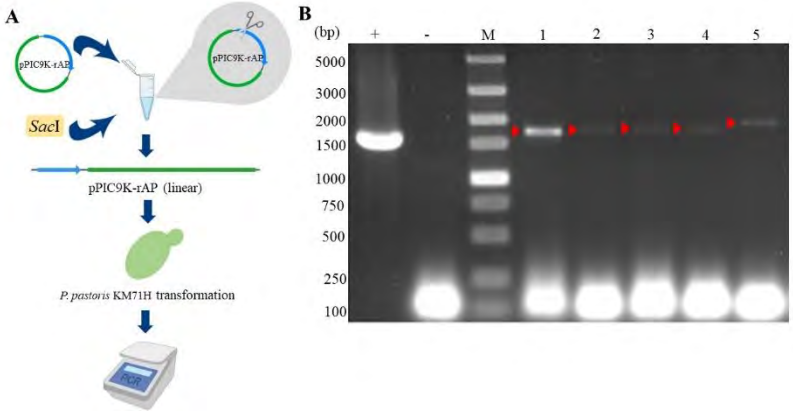

Figure 3 Identification of positive transformant yeast clones by PCR. A) An illustration for yeast transformation and screening via PCR analysis. B) Results of PCR analysis. Lane M, DNA ladder; lane +, Positive control; lane -, Negative control; lane 1-5, PCR results of transformed yeast clone 1-5.

Expression of rAP

The PCR positive *P. pastoris* transformants were cultured and induced via methanol every 24 h. After 7 days of induction, the cell-free supernatant was harvested via centrifugation. The rAP was precipitated via salting out method using ammonium sulfate and removed the remaining salt via dialysis. The crude rAP was then purified via Nickel-affinity chromatography column. Analysis of rAP protein by SDS-PAGE (**Fig. 4A**) and Western Blot (**Fig. 4B**) revealed a single protein band at approximately 35 kDa which was similar to the calculated molecular weight of rAP. Similar results were observed in all 5 clones, no protein band was observed in un-induced sample. Clone 3 and 4 had a higher growth rate in G418 antibiotic-containing growth medium when compared with clone 1, 2 and 5 (data not show) suggesting higher gene copy number. Therefore, clone 3 and 4 were selected for enzyme production and further analyses. rAP was highly expressed by clone 3 and 4 with the crude protein yield of 370.0 and 344.6 mg/L respectively. SDS-PAGE analysis of TCA-precipitated protein samples were shown in **Fig. 4C.**

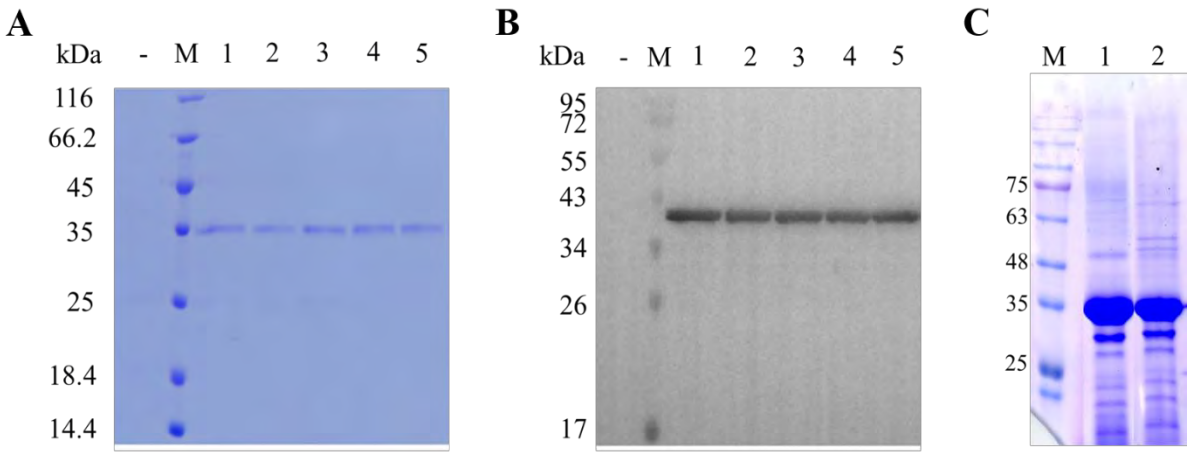

Figure 4 SDS-PAGE and Western Blot analysis of rAP. A) rAP protein samples were analyzed by 10% SDS-PAGE and B) separated proteins were further analyzed by Western Blot. Lane M, Protein Marker; lane -, Un-induced sample; lane 1-5, Induced samples. C) SDS-PAGE analysis of TCA-precipitated protein samples. 200 µL of cell-free supernatant was precipitated using TCA and was subjected to SDS-PAGE analysis. Lane M, Protein Marker; lane 1, culture medium of clone 3; lane 2, culture medium of clone 4.

Determination of rAP activity

In order to screen for protease activity, skim milk agar plate assay was performed. As shown in **Fig. 5A**, cell-free supernatant from *P. pastoris* KM71H pPIC9K-rAP clone 3 and clone 4 showed clear zone, indicating positive for protease activity. Similar result was observed with purified rAP. On the other hand, the cultured medium of non-transformed *P. pastoris* did not show a clear zone, indicating the absence of protease activity.

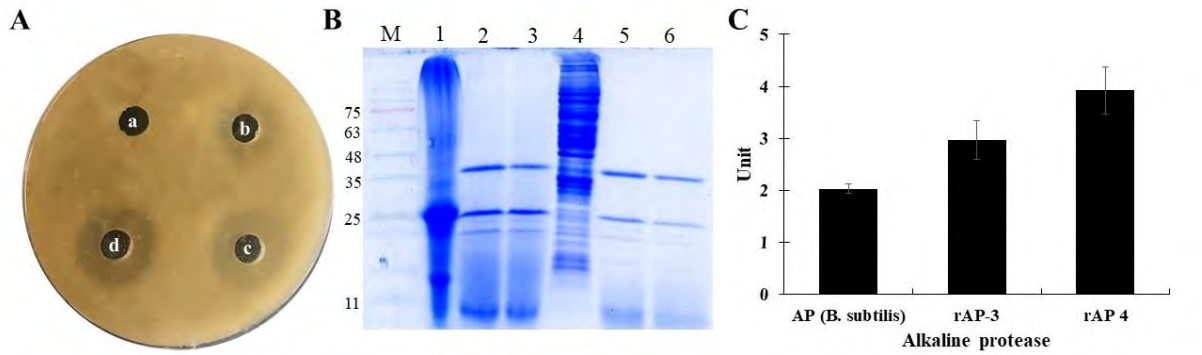

Figure 5 Alkaline protease activity assays. A) Protease activity of rAP was assessed by skim milk agar plate. *a* cell-free supernatant from non-transformed yeast cell culture (negative control), *b* purified rAP 10 µg, *c* cell-free supernatant from *P. pastoris* KM71H pPIC9K-rAP clone 3 and *d* clone 4 culture medium. B) non-digested and digested proteins analyzed by SDS–PAGE, lane M, protein marker; lane 1, non-digested casein; lane 2, casein digested with rAP-3; lane 3, casein digested with rAP-4; lane 4, non-digested cell line lysate; lane 5, cell line lysate digested with rAP-3; lane 6, cell line lysate digested with rAP-4. C) Alkaline protease assay via Folin-phenol method using casein as substrate.

SDS-PAGE results showed that, after 10 min of incubation, rAP completely digested both casein and human cell line lysate as compared with non-digested control (**Fig. 5B**). Alkaline protease activity assay by Folin-phenol method, using casein as a substrate, showed that the enzyme activity of rAP-3 and rAP-4 was 2.966 and 3.923 U, respectively. The activity of rAP from both clones was higher than that of the commercial alkaline proteases from *B. subtilis*, which was 2.026 U (**Fig. 5C**).

DISCUSSION AND CONCLUSION

Aspergillus sojae is known to produce wide variety of proteases including extracellular AP, it has been widely used in food industry for decades [7]. In this study, we utilized DNA technology in order to express and produce rAP in *P. pastoris* KM71H. The resultant protein was approximately 35 kDa, which is similar to a report from previous study [8].

A simple method, skim milk agar plate assay, was performed for screening of protease activity. The method is simple and useful for screening purpose that has been widely used in number of applications [9]. Our results showed that rAP clone 3 and clone 4 were positive for protease activity as shown by the presence of clear zones. It seems that rAP-4 may have stronger protease activity than rAP-3 as shown by wider clear zone. This method maybe used as semi-quantitative or quantitative assay when using standard protease as a calibrator. The rAP was tested for the digestion of casein and total protein from human cell line, we found that rAP-3 and rAP-4 were able to digest both protein samples, suggesting a broad substrate specificity. This is consistent with the previous study demonstrating that alkaline proteases from *Aspergillus spp*. have a wide range of substrates such as soy isolate protein, BSA and glutin (8, 10, 11) . To measure activity of rAP, we utilized Folin-phenol method using casein as a substrate. Although this method is a common test for many proteases, however, we performed the test at 40 °C and the pH 10.0 which is optimal condition for alkaline proteases. This incubation condition was reported previously with AP from *B. subtilis* [11] and rAP from *Aspergillus oryzae* (12).

In conclusion, we successfully produced rAP in *P. pastoris* with satisfactory quantity and activity. Our recombinant yeast clones can be used in various applications and subjected to production on a larger scale in the future.

ACKNOWLEDGEMMENTS

This research was co-supported by National Research Council of Thailand (NRCT) and National Science, Research and Innovation Fund (NSRF) and Prince of Songkla University (Grant No.X650093). Miss Pannaporn Tantimetta was supported by Research Grant for thesis from graduate school of Prince of Songkla University. We would like to thank Dr. Ponsit Sathapondecha for kindly providing us the yeast strain.

REFERENCES

1. Sharma M, Gat Y, Arya S, Kumar V, Panghal A, Kumar A. A Review on Microbial Alkaline Protease: An Essential Tool for Various Industrial Approaches. Ind Biotechnol. 2019; 15(2):69–78.
2. Razzaq A, Shamsi S, Ali A, Ali Q, Sajjad M, Malik A, et al. Microbial Proteases Applications. Front Bioeng Biotechnol. 2019; 7:110.
3. Khan S, Ullah MW, Siddique R, Nabi G, Manan S, Yousaf M, et al. Role of Recombinant DNA Technology to Improve Life. Int J Genomics. 2016; 16(1):1–14.
4. Bill RM. Playing catch-up with *Escherichia coli*: using yeast to increase success rates in recombinant protein production experiments. Front Microbiol. 2014; 85(5):1-5.
5. Çelik E, Çalık P. Production of recombinant proteins by yeast cells. Biotechnol Adv. 2012; 30(5):1108–18.
6. Krainer FW, Dietzsch C, Hajek T, Herwig C, Spadiut O, Glieder A. Recombinant protein expression in *Pichia pastoris* strains with an engineered methanol utilization pathway. Microb Cell Factories. 2012; 11(1):22.
7. Hayashi K, Fukushima D, Mogi K. Isolation of Alkaline Proteinase from *Aspergillus sojae* in Homogeneous Form. Agric Biol Chem. 1967; 31(10):1237–41.
8. Ke Y, Yuan X, Li J, Zhou W, Huang X, Wang T. High-level expression, purification, and enzymatic characterization of a recombinant *Aspergillus sojae* alkaline protease in *Pichia pastoris*. Protein Expr Purif. 2018; 148:24–9.
9. Vijayaraghavan P, Samuel G. A simple method for the detection of protease activity on agar plates using bromocresolgreen dye. J Biochem Tech. 2013; 4(3): 628-630.
10. Adinarayana K, Ellaiah P, Prasad DS. Purification and partial characterization of thermostable serine alkaline protease from a newly isolated *Bacillus subtilis* PE-11. AAPS PharmSciTech. 2003; 4(4):440–8.
11. Mikhailova EO, Mardanova AM, Balaban NP, Rudenskaya GN, Sharipova MR. Isolation and characterization of a subtilisin-like proteinase of *Bacillus intermedius* secreted by the *Bacillus subtilis* recombinant strain AJ73 at different growth stages. Biochem Mosc. 2007; 72(2):192–8.
12. Guo J-P, Ma Y. High-level expression, purification and characterization of recombinant *Aspergillus oryzae* alkaline protease in *Pichia pastoris*. Protein Expr Purif. 2008; 58(2):301–8.

Proceeding PP042

Proteomic analysis of 5-fluorouracil resistant cholangiocarcinoma cell line

Kankamol Kerdkumthong[1], Kawinnath Songsurin[1], Sittiruk Roytrakul[2], Sumalee Obchoei[1,*]

1. Division of Health and Applied Sciences, Department of Biochemistry, Faculty of Science, Prince of Songkla University, Songkhla 90110, Thailand
2. National Center for Genetic Engineering and Biotechnology, National Science and Technology Development Agency, Pathumtani 12120, Thailand

***Email**: sumalee.o@psu.ac.th

ABSTRACT

Resistance to commonly used chemotherapeutic drugs is a major problem of cholangiocarcinoma (CCA) therapy, therefore more effective treatment strategy is urgently needed. Drug resistant cell lines have been used for elucidating drug resistance mechanisms in various cancers leading to the discovery of novel treatments. Here in, we established a 5-Fluorouracil resistant (FR) CCA cell line named KKU-213A-FR, studied its malignant phenotypes and utilized the quantitative LC-MS/MS for the analysis of proteins involved in drug resistance mechanisms. The results showed that KKU-213A-FR had slower growth rate than its parental cell line. Conversely, cell migration and invasion ability were increased significantly. The proteomic analysis identified the total number of 4,284 proteins. In which, 3 were identified only in parental cells, 136 were found only in FR cells, whereas 4,145 were expressed in both cell lines. Volcano plot showed 146 significantly up- and 79 down-regulated proteins in KKU-213A-FR when compared to the control, whereas 4,059 proteins were unchanged. The 25 most up- and down-regulated proteins in KKU-213A-FR were shown by Heatmap analysis, only the up-regulated proteins were focused and further analyzed. Gene ontology revealed that most of these proteins were classified into cellular process group and the protein-protein interaction analysis showed ubiquitin-dependent protein clustering groups. In conclusion, the KKU-213A-FR exhibits highly invasive phenotypes and a unique proteomic profile as compared to KKU-213A parental cells. More in-depth study on the differentially expressed proteins may lead to a better understanding of drug resistance mechanisms and more effective treatments for CCA.

Keywords: drug resistance, cholangiocarcinoma, 5-Fluorouracil, proteomics, LC-MS/MS

INTRODUCTION

Cholangiocarcinoma (CCA) is a malignant cancer that originating from bile duct epithelium (1). Incidence of CCA is increasing worldwide and the highest incidence was noted in the Northeast of Thailand (2). Patients with metastatic CCA is a poor candidate for surgery, therefore the common treatment for these patients is chemotherapy (3). Unfortunately, CCA is highly invasive and highly resistant to chemotherapeutic drugs leading to ineffective treatments and poor overall survival. A better understanding in drug resistant mechanisms might lead to a more effective treatment for CCA. Drug resistant cell lines has been used as a tool for investigating the drug resistant mechanisms and for testing novel therapeutic agents prior to in *in vivo* and clinical uses (4). KKU-213A is a CCA cell line that established from tumor tissues of a Thai CCA patient and is commonly used among CCA researchers (5). 5-FU is one of most

common first-line chemotherapeutic drug that used in CCA treatment. A few 5-FU resistant that established from CCA cell lines such as KKU-M055 and KKU-M214 cell lines were previously established (6).The purpose of this study was to establish a 5-FU-resistant KKU-213A cell line (KKU-213A-FR) using gradually increasing drug concentration (step-wise) method (7). The established cell line was further used for investigation of tumor phenotypic changes namely cell growth, cell migration and invasion. Moreover, proteomic analysis was performed to identify the differentially expressed proteins. Number of bioinformatic tools were utilized to elucidate protein functions and interaction networks.

MATERIALS AND METHODS

Cell lines and cultured conditions

A CCA cell line, KKU-213A, was obtained from the Japanese Collection of Research Bioresources (JCBR) Cell Bank, Osaka, Japan. All cells were maintained in Dulbecco's Modified Eagle Medium (DMEM) supplemented with 10% fetal bovine serum (FBS) and 1% antibiotics/antimycotics, in a humidified atmosphere of 5% CO_2 at 37 °C.

Establishment of chemotherapeutic drug resistant cell line

A chemotherapeutic drug, 5-FU, was purchased from Sigma. Drug resistant cell line was established by step-wise method as described previously (7) with some necessary modifications. To obtain an optimal starting drug concentration the inhibitory concentration 25 (IC_{25}) and the half maximal inhibitory concentration (IC50) of 5-FU in KKU-213A were determined. The cells were initially cultured in DMEM containing 2.5 μM (IC_{25}) of 5-FU. The cell was cultured in the same drug concentration for at least 4 passages before increased 2 times of the previous concentration. Finally, the resultant cell lines that were grown exponentially in the presence of 7 μM 5-FU were obtained and designated as KKU-213A-FR.

Chemotherapeutic drug sensitivity assay

To confirm drug resistant phenotype of the established cell line, cell viability of KKU-213A and KKU-213A-FR were determined by 3-(4,5-dimethylthiazole-2-yl)-2,5-biphenyl tetrazolium bromide (MTT) assay. Briefly, the cells were seed at 3 $x10^3$ cells/well onto 96-well plate and incubated for 24 h. Then the cells were treated with various concentration of 5-FU for 72 h. After that 0.5 mg/mL MTT solution was added to each well and incubated at 37 °C for 2 h and then the medium was replaced with 100 μL dimethyl sulfoxide (DMSO) to solubilize the formazan crystal. The absorbance was measured at 540 nm using microplate reader.

Cell proliferation assay

To compare cell proliferation ability under low FBS condition between parental and FR cell line. The cells ($1.5x10^3$ cells/well) were seeded onto 96-wells plate in DMEM containing 2% FBS. The cell proliferation was examined by MTT at day 0, 2, 4, and 6. The results were calculated and presented as fold change compared with day 0.

Wound healing assay

Cell migration capacity was determined by wound healing assay. Cells in DMEM with 2% FBS were seeded onto 6-well plate at the density of 4.5×10^6 cells/well. After 24 h, the wound was created on a confluent monolayer by sterile pipette tip. The cells were observed under microscope and the images were captured at 0, 6, 12 and 24 h. The cell-free spaces were

measured by imageJ software (8), the percentage of wound closure were calculated and compared. The faster wound closure rate reflects higher migration capacity of the cells.

Boyden chamber assay

The migration and invasion assays were performed by using the modified Boyden chamber method. The cells were seeded onto the, 8-µm porous polycarbonate membrane, upper chamber. For invasion assay, the membrane was coated with 0.5 mg/mL Matrigel (BD Biosciences) prior to use. The complete medium was added to the lower chamber to allow the chemoattractant migration of the cells. After 12 h, the non-migrated cells on upper chamber were wiped off with cotton swab, the membrane was fixed and stained with 0.4% sulforhodamine B (SRB). The numbers of migrated and invaded cells from 6 random low-power fields were counted and compared.

Protein preparation for shotgun proteomics

The cell pellets were lyzed with 0.5% SDS and centrifuged at 10,000xg for 15 min. The supernatant was transferred to a new tube, mixed with 2 volumes of cold acetone, and incubated overnight at -20 ºC. The mixture was thawed and centrifuged at 10,000xg for 15 min. After the supernatant was discarded, the pellet was dried and stored at -80 ºC until use. The tryptic peptide samples (1:20 ratio) of KKU-213A and KKU-213-FR were prepared for injection into an Ultimate3000 Nano/Capillary LC System (Thermo Scientific, UK) coupled to a HCTUltra LC-MS system (Bruker Daltonics Ltd; Hamburg, Germany) equipped with a Nano-captive spray ion source **(Fig. 4A)**. LC-MS data were operated using DecyderMS (9) and searched against a nonredundant UniProt database (Homo sapiens, 20,386 entries from Swiss-Prot; Homo sapiens, 181,774 entries from TrEMBL). The analysis allowed for a maximum of three missed cleavages from tryptic digest. Carbamidomethylation of Cys as a fixed modification, and oxidation of Met as variable modifications. The level of proteins in each sample were expressed as log2 value. A unique peptide was defined as a protein, then proteins that expressed in triplicate samples were further analyzed.

Proteomic analysis

Venn diagrams was generated to show the total number of identified proteins and the proteins that were differentially expressed between samples. Volcano plot was generated by GraphPad Prism version 8 (10) to show differentially expressed protein (fold change ≥4 and False Discovery Rate (FDR) ≤ 0.05) and unchanged proteins in KKU-213A-FR as compared with the parental cells. Log 2 values of the identified proteins were visualized by MultiExperiment Viewer (MeV) (11). The heatmap and bar graphs were generated from the 25 most upregulated and downregulated proteins. The 25 most up-regulated proteins were furthered analyzed by Protein ANnalysis THrough Evolutionary Relationships (PANTHER) classification system (12) for classification of the cellular processes, and were analyzed by the STRING database version 5 (13) for the prediction of functional interaction networks.

Statistical analysis

The data of different groups were compared using Student's t-test. Probability values (P) of < 0.05 was considered as statistically significant.

RESULTS

Establishment of 5-FU resistant cell line

To obtain the optimal starting concentration of 5-FU for establishment of the drug resistant cell line, the parental cell line, KKU-213A, was treated with various concentration of 5-FU for 72 h and then the cell cytotoxicity assay was performed using MTT test. The results were used for calculation of IC_{25} and IC_{50}. The IC_{25} value 5-FU in KKU-213A was 2.96 ± 0.7 µM and the IC_{50} value of that was 5.93 ± 1.39 µM (**Table 1**).

Table 1 IC_{50} and IC_{25} of 5FU in KKU-213A parental cells

	KKU-213A
IC_{50} at 72 h (µM)	5.93 ± 1.39
IC_{25} at 72 h (µM)	2.96 ± 0.70

KKU-213A parental cell line was initially exposed to 5.0 µM of 5-FU which is the concentration below its IC_{50}. Unfortunately, we failed to get the resistant clone. Therefore, the starting concentration was decreased to 2.5 µM of 5-FU which is the concentration below its IC_{25}. After culturing the cells for at least 4 passages in the same drug concentration, the cells were re-exposed to 2 times of previous drug concentration. If the cells were unhealthy, the concentration lower than 2 times was used. The summary of establishment method were shown in **figure 1**. The resultant cells that exponentially grown in 7 µM 5-FU were designated as KKU-213A-FR and were used for the subsequent experiments in parallel with its parental counterpart.

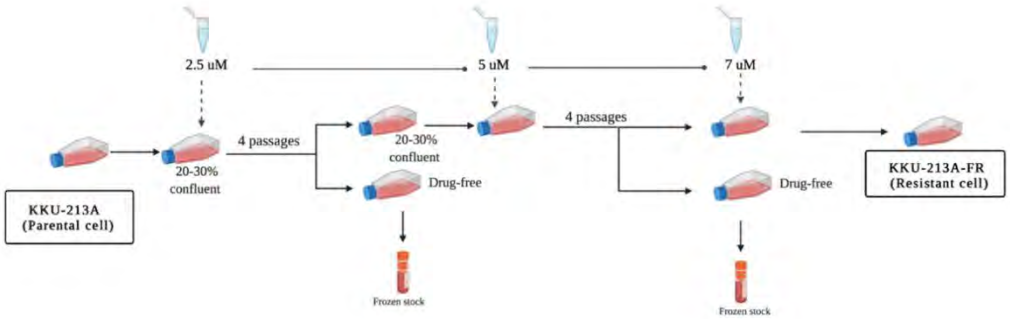

Figure 1 Establishment of 5-FU resistant cell line using step-wise method. The parental CCA cell line, KKU-213A was chronically exposed to step-wise increased concentration of 5-FU as indicated. The resultant cells that grown exponentially in 7 µM 5-FU were designated as KKU-213A-FR and used as a representative of 5-FU resistant cell line.

Confirmation of 5-FU resistant phenotype

The parental and FR cells were subjected to drug sensitivity assay by treating the cells with various concentration of 5-FU followed by MTT assay. The results showed that KKU-213A-FR had significantly higher cell viability when compared to the parental control at the concentration of 1- 400 µM (**Fig. 2**)

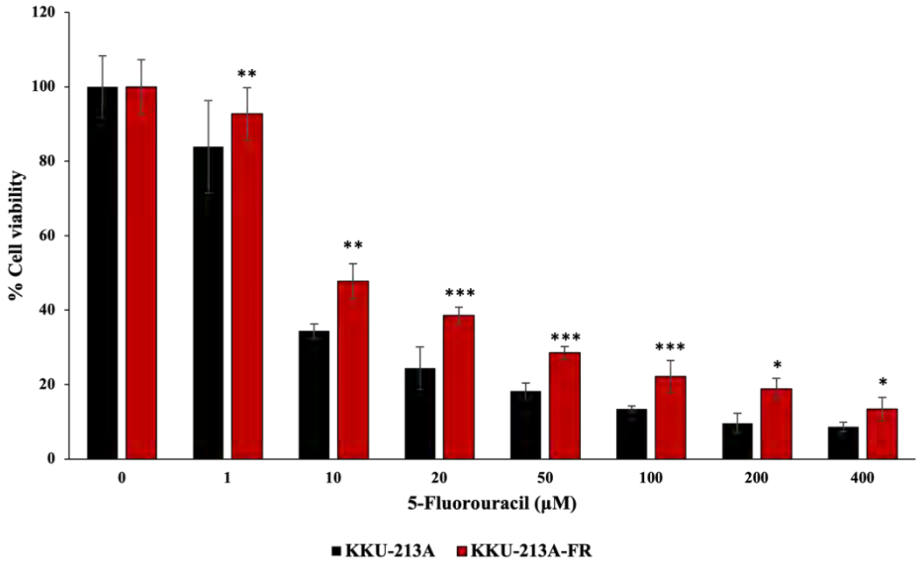

Figure 2 Drug sensitivity assay of parental and 5-FU resistant cells. KKU-213A and KKU-213A-FR were treated with indicated concentration of 5-FU for 72 h and were subjected to MTT test. The cell viability was calculated, from OD_{540}, in comparison with untreated control cells. Data are presented as mean ± SEM of three independent experiments. **P<0.05; **P<0.01; ***P<0.001*.

Study of cellular phenotypic changes in 5-FU resistant cell line

Common malignant phenotypes namely cell proliferation, cell migration and invasion were compared between parental and FR cells. The results showed that KKU-213A-FR had significantly lower cell proliferation rate than the parental cell line (**Fig. 3A**). On the other hand, wound healing assay showed that KKU-213A-FR could migrate and close the wound faster than the parental control as early as 6 h after the wound was created (**Fig. 3B**). Concomitantly, the Boyden chamber assay revealed that FR cell line exhibited higher migration (**Fig. 3A**) and invasion (**Fig. 3B**) ability when compared to parental cell line.

Identification of differentially expressed proteins by proteomic analysis

The proteins that were identified in all three biological replicate samples by LC-MS/MS were applied for further analyses. As shown by Venn diagrams, the total of 4,284 proteins were identified. In which, 3 proteins were identified only in parental cells, 136 proteins were found only in KKU-213A-FR, whereas 4,145 proteins were expressed in both cell lines (**Fig. 4B**). Then the fold changes of differentially expressed proteins were calculated and compared. As shown by volcano plot, 146 proteins were up-regulated, 79 proteins were down-regulated and 4,059 protein were unchanged (**Fig. 4C**). The 25 most up-regulated and down-regulated proteins in KKU-213A-FR as compared with KKU-213A were displayed by heatmap (**Fig. 4D**).

Gene ontology and protein interaction analyses

To better understand the biological pathways involved in 5-FU resistance, the 25 most up-regulated proteins in KKU-213A-FR were annotated with gene ontology (GO) by using Protein ANnalysis THrough Evolutionary Relationships (PANTHER) classification system. As shown in **Fig. 4E**, most of the up-regulated proteins are involved in cellular process (33.3%) followed by response to stimulus, developmental process, multicellular organismal process, and locomotion with the equal distribution (16.7%).

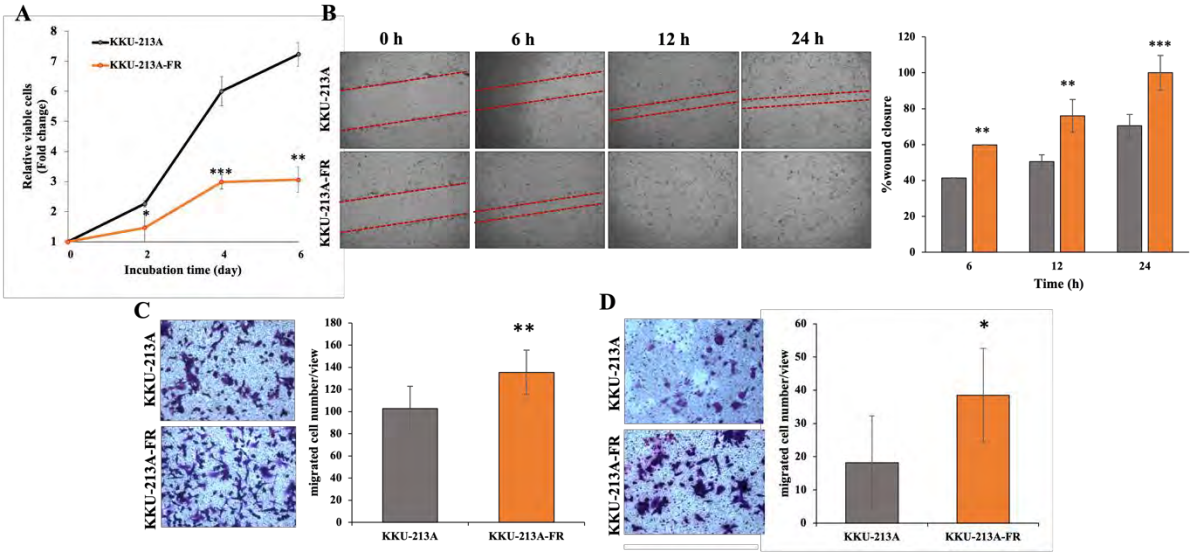

Figure 3 ***Determination of cell growth, cell migration and invasion*** A) Cell proliferation assay. KKU-213A and KKU-213A-FR were grown for 6 days in drug-free medium supplemented with 2% FBS, and the cell number was determined by MTT assay every two days. Growth rate of each cell line was calculated as fold change by normalized with day 0. B) Wound healing assay. The parental and 5-FU resistant cells were seeded and cultured overnight to obtain the confluent cell monolayer. After the wound was generated, the pictures of the cells were taken at 0, 6, 12 and 24 h. Then the percent wound closure was calculated and compared. Cell migration and invasion assay using modified Boyden chamber. C) Cell migration and D) cell invasion assay. The parental and 5-FU resistant cells were seeded and allowed to migrate/invade through the porous membrane of the Transwells for 12 h. The migrated/invaded cells were stained and observed under microscope. The cells from 6 random low-power fields were counted and compared. Data are presented as mean ± SEM from three independent experiments. **P<0.05; **P<0.01; ***P<0.001.***P<0.001.*

Moreover, protein-protein interaction was analyzed by STRING software. The results revealed the strong interaction between 25 input proteins and predicted functional partners (KEAP1, KLHL20, RBX1, NEDD8, DAD1, LRP5, STT3B, RPN1, KCTD5 and KLHL3). Protein clustering by biological function showed that DAD1, RPN1, RPN2, and STT3B involved in protein N-linked glycosylation at asparagine residue. N-linked glycosylation is the glycosylation of protein at the N4 atom of peptidyl-asparagine forming N-acetylglucosaminyl asparagine which have important functions in glycoprotein metabolism and oligosaccharyl transferase complex. A cluster of proteins which include ARIH1, KEAP1, NEDD8 CUL3, RBX1, KCTD5, KLH3 and KLHL20 is related with ubiquitin-dependent protein catabolic process and cellular protein metabolic process. LRPS, CDH2 and NOTCH2 were involved in organic substance **(Fig. 4F)**.

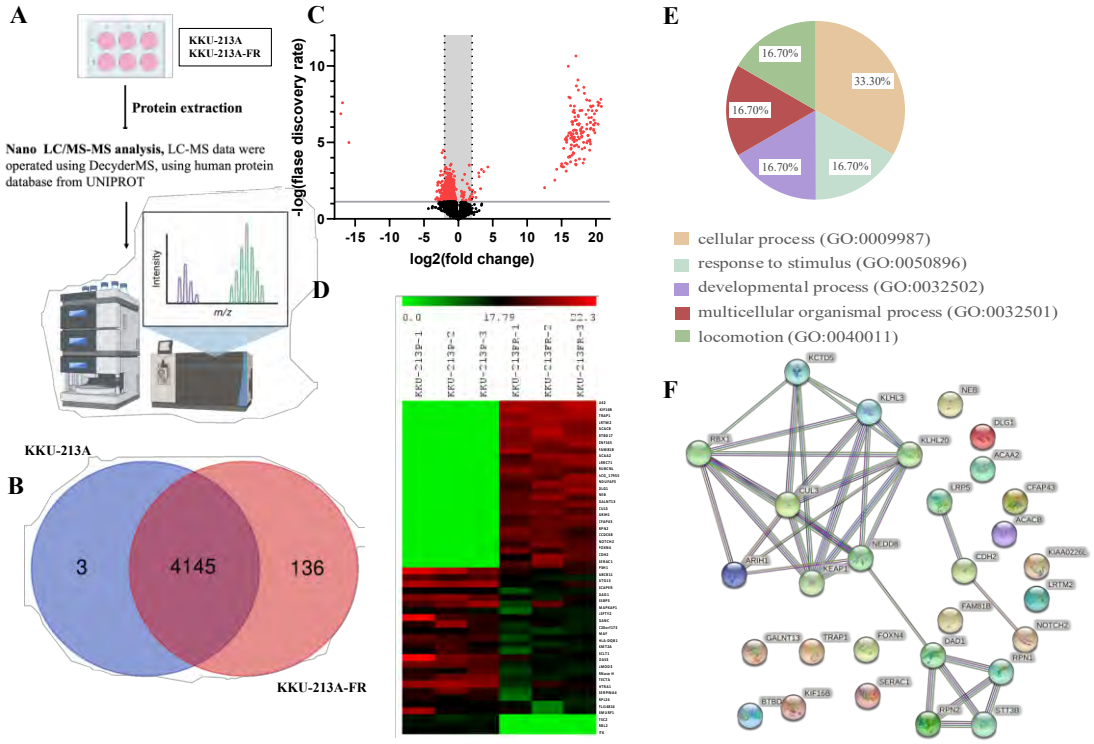

Figure 4 Proteomics and data analyses A) An illustration for Nano LC-MS/MS analysis and protein identification in KKU-213A and KKU-213A-FR B) Venn diagram for demonstration of shared and differentially expressed proteins. C) volcano plot and D) Heatmap for visualization of the 25 most up-regulated and down-regulated proteins. E) Bar graphs for comparison of the 25 most up-regulated and down-regulated proteins in KKU-213A-FR. Y-axis represents Δlog 2 values of the identified proteins. The 25 most up-regulated proteins (≥ 4 folds) were further analyzed. E) Gene ontology analysis based on biological process using PANTHER classification system. F) Protein-protein interaction prediction using STRING software.

DISCUSSION AND CONCLUSION

Chemotherapy is a common treatment for late stage CCA patients who are ineligible for surgery (14). Nonetheless, the overall survival of these patients is still low due to poor responses to chemotherapy. CCA cells can avoid the drug effect and survive by both intrinsic and acquired drug resistant mechanisms (15). The thorough knowledge regarding underlying drug resistance mechanism will lead to the discovery of better treatment strategies. Therefore, in this study we aim to establish a drug resistant CCA cell line, in order to uncover the molecular mechanisms and markers related to the drug resistant phenotypes of CCA.

We successfully established the FR line from a commonly used, KKU-213A parental cell line. The resultant cells are able to grow in medium containing 7 μM 5-FU and also exhibit highly migrative and invasive phenotypes. Concomitant with previous report showing that the established gemcitabine resistant CCA cell lines had higher cell migration and invasion capacity as compared with their parental counterparts (16). Interestingly, the KKU-213A-FR has slower growth rate than the parental cell line. Even though high proliferation is one of the aggressive phenotypes of cancer cells, it was reported that the switching from epithelial to mesenchymal phenotype, during metastasis, renders the cell to more invasive but less proliferative (17). In addition, some slow-cycling cancer cells exhibit highly invasive ability and metabolically active (18).

Using quantitative proteomic analysis, we found that a majority of differentially expressed proteins in FR cells are involved in cellular processes. This is an interesting finding because on the way to resistance of chemotherapeutic drugs, cancer cells usually undergo reprogramming and change their cellular processes in order to increase drug efflux, decrease drug up take, avoid apoptosis, and modify drug targets. The results of protein-protein interactions of differentially expressed proteins show protein clusters that are associated with tumor aggressiveness and drug resistance. For instance, it was reported that NOTCH2 regulates CDH2 (N-cadherin) expression in chronic lymphocytic leukemia cells (19) that leads to activation of epithelial mesenchymal transition (EMT), the mechanism that switches the cancer cells to highly invasive phenotypes (20). These reports were consistent with our phenotypic studies showing that cell proliferation of FR cell was decreased but the migration and invasion ability was increased. In addition, our results show the interaction between input proteins and predicted functional partners for instance the interaction between CUL3 and adaptor proteins, KEAP1 and KLHL20. Functionally, CUL3 plays an important role in the polyubiquitination and subsequent degradation of specific proteins (21). The previous studies showed that in normal condition CUL3/RBX1/KEAP1 complex binds and degrades NFE2-related factor 2 (NRF2) protein but in the condition with high oxidative stress generated by cancer cells themselves (22), KEAP1/NRF2 interaction is easily dissociated and leads NRF2 to positively regulates expression of various oncogenes. The activation of NRF2 and its target genes can result in promotion of cytoprotective and angiogenesis (23). Moreover, the CUL3 adaptor, KLHL20 also have an oncogenic function through promoting ubiquitination of death-associated protein kinase (DAPK), this leads to suppression of cell apoptosis (24). Nevertheless, more studies need to be done to explore 5-FU resistant mechanisms associated with these differential express proteins.

Finally, we expected that this study will provide a beneficial tool for further illustration of drug resistant mechanisms and identification of novel therapeutic targets for development of more effective treatment against drug resistant cancer cells.

ACKNOWLEDGEMMENTS

This study was supported by the budget revenue of Prince of Songkla University to S. Obchoei (SCI6202093S); K. Kerdkumthong was supported by Prince of Songkla University-Ph.D. Scholarship (PSU_PHD2561-001) and Research Grant for thesis from graduate school of Prince of Songkla University; S. Songsurin was supported by the Excellent Biochemistry Program Fund of Prince of Songkla University.

REFERENCES

1. Macias RIR. Cholangiocarcinoma: Biology, Clinical Management, and Pharmacological Perspectives. ISRN Hepatol. 2014; 2014:828074.
2. Sripa B, Pairojkul C. Cholangiocarcinoma: lessons from Thailand. Current Opinion in Gastroenterology. 2008; 24(3):349–56.
3. Banales JM, Cardinale V, Carpino G, Marzioni M, Andersen JB, Invernizzi P, et al. Cholangiocarcinoma: current knowledge and future perspectives consensus statement from the European Network for the Study of Cholangiocarcinoma (ENS-CCA). Nature Reviews Gastroenterology & Hepatology. 2016; 13(5):261–80.
4. Amaral MVS, Portilho AJDS, Silva ELD, Sales LDO, Maués JHDS, Moraes MEAD, et al. Establishment of Drug-resistant Cell Lines as a Model in Experimental Oncology: A Review. Anticancer Research. International Institute of Anticancer Research; 2019; 39(12):6443–55.

5. Rattanasinganchan P, Leelawat K, Treepongkaruna S, Tocharoentanaphol C, Subwongcharoen S, Suthiphongchai T, et al. Establishment and characterization of a cholangiocarcinoma cell line (RMCCA-1) from a Thai patient. World J Gastroenterol. 2006; 12(40):6500–6.
6. Namwat N, Amimanan P, Loilome W, Jearanaikoon P, Sripa B, Bhudhisawasdi V, et al. Characterization of 5-fluorouracil-resistant cholangiocarcinoma cell lines. Chemotherapy. 2008; 54(5):343–51.
7. Coley HM. Development of drug-resistant models. Methods Mol Med. 2004; 88:267–73.
8. Schneider CA, Rasband WS, Eliceiri KW. NIH Image to ImageJ: 25 years of image analysis. Nat Methods. 2012; 9(7):671–5.
9. Johansson C, Samskog J, Sundström L, Wadensten H, Björkesten L, Flensburg J. Differential expression analysis of Escherichia coli proteins using a novel software for relative quantitation of LC-MS/MS data. Proteomics. 2006; 6(16):4475–85.
10. Swift ML. GraphPad Prism, Data Analysis, and Scientific Graphing. J Chem Inf Comput Sci. American Chemical Society; 1997; 37(2):411–2.
11. Howe EA, Sinha R, Schlauch D, Quackenbush J. RNA-Seq analysis in MeV. Bioinformatics. 2011; 27(22):3209–10.
12. Mi H, Muruganujan A, Ebert D, Huang X, Thomas PD. PANTHER version 14: more genomes, a new PANTHER GO-slim and improvements in enrichment analysis tools. Nucleic Acids Research. 2019; 47(D1):D419–26.
13. Szklarczyk D, Franceschini A, Wyder S, Forslund K, Heller D, Huerta-Cepas J, et al. STRING v10: protein-protein interaction networks, integrated over the tree of life. Nucleic Acids Res. 2015; 43(Database issue):D447-452.
14. Bridgewater J, Galle PR, Khan SA, Llovet JM, Park J-W, Patel T, et al. Guidelines for the diagnosis and management of intrahepatic cholangiocarcinoma. J Hepatol. 2014; 60(6):1268–89.
15. Marin JJ, Macias RI. Understanding drug resistance mechanisms in cholangiocarcinoma: assisting the clinical development of investigational drugs. Expert Opinion on Investigational Drugs. Taylor & Francis; 2021; 30(7):675–9.
16. Wattanawongdon W, Hahnvajanawong C, Namwat N, Kanchanawat S, Boonmars T, Jearanaikoon P, et al. Establishment and characterization of gemcitabine-resistant human cholangiocarcinoma cell lines with multidrug resistance and enhanced invasiveness. International Journal of Oncology. Spandidos Publications; 2015; 47(1):398–410.
17. Fares J, Fares MY, Khachfe HH, Salhab HA, Fares Y. Molecular principles of metastasis: a hallmark of cancer revisited. Sig Transduct Target Ther. 2020; 5(1):1–17.
18. Roesch A, Fukunaga-Kalabis M, Schmidt EC, Zabierowski SE, Brafford PA, Vultur A, et al. A temporarily distinct subpopulation of slow-cycling melanoma cells is required for continuous tumor growth. Cell. 2010; 141(4):583–94.
19. Mangolini M, Götte F, Moore A, Ammon T, Oelsner M, Lutzny-Geier G, et al. Notch2 controls non-autonomous Wnt-signalling in chronic lymphocytic leukaemia. Nat Commun. 2018; 9(1):3839.
20. Loh C-Y, Chai JY, Tang TF, Wong WF, Sethi G, Shanmugam MK, et al. The E-Cadherin and N-Cadherin Switch in Epithelial-to-Mesenchymal Transition: Signaling, Therapeutic Implications, and Challenges. Cells. 2019; 8(10):E1118.
21. Chen H-Y, Chen R-H. Cullin 3 Ubiquitin Ligases in Cancer Biology: Functions and Therapeutic Implications. Front Oncol. 2016; 6:113.
22. Szatrowski TP, Nathan CF. Production of large amounts of hydrogen peroxide by human tumor cells. Cancer Res. 1991; 51(3):794–8.

23. Guo Z, Mo Z. Keap1-Nrf2 signaling pathway in angiogenesis and vascular diseases. J Tissue Eng Regen Med. 2020; 14(6):869–83.
24. Lee Y-R, Yuan W-C, Ho H-C, Chen C-H, Shih H-M, Chen R-H. The Cullin 3 substrate adaptor KLHL20 mediates DAPK ubiquitination to control interferon responses. EMBO J. 2010; 29(10):1748–61.

Proceeding PP048

In silico repurposing studies of first-and second-generation antipsychotic drugs in methamphetamine addiction treatment

Kasidit Wiboonkiat[1], Napak Vejsureeyakul[1], Chotiphat Pornthanamongkol[1], Chonlakran Auychinda[1], Jiraporn Panmanee[2], Sujira Mukda[2]*

[1] Department of Biology and Health Science, Mahidol Wittayanusorn School, Nakhon Pathom, Thailand 73170
[2] Research Center for Neuroscience, Institute of Molecular Biosciences, Mahidol University, Nakhon Pathom, Thailand 73170

***Email**: sujira.muk@mahidol.edu

ABSTRACT

Methamphetamine (METH) is a psychostimulant that is associated with psychological morbidity. METH functions through the central nervous system, especially on the reward circuitry. METH passes through a dopamine transporter and induces excess dopamine discharge. Consistently, antipsychotic drugs can efficiently bind with D2 receptors. Thus these drugs may prevent the dopamine overstimulation effects caused by METH. Previous studies in mice indicated that antipsychotics may be used as an intervention for METH-induced hyperlocomotion. Therefore, this project focused on the repurposing of antipsychotics including prochlorperazine, haloperidol, olanzapine, zotepine, and aripiprazole in addiction using computational methods to estimate the binding affinity between drugs and binding sites of the dopaminergic D2 and serotonergic 5-HT2A receptors. Docking scores were calculated by AutoDock Vina. According to the results, five tested antipsychotics displayed a higher binding affinity to the D2 receptor compared to dopamine. They can inhibit the binding of dopamine towards the D2 receptor and suppress neuronal overstimulation. Considering appropriate medications, the most suitable antipsychotic is determined by the lower side effects indicated by lower D2 and higher 5-HT2A binding affinity. In this study, the most appropriate drug is prochlorperazine. The second is olanzapine. Moreover, the relationship between molecular interactions and binding affinities was studied and found that H-bonds, hydrophobic contacts, and amino acid sequences are associated with the binding affinity scores. Taken together, this *in silico* preliminary repurposing study suggests that olanzapine might be a plausible therapeutic target for the treatment of METH addiction. Further *in vitro* and *in vivo* studies are needed for the validation of these findings.

Keywords: Antipsychotic drugs; Dopamine D2 receptor; Methamphetamine; Molecular docking; Serotonin 5-HT2A receptor

INTRODUCTION

METH is a psychostimulant that directly affects the central nervous system (CNS), especially the reward circuitry. The main structures of the reward system related to the drug mechanism are the ventral tegmental area (VTA), the nucleus accumbens (NAc), and the prefrontal cortex (PFC) [1]. The neurotransmitter that plays a key role in the reward system is dopamine [2]. METH induces increased dopamine transmission from the VTA to the NAc and PFC [3]. Long-term effects in METH misusers can be observed such as addiction, mood disturbances, hallucination, and drug use psychotic symptoms similarly found in schizophrenia [4].

With the structural similarity of METH to dopamine, METH enters neurons via the dopamine transporter (DAT) then affects the vesicular monoamine transporter 2 (VMAT2) on the synaptic vesicle, thus the vesicle releases dopamine higher than that in regular conditions. This mechanism causes an increase of dopamine in the cytoplasm and subsequently in the synaptic cleft [5, 6].

Antipsychotic drugs have been used to treat mental illnesses, such as depressive disorder, psychosis, and schizophrenia for more than 60 years [7]. They are divided into two groups: typical/first-generation antipsychotic drugs and atypical/second-generation antipsychotic drugs, in which the second-generation type has fewer side effects, known as extrapyramidal symptoms (EPS) for instance tardive dyskinesia and dystonia, than the first-generation drug class [8]. The mechanism of action of the conventional antipsychotic drug is the inhibition of the dopamine receptor subtype D2, which is different from the new one that inhibits both the D2 receptor and serotonin receptor subtype 5-Hydroxytryptamine receptor 2A (5-HT2A), resulting in fewer EPS [8, 9]. In addition, 5-HT2A/D2 binding ratio can be used to classify drug groups [9-11]. Apart from the diverse inhibition property, the lower affinity of the second generation to the D2 receptor compared to the first generation also has a negative correlation with the EPS occurrence rate [12, 13]. A recent experiment in mice suggested that METH-induced hyperlocomotion was decreased when pretreated with antipsychotic drugs either haloperidol or risperidone. Therefore, D2 antagonist drugs may be useful in METH treatment [14]. In this study, we are repurposing five drugs belonging to the first- and second-antipsychotic generations, comprising prochlorperazine, haloperidol, olanzapine, zotepine, and aripiprazole for METH addiction treatment. Drugs' action via D2 receptor binding may compromise METH-induced overstimulation of dopamine. We also suggest that antipsychotic drugs may have lower EPS according to their selectivity towards the 5-HT2A receptor. Molecular docking was performed to predict the interaction energy between antipsychotic drugs/dopamine/serotonin and D2/5-HT2A receptors and their binding energy was analyzed. Their interactions were illustrated using the 2-dimensional (2D) diagram.

MATERIALS AND METHODS

Tools

1. Protein Data Bank is a website containing protein databases [15]. 3D structures of proteins, amino acid sequences, and ligands were retrieved from this website.
2. NCBI BLASTP is a database for searching proteins by their amino acid sequences [16].
3. AVOGADRO v.1.2 is a software for molecule editing and visualization, designed for cross-platform use in computational chemistry, molecular modeling, bioinformatics, materials science, and related areas [17].
4. UCSF Chimera v.1.15 is a program for interactive visualization and analysis of molecular structures, density maps, trajectories, and sequence alignments [18].
5. AutoDock Vina v.1.2.0 is a program for molecular docking by visualizing molecular interaction between molecules and their targets and calculating the stability of the binding complex [19].
6. LigPlot+ v.2.2.4 is a program generating a 2D diagram of protein-ligand interactions, explaining the distances of interactions of surrounding residues [20].

Receptor Preparation

The crystal structure of dopamine D2 receptor in complex with the atypical antipsychotic drug risperidone and the crystal structure of serotonin 5-HT2A receptor in complex with atypical antipsychotic drug zotepine were retrieved from Protein Data Bank

(PDB code: 6CM4 and 6A94 respectively), the amino acid sequences (FASTA files) of each protein were also downloaded from PDB. The amino sequences derived from Enterobacteria phage T4 or *Escherichia coli* and non-standard residues on the receptors were removed in the UCSF Chimera. The sequence was subjected to perform similarity analysis using NCBI BLASTP. The chain A of both receptors was selected for the docking procedure and further prepared by adding hydrogen atoms and charges using the DockPrep function implemented in the UCSF Chimera where the solvents atoms were removed, and the missing atoms were fixed.

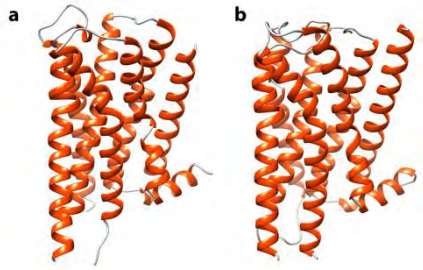

Figure 1 The crystal structure (chain A) of dopamine D2 receptor (**a**, 6CM4) and serotonin 5-HT2A receptor (**b**, 6A94), retrieved from the PDB. Visual images were produced using UCSF Chimera.

Ligand Preparation

Structures of two natural neurotransmitters (dopamine and serotonin), two typical antipsychotic drugs (prochlorperazine and haloperidol), and two atypical antipsychotic drugs (zotepine and aripiprazole) were retrieved from the PDB (PDB code: LDP, SRO, P77, GMJ, ZOT, and 9SC, respectively) in the SDF format. For the atypical antipsychotic drug olanzapine, the structure was created by using AVOGADRO (G09 Method: B3LYP Basis Set: 6-31+G(d)).

Grid Box of the Binding Sites

To define the area of the binding site, we used the previous data on the proteins in complex with antipsychotic drugs, risperidone or zotepine, as references (alpha carbon coordinates) [21, 22]. The grid boxes were created from the center of all interacting residues (alpha carbon coordinates) to cover the binding site pocket. The configuration of x/y/z coordinates was set to size_x=18 Å, size_y=18 Å, size_z=18 Å and center_x 15.35000 Å, center_y -3.61986 Å, center_z 5.13757 Å for the D2 receptor, and was set to size_x=20 Å, size_y=25 Å, size_z=20 Å and center_x 9.07087 Å, center_y 4.52725 Å, center_z -7.89863 Å for the 5-HT2A receptor.

Docking

Molecular docking was performed using AutoDock Vina. In detail, the PDB file of the receptors and the SDF files of the ligands were converted to the PDBQT files. In the AutoDock Vina, the total numbers of the protein-ligand interactions were calculated in each ligand rotation. The binding scores were calculated (kcal/mol). A high negative score shows the favorable binding affinity between the molecules.

2-Dimensional Interaction

The highest affinity coordination was selected for further protein-ligand interaction analysis. We showed diagrams of the complex in 2D by using LigPlot+ to illustrate H-bonds and hydrophobic interactions.

RESULTS AND DISCUSSION

Binding energy score with D2 receptor and 5-HT2A receptor

Regarding the structural similarity of METH and dopamine, an equivalent affinity of -6.5 kcal/mol towards the D2 receptor was found in the current study. We hypothesized that METH might in part act through dopamine receptors and cause the overstimulation of locomotor activity in METH users. The binding scores of protein-ligand interactions and drug information are shown in **Table 1**. Every drug that we have experimented with has a higher negative binding score than dopamine. In other words, antipsychotic drugs have a higher binding affinity with dopamine D2 receptors when compared to dopamine, so they can competitively prevent dopamine from binding with the D2 receptor. This process may decrease the overstimulation caused by METH-induced dopamine release. To examine which drugs are suitable for mitigating the symptoms induced by METH, the medicines will be considered particularly based on their adverse effects.

First-generation antipsychotic drugs are better at binding with D2 and 5-HT2A receptors than second-generation drugs are; however, second-generation antipsychotic drugs are promising for curing patients with METH addiction, regardless of their lower binding affinity towards D2 and 5-HT2A receptors. Drugs with a high affinity to the D2 receptor were shown to cause EPS (**Table 1**) and a cognitive deficit related to the frontal cortex functions [13]. Haloperidol appears to have the highest affinity to the 5-HT2A receptor. However, haloperidol also possesses high affinity to the D2 receptor associated with the EPS found in patients. Therefore, haloperidol is not an appropriate candidate for drug repurposing in METH addiction. When only binding affinity towards the 5HT2A receptor is deliberated, the two most suitable drugs with the highest 5-HT2A/D2 ratio are prochlorperazine (typical; ligand interactions presented in **Fig. 3**) and olanzapine (atypical; ligand interactions presented in **Fig. 4),** respectively. Nevertheless, olanzapine is the most proper drug to treat patients concerning the side effects of the drugs, since olanzapine affects only dyslipidemia and no other severe adverse effects compared to other drugs [23, 24].

Table 1 Binding scores and affinity rank of control, prochlorperazine, haloperidol, olanzapine, zotepine, and aripiprazole with D2 and 5-HT2A receptor.

Ligand	Binding score (kcal/mol)				FDA drug information	Adverse effects [23, 24]
	D2	Affinity rank (lowest to highest)	5-HT2A	Affinity rank (highest to lowest)		
Control	-6.5	1	-6.4	6	neurotransmitters	-
Prochlorperazine	-8	4	-9.8	2	typical	extrapyramidal symptoms
Haloperidol	-10.8	6	-10.4	1	typical	extrapyramidal symptoms
Olanzapine	-7.9	3	-8.7	4	atypical	dyslipidemia, Weight gain
Zotepine	-7.8	2	-8.1	5	atypical	akathisia
aripiprazole	-10.6	5	-9.6	3	atypical	lower risk side effect

Aripiprazole, an atypical antipsychotic drug, has a high binding affinity with D2 receptor but induces low risk of side effects in clinical use. We infer that these lower side effects result from the different action pathways of aripiprazole. Aripiprazole is the only approved antipsychotic drug that acts as a partial agonist with the D2 receptor, while others act

as antagonists [25]. The in-depth underlying mechanism of this drug is still elusive and requires further studies.

Ligand interactions

According to the 2D diagram, haloperidol which has the highest affinity with the D2 receptor also possesses the most hydrophobic interactions with D2 (binding score: -10.8, numbers of hydrophobic: 17). The H-bond interaction is correlated with high affinity to 5-HT2A receptors as two of the highest affinity drugs, including haloperidol (binding score: -10.4. 1st rank) and aripiprazole (binding score: -9.6, 3rd rank), possess H-bond interaction in the binding site. The interaction of the drug and the receptor are illustrated in **Fig 2**.

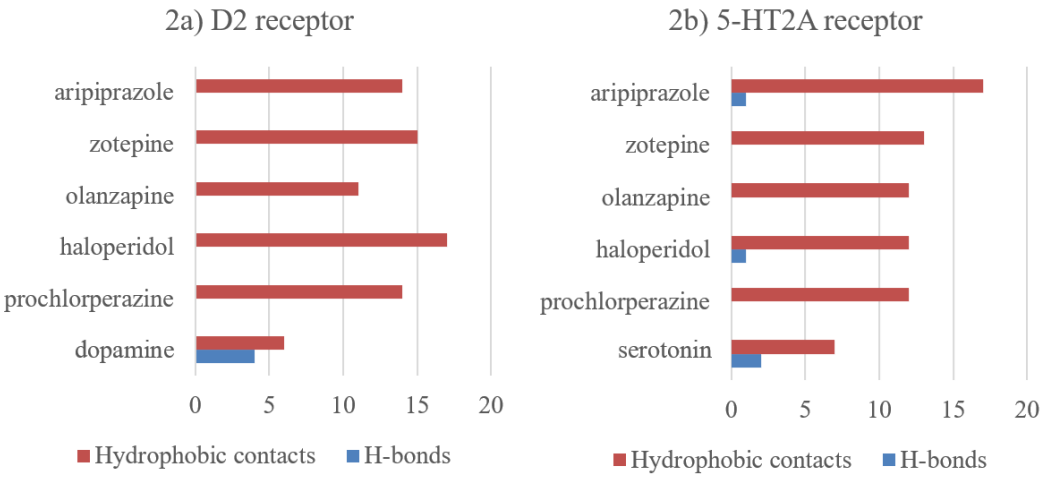

Figure 2 Analysis of the D2 and 5-HT2A receptor interaction from the 2D diagram.

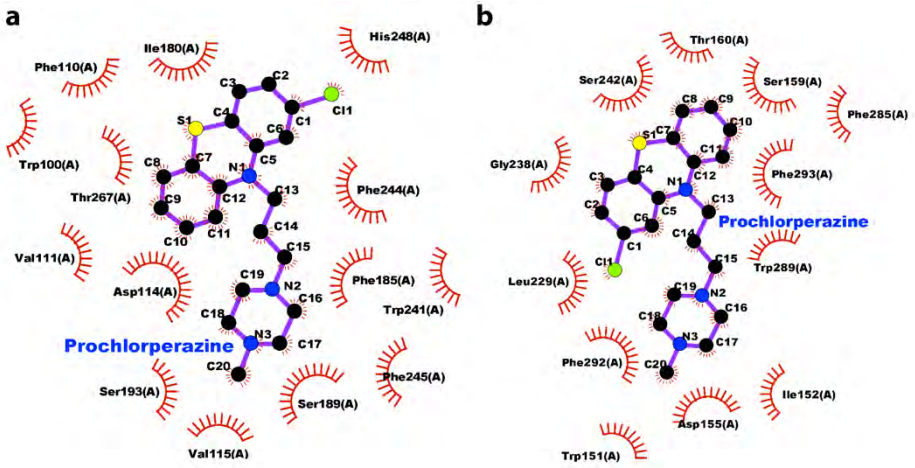

Figure 3 2D diagram from LigPlot+ of prochlorperazine with 2a) dopamine D2 receptor and 2b) serotonin 5-HT2A receptor. The hydrophobic interactions are illustrated as red spoked arcs.

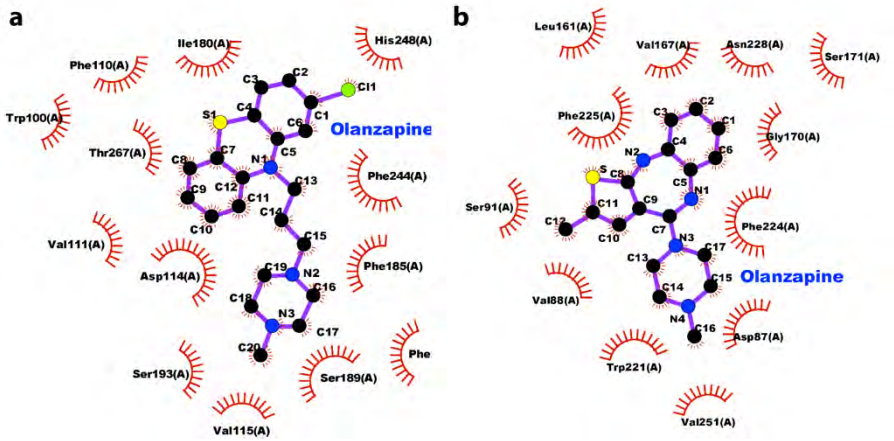

Figure 4 2D diagram from LigPlot+ of olanzapine with 3a) dopamine D2 receptor and 3b) serotonin 5-HT2A receptor. The hydrophobic interactions are illustrated as red spoked arcs.

According to Alka Bali and coworkers (2014), antipsychotic drugs with high binding affinity with D2 receptors were shown to interact with Asp114 and Cys118 and antipsychotic drugs with a high binding affinity with serotonin 5-HT2A receptors were likely to interact with Asp155 [11]. This research is consistent with our result showing that high-affinity drugs interact with the mentioned residues. In addition, haloperidol, which has the highest binding affinity with 5-HT2A, forms an H-bond with Asp155 (2.69 Å) **(Fig. 5 and 6).**

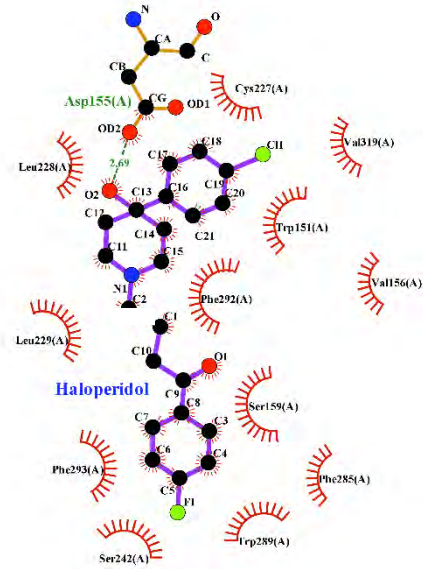

Figure 5 2D diagram from LigPlot+ of haloperidol with serotonin 5-HT2A receptor. The 2D diagram shows the interactions of haloperidol with Trp151, Asp155, Val156, Ser159, Cys227, Leu228, Leu229, Ser242, Trp289, Phe285, Phe292, Phe293, Val319. The hydrogen bonds and hydrophobic interactions are illustrated as green dash lines and red spoked arcs, respectively.

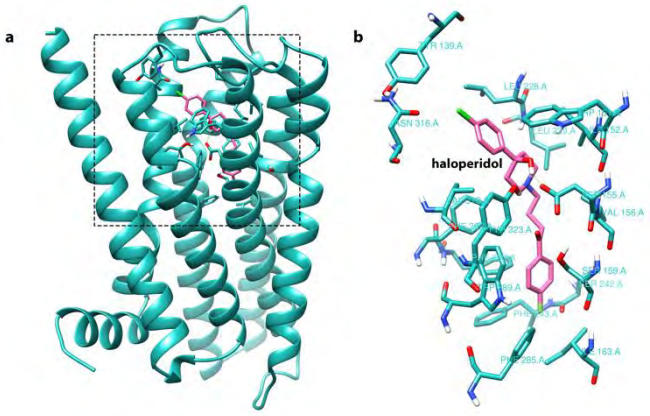

Figure 6 UCSF Chimera visualization shows the best binding conformation of haloperidol on the serotonin 5-HT2A receptor binding site with Trp151, Asp155, Val156, Ser159, Cys227, Leu228, Leu229, Ser242, Trp289, Phe285, Phe292, Phe293, Val319. The hydrogen bond is shown as a green line and amino acid residues forming hydrophobic interactions with haloperidol are shown as sticks.

CONCLUSION

Drug repurposing significantly helps reduce experimentation time intervals in the preclinical phase. Computer-based drug study helps to screen drugs and reduce both time and cost for doing *in vitro* and *in vivo* experiments of compounds with undesirable physicochemical properties. In this study, we explored molecular docking of the five antipsychotic drugs that are generally used for mental disorder treatment including prochlorperazine, haloperidol, olanzapine, zotepine, and aripiprazole acting through their membrane protein receptors including dopamine D2 receptor and serotonin 5-HT2A receptor. The results are compared with those of dopamine and serotonin to repurpose the drugs for treating METH-induced dopamine overstimulation.

Every antipsychotic drug in this study is capable of blocking D2 receptors from dopamine overdose, as suggested by the higher binding affinity in comparison to dopamine. Therefore, the antipsychotics for METH treatment were mainly selected based on their EPS side effects. Suitable drugs for decreasing EPS side effects should have lower D2 binding affinity and higher 5-HT2A binding affinity. Consequently, the most suitable drug determined is prochlorperazine which is the typical antipsychotic drug, followed by olanzapine which is the atypical drug. The previous study on cluster analysis on rat brains identified that the 5-HT2A/D2 ratio was the most potent means of utilizing this data for EPS prognosis with 92% accuracy [9]. However, a suitable indicator used to classify typical and atypical antipsychotics is EPS side effects. Since typical antipsychotic drugs are defined by their adverse side effects such as EPS, prochlorperazine clinically displays EPS side effects regardless of its high 5-HT2A/D2 ratio. Therefore, we conclude that olanzapine is the most suitable antipsychotic drug of the five selected drugs used in this study. The preliminary results obtained from the current study are needed for further investigation using *in vitro and in vivo* studies.

ACKNOWLEDGEMENTS

In this work, graphic images were produced using the UCSF Chimera package from the Resource for Biocomputing, Visualization, and Informatics at the University of California, San Francisco (supported by NIH P41 RR001081). Further, the authors would like to thank Mahidol Wittayanusorn school and the Institute of Molecular Biosciences for providing all research facilities

REFERENCES

1. Vollm BA, de Araujo IE, Cowen PJ, Rolls ET, Kringelbach ML, Smith KA, et al. Methamphetamine activates reward circuitry in drug naive human subjects. Neuropsychopharmacology. 2004;29(9):1715-22.
2. Arias-Carrion O, Stamelou M, Murillo-Rodriguez E, Menendez-Gonzalez M, Poppel E. Dopaminergic reward system: a short integrative review. Int Arch Med. 2010;3:24.
3. Marshall JF, O'Dell SJ. Methamphetamine influences on brain and behavior: unsafe at any speed? Trends Neurosci. 2012;35(9):536-45.
4. Hsieh JH, Stein DJ, Howells FM. The neurobiology of methamphetamine induced psychosis. Front Hum Neurosci. 2014;8:537.
5. Kish SJ. Pharmacologic mechanisms of crystal meth. CMAJ. 2008;178(13):1679-82.
6. Yang X, Wang Y, Li Q, Zhong Y, Chen L, Du Y, et al. The Main Molecular Mechanisms Underlying Methamphetamine- Induced Neurotoxicity and Implications for Pharmacological Treatment. Front Mol Neurosci. 2018;11:186.
7. Zhang J-P. Life-threatening effects of antipsychotic drugs. In: Manu P, Flanagan RJ, Ronaldson KJ, editors. The benefits of antipsychotic drugs: Symptom control and improved quality of life: Elsevier Academic Press.; 2006. p. 295–309.
8. Gardner DM, Baldessarini RJ, Waraich P. Modern antipsychotic drugs: a critical overview. CMAJ. 2005;172(13):1703-11.
9. Meltzer HY, Matsubara S, Lee JC. The ratios of serotonin2 and dopamine2 affinities differentiate atypical and typical antipsychotic drugs. Psychopharmacol Bull. 1989;25(3):390-2.
10. Aranda R, Villalba K, Ravina E, Masaguer CF, Brea J, Areias F, et al. Synthesis, binding affinity, and molecular docking analysis of new benzofuranone derivatives as potential antipsychotics. J Med Chem. 2008;51(19):6085-94.
11. Bali A, Sen U, Peshin T. Synthesis, docking and pharmacological evaluation of novel indole based potential atypical antipsychotics. Eur J Med Chem. 2014;74:477-90.
12. Kapur S, Seeman P. Does fast dissociation from the dopamine d(2) receptor explain the action of atypical antipsychotics?: A new hypothesis. Am J Psychiatry. 2001;158(3):360-9.
13. Sykes DA, Moore H, Stott L, Holliday N, Javitch JA, Lane JR, et al. Extrapyramidal side effects of antipsychotics are linked to their association kinetics at dopamine D2 receptors. Nat Commun. 2017;8(1):763.
14. Jing L, Liu B, Zhang M, Liang JH. Involvement of dopamine D2 receptor in a single methamphetamine-induced behavioral sensitization in C57BL/6J mice. Neurosci Lett. 2018;681:87-92.
15. Berman HM, Westbrook J, Feng Z, Gilliland G, Bhat TN, Weissig H, et al. The Protein Data Bank. Nucleic Acids Res. 2000;28(1):235-42.
16. Ye J, Coulouris G, Zaretskaya I, Cutcutache I, Rozen S, Madden TL. Primer-BLAST: a tool to design target-specific primers for polymerase chain reaction. BMC Bioinformatics. 2012;13:134.
17. Hanwell MD, Curtis DE, Lonie DC, Vandermeersch T, Zurek E, Hutchison GR. Avogadro: an advanced semantic chemical editor, visualization, and analysis platform. J Cheminform. 2012;4(1):17.
18. Pettersen EF, Goddard TD, Huang CC, Couch GS, Greenblatt DM, Meng EC, et al. UCSF Chimera--a visualization system for exploratory research and analysis. J Comput Chem. 2004;25(13):1605-12.

19. Eberhardt J, Santos-Martins D, Tillack AF, Forli S. AutoDock Vina 1.2.0: New Docking Methods, Expanded Force Field, and Python Bindings. J Chem Inf Model. 2021;61(8):3891-8.
20. Laskowski RA, Swindells MB. LigPlot+: multiple ligand-protein interaction diagrams for drug discovery. J Chem Inf Model. 2011;51(10):2778-86.
21. Kimura KT, Asada H, Inoue A, Kadji FMN, Im D, Mori C, et al. Structures of the 5-HT2A receptor in complex with the antipsychotics risperidone and zotepine. Nat Struct Mol Biol. 2019;26(2):121-8.
22. Wang S, Che T, Levit A, Shoichet BK, Wacker D, Roth BL. Structure of the D2 dopamine receptor bound to the atypical antipsychotic drug risperidone. Nature. 2018;555(7695):269-73.
23. Kondo T, Otani K, Ishida M, Tanaka O, Kaneko S, Fukushima Y. Adverse effects of zotepine and their relationship to serum concentrations of the drug and prolactin. Ther Drug Monit. 1994;16(2):120-4.
24. Muench J, Hamer AM. Adverse effects of antipsychotic medications. Am Fam Physician. 2010;81(5):617-22.
25. de Bartolomeis A, Tomasetti C, Iasevoli F. Update on the Mechanism of Action of Aripiprazole: Translational Insights into Antipsychotic Strategies Beyond Dopamine Receptor Antagonism. CNS Drugs. 2015;29(9):773-99.

PP058

A protein engineering to create the high thermostable formate dehydrogenase enzyme for biocatalysis applications

Rattima Boonkumkrong[1], Paweenapon Chunthaboon[1], Ruchanok Tinikul[2]

[1] Student of Department of Biochemistry and Center of Excellence in Protein and Enzyme Technology (CPET), Faculty of Science, Mahidol University, Bangkok 10400, Thailand
[2] Assistant Professor, Department of Biochemistry and Center of Excellence in Protein and Enzyme Technology (CPET), Faculty of Science, Mahidol University, Bangkok 10400, Thailand

***Email:** rattima2014@gmail.com, rattima.boo@student.mahidol.edu

ABSTRACT

Formate dehydrogenase (FDH) catalyzes the generation of NADH from NAD^+ by oxidation of formate to carbondioxide. The enzyme is useful for coenzyme regenerating systems, in which NADH is continuously generated by the FDH enzyme to support the main synthesis enzyme reaction in biotransformations. The novel FDH from *Bacillus simplex* (BsFDH) was recently characterized and revealed the highest catalytic efficiency. However, the major painpoint of BsFDH is low thermostability. Therefore, in this study, we employed a FireProt computational prediction to rational engineer to improve the thermostability of BsFDH. The program suggested 61 variants that may have more thermostability than the wild-type. By complement three criteria, we selected 9 candidate variants to perform site-directed mutagenesis and 7 variants were successfully overexpressed and purified. The enzyme activity and thermostability were investigated in comparison with wild-type enzyme. The results showed that the Q125L, A216I, S50L, and T213C exhibited comparable activity to the wild-type enzyme, while only Q125L had higher thermostability than the wild-type. At 55ºC incubation, the Q125L was able to retain more than 50% after 6 h of incubation, while the wild-type activity dropped 35% activity. This result suggests that the Q125L variant of the BsFDH might be suitable for biosynthesis.

Keyword: Thermostability, Formate dehydrogenases, Biocatalysis, Coenzyme regenerating system, FireProt

INTRODUCTION

NAD(P)H-dependent oxidoreductases are critical biocatalysts in the chiral compound synthesis reaction [1,2]. The enzymes mostly require nicotinamide cofactors (NAD(P)H) to participate in the reactions. Because the NAD(P) H cofactor is expensive, in situ NADH regeneration is required for preparative applications [3,4]. A common strategy is to combine the second oxidoreductase reaction with the main synthesis reaction to continuously regenerate a reduced form of cofactor.

$NAD(P)^+$- dependent formate dehydrogenase (FDH) is an abundant enzyme found in methylotrophic microorganisms. The enzyme catalyzes the oxidation of formate to carbon dioxide and transfers two electrons to $NAD(P)^+$ to produce NAD(P)H. FDH has several advantages for applying in NAD(P)H regenerating, including, (1) The formate oxidation reaction is almost irreversible, allowing high efficiency to produce NAD(P)H; (2) The substrate, formate, is low-cost and also applicable as buffer matric for reaction; (3) The final

product of reaction, CO_2 gas, can easily release from the reaction, thus tedious purification process is not required, and (4) there are many FDHs that have ability to transfer reduced energy of formate to $NAD(P)^+$. Therefore, FDH is one of the most appropriate enzymes to be used as a co-enzyme regenerating system for biocatalysis [5,6]. However, current FDHs have the drawback of low specific activity, which leads to the use of larger quantities of FDH to be applied in biosynthesis. Finding new FDH with high catalytic efficiency would be beneficial. Previously, our research team has characterized a novel FDH enzyme from *Bacillus simplex* (BsFDH). The enzyme has high activity, providing 4.4-fold greater specific activity than that of FDH from *Pseudomonas* sp101 (PsFDH, a commercial FDH used in real industry). Unfortunately, pain point of low thermostability of this enzyme still hampers its robustness. For usage in industrial processes, the FDH enzyme must have high tolerance toward harsh conditions such as high solvent, salt, acidic or basic conditions, in the presence of oxidizing and reducing agents, and especially high temperatures. Therefore, this research project aims to engineer the BsFDH enzyme to improve its thermostability by using a rational design strategy.

MATERIALS AND METHODS

1. Computational prediction of hotspot residues for improved thermostability

1.1 Program calculation to generate a list of mutations

The thermostable variants were predicted with FireProt (https://loschmidt.chemi.muni.cz/fireprot/), that is the web server for automated design of thermostable protein to predict enzyme variants that may have more thermostability than the original wild-type enzyme [7-11].

1.2 Candidate residue analysis and selection for rational engineering

The candidate mutations were introduced into the model structure of BsFDH. Next, to consider which particular position and type of residues should be mutated, we implemented three rational criteria for selecting candidate variants for further experimental characterization based on knowledge of enzyme structure and function [10]. The first criterion was to eliminate candidate residues in the area of active site. The second criterion was based on Gib's free energy value, calculated by energy and evolution base. And the final criterion was to select mutated residues that could form interactions with neighboring residues.

2. Construction of BsFDH variants

2.1 Site-directed mutagenesis

The *Bsfdh*-pET11a plasmid was used as the mutagenesis template. This pET11a vector carries 1030 nucleotides of the *fdh* gene from *B. simplex*. Site-directed mutagenesis was performed using PCR. The reactions were composed of the *Bsfdh*-pET11a template, 500 nM of forward and reverse primers, 200 μM of dNTPs, and 2.5 units of Phusion DNA polymerase in 1x buffer HF. The thermocycler program began at 98 °C for 5 min for initial denaturation, followed by 16 cycles of denaturation at 98 °C for 45 s, annealing at 50-55 °C for 1 min (depending on the Tm of the primer), extension at 72 °C for 4 min, and final extension at 72 °C for 10 min. PCR products were analyzed by agarose gel electrophoresis and treated with *Dpn*I, a restriction enzyme, to remove the wild-type template for overnight at 37°C before being transformed into XL1Blue competent cells supplemented with 100 μg/mL amplicillin. The plasmids were extracted by using the FavorPrep kit and confirmed by DNA sequencing (Macrogen Inc., South Korea)

3. Expression of wild-type and mutant FDH enzymes

The enzyme was overexpressed in *E. coli* BL21(DE3) using auto-induction media. The starter culture was inoculated at 1% v/v into 650 mL of ZYM-5052 media containing 50 μg/mL of ampicillin. The cells were grown at 37 °C and 220 rpm until OD_{600} reached around 1.0, then the temperature was reduced to 25 °C for 16 hr to allow protein expression. Cells were harvested by centrifugation at 8000 rpm for15 min at 4 °C, then cell paste was stored at -80 °C until used.

4. Purification of wild-type and mutant FDH enzymes

The frozen cell paste was thawed and then resuspended in ice-cold lysis buffer (1 mM DTT, 60 μM PMSF and 0.5 mM EDTA in 50 mM sodium phosphate buffer pH 7) and disrupted by sonication. The lysate was clarified by centrifugation at 15,000 rpm for 45 min at 4°C. The supernatant was first precipitated with 0.5% w/v of polyethylenimine (PEI), and the supernatant was collected after centrifugation at 15,000 rpm for 1 hr at 4 °C. Next, the enzyme solution was precipitated at 40-60% ammonium sulfate saturation and the pellet was gently resuspended in ice-cold 50 mM sodium phosphate buffer pH 7. The protein was dialyzed overnight at 4 ºC in 2 L of 50 mM sodium phosphate buffer pH 7. The dialyzed protein was clarified by centrifugation at 15,000 rpm for 10 min at 4 °C, before being loaded onto the DAEA column.

The DEAE-sepharose column was pre-equilibrated with 50 mM sodium phosphate buffer pH 7.0 for 10 column volumes. Then, the clarified protein solution was loaded into DEAE column and washed with 50 mM sodium phosphate buffer pH 7.0 containing 50 mM NaCl for 10 column volumes, and the enzyme was eluted with 10 column volumes of a linear gradient of 50 mM sodium phosphate buffer pH 7.0 containing 50 to 350 mM NaCl (until the UV 280 nm band reached the baseline level). The eluted protein was checked using a spectrophotometer at 280 nm and analyzed using SDS-PAGE to confirm BsFDH protein. The enzymes were pooled and concentrated by concentrator-stirrer with 10 kDa MW cut-off. The concentrated protein was de-salted using sephadex-G25. Finally, cryoprotectant, 10% v/v glycerol was added to enzyme solution and kept at -80 °C. The quantity and quality were determined using the Bradford assay and SDS-PAGE (12%) with Coomassie brilliant blue staining and compared to standard protein markers (Enzmart Biotech, Thailand). The Extinction coefficient (ε_{280}) of 37.47 $mM^{-1}cm^{-1}$ at pH 7 was used to calculate the protein concentration.

5. Investigation of formate dehydrogenase enzyme activity

The FDH activity was measured based on the formation of NADH as can be monitored at absorbance 340 nm. The assay reactions were conducted in 50 mM sodium phosphate buffer pH 7.0 consisting of 0.4 mM NAD^+, 800 mM sodium formate and 0.25 μM FDH enzyme. The reaction was monitored according to the increase in absorbance of 340 nm at 25 °C after being initiated by adding the FDH enzyme. An initial velocity obtained from the initial slopes of each assay reaction was used for activity calculation. One unit of FDH enzyme is defined as the enzyme quantity that catalyzes 1 μmol product formation (NADH) per min at 25ºC.

6.Thermostability assay

6.1 Investigation of proteins stability by ThermoFluor assay

In this experiment, the protein stability was determined using a real-time PCR machine and SYPRO Orange dye as a hydrophobic dye. A total of 20 μL of 40 μM BsFDHs, wild-type and variants, were mixed with 50 mM sodium phosphate buffer pH 7.0 and 10X SYPRO orange

dye in a PCR tube. The intrinsic fluorescence signal was monitored while the temperature was increased from 10 to 95°C with the constant increasing rate of 1°C per min. The protein melting curve for each BsFDH variant was obtained from the plot of the intrinsic fluorescence signal against reaction temperature and used for determining the T_m value.

6.2 Investigation of proteins thermostability by activity assay

The time-dependent thermal inactivation assay of BsFDH enzymes was investigated for estimation of the enzyme thermotolerance. The BsFDH variant and wild-type in 50 mM sodium phosphate buffer pH 7.0 was incubated for 0–1440 min at 50, 55 and 60 °C. At various time points, the enzyme was taken for assay reaction under the conditions described previously in Section 5. The enzyme activity before heating was used as the value for time zero and was set as the value for 100% activity. The percentage of residual activity of FDH at various time points was calculated. The assay was performed in triplicate and the data was presented as mean ± SD.

RESULTS

1. FireProt program prediction for thermostable variants and selection criteria.

As there is no three-dimensional structure of BsFDH available, the BsFDH model structure was first constructed from the SWISS-model program using FDH from *C. boidinii* that shares 46.09% identity with BsFDH as a template. The resultant model had 0.83 of GMQE, 0.89 of QSQE, indicating a good quality of the model. To identify candidate residues that may be beneficial for enzyme thermostability, the BsFDH model was submitted to the FireProt program. The program consists of three strategic approaches; an energy-based approach, or an evolution-based approach, or a combination of both. After calculation, the FireProt program provided 61 candidates of single-point mutation introduced into protein structure. To reduce a number of clones to be constructed. We implemented three rational criteria for selecting candidate variants for further characterization based on knowledge of enzyme structure and function. The first criterion is to avoid any changing residue near the active site area, as it might perturb BsFDH activity, and the residue should not be a conserved residue. From this criterion, 12 candidates were eliminated. The second criterion, we selected the variants that showed a negative value of delta Gibbs free energy. The delta Gibb's free energy was calculated from energy- and evolution-based FirePort. Target residues were made *in silico* site-saturated mutagenesis to investigate the suitable mutants and value of different folding free energy ($\Delta\Delta G^{fold}$) calculated from the subtraction of folding free energy of wild-type ($\Delta\Delta G^{fold\ WT}$) from the folding free energy of mutant ($\Delta\Delta G^{fold\ mutant}$) according to **Equation 1**

$$\Delta\Delta G^{fold} = \Delta G^{fold\ mutant} - \Delta G^{fold\ WT} \quad \text{---------- (1)}$$

Negative value of $\Delta\Delta G^{fold}$ indicates the more structure stability of the variant compared to the wild-type, therefore, candidates with the $\Delta\Delta G^{fold}$ less than -1 kcal/mol were selected and at this step, only 23 candidates passed for further analysis.

The final criterion is the finding of residues located near the subunit interface and able to form interactions with residues from neighboring subunits. This is based on the notion that the more stable protein is a consequence of interaction via salt bridges, hydrogen bonding, hydrophobic interaction between subunits. When this criterion was applied to 23 candidates from the previous criterion, only 4 candidates could pass. Moreover, among 23 candidates, we also selected another 5 candidates, which had the most negative value of $\Delta\Delta G^{fold}$. The 9 selected candidates are listed in **Table 1,** and relative positions in the model structure of BsFDH are illustrated in **Figure 1.**

Table 1 A summary of 9 selected candidates from FireProt analysis for BsFDH thermostability improvement.

No.	Mutation information			Not conserved	$\Delta\Delta G^{fold}$
	Position	Reference	Alter		
1	43	T	M	/	-1.64029
2	125	Q	L	/	-2.28385
3	136	G	Y	/	-1.89273
4	216	A	I	/	-4.62761
5	50	S	L	/	-1.10108
6	196	L	W	/	-1.87339
7	213	T	C	/	-1.06358
8	151	G	Q	/	-1.30168
9	69	A	F	/	-1.29088

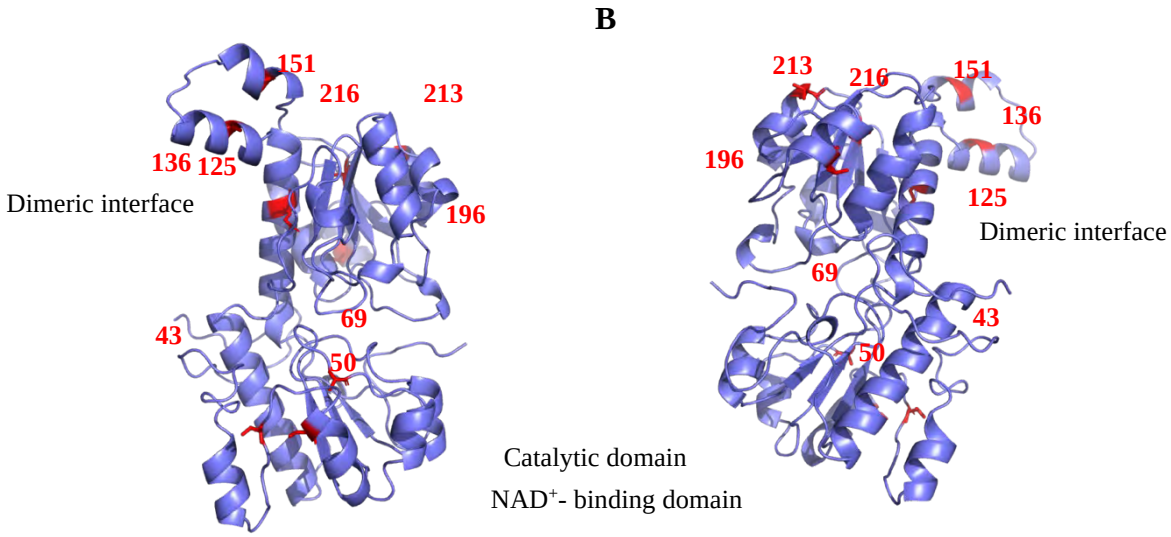

Figure 1 Positions of 9 selected candidate residues in the BsFDH model structure (A: front view, B: back view)

2. Construction, overexpression and purification of BsFDH variants

Specific primers were designed and site-directed mutagenesis was performed using PCR. The *bsfdh*-pET11a plasmid was used as the mutagenesis template. Only 8 mutant genes were successfully constructed and the sequences were confirmed by DNA sequencing (Macrogen Inc., South Korea).

The BsFDH mutants were expressed in 1.3 L auto-induction (ZY) media at 25°C for 16 h. The cell paste of each mutant was weighed as follows: 19.68g (T43M), 22.29g (Q125L), 20.92g (G136Y), 15.79g (A216I), 20.73g (S50L), 14.38g (L196W), 19.04g (T213C) and 19.89g (G151Q). All mutant enzymes were purified according to the protocol used for wild-type purification. The crude extract was first precipitated by 0.5% (w/v) polyethyleneimine (PEI) and followed by 40-60% of ammonium sulfate saturation. The enzyme solution was dialyzed before loading onto the DEAE-sepharose column and removing salt by G-25 gel filtration. The quantity and quality of BsFDH mutant proteins were determined using Bradford assay and SDS-PAGE with Coomassie brilliant blue staining. All mutants were successfully

purified except for the L196W variant, due to the enzyme not being expressed at the employed condition. The enzymes showed overexpression bands with an approximate size of around 38.5 kDa and obtained more than 95% purity judged by SDS-PAGE analysis (**Figure 2**).

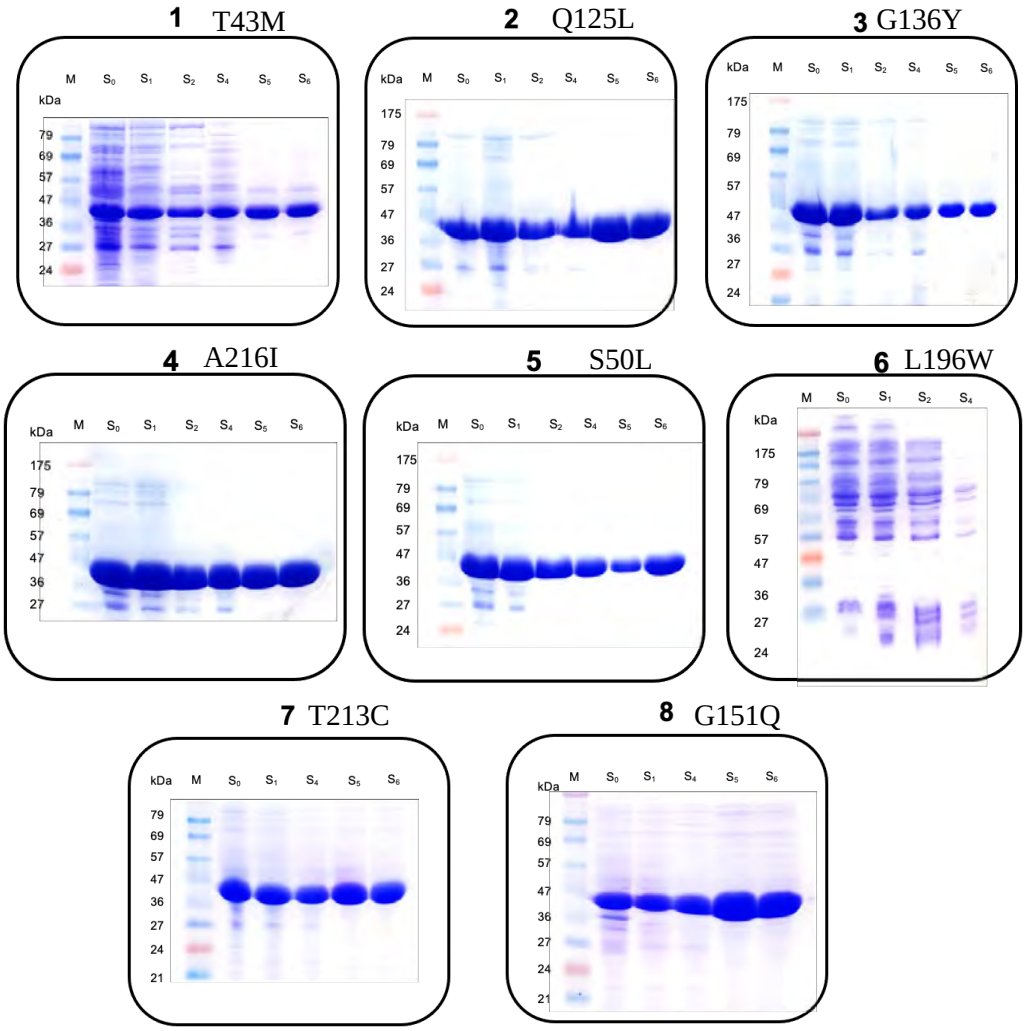

Figure 2 SDS-PAGE analysis of BsFDH mutants in each purification step. A 20 μg protein from each purification step was examined using 12% SDS-PAGE . Lane M; protein marker, Lane S_0; crude extract, Lane S_1; protein after precipitated by 0.5% (w/v) polyethyleneimine, Lane S_2; protein after precipitated by 40-60% ammonium sulfate, Lane S_4; protein after dialysis, Lane S_5; protein after purified by DEAE-Sepharose column, Lane S_6; protein after Sephadex-G25 gel filtration.

3. Investigation of formate dehydrogenase enzyme activity

To investigate whether the variants have efficient catalysis, the FDH activity assay was performed in the variants and compared with the wild-type BsFDH enzyme. Therefore, 8 mutants were successfully constructed and expressed but for the L196W variant was low protein expression at the employed condition. So, the 7 mutants were investigated of formate dehydrogenase enzyme activity. The results revealed that the Q125L, A216I, S50L and T213C had similar specific activities to those of the wild-type BsFDH, while mutations of T43M, G136Y and G151Q resulted in decreased enzyme activity (**Figure 3**). It is also noted that the BsFDH wild-type and Q125L, A216I, S50L and T213C variants provide 1.5 - 2-fold greater

specific activity as compared with PsFDH. Therefore, Q125L, A216I, S50L and T213C were selected to further investigate their thermostability.

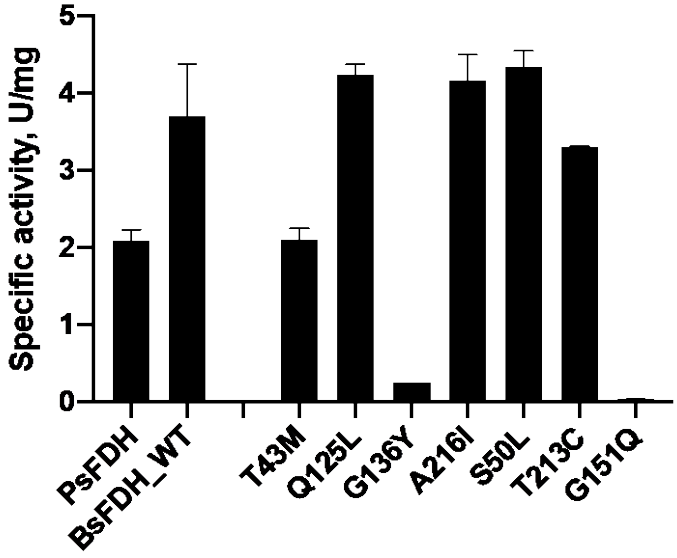

Figure 3 The specific activity of wild-type and mutant BsFDHs. The FDH activity was measured based on the formation of NADH. The assay reactions were conducted in 50 mM sodium phosphate buffer pH 7.0 and consisted of 0.4 mM NAD^+, 800 mM sodium formate and 0.25 μM FDH. The reaction was monitored at a wavelength of 340 nm at 25 °C.

4. Investigation of protein stability by ThermoFluor assay

To investigate structural stability, the ThermoFluor assay was performed on wild-type and mutant BsFDHs. T_m is calculated from the plot between integrated relative fluorescence units (RFU) and temperature **(Figure 4)**. The results showed that there was no significant difference in T_m calculated from wild-type and mutant as the T_m of 59.5 ± 0.289, 61 ± 0.577, 59.5 ± 0.5, 59.5 ± 0.289 and 59.5 ± 0.289 ^oC were obtained from wild-type, Q125L, A216I, S50L, and T213C mutants, respectively. The data indicate the similarity of the overall integrity of wild-type and mutant structures.

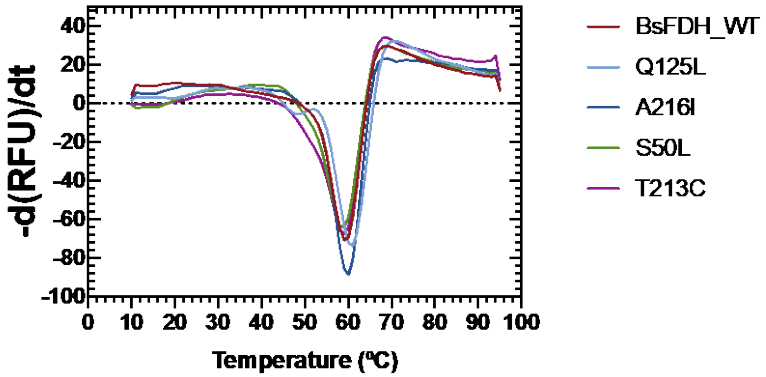

Figure 4 The melting curves of BsFDH wild-type and mutants. The melting curves are presented by plotting the first derivative of the fluorescence emission as a function of temperature. The T_m corresponds to the lowest point of the first derivative graph and the assay was performed in triplicate.

5. Thermostability assay

The thermostability of wild-type BsFDH was first investigated by incubating the enzyme at 50, 55 and 60 ^{o}C for various time points. The results showed that the wild-type BsFDH was stable at 50^{o}C as no significant change of enzyme activity was observed over 180 min incubation. At 55 ^{o}C incubation, the enzyme retained around 60% activity, while at 60 ^{o}C, enzyme activity was dramatically reduced and completely lost after 120 min incubation (**Figure 5A**).

To explore if the variants can exert higher thermostability, time course thermal inactivation at 55 ^{o}C was investigated in BsFDH variants compared with BsFDH wild-type. The result in **Figure 5B** clearly indicated that mutation at Q125L could enhance enzyme thermostability, in which the Q125L was able to retain >50% after 6 h incubation, while the wild-type activity dropped to less than 35% activity. When the thermostability of Q125L was compared with benchmark PsFDH by incubating at 60^{o}C. We use PsFDH as a benchmark PsFDH because it is known to be the thermostable FDH enzyme and has recently been utilized in the biocatalysis industry. The results in **Figure 5C** can confirm the higher stability of the Q125L compared to the wild-type BsFDH. The activity of Q125L gradually decreased over time, and it retained more than 50% after 100 min of incubation. While the PsFDH was stable over the incubation time. However, when the enzyme originally had lower specific activity relative to the BsFDH, it turned out that the actual activity was compared, and the Q125L could provide higher specific activity than that of the PsFDH over 100 min of incubation.

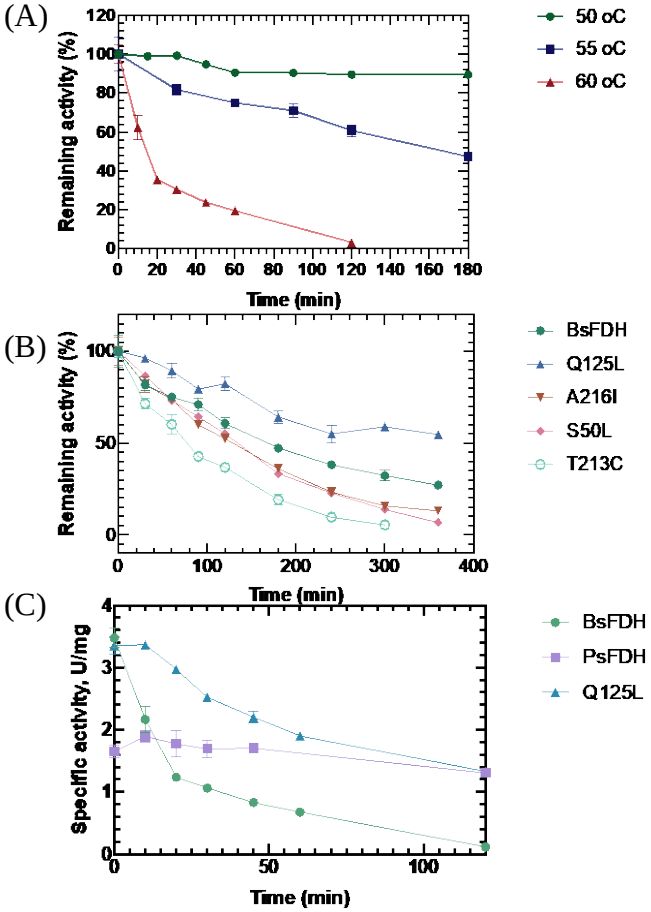

Figure 5 Thermostability assay. (A) Thermal inactivation of wild-type BsFDH at different incubation temperatures. Thermostability assay at 55 ^{o}C of wild-type and BsFDH variants. Percent remaining activities were calculated relative to the activity at time 0 and the assay was

carried out in triplicate. (C) Thermostability assay at 60 ºC and the specific activities are presented.

DISCUSSION AND CONCLUSION

This study used *in silico* approaches to rationally design variants of BsFDH with improved thermostability. Although more than 60 target variants were suggested by the program. We implemented three rational criteria for selecting candidate variants based on knowledge of enzyme structure and function to reduce the number of candidates to be studied [12]. The first criterion was to eliminate candidate residues in the active site, residues that have been reported to participate in FDH catalysis and be conservative residues of FDHs. This is because changing those residues might affect enzyme activity. The second criterion was based on Gibb's free energy value, and the final criterion was to select residues that could form interactions with neighboring residues. This is based on the idea that more stable proteins result from interactions such as salt bridges, hydrogen bonding, and hydrophobic interaction [13]. The results showed the thermostability improvement of Q125L variant. The Gln125 position is located near to the dimeric interface, where the residues 4 Å-around Gln125 position in protein structure are mostly hydrophobic amino acids. The changing of Gln to Leu, which possesses hydrophobic property, may support the hydrophobic interaction, leading to more thermostability of the Q125L variant. In addition, Q125 may be a potential position for further improvement of BsFDH thermostability by site-saturation mutagenesis.

ACKNOWLEDGEMMENTS

The authors acknowledge Development and Promotion of Science and Technology Talents Project (DPST) (to RB), and a Research Grant for New Scholar (Office of the Ministry of Higher Education, Science, Research and Innovation, Grant number: RGNS 63-179) (to RN), Faculty of Science, Mahidol University, Department of Biochemistry and Center of Excellence in Protein and Enzyme Technology (CPET), Faculty of Science, Mahidol University for the technical support.

REFERENCES

[1] Fischer T, Pietruszka J (2010) Key building blocks via enzyme-mediated synthesis. Top Curr Chem 297:1–43

[2] Wohlgemuth R (2010) Asymmetric biocatalysis with microbial enzymes and cells. Curr Opin Microbiol 13:283–292

[3] van der Donk R, Zhao H (2003) Recent developments in pyridine nucleotide regeneration. Curr Opin Biotechnol 14:421–426

[4] Wichmann R, Vasic-Racki D (2005) Cofactor regeneration at the lab scale. Adv Biochem Engin/Biotechnol 92:225–260

[5] Hummel, W.; Groger, H. Strategies for regeneration of nicotinamide coenzymes emphasizing self-sufficient closed-loop recycling systems. J. Biotechnol. 2014, 191, 22−31.

[6] Babel, W. The Auxiliary Substrate Concept: From simple considerations to heuristically valuable knowledge. Eng. Life Sci. 2009,9, 285−290.

[7] M. Musil, J. Stourac, J. Bendl, J. Brezovsky, Z. Prokop, J. Zendulka, T. Martinek, D. Bednar, J. Damborsky, *Nucleic Acids Res.* 2017, 45(W1), W393-W399.

[8] Bednar, D., Beerens, K., Sebestova, E., Bendl, J., Khare, S., Chaloupkova, R., Prokop, Z., Brezovsky, J., Baker, D., & Damborsky, J. (2015) FireProt: energy- and evolution-

based computational design of thermostable multiple-point mutants. PLoS Comput Biol, 11, e1004556– e1004575.

[9] Dvorak, P., Bednar, D., Vanacek, P., Balek, L., Eiselleova, L., Stepankova, V., Sebestova, E., Kunova, M., Chaloupkova, R., Brezovsky, Prokop, Z., Krejci, P., Dvorak, P., Damborsky. Computer-assisted engineering of hyperstable fibroblast growth factor2. *Biotechnology and bioengineering.* 2017; 115,4.

[10] Pongpamorn, P., Watthaisong, P., Pimviriyakul, P., Jaruwat, A., Lawan, N., Chitnumsub, P., & Chaiyen, P. (2019) Identification of a Hotspot residue for Improving the thermostability of a flavin-dependent monooxygenase. *ChemBioChem*. 10.1002/cbic.201900413.

[11] Ashraf, N.M., Krishanagopal, A., Hussain, A., Kastner, D., Sayed, A.M.M., Mok, Y-K., Swaminathan, K., Zeehan, N. Engineering of serine protease for improved thermostability and catalytic activity using rational design. *International Journal of Biological Macromolecules*. 2019; 126.

[12] Maenpuen S, Pongsupasa V, Pensook W, Anuwan P, Kraivisitkul N, Pinthong C, Phonbuppha J, Luanloet T, Wijma HJ, Fraaije MW (2019) Creating flavin reductase variants with thermostable and solvent-tolerant properties by rational-design engineering. Chembiochem 21(10):1481–1491

[13] J. Bendl, J. Stourac, E. Sebestova, O. Vavra, M. Musil, J. Brezovsky, J. Damborsky, Nucleic Acids Res. 2016, 44, W479 – W487.

COMPANY SPONSORS

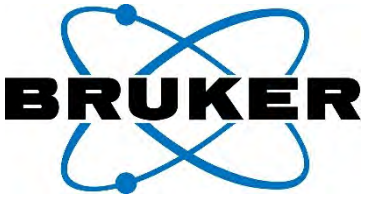

Abstracts and Proceedings
16th International Online Mini-Symposium
of the Protein Society of Thailand

Protein Society of Thailand
http://www.proteinsocthai.net

pstsymposium2021@gmail.com
https://science.mahidol.ac.th/pst2021
Mahidol Science
The Protein Society of Thailand